Microplastic in Beach Sediment from Mary's Point, Shepody National Wildlife Area, Southeastern New Brunswick

by

Claire Gullison

Bachelor of Science, Honours, The University of New Brunswick, 2023

Bachelor of Education, St. Thomas University, 2026

A Thesis Submitted in Partial Fulfillment
of the Requirements for the Degree of

Master of Science

in the Graduate Academic Unit of Earth Sciences

Supervisor: Dave Keighley, PhD, PGeo, Earth Sciences

Examining Board: Cliff Shaw, PhD, Earth Sciences
Myriam Barbeau, PhD, Biology

This thesis is accepted by the Dean of Graduate Studies

THE UNIVERSITY OF NEW BRUNSWICK

August 2026

© Claire Gullison, 2026

Abstract

Microplastic pollution has become an increasingly pervasive global contaminant, yet protected coastal environments remain insufficiently characterized. A baseline assessment is established here for microplastics within the beach sediments of Mary's Point, a nationally and internationally protected site of high ecological significance in the upper Bay of Fundy. Fourteen sediment cores collected in 2022 and 2024 were analyzed using a five-stage extraction protocol integrating sequential density separations with an oleophilic phase, enabling the recovery of a broad range of polymer densities. A total of 1,806 microplastic particles were identified, with secondary fibres (resulting from the degradation of larger plastic items) more than 90% of all particles. Mean abundances declined significantly from 990.8 microplastics per kilogram of sediment (MP/kg) in 2022 to 343.5 MP/kg in 2024, driven by episodic, high-energy storm reworking. While storm surges scoured upper sediment layers, the macroscopic sand matrix exhibited geomorphic resilience, showing no statistically significant temporal shift in median grain size. Lateral and vertical heterogeneity in microplastic distribution reflects dynamic sedimentary processes. Findings demonstrate that even remote, protected shorelines function as dynamic sinks for long-range microplastic contamination modulated by episodic high-energy events.

Dedication

To my family and friends, who supported me through every stage of this journey and believed in me even when I doubted myself.

Acknowledgements

I would like to express my sincere appreciation to Dr. Dave Keighley, my supervisor, for his guidance and support throughout this research. I am also grateful to Dr. Allison Enright for providing laboratory materials and insightful analytical consultation, and to Dr. Cliff Shaw for access to laboratory equipment, including the oven used in sample preparation. I would like to extend my thanks to the UNB Chemistry Department for their assistance with FTIR (Fourier-Transform Infrared) analytical methods. Fieldwork for this project was made possible through sampling permits issued by Environment and Climate Change Canada in 2022 and 2024. I further acknowledge the staff of the UNB Chemistry Store for their helpful consultation and support in obtaining the necessary laboratory supplies. I also acknowledge the financial support received through the University of New Brunswick's Accelerated MSc program, which contributed significantly to the completion of this thesis.

Table of Contents

Abstract ii

Dedication iii

Acknowledgements iv

Table of Contents v

List of Tables ix

List of Figures xii

List of Symbols, Nomenclature, or Abbreviations xx

1. Introduction 1

1.1. Definitions 2

1.1.1. Types of plastic waste 2

1.1.2. Microplastic size classifications 2

1.1.3. Microplastic shape classifications 5

1.1.4. Abundance or concentration units 7

1.1.5. Compositional and degradation terms 7

1.2. Environmental impact of waste plastic 10

1.2.1. Plastic degradation and additive leaching 11

1.2.2. Transport and deposition in sedimentary systems 12

1.2.3. Ecological and human health effects 14

1.2.4. Broader environmental and economic impacts 15

1.3. Research rationale 16

2. Research Review of Microplastics in Beach Sediment 18

2.1. Overview of previous research 18

2.1.1. Foundational research 18
2.1.2. Recent research trends 21
2.1.3. Global coverage and disparities 26
2.1.4. Research on environmentally sensitive beaches 28
2.2. Overview of sampling methods 30
2.2.1. Sampling strategies 30
2.2.2. Sampling zones 31
2.2.3. Sampling depths 32
2.3. Overview of microplastic-extraction methods 33
2.3.1. Visual Extraction Using a Binocular Microscope 35
2.3.2. Density-based separations 35
2.3.3. Oil and hybrid separations 36
2.3.4. Alternative extraction methods 37
2.3.5. Organic-matter removal 38
2.4. Microplastic identification techniques 41
2.4.1. Visual sorting and hot needle testing 42
2.4.2. FTIR and Raman Spectroscopy 43
2.4.3. Other tools 43
2.5. Contamination control and quality assurance 44
2.6. Synthesis of methodological variability 46
3. Geological and Natural Setting of the Study Area 48
3.1. Geological evolution of Chignecto Bay 50
3.2. Modern hydrodynamic and sedimentary environment of Chignecto Bay 52

3.3. Mary's Point 54
3.4. Site importance 57
3.4.1. Fundy Biosphere Region 57
3.4.2. National Wildlife Area 59
3.4.3. Western Hemisphere Shorebird Reserve Network 60
3.4.4. Ramsar Wetland of International Importance 61
3.5. Ecological threat of microplastics 62
4. Methodology 65
4.1. Field Methods 65
4.2. Sediment preparation and analyses 68
4.3. Microplastic Extraction 70
4.4. Particle Identification and Quality Control 72
4.4.1. Visual sorting and classification 72
4.4.2. Organic matter digestion 73
4.4.3. Quality control 74
4.4.4. Omission of additional identification steps 75
4.5. Statistical Tests 76
5. Results 77
5.1. Sampling Overview 77
5.1.1. Sediment characteristics 77
5.1.2.-Temporal grain-size variation 78
5.1.3. Spatial variation in grain size 79
5.2. Microplastic abundance 79

5.2.1. Temporal Variation 81
5.2.2. Variation of microplastic characteristics 81
6. Discussion 84
6.1. Sediment Characteristics 84
6.2. Microplastic Abundance and Distribution 90
6.2.1. Temporal and Spatial Variability 90
6.2.2. . Microplastic Characteristics: Density, Shape and Colour 93
6.3. Mary's Point Microplastic Pollution in a Global Context 99
7. Summary and Future Work 105
7.1. Summary of key findings 105
7.2. Limitations and future work 107
7.3. Broader implications and concluding remarks 110
Bibliography 111
Appendix A – Sample ID's 149
Appendix B – Microplastic Abundance Results 151
Appendix C – Sediment Analysis 154
Appendix D – Meta-Analysis of Data 171
Curriculum Vitae

List of Tables

Table 1.1. Plastic types along with their origin (Plastics Europe, 2021), demand in 2019 (Plastics Europe, 2021), and density ranges reported by Hidalgo-Ruz et al. (2012) (density range 1) and SpecialChem SA (density range 2). 8

Table 1.2. Density range of plastic particles in groups of < 1.0 g/cm^3, < 1.00 – 1.18, g/cm^3, < 1.18 – 1.30 g/cm^3, < 1.30 – 1.50 g/cm^3, > 1.50 g/cm^3. Plastic types in black are the baseline-defined density of the resin. Those in grey italics are resins with an increased density compared to their baseline defined density in black, due to the addition of compounds such as flame retardants, elasticizers, lubricants, etc. Numbers in brackets correspond to their recycling number. 10

Table 2.1. Published microplastic studies on beaches using a density extraction method between 2011 and 2024. See Appendix D, Table D1 for a complete list of studies..... 22

Table 2.2. Summary of common extraction techniques used in microplastic studies, highlighting their respective strengths, limitations, and typical use contexts. Techniques range from low-cost visual extraction to advanced electrostatic and depolymerization methods. 34

Table 2.3. Selected beach microplastic studies incorporating chemical digestion (H_2O_2 or KOH) for organic-matter removal and subsequent polymer identification via FTIR or Raman spectroscopy. Abbreviations: PE = Polyethylene; PP = Polypropylene; PET = Polyethylene Terephthalate; PS = Polystyrene; EPS = Expanded Polystyrene; dw = dry weight..... 40

Table 2.4. Summary of common analytical techniques used in microplastic identification, highlighting their respective strengths, limitations, and typical use contexts (Simon-Sánchez et al. 2022; Soursou et al. 2023; Volgare et al. 2021; Hidalgo-Ruz et al. 2012). Techniques range from low-cost visual sorting to advanced spectroscopic and thermal methods, with ongoing efforts to strike a balance between analytical accuracy, cost, and accessibility in environmental studies. 41

Table 4.2. Samples collected during 2024 field work on July 8th at Mary's Point Beach. Seven cores were extracted along the beach from east to west at randomly generated coordinates, along the spring high tide line. The spring high tide line was identified based on the continuous wrack present. Core 1 indicated the eastern-most location. 68

Table 4.1. Samples collected during 2022 field work on July 5th at Mary's Point Beach. Seven cores were extracted along the beach from east to west at randomly generated coordinates, along the spring high tide line. The spring high tide line was identified based on the continuous wrack present. Core 1 indicated the eastern-most location. 68

Table 6.1. Summary of reported microplastic abundances in protected coastal environments worldwide, highlighting that even ecologically significant or conservation-designated sites exhibit measurable levels of contamination across a range of geographic and environmental contexts. 103

Table A1. Core ID's and microplastic extraction ID's for 2022. 149

Table A2. Core ID's and microplastic extraction ID's for 2024. 150

Table B1. Microplastic abundance results per sample (by depth and core) in 2022 151

Table B2. Microplastic abundance results per sample (by depth and core) in 2024 151

Table B3. 2022 microplastic abundance results per sample (by depth and core)..... 152

Table B4. 2024 microplastic abundance results per sample (by depth and core)..... 153

Table C1. Grain size analysis of samples collected in 2022..... 168

Table C2. Grain size analysis of samples collected in 2024..... 169

Table C3. Mean grain size by core in 2022 and 2024. 170

Table D1. Summary of peer-reviewed beach sediment microplastic studies (2011–2024) 171

List of Figures

Figure 1.1. Example classifications of particle (sediment) size in the scientific literature and the different boundaries being used to classify different sizes of plastic particles. In sedimentology, a common classification is based on Udden (1914), Wentworth (1922), and Blair & McPherson (1999); in soil science, the scheme of the Soil Survey Staff (1951) in the US Dept. of Agriculture; in engineering, AASHTO, the American Association of State Highway and Transportation Officials (AASHTO) (1997)..... 4

Figure 1.2. Visual representation of shape categories defined by Zingg's three-axis particle geometry (a, b, and c axes). 5

Figure 3.1. Map of the Bay of Fundy, New Brunswick, Canada. The study region of Mary's Point is circled in red. Identified areas include (A) Bay of Fundy, (B) Chignecto Bay, (C) Shepody Bay, (D) Cumberland Basin, (E) Minas Basin, (F) Cape Maringouin, (G) Hopewell Rocks Provincial Park, (H) Petitcodiac River, (I) Waterside Beach. 49

Figure 3.2. Google Earth Image of Mary's Point, NB, identifying the Quaternary Cliffs (red arrows), the Carboniferous Cliffs (yellow arrows), wave-cut platforms (blue arrow), and the New Horton Mud Flats..... 54

Figure 3.3: Map of the Fundy Biosphere Region, New Brunswick, Canada (Canadian Geographic, 2013)..... 58

Figure 3.4. Protected regions under the designation of the Shepody National Wildlife Area (green) by the Government of Canada (Environment and Climate Change Canada, 2023). 59

Figure 3.5. Map of the Americas showing the migratory route of eastern Semipalmated Sandpipers, illustrating their journey between Arctic breeding grounds and South American wintering sites (Species at Risk, 2006). 60

Figure 3.6. Mary's Point and other nearby WHSRN sites (WHSRN, n.d., Retrieved June 29, 2022). 61

Figure 3.7. Map of Mary's Point unit of the Shepody NWA, and its additional RAMSAR Wetland of International Importance designation (Ramsar, Retrieved April 8, 2025)..... 62

Figure 4.1. Fourteen core samples were taken from Mary's Point, New Brunswick, Canada, 3 m below the spring high tide line in 2022 and 2024. Samples were taken at randomly generated longitudes between the western (064º38'48.00" W) and eastern (064º39'45.00" W) ends of the beach. 67

Figure 4.2. Illustration of methodology showing samples sequentially passed through increasing-density solutions, with decanting and filtration steps between each phase, concluding with an oleophilic extraction to remove particles with densities greater than 1.5 g/cm^3. 71

Figure 5.1. Core sample locations along the beach transect, with extrapolated heatmaps displaying mean grain size as a function of depth. Lighter colours represent coarser sediment (lower ϕ), and darker shades rrepresent finer material (higher ϕ). For descriptive display only; depth parameters were statistically aggregated by core to preserve strict data independence during temporal hypothesis testing (n = 14) 78

Figure 5.2. Spatiotemporal distribution of microplastic abundance (MP/Kg) by core and depth for (a) 2022 and (b) 2024. Cores are arranged along a relative west-to-east transect

for each sampling year. Each cell represents the number of microplastic particles per gram recovered from a 4 cm sediment interval. Note that core numbers represent relative position only and are not co-located between years. The colour scale is standardized across both panels to allow for direct comparison of the overall abundance patterns, highlighting the higher concentrations found in 2022. This figure is for descriptive display only; depth parameters were statistically aggregated by core to preserve strict data independence during temporal hypothesis testing (n = 14) 80

Figure 5.3. Relative abundance (%) of microplastic shapes (pellets, fibres, films, fragments, and fibre balls) recovered from sediment samples in 2022 and 2024, highlighting the consistent dominance of fibres across both sampling years. 82

Figure 5.4. Relative abundance (%) of microplastic colours identified in 2022 and 2024, showing a stable colour profile between years with white/clear, black, and blue particles being the most prevalent. 83

Figure 6.1. NOAA Historic Hurricane tracks showing hurricanes passing through a 180 Nautical Mile radius of Mary's Point, NB, Canada from 2019 to 2023. 85

Figure 6.2. (a) Hydrodynamic processes at the study site, shown on satellite imagery from Google Earth. (b) The dominant southwest wave approach (blue line) relative to the shoreline (yellow line), indicating the potential for westward longshore drift (red arrows); (c) Wave diffraction around the eastern headland, which creates a sheltered, low-energy zone at the eastern end of the beach. 87

Figure 6.3. Conceptual sketch illustrating the effect of surface erosion on apparent core depth between 2022 and 2024. 92

Figure 6.4. Schematic showing the dilution of microplastic contamination in the upper sedimentary layers. (i) initial environment, (ii) constant rate of microplastic accumulation from various sources, (iii) slope stability breached on backshore, (iv) increased sediment load deposition, (v) constant rate of microplastic accumulation from various sources, (vi) bioturbation and sediment reworking. 94

Figure 6.5. Frequency of dominant microplastic shapes reported in global beach and coastal sediment literature from recent studies (n=38). The chart illustrates the number of studies in which fibres, fragments, foam, or pellets were identified as the most prevalent shape Note: In cases where two shapes were reported as equally dominant (e.g., fibre and fragment in Godoy et al., 2020), the study was included in the count for both categories. (Ballent et al., 2016; Retama et al., 2016; Lots et al., 2017; Hengstmann et al., 2018; Koongolla et al., 2018; Li et al., 2018; Lo et al., 2018; Zhang et al., 2018; Zhao et al., 2018; Ghaffari et al., 2019; Sathish et al., 2019; Tziourrou et al., 2019; De-la-Torre et al., 2020; Godoy et al., 2020; Nguyen et al., 2020; Prarat et al., 2020; Rahman et al., 2020; Carvalho et al., 2021; Hossain et al., 2021; Jualaong et al., 2021; Manbohi et al., 2021; Schröder et al., 2021; Veerasingam et al., 2021; Wu et al., 2021; Abidli et al., 2022; Asensio-Montesinos et al., 2022; Gao et al., 2022; Jones et al., 2022; Kaviarasan et al., 2022; Nhon et al., 2022; Pervez & Wang, 2022; Terzi et al., 2022; Zhang et al., 2021; Khaleel et al., 2023; Le et al., 2023; Şener & Yabanli, 2023; Tasnim et al., 2023; Arjun et al., 2024; Bobchev et al., 2024; Borah et al., 2024; Gül, 2024; Hamdy et al., 2024; Piyumali et al., 2024). 95

Figure 6.6. Global distribution of microplastic abundances (MP/kg) reported in beach-sediment studies between 2011 and 2024 (see Appendix D, Table D1). Studies are

grouped into 13 bins of 250 MP/kg, with the final bin representing values > 3000 MP/kg. Panel (a) includes studies using low-density NaCl extraction (n = 112; ~1.18 g/cm^3), while panel (b) includes studies using higher-density extraction solutions (n = 84; e.g., $CaCl_2$, $ZnCl_2$, NaI, NaH_2PO_4). Vertical lines indicate mean microplastic abundance at Mary's Point: solid lines in panel (b) represent values derived from the full multi-step extraction protocol used in this study, whereas dashed lines in panel (a) show where the same samples would plot if only NaCl extraction had been employed. 100

Figure 6.7. Global distribution of microplastic (MP) abundances in beach sediments reported in density-base extraction studies. Results are grouped by low-density NaCl extraction (~1.18 g/cm^3) and higher-density extraction solutions (e.g., $CaCl_2$, $ZnCl_2$, NaI, NaH_2PO_4, and Na_2WO_4), capable of recovering denser polymers. Boxes show the interquartile ranges (IQR), medians, means (x), and 1.5xIQR whiskers; outliers represent highly contaminated sites. For NaCl-only studies, Q1 = 89, Q3 = 433, IQR = 345, mean = 481, median = 221. For higher-density extraction studies, Q1 = 56, Q3 = 564, IQR = 508, mean = 1226, median = 204. Diamonds indicate mean MP abundance at Mary's Point for 2022 and 2024 derived from the multistep extraction (blue) and estimated NaCl-only recovery (green). 102

Figure C1. Core 22-1. Stratigraphic log for Core 22-1, collected on July 5th, 2022. The core consists of brown medium-sandstone and reached a total recovery of 19.0 cm. The log illustrates consistent grain size throughout, while microplastic (MP) abundance shows vertical variability, notably featuring a localized lens of high contamination at 12–16 cm. 154

Figure C2. Core 22-2. Stratigraphic log for Core 22-2, collected on July 5th, 2022. Composed of brown medium-sandstone with a total recovery of 14.0 cm, the log illustrates consistent grain size and variable MP abundance. Notable peaks in contamination occur at the surface (0–4 cm) and at depth (12–14 cm). 155

Figure C3. Core 22-3. Stratigraphic log for Core 22-3, collected on July 5th, 2022. The core reached a total recovery of 15.0 cm and is characterized as brown medium-sandstone. While grain size remains consistent, MP abundance varies vertically, with high contamination observed at depth (8–15 cm). 156

Figure C4. Core 22-4. Stratigraphic log for Core 22-4, collected on July 5th, 2022. Reaching a total recovery of 13.0 cm, this brown medium-sandstone core exhibits consistent grain size. The log reveals vertical variability in MP abundance, highlighted by a localized lens of low contamination at 8–12 cm. 157

Figure C5. Core 22-5. Stratigraphic log for Core 22-5, collected on July 5th, 2022. Total core recovery reached 13.0 cm. The lithology transitions from brown fine-sandstone to medium-sandstone at a depth of 4 cm. The log illustrates slight variability in both grain size and MP abundance throughout the profile. 158

Figure C6. Core 22-6. Stratigraphic log for Core 22-6, collected on July 5th, 2022. The core reached 13.0 cm and consists primarily of brown medium-sandstone, featuring a medium-coarse lens from 8–12 cm. The log illustrates slight variability in grain size and a generally lower MP abundance. 159

Figure C7. Core 22-7. Stratigraphic log for Core 22-7, collected on July 5th, 2022. Composed of brown medium-sandstone with a total recovery of 20.0 cm, the log

illustrates consistent grain size and MP abundance. A localized low-contamination lens is noted at 16–20 cm. 160

Figure C8. Core 24-1. Stratigraphic log for Core 24-1, collected on July 8th, 2024. Total recovery reached 12.0 cm, with the lithology transitioning from brown to red-brown medium-sandstone at 8.5 cm. The log illustrates an increase in grain size and a corresponding decrease in MP abundance with depth. 161

Figure C9. Core 24-2. Stratigraphic log for Core 24-2, collected on July 8th, 2024. The core reached a total recovery of 14.0 cm, shifting from brown medium-sandstone to red-brown at 10.5 cm. Pebble and conglomerate lenses are present at 8–10 cm and 12–14 cm. MP abundance is variable, with high contamination localized at 12–14 cm. 162

Figure C10. Core 24-3. Stratigraphic log for Core 24-6, collected on July 8th, 2024. Total recovery reached 17.0 cm, with a lithological transition from brown sandstone to red-brown conglomerate at 12 cm. The log illustrates variable MP abundance, featuring high contamination at the surface (0–4 cm) and at depth (16–17 cm). 163

Figure C11. Core 24-4. Stratigraphic log for Core 24-4, collected on July 8th, 2024. Composed of brown medium-grained sandstone with a total recovery of 12.0 cm, the log illustrates consistent grain size and MP abundance throughout the profile. 164

Figure C12. Core 24-5. Stratigraphic log for Core 24-5, collected on July 8th, 2024. The core consists of brown sandstone and reached 17.0 cm; a small pebble/conglomerate lens at 16 cm inhibited deeper coring. The log illustrates near-consistent grain size and variable MP abundance, with a localized high-contamination lens at 16–17 cm. 165

Figure C13. Core 24-6. Stratigraphic log for Core 24-6, collected on July 8th, 2024. Total recovery reached 17.0 cm, with a lithological transition from brown sandstone to red-brown conglomerate at 12 cm. The log illustrates variable MP abundance, featuring high contamination at the surface (0–4 cm) and at depth (16–17 cm)..... 166

Figure C14. Core 24-7. Stratigraphic log for Core 24-7, collected on July 8th, 2024. The core reached 18.0 cm, transitioning from brown to red-brown sandstone at 9 cm. The log illustrates near-consistent grain size and variable MP abundance, notably a localized lens of higher contamination at 16–18 cm. 167

List of Symbols, Nomenclature, or Abbreviations

ϕ: phi, logarithmic scale for classifying sediment grain sizes. The phi scale is a transformation of the Udden-Wentworth grain size scale and is calculated using the formula $\phi = -\log_2(d)$, where 'd' is the particle diameter in millimeters.

BPA: Bisphenol-A

BS: Back Shore

D: Dune

EDS: Energy-dispersive X-ray spectroscopy

FS: Fore Shore

FTIR: Fourier-Transform Infrared

HDP: High Density Plastic

HT: High Tide

IT: Intertidal

LDP: Low Density Plastic

LT: Low Tide

MDP: Moderate Density Plastic

MP: Microplastic

MP/kg: Microplastic per kilogram

NIR-HIS: Near-Infrared Hyperspectral Imaging

PE: Polyethylene

PET: Polyethylene Terephthalate

POP: Persistent organic pollutant

PP: Polypropylene

PVC: Polyvinyl chloride

Py-GC-MS: Pyrolysis-Gas Chromatography-Mass Spectrometry

QA/QC: Quality assurance and quality control

SEM: Scanning Electron Microscope

SPT: Sodium polytungstate

StL: Strand Line

VHDP: Very-High Density Plastic

VLDP: Very-Low Density Plastic

1. Introduction

Approximately 79–80% of all plastic ever produced ends up in landfills or the natural environment (Geyer et al., 2017). This inefficiency stems from a production trajectory that has grown exponentially since the 1950s and is projected to reach a total of 736 million tonnes by 2040 (OECD, 2024), while global recycling rates remain stagnant at a mere 6–9% (Geyer et al., 2017; Thompson & De Falco, 2020; Kumar et al., 2021; Reddy et al., 2022; Fonseca et al., 2024). The resulting plastic pollution is particularly severe in low- and middle-income countries that often lack sufficient waste management systems, leading to high leakage rates into the environment (Borrelle et al., 2020). However, challenges persist even in regions with advanced recycling programs, which are often hindered by plastic contamination, complex multi-layered product designs, and other design limitations (Hopewell et al., 2009; Andrady, 2011).

Once released, plastic debris becomes a sedimentary particle and, alongside its natural counterparts, can be transported over long distances by air, water, and biotic vectors (Zalasiewicz et al., 2016), thereby increasing its exposure and ecological impact across terrestrial and aquatic systems (Rahman et al., 2023). Mitigating this global issue requires comprehensive strategies, including extended producer responsibility programs, bans on single-use plastics, and investment in recycling infrastructure and technologies, such as chemical recycling (Rahimi & Garciá, 2017; OECD, 2024). As plastic production and waste continue to escalate, understanding the pathways and impacts of plastics in different environments becomes imperative for effective mitigation efforts.

1.1. Definitions

Definitions relating to plastic waste vary significantly across scientific disciplines creating a significant barrier to cross-study comparisons, meta-analyses, and regional assessments (Frias & Nash, 2019; Hartmann et al., 2019). This lack of consensus undermines the reliability of large-scale pollution evaluations and complicates efforts to synthesize findings across geographic and temporal scales (Rochman et al., 2016; Pagter et al., 2018). Given that consensus on terminology is difficult to achieve, and to facilitate cross-disciplinary understanding, this study defined the terminology, measurement units, and classification criteria used to categorize microplastics.

1.1.1. Types of plastic waste

Plastic waste can be broadly categorized into two categories: Primary and secondary plastic. Primary plastic includes microparticles that are intentionally manufactured at small sizes for industrial or commercial use, such as microbeads in personal care products. Secondary plastics, result from the physical, chemical, and biological degradation of larger plastic items, such as packaging, fishing gear, or construction materials (Pieper et al., 2020; Mao et al., 2022). Once released or fragmented, these resulting microplastics persist in the environment for extended periods (Cole et al., 2011; Zhang et al., 2021).

1.1.2. Microplastic size classifications

The literature reveals considerable disparities in both size detection limits and classification schemes for microplastics, resulting in large variations in reported data and making comparisons across studies challenging (Leusch et al., 2023). The term

"microplastics," was first coined by Thompson et al. (2004). Following the first size-based definition of "5 mm and less" proposed at the 2008 "International Research Workshop of the Occurrence, Effects, and Fate of Microplastic Marine Debris," this 5 mm upper boundary has been commonly used (e.g., NOAA 2019; Munari et al., 2017; Tirkey and Upadhyay, 2021; Soursou et al., 2023). However, other researchers and standardization bodies, including ISO 24187, support an upper limit of 1 mm, arguing it better reflects environmental conditions (e.g., Browne et al., 2011; Duncan et al., 2018; Frias and Nash, 2019; Hartmann et al., 2019; Kumar et al., 2021; Jaouani et al., 2022). At the lower end, a boundary of 1 μm is commonly adopted, with smaller particles typically classified as "nanoplastics" (e.g., Frias and Nash, 2019; Pieper et al., 2020; da Silva et al., 2020; Fong et al., 2024). The sorting methods used, such as mesh sizes for filtration or the capabilities of analytical tools including FTIR and Raman spectroscopy, significantly influence the size range that can be reliably analyzed (Sunil et al., 2024; Zhang et al., 2025).

In sedimentology, particle size refers to the intermediate axis, which determines if it can pass through a sieve mesh. As illustrated in Figure 1.1, an upper boundary of 1 mm corresponds to 0 phi (ϕ), the boundary between coarse and very coarse sand in the Udden-Wentworth classification, and the US Standard Sieve size #18. In contrast, 5 mm corresponds to ~ -2.32 ϕ, which lies within the fine pebble classification, and no US Standard Sieve # exists (however, 5 mm meshes are manufactured elsewhere). The lower boundary of 1 μm (10^{-6} m) approximates to +10 ϕ (= 0.9765625 μm), falling within clay fraction of the Udden-Wentworth classification (Udden, 1914; Wentworth, 1922; Blair & McPherson, 1999). Based on these considerations and the recommendations of Hartmann

et al. (2019) and ISO 24187, I have adopted a working definition of microplastics as particles > 1 µm and < 1 mm.

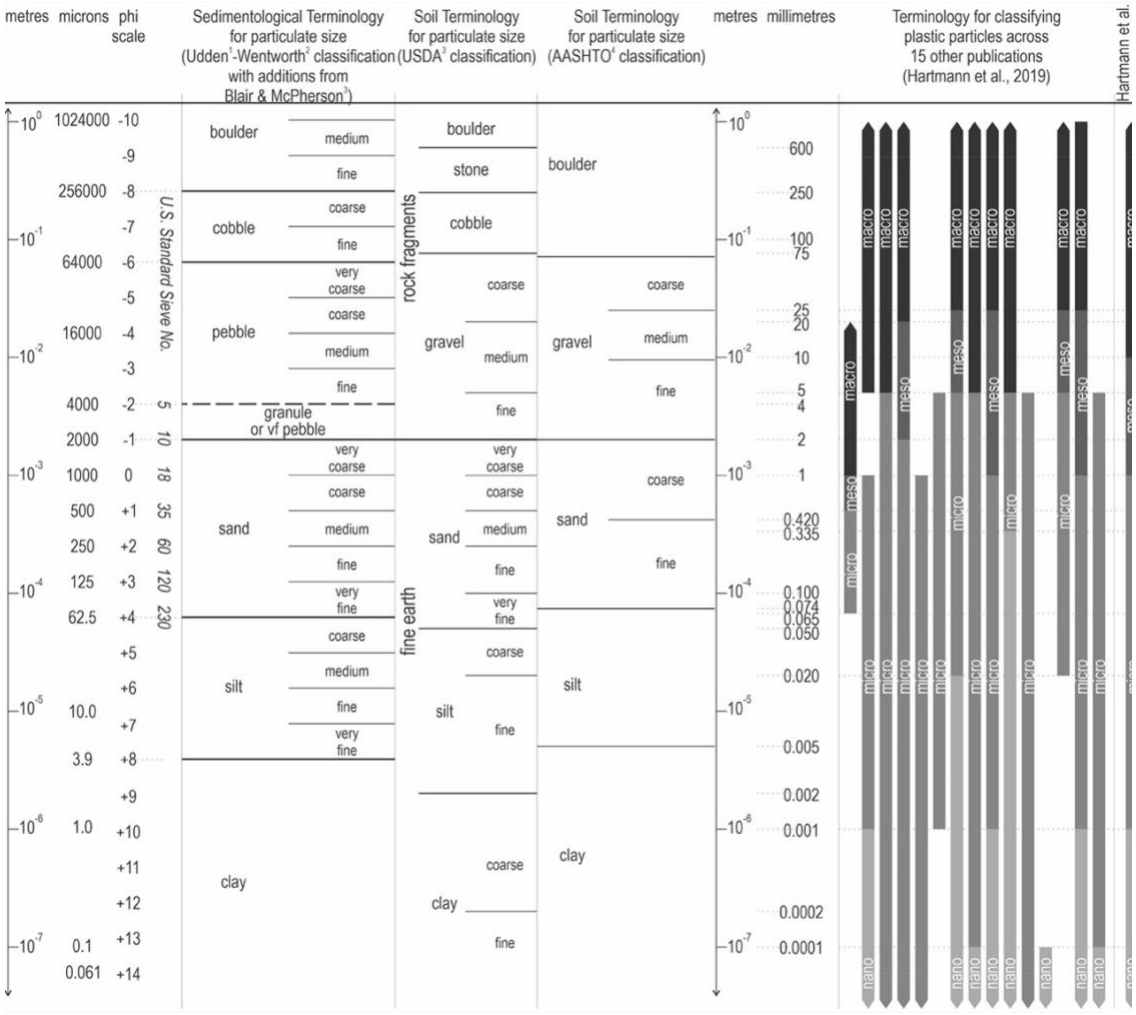

Figure 1.1. Example classifications of particle (sediment) size in the scientific literature and the different boundaries being used to classify different sizes of plastic particles. In sedimentology, a common classification is based on Udden (1914), Wentworth (1922), and Blair & McPherson (1999); in soil science, the scheme of the Soil Survey Staff (1951) in the US Dept. of Agriculture; in engineering, AASHTO, the American Association of State Highway and Transportation Officials (AASHTO) (1997).

1.1.3. Microplastic shape classifications

The original plastic item and its subsequent environmental degradation largely determine the shape of a microplastic particle. The literature contains a wide variety of descriptive terms, such as pellets, fragments, fibres, films, foams, ropes, filaments, sponges and microbeads, but there is no universal standard for classifying these shapes, leading to inconsistencies (Hidalgo-Ruz et al., 2012; Frias & Nash, 2019; Carretero et al., 2021). Furthermore, reliance on visual identification introduces subjectivity and operator bias. Microplastic particles were assigned a shape based on modified criteria from Zingg (1935) (Figure 1.2).

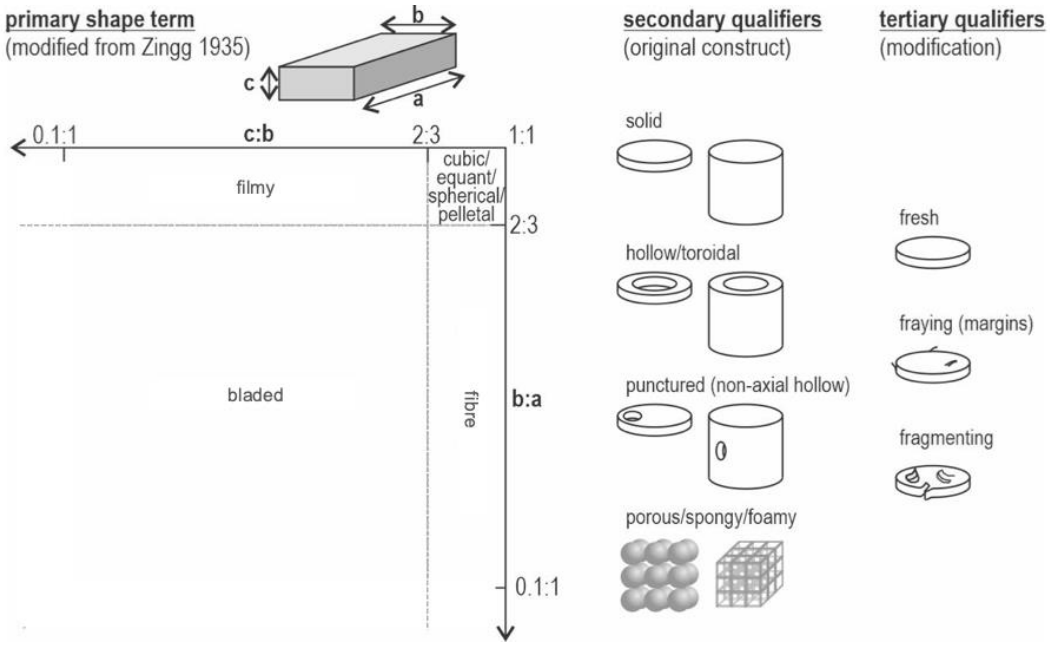

Figure 1.2. Visual representation of shape categories defined by Zingg's three-axis particle geometry (a, b, and c axes).

These shape assignments are determined by the particle's three-dimensional geometry: long (a), intermediate (b), and short (c) dimensions. Because sieving procedures naturally separate particles based on their intermediate axis, this study maintains consistency by using the same dimension for size measurements conducted under microscopy. Where all three dimensions are utilized to define a specific shape, the classification adheres to the standard sedimentological parameters established by Zingg (1935).

Based on the geometric ratios described above, four primary shape categories are used: equant, bladed, prolate, and oblate. Herein, equant particles are synonymous with pellets, bladed particles with fragments, prolate particles with fibres, and oblate particles with films. Also, a fifth shape category is applied to particles composed of "intertwined" fibres, which were not disaggregated to avoid the risk of breakage, which could introduce artificially elevated numbers of microplastics. Secondary qualifiers describe the particle's original structure, such as the presence of holes or pores, while tertiary qualifiers address post-depositional modifications, such as fraying or fragmentation. Unlike some studies, I excluded the term "foam" from the primary shape analysis, including it as a secondary qualifier because it is characterized by a porous, gas-filled structure rather than a distinctive geometry.

These shapes can provide clues about the particle's origins; for instance, fibres are often associated with textiles, films with packaging, and fragments with the mechanical breakdown of larger plastic items (Yang et al., 2021). Surface textures, such as grooves, cracks, adhered particles, and flakes, observed on fragments and pellets further reflect the

mechanical wear and chemical weathering processes that contribute to plastic degradation.

1.1.4. Abundance or concentration units

Plastic pollution is reported using several different units, including counts per unit surface area (e.g., items or microplastics, MP/m^2), total mass, items/counts per unit volume of sediment (e.g., MPs/cm^3), and items/counts per unit dry weight of sediment (e.g., MPs/kg dw). Microplastic pollution was reported as the number of microplastic counts per kilogram of dry sediment (MP/kg). This metric is considered more consistent and reproducible than volume-based measurements, which can be skewed by sediment compaction, or mass-based measurements (mass of the microplastics), which can overemphasize denser polymers. Standardizing results by dry weight facilitates more reliable comparisons across studies and enables data aggregation for meta-analysis (Uddin et al., 2020; Yang et al., 2021).

1.1.5. Compositional and degradation terms

There are ongoing discrepancies in how the term “plastic” is defined compositionally (Hartmann et al., 2019). Some definitions exclude materials such, as elastomers, polymer blends, cellulose acetate (the primary component of cigarette butts), despite their persistence as sources of anthropogenic waste. Notably, the European Chemicals Agency has considered classifying cellulose acetate cigarette filters as single-use plastics (Araújo et al., 2022). Given the diversity of plastic formulations and chemical additives used to enhance their properties, creating a manageable and comparable classification system remains a considerable challenge.

While analytical constraints precluded polymer-specific identification, evaluating the general density ranges and commercial applications of common plastics allows for robust inferences regarding synthetic particle behaviour in clastic sediment systems. Table 1.1 lists the frequently encountered plastic types, their common uses, abbreviations, and recycling codes (e.g., PET, Nylon, PVC), production demand (as of 2019), and reported density ranges from two major sources (Hidalgo-Ruz et al., 2012; SpecialChem SA, accessed February 21st, 2023).

Table 1.1. Plastic types along with their origin (Plastics Europe, 2021), demand in 2019 (Plastics Europe, 2021), and density ranges reported by Hidalgo-Ruz et al. (2012) (density range 1) and SpecialChem SA (density range 2).

Abbreviation {Recycle #}	Common name	Origin (Plastics Europe 2021)	Demand 2019 (Plastics Europe 2021)	Density range (g/mL; Moret-Ferguson et al. 2010)	Density range (specific gravity, Andrady 2011)	Density range (g/mL; Zhang 2020)	Density range (g/cm^3; Hidalgo-Ruz et al 2012, Bellasi et al. 2021)	Density range (g/cm^3; SpecialChem)
PP {5}	PolyPropylene	Food packaging, sweet and snack wrappers, hinged caps, microwave containers, pipes, automotive parts, bank notes, etc., Rope, bottle caps, netting, microbeads	9.87MT	0.85-0.92	0.83-0.85	0.9	0.9-0.91	0.88-0.91 ^up to 1.25
(L)LDPE {4}	(Linear) Low Density PolyEthylene	Reusable bags, trays and containers, agricultural film, food packaging film, etc. six-pack rings, bottles, netting, straws	8.85MT	0.89-0.93	0.91-0.93	0.9-1.0	0.91-0.96	0.91-0.95
HDPE {2}	High Density PolyEthylene	toys, milk/juice bottles, shampoo bottles, pipes, houseware, etc.	6.29MT	0.94-0.97	0.94			0.94-0.97
PVC {3}	PolyVinyl Chloride	Window frames, profiles, floor and wall covering, pipes, cable insulation, hoses, inflatable pools, etc. cups, bottles, fabric	5.09MT	1.16-1.41	1.38	1.4	1.16-1.58	1.15-1.70
PU (TPE)	PolyUrethane (Thermoplastic elastomers)	Building insulation, pillows and mattresses, insulating foams for fridges, etc plastic pellets	4.01MT				1.2	
PET {1}	PolyEthylene Terephthalate (Polyester)	Bottles for water, soft drinks, juices, cleaners, etc. plastic pellets	3.99MT	1.38-1.41	1.37	1.4-1.6	1.37-1.45	1.30-1.40 ^up to 1.6

Table 1.1. (continued)

Abbreviation {Recycle #}	Common name	Origin (Plastics Europe 2021)	Demand 2019 (Plastics Europe 2021)	Density range (g/mL; Moret-Ferguson et al. 2010)	Density range (specific gravity, Andrady 2011)	Density range (g/mL; Zhang 2020)	Density range (g/cm^3; Hidalgo-Ruz et al 2012, Bellasi et al. 2021)	Density range (g/cm^3; SpecialChem)
PS {6}	PolyStyrene	Food packaging (dairy, fishery), building insulation, electrical & electronic equipment, inner liner for fridges, eyeglasses frames, etc. utensils	1.58MT	1.04-1.08	1.05	1.05	1.04-1.1	1.04-1.05 ^up to 1.25
(F)(E) PS	(Foamed) (Expanded) PolyStyrene	As above; Floats, bait boxes, foam cups	1.54MT		Not given			
PA	PolyAmide (Nylon)	Netting, traps, fabric	1.02MT	1.15	Not given		1.02-1.05	1.01–1.19 ^up to 1.60
ABS/SAN	Acrylonitrile Butadiene Styrene/ Styrene-AcryloNitrile copolymer	Pipe, automobile, thermal insulation	0.97MT					1.00-1.20 ^up to 1.40
PC	Polycarbonate	Glass alternative, barriers	0.77MT					1.15-1.20 ^up to 1.60
PMMA	PolyMethyl MethAcrylate	Glass alternative, touchscreens	0.26MT					1.17-1.25
e.g.	(Other thermoplastic)		(2.7MT)					
PBT	Polybutylene Terephthalate	Domestic heaters, electric insulation	--					1.30-1.40 ^up to 1.60
PLA	PolyLactic Acid	Films, bottles, biodegradable med-devices	--					1.23-1.26
PTFE	PolyTetroFlouroEthylene	Containers, pipe, airplane wings, cookware	--					2.10-2.20 ^up to 2.30
PAI	PolyAmide-Imide	Wire coating, valves	--					1.40-1.50 ^up to 1.60
CA	Cellulose Acetate	Cigarette filters	--		Not given			1.22-1.34
e.g.	(Other plastics)		(3.8MT)					
PF	Phenol Formaldehyde (Bakelite, formica)	Wire coating, sockets, jewelry, kitchenware, car parts, toilet seats	--					
	vulcanized rubber	Tires, seat belts, toys, hoses	--					

Table 1.2. Density range of plastic particles in groups of < 1.0 g/cm^3, < 1.00 – 1.18, g/cm^3, < 1.18 – 1.30 g/cm^3, < 1.30 – 1.50 g/cm^3, > 1.50 g/cm^3. Plastic types in black are the baseline-defined density of the resin. Those in grey italics are resins with an increased density compared to their baseline defined density in black, due to the addition of compounds such as flame retardants, elasticizers, lubricants, etc. Numbers in brackets correspond to their recycling number.

	Density range of plastic particles				
	<1.0 g/cm^3	<1.18 g/cm^3	<1.3 g/cm^3	<1.5 g/cm^3	>1.5 g/cm^3
Plastic	HDPE {2} LDPE {4} PP {5}	PS {6} PC {7} PMMA {7} PA {PA} ABS/SAN {ABS} *PP {5}*	PET {1} TPE {7} PMMA {7} PC {7} *PP {5}* *PS {6}* *PS {7}* *PA {PA}* *ABS/SAN {ABS}*	*PET {1}* *PS {6}* *PC {7}* *PA {PA}* *ABS/SAN {ABS}*	*PET {1}* *PC {7}* *PA {PA}*

To aid interpretation, the data in Table 1.1 are further condensed into Table 1.2, which organizes plastic types into five groups based on their density: < 1 g/cm^3 (Very Low-Density Plastic, VLDP), 1.00 to 1.18 g/cm^3 (Low Density Plastic, LDP), 1.18 to 1.30 g/cm^3 (Moderate Density Plastic, MDP), 1.30 to 1.50 g/cm^3 (High Density Plastic, HDP), and > 1.50 g/cm^3 (Very High Density Plastic, VHDP). Most widely used polymers fall within the lower density ranges (< 1.30 g/cm^3), which increases their likelihood of remaining buoyant in aquatic systems.

1.2. Environmental impact of waste plastic

Once plastic waste enters the environment, it becomes a persistent contaminant, subject to a complex interplay of physical, chemical, and biological processes that determine its transport, fate, and ecological impact.

1.2.1. Plastic degradation and additive leaching

In the natural environment, plastics undergo a slow process of degradation and fragmentation. Physical degradation begins by mechanical abrasion with other sedimentary particles from forces such as wind and wave action, which breaks larger items into smaller pieces including microplastics (Johannessen & Shetranjiwalla, 2021; Zhang et al., 2021; Rezaie & Forghani, 2022). This process is accelerated by photodegradation, where ultraviolet (UV) radiation from sunlight makes the plastic brittle, and by chemical degradation processes, including oxidation (Rezaie & Forghani, 2022; Jarosz et al., 2024; Lv et al., 2024). Over time, microorganisms such as bacteria and fungi can colonize plastic surfaces, further breaking them down into microplastics and nanoplastics through enzymatic activity (Scaria et al., 2023; Sharma & Vuppu, 2023; Lv et al., 2024; Pal et al., 2024).

A significant chemical risk arises from additives, such as plasticizers, flame retardants, stabilizers, and lubricants, incorporated during manufacturing (Hahladakis et al., 2018). These compounds are often not chemical bonded to the polymer and can leach into the environment as the plastic degrades. The leaching is influenced by environmental factors, such as temperature and pH, and is amplified in particles with high surface area-to-volume ratios, including the filmy particles (Obuzor & Onyedikachi, 2023; Pohl & Bodzek, 2023; Li et al., 2024). A primary example of this behavior involves phthalates; a class of plasticizers commonly used in PVC to increase flexibility. Research has documented that phthalates can rapidly migrate out of the polymer matrix, particularly under elevated temperatures or in acidic and alkaline environments (Kodavanti & Loganathan, 2016). In high-surface-area microplastics, this leaching is markedly faster

compared to larger, denser fragments, leading to higher concentrations of these compounds in surrounding water systems. Once released, many of these additives, including phthalates, exhibit potent endocrine-disrupting properties and contribute substantially to the overall toxicological risk profile of plastic pollution (Kodavanti & Loganathan, 2016; Tyler et al., 2019)

1.2.2. Transport and deposition in sedimentary systems

The transport, distribution, and deposition of microplastics is governed by a complex interplay between particle-specific properties, hydrodynamic forces, and sedimentary characteristics. Density is a primary factor. Denser polymers such as polyvinyl chloride (PVC) and polyethylene terephthalate (PET) tend to sink and accumulate in depositional areas, behaving akin to mineral grains. In contrast, low-density plastics such as polyethylene (PE) and polypropylene (PP) are buoyant and can remain suspended in the water column or be transported long distances on the surface before being washed ashore (Li et al., 2020). Particle size and shape also influence transport, with smaller, irregularly shaped particles being more prone to prolonged suspension (Zhang, 2017; Ho & Not, 2019).

In coastal environments, tidal currents, wave dynamics, and wind are the primary mechanisms for mobilizing microplastics, particularly in estuarine systems where bidirectional flow enhances both vertical mixing and horizontal redistribution (Jiang et al., 2024; Pasquier et al., 2024; Shen & Worrell, 2024). Wind-driven surface transport processes, such as Ekman drift, Stokes drift, and windage, contribute to the lateral movement of the buoyant low-density plastics, including PE and PP (Zhang, 2017; Ho & Not, 2019). Storm events represent an episodic but powerful driver of microplastic

remobilization. These events can intensify bed disturbance, cause shoreline erosion, and resuspend buried particles. For instance, microplastic levels in Galveston Bay, Texas, were significantly elevated following Hurricane Harvey due to these hydrodynamic disruptions (Summers et al., 2024). Such findings underscore the vulnerability of coastal systems to sudden shifts in microplastic abundance and vertical distribution during high-energy conditions.

The local geology dictates how well microplastics are retained, as the structure and grain size of sediments also influence the accumulation and retention of microplastics. Finer-grained substrates, such as silts and clays, show greater microplastic retention due to their cohesive properties and smaller pore spaces (Adjornor et al., 2024; Furlan et al., 2024). Vegetated coastal environments, such as mangrove systems, can also facilitate burial and reduce resuspension through root entanglement and sediment trapping (Xu et al., 2023).

Biofouling, the colonization of particles by microorganisms, alters the surface properties and effective density of plastics, potentially causing even buoyant particles to sink (Raimundo et al., 2020; Li et al., 2023). Filter-feeding organisms can ingest microplastics and excrete them in dense fecal pellets, which enhances their deposition in benthic zones (Raimundo et al., 2020; Ahmed Dar et al., 2024). Finally, bioturbation by burrowing invertebrates facilitates the burial of microplastics, reworking them into deeper sediment layers and promoting long-term retention within the geologic record (Raimundo et al., 2020).

1.2.3. Ecological and human health effects

Microplastics are a pervasive pollutant across nearly all ecosystems, impacting ecosystem functions, wildlife, and human health. They degrade habitat quality in sensitive environments, including mangroves and coral reefs, disrupt nutrient cycling, and have been found in virtually all studied vertebrate and invertebrate species (Walther & Bergmann, 2022; Koh et al., 2023; Tuuri & Leterme, 2023; Garcês & Pires, 2024). For wildlife, the consequences are severe: ingestion of plastic mistaken for food leads to starvation and internal injuries, while entanglement in bags and discarded fishing gear often results in suffocation, internal injuries, limb loss, and death (Rahman et al., 2023; Tuuri & Leterme, 2023; Garcês & Pires, 2024). Some bird species have been observed incorporating plastic materials into their nests, inadvertently causing entanglement and fatal injuries in nestlings (Garcês & Pires, 2024). Beyond direct physical harm, microplastics act as vectors, transporting invasive species, pathogens, and adsorbed environmental toxins, such as persistent organic pollutants (POPs) and heavy metals (Courtene-Jones et al., 2022; Mondal et al., 2023; Pan & Umapathy, 2024).

The chemical risks associated with microplastics extend directly to human health. Additives used in plastic manufacturing, such as bisphenol A (BPA) and phthalates, and brominated flame retardants, are of particular concern, as they are known endocrine disruptors linked to thyroid dysfunction, neurodevelopmental impacts, and reproductive harm (Kodavanti & Loganathan, 2016; Tyler et al., 2019). Human exposure occurs through the ingestion of contaminated food and water, as well as inhalation, and is increasingly associated with immunotoxicity and chronic endocrine disruption (Rahman et al., 2023; Yu & Singh, 2023; Habumugisha et al., 2024). The physiological threat is

further compounded by particle size; microplastics as small as 1 μm possess the bioavailability to cross critical biological membranes, including the blood–brain barrier and the placenta. This suggests that the presence of these particles in the human body may have profound, long-term impacts on neurological function and fetal development (Fong et al., 2024).

1.2.4. Broader environmental and economic impacts

Plastic pollution drives widespread habitat degradation in both marine and terrestrial ecosystems. In coral reefs, plastic waste smothers corals and sponges, obstructing essential light and oxygen exchange, which leads to decreased photosynthetic activity and increased coral mortality (Rahman et al., 2023). In soil systems, microplastics interfere with key biological processes by negatively impacting decomposer communities such as nematodes and microarthropods, which are critical for nutrient cycling and organic matter breakdown (Garcês & Pires, 2024). These disruptions cascade through ecosystems and may ultimately result in declines in biodiversity, altered food web dynamics, and reduced ecosystem resilience. Moreover, the persistence and mobility of microplastics contribute to their spread into previously unaffected regions, exacerbating environmental stress in already vulnerable systems.

The consequences of plastic pollution extend into the socioeconomic sphere. Coastal tourism and fisheries often suffer economic losses due to polluted shorelines and degraded habitats. Aesthetic degradation leads to reduced tourist appeal, while cleanup operations strain municipal budgets (Thushari & Senevirathna, 2020; Rahman et al., 2023). Plastic waste in the ocean can also damage marine vessels and fishing gear, resulting in increased operational costs and safety hazards for maritime industries. On a

broader scale, the incineration and degradation of plastic waste contribute to greenhouse gas emissions. As plastics decompose, especially under ultraviolet (UV) radiation, they release methane, ethylene, and other greenhouse gases that contribute to climate change (Rahman et al., 2023). These emissions further complicate global efforts to limit warming and reduce the environmental footprint of human activities.

1.3. Research rationale

The preceding sections have outlined the global scope, persistence, and environmental complexity of plastic pollution, with particular emphasis on the diverse characteristics and behaviours of microplastics. These particles are increasingly recognized as persistent sedimentary contaminants whose fate is influenced by a suite of interacting factors, including particle density and shape, tidal currents, sediment type, and biological processes such as ingestion and bioturbation. Microplastics also pose chemical risks due to the leaching of additives and their potential to transport other pollutants, raising concerns not only for ecological integrity but also for human health.

Despite this growing body of research, knowledge gaps remain, particularly in sediment-dominated, conservation-sensitive coastal ecosystems. Protected areas with fine-grained intertidal zones and dynamic tidal regimes are often critical habitats for migratory species and provide essential ecosystem services. Yet, few studies have quantified microplastic abundance or characterized the types of plastics present within their sediments. The baseline data gathered here addressed a portion of this research gap by establishing an initial assessment of microplastic contamination within the beach sediments of Mary's Point, situated inside the Shepody National Wildlife Area of the upper Bay of Fundy, New Brunswick. Using sediment cores collected across two field

seasons (2022 and 2024), this work contributes new insights into microplastic transport and retention in a high-energy, ecologically protected setting. Introducing a multi-step, low-cost, environmentally sensitive extraction method designed to recover particles across a broad density spectrum will hopefully aid in subsequent research and comparison of other beach ecosystems around the world.

Chapter 2 reviews the current state of microplastic research in coastal sediments, examining key methodologies, sampling strategies, and classification systems. This synthesis lays the foundation for the analytical approach adopted in the present study. Chapters 3 to 6 describe the Mary's Point case study, outlining the site context, field sampling, and multi-step extraction methods, followed by results on spatial and temporal microplastic patterns, contamination pathways, and their comparison to global trends.

2. Research Review of Microplastics in Beach Sediment

The present chapter provides a review of existing research on microplastic pollution in beach sediments. It includes an overview of foundational studies, recent research trends, and the global distribution of sampling efforts, with a particular focus on gaps in protected and remote coastlines. The chapter also examines the methodological landscape that has shaped current understanding of beach microplastic pollution, spanning sample collection, extraction procedures, particle identification, and the persistent challenge of cross-study comparability.

2.1. Overview of previous research

Concern over microplastic pollution in coastal marine sediments is growing, as beaches act as both sinks and transport zones for plastic debris (Ho & Not, 2019). Numerous international studies (see Appendix D, Table D1) document the prevalence, abundance, and composition of microplastics; however, they differ widely in analytical scope, sampling depth, and geographic coverage, which limits meaningful comparisons.

2.1.1. Foundational research

The evolution of microplastic science has transitioned from early, isolated observations of synthetic debris to a multi-disciplinary field focused on detailed experimental work and global modelling. However, as the discipline has grown, it has been characterized by a persistent lack of universal standardization in sampling, extraction, and classification. Collectively, the studies discussed below form the backbone of contemporary research, categorized here by their primary contributions to the understanding of global dispersion, methodological development, and systemic risk.

The earliest contributions to the field established that synthetic debris was globally dispersed and bioavailable decades before "microplastic" became a formal scientific term. One of the earliest published accounts came from Kenyon and Kridler (1969), who documented plastic ingestion in Laysan albatross chicks from Southeast Island (Pearl and Hermes Reef) in the Hawaiian Islands National Wildlife Refuge. Their analysis of stomach contents revealed a variety of debris, including fragments, caps, and pellets, proving that plastic was already reaching remote Pacific regions. This global dispersion was further confirmed by Rothstein (1973), who reported plastic ingestion by Leach's Storm-Petrels (*Oceanodroma leucorhoa*) collected as early as the 1960s from colonies in Newfoundland and New Brunswick, Canada. During the same period, researchers identifying floating particles in marine surface waters such as Carpenter and Smith (1972) in the Sargasso Sea and Colton et al. (1974) in the northwestern Atlantic provided evidence of widespread contamination. Cundell (1974) also identified plastic accumulation in the sediments of Narragansett Bay, New England, documenting the entry of these materials into benthic environments. Because these studies predated formal classification schemes, they relied on *ad hoc* descriptors and lacked size-based definitions, illustrating an early and enduring challenge in the field: the lack of a cohesive, standardized framework for describing synthetic particles.

A pivotal shift in the field's nomenclature occurred with Thompson et al. (2004), who officially introduced the term "microplastics" based on the discovery of ~20 µm sized particles in sediments. Beyond the name, Thompson et al. (2004) expanded the spatial scope of the problem by documenting microplastics embedded within benthic substrates across multiple sedimentary environments in the United Kingdom. The

authors proposed that most microplastics originate from the fragmentation of larger debris, a key assumption that remains central to degradation models today. As research intensified, the focus shifted toward developing replicable extraction methods, though true standardization remained elusive. Claessens et al. (2011) provided one of the first quantitative assessments of abundance in coastal environments by applying NaCl-based flotation and stereomicroscopic sorting. Their stepwise, low-cost procedure offered a practical baseline for early beach sediment surveys, yet it also highlighted the limitations of using a single density solution for diverse polymer types. This fragmentation of methods was formally addressed by Hidalgo-Ruz et al. (2012), whose comprehensive review of sampling and extraction techniques revealed significant variation in mesh sizes and sampling depths across the literature. Rather than solving the issue of consistency, their work exposed the subjectivity and operator bias that remains a primary hurdle in comparing global datasets.

Beyond physical presence, foundational research has worked to define microplastics as complex chemical and biological stressors. Cole et al. (2011) integrated the field of toxicology into microplastic science by reviewing both primary and secondary microplastics as vectors for sublethal toxicity and endocrine disruption. This theoretical framework was empirically substantiated by Browne et al. (2011), who demonstrated in a controlled laboratory setting that microplastic ingestion in sediment-dwelling lugworms (*Arenicola marina*) directly impaired energy reserves and facilitated the transfer of hydrophobic organic contaminants into benthic food webs. This moved the academic discussion from speculation regarding bioavailability to measurable biological outcomes. Jambeck et al. (2015) introduced a global systems perspective by

quantifying annual ocean-bound inputs, prompting a shift toward land-based waste management policy. By modeling that approximately 8 million metric tonnes of plastic waste enter the world's oceans each year, they identified inadequate infrastructure as the primary driver of leakage. This study transformed microplastic pollution from a localized marine issue into a systemic outcome of global consumption. However, the sheer scale of these models continues to underscore the need for more refined, standardized classification methods, as global estimates remain dependent on localized data collected through often incomparable methods.

2.1.2. Recent research trends

Over the past decade, research on microplastics in beach sediments has grown significantly and shifted from exploratory surveys to more targeted investigations of spatial and temporal variability. Since 2011, there have been over 200 published studies investigating the presence of microplastics in beach sediment using density extraction methods (Appendix D, Table D1). As shown in Table 2.1, there is a stark lack of methodological uniformity in the solutions used for these extractions. While NaCl remains the most frequently cited solution (n = 112), likely due to its low cost and accessibility, its lower density (1.2 g/cm^3) may result in the underreporting of denser polymers compared to more specialized solutions, including sodium tungstate ($Na_6O_{41}W_{12}$), which appears in 49 unique studies. This reliance on varying extraction media underscores the ongoing challenges in comparing results across different regional studies and reinforces the need for standardized classification approaches, as discussed in the present chapter.

Table 2.1. Published microplastic studies on beaches using a density extraction method between 2011 and 2024. See Appendix D, Table D1 for a complete list of studies.

Extracting Solution	**# mentions (in unique studies)**	**Reference(s)**
NaCl	112	Claessens et al. (2011)
CsCl	1	Dodson et al. (2020)
$CaCl_2$	6	Li et al. (2018)
NaH_2PO_4	1	Zhang et al. (2020)
$Na_6O_{39}W_6 \cdot H_2O$	2	Lenz et al. (2023) Llyod-Jones et al. (2023)
KI	2	Abayomi et al (2017) Aslam et al. (2020)
NaI	11	van Cauwenberghe et al. (2013)
$ZnCl_2$	55	Liebezeit & Dubaish (2012)
Na_2WO_4	2	Ballent et al. (2016)
Oil	2	Paradinas et al. (2021)

Recent work has expanded beyond presence/absence data to investigate how local sediment texture, shoreline slope, and adjacent land use influence the deposition of microplastics. Of note, Godoy et al. (2020) highlighted the role of geomorphological characteristics, such as beach slope and grain size, in shaping microplastic accumulation along Spain's coastline, finding that gentler, shallower slopes and finer sediments tend to promote greater microplastic retention.

Flores-Cortés et al. (2022) examined the composition and distribution of microplastics on Tecolutla Beach in the Gulf of Mexico, demonstrating how coastal form and wave dynamics influenced the retention of pellets, films, and fragments, with sheltered embayments accumulating more microplastics than exposed ones.

Sediment texture and shoreline geometry have emerged as primary controls on particle distribution. For instance, grain size variability and beach slope were found to be decisive factors in microplastic exposure levels along the Uruguayan coast, where finer

sediments and shallower profiles promoted greater retention (Vermeiren et al., 2021). This is consistent with findings from the Gulf of Mexico, where coastal form and wave dynamics specifically influenced the spatial sorting of different microplastic shapes; sheltered embayments at Tecolutla Beach were found to accumulate significantly higher concentrations of pellets, films, and fragments compared to exposed, high-energy stretches of the same coastline (Flores-Cortés et al., 2022).

The interplay between coastal energy and terrestrial inputs further complicates these accumulation patterns. In many North Atlantic and South American coastal systems, the presence of low-energy, embayed morphology acts as a trap for debris, a process often amplified by proximity to urban infrastructure. For example, research in Portugal and Uruguay has documented that sheltered "pocket" beaches adjacent to urbanized watersheds and stormwater outfalls receive disproportionately high loads of microplastics compared to rural or high-energy coastlines (Vermeiren et al., 2021; Godoy et al., 2023). These findings are of particular relevance to the study of Mary's Point; while the site is largely rural, its status as a high-energy, macrotidal environment in the Bay of Fundy provides a necessary contrast to the low-energy, urban-dominated sites that currently characterize much of the literature.

Researchers are now paying greater attention to the vertical and horizontal distribution of microplastics within beach profiles. Beyond surface sampling, recent studies have begun to explore stratigraphic variability. Lefebvre et al. (2021) conducted monthly sampling in Arcachon Bay, France, showing that samples at the high tide line typically contained more microplastics due to enhanced exposure to wind, waves, and litter deposition, compared to lower down the beach. Similarly, Machendiranathan et al.

(2022) examined vertical profiles up to 30 cm deep in Donghai Island, China, and found substantial variability across layers, with synthetic fibres dominating at all depths.

Several recent studies have also highlighted that microplastic concentrations vary substantially between seasons, often in response to rainfall events, monsoonal patterns, and beach usage cycles. Monsoon flooding and runoff were associated with elevated microplastic inputs and redistribution in coastal Kerala, India (Kumar & Varghese, 2021) and Mumbai, India (Dutta et al., 2022; Arjun et al., 2024). Similarly, Arjun et al. (2024) reported higher microplastic concentrations during the monsoon season in Mumbai. On the other hand, Tasnim et al. (2023) observed significantly higher microplastic concentrations in winter compared to the monsoon season on Bangladeshi beaches, likely due to reduced dilution and increased retention during the dry season.

In addition to seasonal and hydrological influences, extreme weather events, such as hurricanes and typhoons, have also been shown to alter the distribution of microplastics significantly. Following Hurricane Harvey, microplastic concentrations in Galveston Bay, Texas, increased fivefold, mainly due to enhanced surface loading and the resuspension of bed-stored particles (Zhang et al., 2021). Further work on the aftermath of Hurricane Harvey later confirmed these findings on the resuspension of bed-stored particles (Summers et al., 2024). Similarly, Typhoon Mangkhut led to an 11-fold increase in macro-debris and a substantial rise in microplastic density along South China's beaches, indicating the decisive role of storm-driven over wash in mobilizing plastics across coastal systems (Liu et al., 2022). When Hurricane Larry hit Newfoundland in 2021, researchers found a significant increase in microplastic deposition during the peak of the storm (Ryan et al., 2023). After the storm passed,

deposition levels decreased considerably from this peak. Still, they did not immediately return to the lowest pre-storm values, remaining somewhat elevated for a period following the event.

The influences of human activity on microplastic loading have also emerged as a significant focus. Numerous studies have documented the strong correlations between increased beach tourism intensity and urban development, and increased microplastic concentration. Luo et al. (2022) attributed high microplastic abundances in Qingdao, China, to the proximity of aquaculture facilities, harbours, and sewage discharge points, while Dutta et al. (2022) reported higher microplastic concentrations along heavily trafficked beaches in Mumbai, India. Similarly, Gao et al. (2023) found significantly higher microplastic levels on resort beaches in China compared to less frequently used rural sites. Gül (2024) identified spatial and vertical variability in Turkish Black Sea beaches, driven in part by seasonal tourist activity and shifting sediment dynamics.

Wastewater discharge has been increasingly recognized as a significant pathway for microplastic contamination, particularly through the release of synthetic microfibres. An early study by Browne et al. (2011) detected fibres of polyester and acrylic in marine sediments and suggested they originate from domestic discharge. This pathway was later confirmed by multiple studies; for instance, Leslie et al. (2017) and Doucet et al. (2021) both report that wastewater treatment plants (WWTPs) serve as point sources for microplastic pollution, discharging fibres into both freshwater and marine systems even after partial filtration. De Falco et al. (2019) quantified microplastic loads in washing machine discharge and demonstrated that substantial fibre release occurs during standard laundering of synthetic garments. Extending this understanding, Volgare et al. (2021)

showed that the type of detergent used can significantly affect the rate of fibre release during laundering, suggesting that both consumer behaviour and treatment technology shape the extent of grey-water-derived pollution.

2.1.3. Global coverage and disparities

Although microplastic pollution is a global concern, researchers concentrate their efforts in specific regions, typically where monitoring programs and research infrastructure are already well-established. This uneven distribution reflects disparities in scientific funding, institutional capacity, and long-term environmental datasets (Strady et al., 2021; Simon-Sánchez et al., 2022; Dahms & Greenfield, 2024). These factors complicate both regional and global synthesis efforts, as inconsistencies in sampling intensity, methodology, and data accessibility limit the comparability of results across coastal systems (Strady et al., 2021; Simon-Sánchez et al., 2022). Identifying areas of overrepresentation, as well as regions where data are critically lacking, remains essential for guiding future research, refining global monitoring frameworks, and ensuring that geographically diverse datasets inform mitigation strategies.

Europe and Asia have seen the highest research activity, though the scope and standardization of studies differ markedly between them. In Europe, coordinated efforts have enabled large-scale transboundary assessments. A notable example is Lots et al. (2017), which examined 23 beaches across 13 countries using harmonized sampling protocols and citizen science to enable cross-border comparisons at the continental scale. Asia, by contrast, exhibits high research output concentrated in rapidly urbanizing or industrialized coastal zones, though with more variation in methodology and scope. Across South and Southeast Asia, studies have linked microplastic abundance to

population density, land use, and variations in infrastructure. Strady et al. (2021) reported elevated microplastic concentrations across both urban and rural sampling sites relative to less-impacted sites, including rural reservoirs and certain bays (e.g. Red River, Vietnam), emphasizing the importance of context-specific methodological adaptations in lower-resource settings. Similarly, Arjun et al. (2024) found a positive correlation between increasing coastal population density and increasing microplastic abundance in beach sediments, with the highest loads recorded adjacent to densely populated fishing villages, harbour areas, and urbanized tourism hubs, and lower abundances at sparsely populated, less-developed rural beaches. Their survey of 25 beaches along India's Kerala coast highlighted that fishing-related land use – including boat landing sites and net-drying areas – persistently contributed high proportions of nylon fibres, while tourism-oriented land use (resorts, recreational beaches) and religious congregation sites were associated with a more diverse mix of fibres, fragments, and films. In contrast, beaches adjoining predominantly natural or low-intensity agricultural hinterlands exhibited comparatively low particle counts.

Research across South America and Africa remain sparse and patchy, with few long-term datasets and limited replication. Exceptions include Argentine beaches, where Ronda et al. (2023) found a positive correlation between increased tourism intensity and increased microplastic abundance. Recent studies have begun targeting hard-to-access locations, including remote Pacific islands and polar coastlines, to more accurately represent global transport dynamics. Antarctic beach sediments near the Mario Zucchelli research station provide further evidence of microplastics' dispersal and long-range transport potential, as Munari et al. (2017) detected synthetic fibres and fragments in a

remote, sparsely populated area with no significant local plastic sources, indicating deposition via ocean currents, sea ice rafting, and atmospheric fallout. Likewise, in the South Pacific, Mylius et al. (2023) documented microplastic contamination in beach sediments from the Solomon Islands and Vanuatu, two nations with minimal local plastic production, suggesting that long-range marine transport is a dominant source.

Despite recent advances, substantial blind spots remain in global datasets. African shorelines, Arctic coastlines, and many small islands continue to receive minimal research attention, primarily due to limited access to field equipment, laboratory facilities, and analytical infrastructure (Walther & Bergmann, 2022; Dahms & Greenfield, 2024). As long as these barriers persist, many low-income or geographically isolated regions remain excluded from global synthesis efforts. Bridging these gaps will require the adoption of standardized, low-cost extraction protocols, long-term international collaboration, and investment in regional research capacity. As the field advances, ensuring more equitable geographic coverage will be crucial for producing assessments that are globally representative and capable of supporting localized mitigation strategies.

2.1.4. Research on environmentally sensitive beaches

Although beach microplastic pollution has received variable attention globally, protected coastal environments – including National Wildlife Areas and Ramsar wetland sites – also remain substantially underrepresented in the literature. Where such studies do exist, findings consistently demonstrate that the designation of an environmentally protective status does not equate to immunity from plastic pollution. For instance, Antarctic Specially Protected Areas exhibit low but detectable levels of microplastics,

likely resulting from long-range transport and deposition in high-energy environments (de Miranda et al., 2023). The Xuwen Coral Reef Reserve in China and Can Gio Biosphere Reserve in Vietnam both report notable microplastic concentrations, especially of persistent fibres and PE fragments (Nhon et al., 2022; Machendiranathan et al., 2025). In Sri Lanka, the accumulation of microplastics in Bundala and Hikkaduwa Marine National Parks poses risks to sea turtle nesting and coral reef systems (Sevwandi et al., 2021).

Meanwhile, studies in Colombian and Irish conservation zones report notable pollution despite their protected status (Ordóñez, 2022; Kneel et al., 2024). Canadian sites remain vastly underrepresented in the published literature. Most Canadian studies to date have focused on urban or industrialized freshwater systems, particularly the Great Lakes region (Corcoran et al., 2015; Ballent et al., 2016), with limited research on coastal sediments. In 1992, the protected Sable Island (Nova Scotia, Canada) was surveyed for persistent macro-litter, as the Island is a National Park Reserve with limited access (Lucas, 1992). Very few published studies have investigated microplastic contamination in ecologically protected or remote coastal zones such as Alava et al. (2021) at Cowichan-Koksilah Estuary, Noël et al. (2022) along the British Columbia coast, and Morra (2021) in Clayoquot Sound and Orchid Lake. Notable gaps exist along the Atlantic coast, including the Bay of Fundy region. Apart from an unpublished MSc thesis that sampled in Fundy National Park (Forsythe, 2016), no sediment-focused microplastic studies have been conducted in protected zones. This lack of baseline data limits our understanding of plastic pollution within Canada's protected coastal zones,

hindering the assessment of potential impacts on habitat quality, sediment dynamics, and ecosystem function.

2.2. Overview of sampling methods

Reliable assessments of microplastic pollution in beach sediments depend on consistent and well-documented sampling techniques. This section reviews commonly employed sampling strategies, locations, and depth intervals used in recent studies, underscoring how the lack of methodological consistency, added to the lack of consistency of terminology discussed in Chapter 1.1, continues to limit reliable comparisons across regions and studies.

2.2.1. Sampling strategies

The different sampling strategies are typically classified into three primary categories: selective, volume-reduced, and bulk (Zobkov & Esiukova, 2018). Selective sampling involves visually identifying and manually collecting plastic debris on the sediment surface. This two-dimensional visual approach is effective for capturing larger or brightly coloured particles visually distinct from the surrounding substrate. However, it does not account for microplastics embedded in the sediment column, and therefore risks underrepresenting small, transparent, or buried particles not visible from above.

Volume-reduced sampling uses tools such as sieves or scoops with standardized dimensions to constrain the amount of sediment being extracted. This reduction facilitates more efficient processing but introduces potential bias when sieve sizes, scoop dimensions, or collection angles vary, even slightly, between sites or operators (Zobkov & Esiukova, 2018).

Bulk sampling involves initially collecting entire sediment volumes from defined areas, typically using shovels, trowels, or corers. As with volume-reduced methods, samples are often extracted to shallow depths (e.g. up to 5 cm) to represent surface-layer contamination. While this method enables a more representative assessment of total microplastic content, it requires substantial laboratory processing to separate plastics from the sediment matrix. Volume-reduced methods are often employed after bulk sample collection to reduce the amount and/or remove the sediment matrix from the samples.

2.2.2. Sampling zones

Most studies focus on the high tide, or strandline – the area of the beach where floating debris is deposited at the peak of the tidal cycle – as it is typically the zone with the highest concentration of microplastics (e.g., Browne et al., 2011; Turra et al., 2014). Some expand sampling to include mid- and low-intertidal zones or perpendicular transects (e.g., Jones et al., 2022; Ronda et al., 2023) across the beach profile to capture spatial variation. However, few explicitly account for the dynamic environmental conditions during sampling, such the tidal cycle and beach morphology, which can significantly influence microplastic distribution (Zhang et al., 2021).

The timing of sampling relative to the lunar tidal cycle is an important but often overlooked variable. Sampling during or after a spring tide, when the tidal range is at its maximum, will capture deposition at the highest point on the beach profile. In contrast, sampling during a neap tide, when the tidal range is minimal, will reflect deposition in a lower, more frequently reworked zone. This variation in the vertical extent of wave influence means that the location and concentration of the primary debris line can shift

significantly, impacting the comparability of studies conducted at different times in the lunar cycle (Godoy et al., 2020; Vermeiren et al., 2021).

Furthermore, beach morphology and sediment type fundamentally control how microplastics are retained or transported (Godoy et al., 2020; Vermeiren et al., 2021). Flatter, more sheltered environments, such as those behind coastal barriers or within protected embayments tend to trap more particles and act as microplastic sinks, whereas steeper, high-energy coastlines are more likely to be transport zones (Flores-Cortés et al., 2022). These uncontrolled variables can significantly influence reported microplastic concentrations, complicating efforts to identify broader spatial or temporal trends (Hidalgo-Ruz et al., 2012).

2.2.3. Sampling depths

While most beach microplastic studies bulk sample only to depths of 5 cm or less, research increasingly recognizes both the value and the technical challenge of collecting samples from greater sediment depths. Veerasingam et al. (2021) extended sampling to 30 cm along the coast of Qatar. Still, they reported that physical barriers within the sediment, such as compaction and embedded debris, frequently limited core penetration and precluded obtaining uniform depth samples across all sites. Pervez & Wang (2022) attempted both short (70 cm) and long (up to 8 m) sediment cores. They documented that deeper sampling was often hindered by dense roots, consolidated substrate, or shell layers, which could lead to core refusal or partial recovery. Similarly, Machendiranathan et al. (2022) noted that on Donghai Island, China, field teams encountered substrate hardness and heavy debris loads that in some locations restricted coring to surface layers, emphasizing the logistical variation even across a single study

area. In a different setting, Gül (2024) found that achieving sediment profiles down to 105 cm along the Turkish Black Sea required substantial effort and that full-depth recovery was not always feasible in anthropogenically influenced or laminated sediments. Further, Sivaraman et al. (2024) emphasized that even relatively shallow stratified sampling, with intervals as narrow as 0–5 cm and 5–10 cm, could be complicated by local sediment properties and required the selection of suitable coring equipment.

These studies demonstrate that while deep or stratified coring can provide essential information on vertical microplastic occurrence, practical limitations imposed by sediment compaction, organic content, or coarse materials often set the achievable depth and integrity of recovered samples. Explicitly reporting such methodological constraints is critical, as these factors affect the reliability and comparability of vertical beach microplastic studies.

2.3. Overview of microplastic-extraction methods

A critical step in microplastic analysis involves separating subsurface plastic particles from the complex sediment matrix in which they are embedded and extracted (see Table 2.2). This matrix is typically a mixture of inorganic and organic components. The inorganic fraction consists of mineral grains of varying sizes, shapes, and mineralogies (such as quartz and feldspars), and which may be bound together by cementing materials, including iron oxides or carbonates. The organic fraction is equally diverse, comprising natural debris such as plant fragments, root systems, microbial biofilms, and the exoskeletons of small organisms.

Table 2.2. Summary of common extraction techniques used in microplastic studies, highlighting their respective strengths, limitations, and typical use contexts. Techniques range from low-cost visual extraction to advanced electrostatic and depolymerization methods.

Technique	Strengths	Limitations	Common Use Context
Visual	Inexpensive, accessible	Ambiguous particles, underestimate	Preliminary screening and quantification before spectroscopic analysis
Density	Isolates from a variety of matrices, tailored	Costly, toxic solutions	NaCl is inexpensive and safe, $ZnCl_2$ and NaI are often used
Oil & Hybrid	Density-independent, environmentally friendly, less sensitive to organic matter	Oil traces remain, post extraction cleaning	Useful alongside density solutions (hybrid)
Electrostatic	Near complete separation	High equipment costs and operational complexity	Pilot studies and some advanced research for dry sediment
Pressurized fluid extraction	Wide range of particle sizes	High equipment costs, operationally complex	Specialized research for complex matrices
Solvent based depolymerization	Polymer specific quantification, accurate chemical identification and quantification	Destroys original polymer structure, advances laboratory setup	Used for polymer identification and quantification
Magnetic separation	Effective for small or nano-sized particles, recovers particles with magnetic qualities	In experimental stage, not widely validated. Requires modification of microplastics or addition of magnetic reagents	Investigated for environmental samples, particularly for recovery of nano/microplastics in water
Ultrasonic	Assists in breaking up aggregates and releasing MPs from matrices, useful for stubborn or fine-grained samples	Sophisticated preparation and instrumentation; not standardized. Can cause breakage or alteration of MP particles	Complimentary strategy to density of chemical extraction

The primary challenge of any extraction method is to effectively isolate the target plastic particles from this varied background. The effectiveness of this separation step directly influences the accuracy of the final reported abundance, size distribution, and polymer types (Claessens et al., 2011; Hidalgo-Ruz et al., 2012).

2.3.1. Visual Extraction Using a Binocular Microscope

Visual extraction (manual picking and sifting) supported by low-magnification binocular microscopy is widely used in beach-sediment microplastic studies because it is low cost, rapid, and does not require specialized instrumentation (Hidalgo-Ruz et al., 2012; Simon-Sánchez et al., 2022; Soursou et al., 2023). However, this approach inherently reflects the same bias as selective sampling: visually obvious particles are preferentially detected, while small, transparent, weathered, or sediment-coated particles are easily missed, resulting in systematic under-representation of less conspicuous microplastics (Zobkov & Esiukova, 2018; Simon-Sánchez et al., 2022). In addition, identification by appearance alone is uncertain because organic fibres and debris can be misclassified as plastics, especially where particles are degraded or fibrous, contributing to both false positives and false negatives (Lusher et al., 2020; Simon-Sánchez et al., 2022; Soursou et al., 2023). Consequently, best-practice protocols emphasize quality assurance and quality control (QA/QC) when microscopy-based sorting is used, including avoiding plastic labware, limiting airborne fibre exposure, and running procedural blanks to quantify background contamination and improve confidence in reported counts (Masura et al., 2015; Yang et al., 2021; GESAMP, 2019; Gao et al., 2023).

2.3.2. Density-based separations

As noted in section 2.1.2 and Table 2.1, density separation is the most widely applied technique for isolating microplastics from sediments. The technique is based on differences in buoyancy between plastic particles and inorganic sediment grains (Zobkov & Esiukova, 2018; Yang et al., 2021). A room temperature saturated sodium

chloride (NaCl) solution is most often used due to its low cost, availability, and non-toxicity, as well as its ease of environmental disposal (Yang et al., 2021; Simon-Sánchez et al., 2022) (supplemental data). The mixture is gently stirred to allow the sediment and microplastics to fully interact with the separation solution. Once agitation stops, the sample is left undisturbed so that heavier mineral grains settle to the bottom while plastic particles, which are less dense than the solution, remain suspended or float to the surface. The floating fraction (supernatant) is then carefully decanted and filtered to collect the microplastics. However, NaCl solutions have a density of 1.18 g/cm^3. They will not separate any high-density plastic polymers such as PVC, polyethylene terephthalate (PET), and polycarbonate, which have densities exceeding 1.3 g/cm^3.

To improve the recovery of these denser polymers, alternative solutions with higher density have been used. These include zinc chloride ($ZnCl_2$, ~1.6-1.7 g/cm^3), sodium iodide (NaI, ~1.6 g/cm^3), calcium chloride ($CaCl_2$, ~1.45 g/cm^3), and sodium polytungstate (SPT, > 1.6 g/cm^3). While these brines improve extraction efficiency, particularly for small or dense microplastics, they introduce challenges related to cost, toxicity, and disposal safety (Pagter et al., 2018; Tiwari et al., 2023). As a result, many researchers select a separation fluid based on trade-offs between recovery performance and environmental or budgetary constraints.

2.3.3. Oil and hybrid separations

To overcome the drawbacks of the various salt solutions, some studies have recently trialled oil-based separation. This method exploits the tendency of plastic to bind with nonpolar liquids, such as vegetable oils (Crichton et al., 2017; Dodson et al., 2020). When mixed with sediment in the presence of water, plastic particles

preferentially migrate to the low-density oil phase while denser sediment grains settle out (Crichton et al., 2017). Recovery rates can vary substantially depending on the oil-to-sediment ratio, agitation duration, and the type of sediment. In addition, multiple extraction rounds are often required to achieve acceptable recovery efficiency, especially for particles < 1 mm, which may be missed in single-pass extractions (Yang et al., 2021; Soursou et al., 2023). Olive and canola oils, in particular, offer a cheaper and non-toxic, hence safer and more sustainable, alternative to traditional metal salt solutions, especially when recovering high-density particles.

Some recent studies have introduced hybrid protocols that combine sequential salt- and oil-based extractions to optimize recovery across a broader range of polymer densities. For example, Dodson et al. (2020) employed a NaCl flotation followed by an oil-based extraction to capture particles that remained after the initial density separation. This integrative approach enhances the likelihood of recovering both low-density and high-density plastics while minimizing environmental and financial costs. However, few protocols provide detailed validation of oil-based methods, highlighting a need for standardized evaluation across sediment types.

2.3.4. Alternative extraction methods

In addition to standard microplastic separation methods such as density separation, oil-based extraction, and visual/manual sorting, other authors have developed alternative techniques. For example, electrostatic separation, using devices such as the Korona-Walzen-Scheider (KWS), harnesses the distinct conductive properties of plastics and mineral particles to achieve near-complete separation (Felsing et al., 2018; Bellasi et al., 2021). Pressurized fluid extraction, such as that reported by Fuller & Gautam (2016),

achieves separation using specialized pressurized equipment. Solvent-based depolymerization methods have also been deployed, such as alkaline depolymerization of PET, which allows for polymer-specific quantification, but this also destroys the original polymer structure (e.g., Misra et al., 2020). Similarly, ultrasonic, microwave-assisted, or magnetic separation has been explored, such as the use of magnetic nanoparticles to bind and extract microplastics (Sujathan et al., 2017; Grbic et al., 2019). While some of these advanced methods can achieve high recovery or specificity, they are generally discounted for widespread environmental monitoring due to high cost, technical demands, or limited applicability, leaving density and oil-based techniques as the most practical and adaptable options for most studies (Bellasi et al., 2021).

2.3.5. Organic-matter removal

Another critical step in microplastic extraction is the removal of organic matter from the sediment. Organic matter can interfere with both visual sorting and spectroscopic identification by masking particles or, in the case of root systems or microbial biofilms, by binding them into aggregates that resist visual or spectroscopic confirmation. Additionally, organic material often has a density similar to or lower than many plastics, which can cause it to co-separate with microplastics during density-based extraction methods, leading to contamination of the extracted fraction and potential overestimation of microplastic abundance.

Oven burning, also known as loss-on-ignition (LOI), is a well-established technique for quantifying total organic matter in environmental samples by combusting materials at high temperatures (typically 550 ^{o}C) (Prata et al., 2019). However, due to the thermal degradation and destruction of plastic polymer particles at these

temperatures, LOI is not suitable for organic matter removal in microplastic extraction protocols (Prata et al., 2019).

To address these issues, researchers often employ oxidative digestion techniques using reagents such as hydrogen peroxide (H_2O_2), Fenton's reagent (a combination of H_2O_2 and Fe^{2+} ions), bleach (NaClO) (Pfeiffer & Fischer, 2020), or enzymatic digestion methods (Hurley et al., 2018). The aim is to break down organic debris while preserving the synthetic particles, a balance that depends on reagent strength and exposure time. Reagents must be carefully controlled to avoid degrading certain plastic types or altering the morphology of fragile particles. Recent studies have emphasized the importance of temperature regulation, reaction time, and post-digestion neutralization in protecting the integrity of microplastic samples (Soursou et al., 2023; Tiwari et al., 2023). Notably, in samples with abundant organic matter, this oxidative treatment is frequently performed as a first step before density or oil-based separation because removing organic compounds at the outset minimizes aggregation and co-extraction of debris, thereby improving separation efficiency and ensuring more accurate identification and quantification of microplastics (Razeghi et al., 2021; Monteiro et al., 2022; Tuuri & Leterme, 2023).

Additional comparative evaluations of digestion strategies provide useful methodological context. Several widely used protocols rely on oxidative digestion with hydrogen peroxide (H_2O_2), either alone or as Fenton's reagent ($H_2O_2 + Fe^{2+}$), while others apply alkaline digestion (e.g., KOH) or commercial bleach (NaClO). These approaches differ in their efficiency, reaction time, and potential to damage polymers. Numerous laboratory intercomparison studies have assessed their relative performance.

Building on this work, the studies summarized in Table 2.3 compare organic-matter removal agents, polymer stability, and analytical compatibility, and collectively illustrate the methodological diversity that continues to complicate cross-study comparability.

Table 2.3. Selected beach microplastic studies incorporating chemical digestion (H_2O_2 or KOH) for organic-matter removal and subsequent polymer identification via FTIR or Raman spectroscopy. Abbreviations: PE = Polyethylene; PP = Polypropylene; PET = Polyethylene Terephthalate; PS = Polystyrene; EPS = Expanded Polystyrene; dw = dry weight.

Study	Location / Setting	Digestion Agent	Polymer Identification	Common Identified Polymers	Key Findings / Methodological Contribution
Masura et al. (2015)	USA (NOAA Protocol)	H_2O_2 with Fe(II) catalyst (Fenton's Reagent)	Visual, with optional FTIR confirmation	Protocol designed for all common polymers (PE, PP, PS, PVC, etc.)	Established the foundational NOAA protocol for digesting organic material in marine sediment and water samples, becoming a global standard.
Karami et al. (2017)	Lab-based evaluation (Malaysia)	Compared H_2O_2, KOH, HNO_3, and HCl	FTIR & SEM	Tested effects on PE, PP, PS, and PVC particles	Assessed the effectiveness of different digestion agents and their potential to degrade or damage the target microplastics, providing critical guidance on method selection.
Prata et al. (2019)	Lab-based evaluation (Portugal)	Optimized H_2O_2 protocol	Not specified (methodological focus)	Focused on the integrity of common polymers post-digestion	Provided key recommendations for optimizing digestion parameters (temperature, duration, concentration) to maximize organic removal while minimizing polymer damage.
Pfeiffer & Fischer (2020)	Lab-based evaluation (Germany)	Compared H_2O_2, Fenton's Reagent, and other agents	Raman and/or FTIR	Protocol tested on sediment samples spiked with PE, PP, PET, PS, etc.	Provided a comprehensive review and comparison of digestion protocols specifically for challenging sediment matrices, confirming the efficacy of oxidative methods.

2.4. Microplastic identification techniques

Once separated from beach sediment, the identification of presumptive microplastics relies on a blend of approaches, chosen based on available resources, cost, and the desired level of analytical certainty (see Table 2.4).

Table 2.4. Summary of common analytical techniques used in microplastic identification, highlighting their respective strengths, limitations, and typical use contexts (Simon-Sánchez et al. 2022; Soursou et al. 2023; Volgare et al. 2021; Hidalgo-Ruz et al. 2012). Techniques range from low-cost visual sorting to advanced spectroscopic and thermal methods, with ongoing efforts to strike a balance between analytical accuracy, cost, and accessibility in environmental studies.

Technique	Strengths	Limitations	Common Use Context
Visual Sorting	Low cost, quick, and accessible in low-resource settings	Subjective, prone to false positives/negatives, misses small or transparent particles	Initial screening of particles >500 µm in lab or field studies
FTIR	Polymer-specific, non-destructive, widely used	Limited resolution for small or complex particles; requires flat, dry samples	Routine lab-based polymer confirmation of visually sorted particles
µ-FTIR	High resolution, particle-level ID down to ~10 ¬µm	Longer scan times, expensive, and technical expertise are required	Advanced research needs particle-level mapping and quantification
Raman	Polymer-specific, can identify pigments, and works on small particles	Fluorescence interference; less effective on weathered samples	Supplement or alternative to FTIR, especially for small or coloured microplastics
µ-Raman	High spatial resolution, minimal sample prep	Slow, requires specialized optics, sensitive to interference	High-resolution validation of fibre-like or sub-20 µm microplastics
Py-GC-MS	Highly accurate polymer ID, independent of particle shape or contamination	Destructive method, requires expensive instrumentation, and technical skill	Source tracking, advanced compositional studies, and method validation
HIS-NIR	Non-destructive, allows in situ scanning of environmental matrices	Underdeveloped in MP research, requires calibration and technical expertise	Emerging method for rapid surveys or field-deployable platforms
Hot Needle Test	Extremely simple, no equipment beyond a heated needle; detects melting behaviour	Cannot distinguish polymer type; risk of misclassification with organic matter	Field tests or quick confirmation in the absence of lab tools
SEM	High-resolution surface imaging is helpful for morphology and elemental analysis	Requires vacuum, costly, not polymer-specific unless paired with EDS	Morphological characterization, sometimes paired with chemical analysis (EDS)

Table 2.4. (continued)

Technique	Strengths	Limitations	Common Use Context
Flow Cytometry	Rapid detection and counting of particles in suspension allows size/shape gating	Expensive, best for small/transparent MPs in liquids, not yet standard in MP work	Emerging applications for MP analysis in liquid samples

2.4.1. Visual sorting and hot needle testing

Visual sorting of the separated, putative microplastic particles remains the most widely used method, mainly because it requires no specialized equipment and can be applied fairly rapidly to large amounts of particles. However, visual sorting may misclassify any remaining organic debris as plastics, and the method tends to overlook degraded or translucent fibres, particularly when particles are weathered (Simon-Sánchez et al., 2022; Soursou et al., 2023). Researchers typically rely on visual cues, such as shape (e.g., fibre, film), colour (e.g., red, blue), and surface texture (e.g., porous), to identify plastic particles. Standardized visual protocols have been proposed to improve consistency, but even with visual standards in place, detection remains unreliable, particularly for particles approaching the lower size threshold (Lusher et al., 2020).

To improve identification reliability of visual sorting, the hot needle test is often used as a supplementary step to confirm if a particle is a synthetic polymer. The procedure involves heating a metal needle and gently touching it to the surface of a suspect particle while under microscopic observation. The key to a successful test is maintaining a suitable needle temperature. The needle must be hot enough to melt common plastics (melting points of 110^{o}C for low-density PE and over 330^{o}C for Teflon) but not so hot as to cause immediate combustion (Lusher et al., 2020; Yang et

al., 2021). Care must be taken not to overheat the needle, as excessive temperatures can cause burning rather than simple melting, leading to charring, discoloration, and the potential destruction of the sample, which can make identification inconclusive. The test is especially valuable for distinguishing plastics from similarly appearing organic or mineral debris when visual identification is ambiguous. However, the test is less effective for very small or thin particles that may be damaged or difficult to observe (Lusher et al., 2020; Yang et al., 2021).

2.4.2. FTIR and Raman Spectroscopy

FTIR and Raman spectroscopy are commonly used for confirming a plastic source as well as a detailed polymer identity, offering greater reliability than visual sorting, especially for ambiguous or weathered particles. FTIR identifies the separated particles by matching infrared absorption spectra to known polymer reference libraries. When used in its microscopic form (μ-FTIR), this technique allows particle-level identification down to ~10 μm with minimal sample preparation (Soursou et al., 2023). Raman spectroscopy is efficient for coloured or pigmented plastics, although its use can be limited by interference from fluorescent compounds. Both methods preserve the particle during analysis, making them ideal for confirmation after visual sorting; however, their use requires expensive equipment, considerable time, and specialized technical training (Asensio-Montesinos et al., 2020; Soursou et al., 2023).

2.4.3. Other tools

Beyond FTIR and Raman techniques, advanced tools such as Pyrolysis-Gas Chromatography-Mass Spectrometry (Py-GC-MS), Scanning Electron Microscopy

(SEM), and Hyperspectral Imaging (HIS-NIR) have also been attempted. Py-GC-MS enables the quantification and identification of polymers based on thermal decomposition products, making it particularly useful for particles too small, damaged, or complex for optical techniques. However, the pyrolysis step destroys the sample, preventing any further morphological or physical analysis (Soursou et al., 2023). SEM captures fine-scale surface textures and particle shape, but cannot confirm polymer identity unless paired with techniques comparable to energy-dispersive X-ray spectroscopy (EDS), and issues such as static charging make careful sample mounting a critical step. HIS-NIR remains in early development but is gaining attention for its potential in real-time or automated identification. Currently, its uptake is limited by the high cost of specialized equipment and the need for calibration standards (Tirkey & Upadhyay, 2021; Soursou et al., 2023).

2.5. Contamination control and quality assurance

Accurate reporting of microplastic pollution in sediment also hinges on strong contamination control and quality assurance protocols, as microfibres and other fine particles from the laboratory environment can be easily introduced during sample handling and analysis. To mitigate this risk, a multi-faceted approach incorporating procedural, environmental, and material controls is essential.

Key environmental controls focus on minimizing airborne contamination. Anti-static precautions are critical because static electricity can attract airborne fibres and fine microplastics to surfaces and samples. This risk can be mitigated by using anti-static work surfaces or wearing anti-static lab coats (Gao et al., 2023). Air circulation must be carefully managed, as uncontrolled airflow can redistribute laboratory dust and fibres

onto samples. It is therefore recommended to minimize unnecessary air movement and, ideally, to analyze samples within a laminar flow hood or a clean air cabinet to create a particle-free work environment (Gao et al., 2023).

Material selection is another critical component. To prevent cross-contamination, avoiding the use of plastic instruments and storage containers is paramount, because common labware materials such as PP tubes, PE bottles, or plastic tweezers, can shed particles into samples. Instead, glass or metal laboratory ware is preferred such as glass beakers, stainless steel sieves, and aluminum foil to cover samples during drying and storage (Gao et al., 2023).

Finally, procedural controls are necessary to quantify and account for any background contamination that does occur. The use of procedural blanks (samples processed with all reagents but without any environmental sample) is a standard practice recommended by authoritative bodies, such as the NOAA (Masura et al., 2015) and the GESAMP working group (GESAMP, 2019). These blanks allow laboratories to identify and quantify any contamination introduced during processing. Similarly, using filtered reagents (e.g., filtering solutions through 0.2–1 μm membranes before use) ensures that chemicals themselves do not introduce new microplastic particles into the samples (Yang et al., 2021; Gao et al., 2023). By subtracting the types and quantities of microplastics found in the blanks from the environmental sample counts, researchers can improve the accuracy and reliability of their final data (Yang et al., 2021; Gao et al., 2023).

2.6. Synthesis of methodological variability

As established in Chapter 1, the lack of harmonized terminology presents a foundational challenge to microplastic science. This issue is compounded by marked divergences in methodology across sampling design, extraction protocols, and analytical confirmation, each influencing data quality and interpretation. This methodological disarray continues to impede coordinated global monitoring and undermines the feasibility of reliable meta-analysis.

Studies vary significantly in sampling strategies, where choices in depth, equipment type, and mesh size strongly affect which particles are captured and can lead to vastly different reported counts (Hidalgo-Ruz et al., 2012; Simon-Sánchez et al., 2022). Normalization of concentrations by area, volume, or weight further complicates direct comparisons between studies (Yang et al., 2021). Separation techniques are also inconsistent, ranging from common low-density (NaCl) solutions to high-density ($ZnCl_2$, NaI, SPT) or oleophilic extractions (Pagter et al., 2018; Yang et al., 2021; Soursou et al., 2023). Each method involves critical trade-offs between polymer recovery efficiency and practical constraints, including cost and toxicity, yet these choices fundamentally alter reported microplastic loads.

This variability is compounded by inconsistent analytical validation. Many studies rely on visual sorting, but the extent of more rigorous spectroscopic confirmation (e.g., FTIR, Raman) is inconsistent and often lacks the transparency needed for replication (Simon-Sánchez et al., 2022; Soursou et al., 2023). Critical details, such as extraction protocols, solution concentrations, alongside QA/QC procedures, such as procedural blanks, are too often omitted, hindering reproducibility and complicating

cross-study comparisons (Tiwari et al., 2023; Thompson et al., 2024). These persistent challenges highlight an urgent need for protocols that balance analytical rigour with practicality. Until such standards are widely adopted, transparent and comprehensive reporting of all methodological details remains critical for advancing the field (Mataji et al., 2020).

3. Geological and Natural Setting of the Study Area

Building on the methodological review and identification of knowledge gaps outlined in Chapter 2, the present chapter introduces the geological and natural context of the study site. While coastal microplastic research has expanded globally, studies focused on environmentally sensitive and protected beaches, particularly in Canada, remain scarce in the literature. The study site is a beach adjacent to Mary's Point, situated on the northeastern margin of the Bay of Fundy (Figure 3.1). Selecting this location directly addresses the identified research gap, providing an opportunity to investigate microplastic dynamics within a high-energy, ecologically significant, and UNESCO-recognized coastal setting.

The Bay of Fundy is renowned for having the world's highest tidal ranges, and the nearby estuaries play a crucial role in the region's ecology (Amos & Zaitlin, 1991). The northeast of the Bay is divided into three distinct physiographic provinces: the outer Chignecto Bay (sensu stricto), and the inner estuaries of Shepody Bay and the Cumberland Basin. Mary's Point is a narrow finger of land extending out from the southeastern coast of New Brunswick, roughly dividing the outer Chignecto Bay from the inner Shepody Bay (Amos & Zaitlin, 1991).

The broader region around Mary's Point contains diverse habitats, including eroding cliffs, salt marshes, sand and gravel beaches, and extensive intertidal mudflats. Onshore, the environment is primarily rural, characterized by agriculture, forestry, and small local wharves, with the fishing village of Alma located approximately 25 km to the southwest. The major industrial centre (oil refineries, paper mills, ports) is Saint John, about 120 km to the southwest. The commercial centre of Moncton, around 40 km

to the north, has seen environmental changes following the removal of a causeway that previously blocked tidal movement up the Petitcodiac River between 1968 and 2010 (Gerwing et al., 2017).

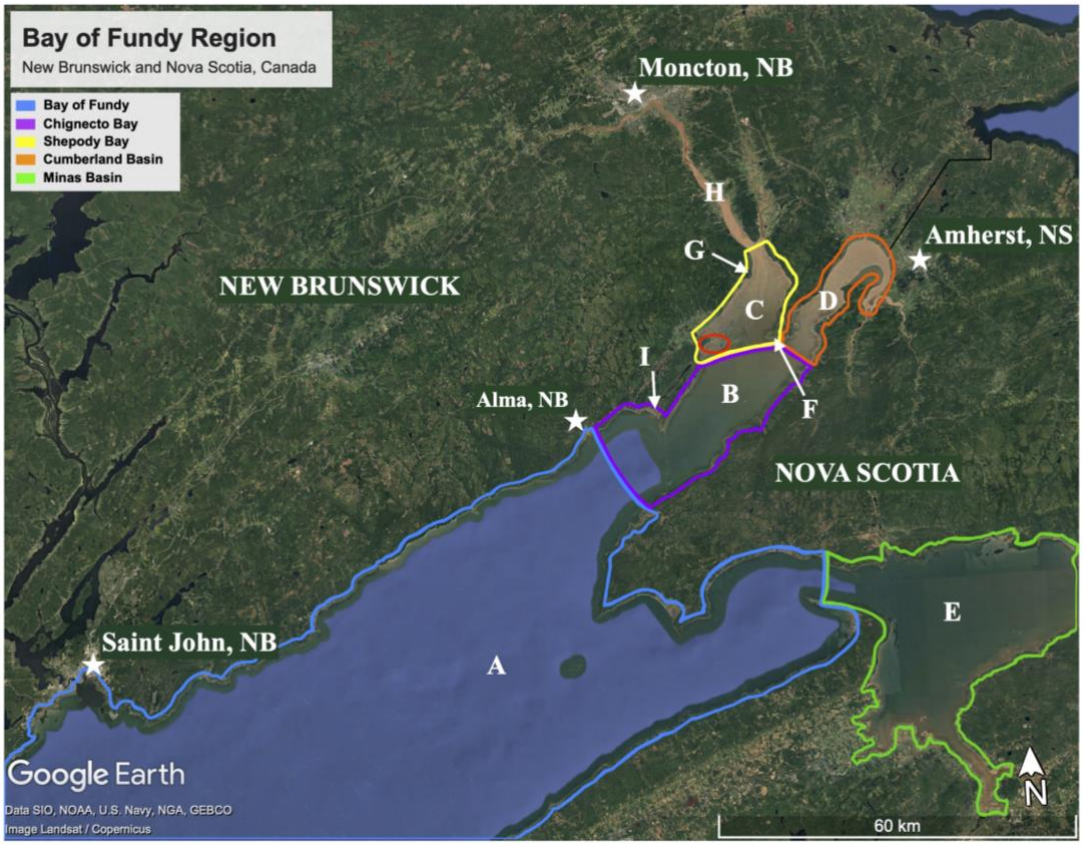

Figure 3.1. Map of the Bay of Fundy, New Brunswick, Canada. The study region of Mary's Point is circled in red. Identified areas include (A) Bay of Fundy, (B) Chignecto Bay, (C) Shepody Bay, (D) Cumberland Basin, (E) Minas Basin, (F) Cape Maringouin, (G) Hopewell Rocks Provincial Park, (H) Petitcodiac River, (I) Waterside Beach.

3.1. Geological evolution of Chignecto Bay

The broad morphology of the Bay of Fundy is the result of Paleozoic tectonics. Approximately 430 million years ago, the Acadian Orogeny initiated the formation of pull-apart basins that became filled with Devonian-Carboniferous sediment. Ongoing tectonic activity, including salt diapirism, resulted in the folding and thrusting of these lithified sediments and earlier Precambrian to Early Paleozoic rocks. The later opening of the Atlantic during the Mesozoic induced tensional stresses, leading to the development of half-grabens and the deposition of red-bed facies within the Fundy Basin, which correlates spatially with the central Bay of Fundy and Minas Basin (Craggs et al., 2017).

Amos & Zaitlin (1991) summarized that the Chignecto Bay region has undergone subsequent geological changes driven by glacial processes, sea level fluctuations, and tidal dynamics over the past 15,000 years. Before 13,300 BP, the Chignecto Bay area was dominated by thick glacial ice associated with the Chignecto Phase. At approximately 15,000 BP, this ice loading had caused significant submergence, with relative sea levels approximately 55 m above present sea level. As the Chignecto ice sheet retreated, sandy deltas formed along its front, depositing sediments into the inundated Bay of Fundy. Following deglaciation (13,300–10,000 BP) and accompanying sea-level rise, strong tidal currents reworked these pro-glacial deposits, redistributing them into extensive gravel beds. This period coincided with a brief phase of macrotidal conditions, which peaked around 12,000 BP (Amos & Zaitlin, 1991).

Isostatic uplift rates during this period peaked at approximately 2 metres per century. Continued, but slowed, isostatic rebound eventually regressed sea levels to 25 m below the present day by ~7,000 BP. During that time, a barrier or spit formed across the lower Bay, sheltering a lagoon and estuarine deposits where sand and mud rapidly accumulated under microtidal conditions, while fluvial valleys developed in what is now Shepody Bay and the Cumberland Basin. Between 6,000 and 3,000 BP, the barrier was eventually flooded, leading to the development of the present-day storm-influenced macrotidal system that actively resuspends and reworks previously deposited sediments (Amos & Zaitlin, 1991). This long-term Holocene transgression, with mean sea level rising steadily at approximately 15 cm per century and tidal range increasing by 30 cm per century since 7,000 BP, resulted in the deposition of nearly 20 meters of fine-grained "lagoonal" muds in the sub-estuaries. The barrier flood was likely first documented in the Mi'kmaw Nations oral traditions, which involves the giant Kluscap ("Glooscap"), the beaver, and the whale (Reid, 2013).

The bedrock geology in the vicinity of Mary's Point therefore consists of Paleozoic fluvial and deltaic sedimentary rock that filled the pull-apart basins. Subsequent bedrock flexing, due to tectonic and diapiric activity, upthrust and steeply folded much of the material, now forming the eroded cliffs of the bay. The bedrock consists primarily of siltstone and shale, which now shed significant quantities of weathered fine-grained sediment into the bay.

The surficial sediments of the study area reflect the local bedrock lithology, shaped by multiple overlapping processes. These include glacial erosion, postglacial tidal deposition, and the ongoing weathering of glacial sediments exposed along the

cliffs and intertidal zones at Mary's Point. In addition to these terrestrial inputs, fine-grained, clay-rich glacial and postglacial sediments– often containing muddy gravel – dominate the seabed of the outer Bay of Fundy and Chignecto Bay. These seabed deposits, presently undergoing active erosion, contribute a further supply of fine-grained material to the suspended sediment load (Amos & Zaitlin, 1991). The combined influence of coastal erosion, seabed reworking, and sediment inputs from upland exposures creates a dynamic sedimentary environment that continually replenishes fine-grained material in the system.

3.2. Modern hydrodynamic and sedimentary environment of Chignecto Bay

The Bay of Fundy, renowned for having the world's highest tides, exhibits a dynamic sedimentary environment shaped by distinctive hydrodynamic processes. As summarized by Amos (1987) and (Amos & Zaitlin, 1991), the bay's northeast–southwest orientation aligns with the prevailing wind direction, exposing it to significant storm-wave activity. These energetic conditions strongly influence sediment transport and deposition patterns throughout the system.

At Mary's Point, wind-driven sediment redistribution (aeolian transport) and storm-induced backshore flooding play important roles in shaping the spatial variability of surface sediments across the beach system. Strong southwesterly winds, which dominate much of the region, can entrain and transport dry, fine-grained sand landward, contributing to localized accumulation patterns and the development or reworking of small aeolian bedforms (Rey et al., 2021; Dimante-Deimantovica et al., 2023; Tasnim et al., 2023). During high-energy events, storm surges and wave over wash further mobilize sediment across the intertidal and backshore zones, redistributing both fine and

coarse fractions and enhancing the patchiness of sediment textures observed along the beach face. These processes operate alongside tidal currents and wave action, collectively governing short-term sediment mobility and playing a critical role in the continual reworking of the Mary's Cove shoreline.

In general, tidal currents in the Bay of Fundy flow parallel to the margins of its main tidal channels and embayments, closely following the natural contours of the seafloor and NE-SW coastline. However, in Shepody Bay, residual (net) currents show a north–northwest trend, deviating from this general pattern. Winds blowing from the southwest up the length of the Bay generate locally significant waves that can affect the entire Chignecto Bay System. While wave energy is typically greatest within the open waters of Chignecto Bay, it also reaches the mouths of Shepody Bay and Cumberland Basin, as these inlets are aligned with the dominant wind direction.

The Bay of Fundy's tidal regime is dominated by a lunar semidiurnal cycle, producing two high and two low tides each day. This cycle is nearly resonant with the natural oscillation of the Gulf of Maine, a condition that amplifies tidal ranges and drives exceptionally strong tidal currents (Amos & Zaitlin, 1991). The Bay's strong tidal currents facilitate the rapid transport of fine-grained sediments in suspension. Large-scale sediment bedforms such as sand waves, mega-ripples, and sand ribbons are prevalent in offshore and subtidal areas of the outer Bay of Fundy and Chignecto Bay. Seasonal gravel distribution in these offshore zones occurs via ice rafting during the winter months (Amos & Zaitlin, 1991). However, these features are not characteristic of the intertidal flats or backshore at Mary's Point.

The inner Chignecto Bay functions as a muddy estuary, where sediment deposition is primarily composed of eroded Paleozoic mudstone, sandstone, and Quaternary silts and clays. These sources are influenced mainly by cliff and seabed erosion. Notable formations resulting from cliff-line erosion include the Hopewell Rocks, also known as Flowerpot Rocks, which are sea stacks that stand 12–21 m tall (Trenhaile et al., 1998). Cliff-line erosion accounts for approximately 1.03×10^6 m^3 of sediment annually. Rivers add 3.5×10^5 m^3 of sediment per year. The net input of recent sediment is estimated at 1.3×10^6 m^3 per year, with approximately 93% comprising fine-grained material. Seabed reworking introduces an additional 6.0×10^6 m^3 of fine-grained sediment into suspension annually (Amos, 1987; Amos & Zaitlin, 1991).

3.3. Mary's Point

Today, the peninsula of Mary's Point extends easterly into the Bay of Fundy and consists of a mixed back shore of salt marsh and up to 20 m high eroding cliffs of both resistant Carboniferous sandstone (little mudstone is exposed in the vicinity) and of poorly consolidated Quaternary glacio-marine-delta sand and gravel (Figure 3.2) (Stea et al., 2011). On the southeastern and eastern tips of Mary's Point, the cliffs have eroded back, leaving an extensive wave-cut platform of exposed Carboniferous bedrock. West of the tip, the foreshore forms gently sloping beaches of varying width. The south-facing beach represents the study area and is from < 20 m (east) to > 60 m wide (west). Based on the sandier beach deposits adjacent to the foot of the unconsolidated, sandier Quaternary cliffs, these cliffs are probably the primary source of material for the south beach. Extensive intertidal mudflats located further seaward, such as the ~2-km-wide New Horton Flats (Figure 3.2), are inundated diurnally by the tides of up to 13.5 m

range (Government of Canada, 2022). Although winds are predominantly from the southwest (Amos & Asprey, 1979), the southward curve of the Mary's Cove shoreline westward from the peninsula and headland at Upper New Horton likely shelters the south beach from waves energized at these times. Accordingly, more southerly winds and wave diffraction in the embayment of New Horton Flats likely produce a predominantly westerly longshore drift on the south beach.

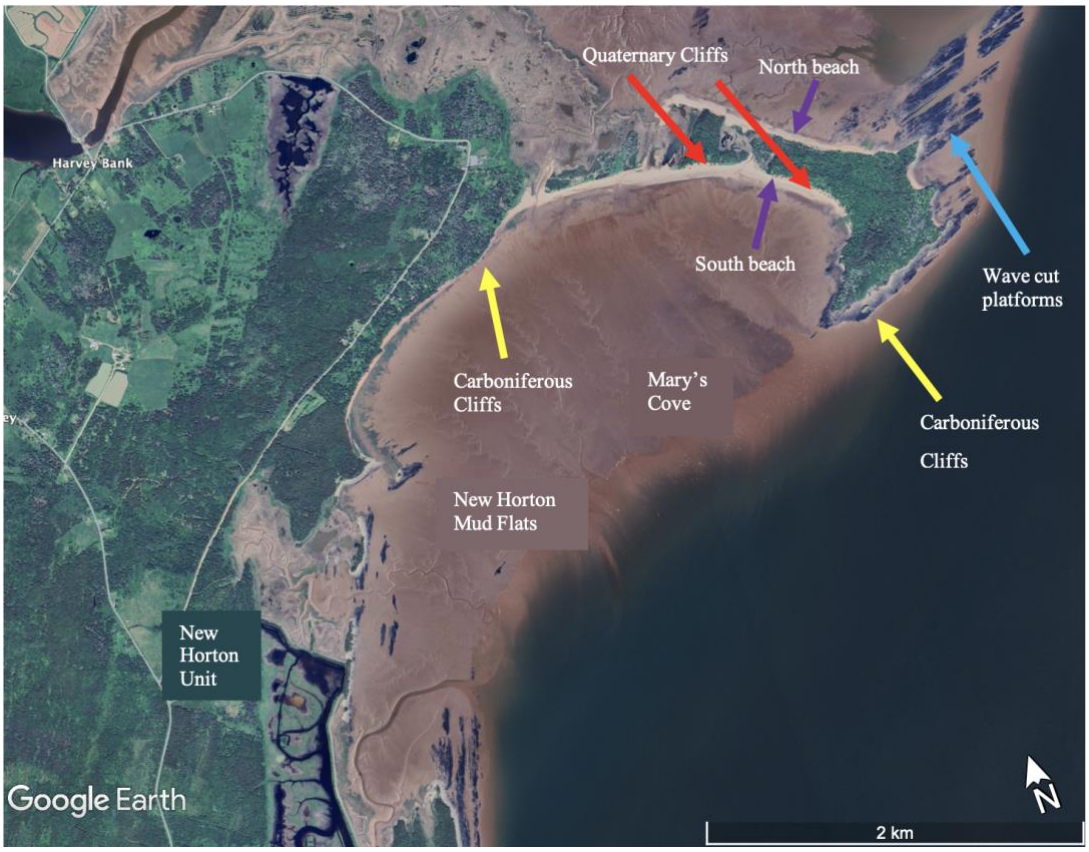

Figure 3.2. Google Earth Image of Mary's Point, NB, identifying the Quaternary Cliffs (red arrows), the Carboniferous Cliffs (yellow arrows), wave-cut platforms (blue arrow), and the New Horton Mud Flats.

The seabed of the outer Bay of Fundy and Chignecto Bay contains fine-grained, clay-rich glacial and postglacial sediments, along with muddy gravel, which serves as a source of the fine-grained suspended sediments of the Bay. While mudflats in the inner estuaries act as depositional environments, sediment accumulation is ephemeral, with deposits subject to resuspension and redistribution. The pattern of suspended sediment transport remains complex, as evidenced by measurements from the mouths of Shepody Bay and Cumberland Basin, which indicate both import and export of sediment over time (Amos & Zaitlin, 1991).

No sedimentological studies have been published specifically on the beaches of Mary's Point. A nearby beach, Waterside Beach (Figure 3.1), was studied by Dashtgard et al. (2006), who reported on the sedimentology and stratigraphy of this transgressive, muddy gravel beach. Subsequently, Dashtgard & Gingras (2007) examined the tidal controls on the morphology and sedimentology of three beaches, including Waterside Beach. Other studies in the Bay of Fundy region (e.g., Fader et al., 1977; Amos & Asprey, 1979; Nadon & Middleton, 1985; Amos, 1987; Amos & Zaitlin, 1991; Fader, 2005) describe the overall geology and sedimentology of the broader area but do not provide a focused, site-specific sedimentological analysis of Mary's Point Beach. One unpublished study (Forsythe, 2016) examined microplastic pollution along the southwestern coast of New Brunswick and a beach in Fundy National Park. In contrast, nearby beaches and mudflats, particularly those in the Shepody Bay and Cumberland Basin regions, have been widely studied for biological purposes because of the region's ecological importance, for example, Gerwing et al. (2015) reported on the variation in

biotic and abiotic features of various intertidal mudflats in the upper Bay of Fundy, including Mary's Point.

3.4. Site importance

The study area at Mary's Point holds exceptional ecological value, a fact recognized by its designation under five distinct international and national conservation frameworks. It is a core component of the United Nations Educational, Scientific, and Cultural Organization's (UNESCO) Fundy Biosphere Region (Fundy Biosphere, retrieved March 6, 2025), a federally protected National Wildlife Area (Government of Canada, 2016; Environment and Climate Change Canada, 2023), a Ramsar Wetland of International Importance (Ramsar, Retrieved April 8, 2025), a globally recognized Important Bird and Biodiversity Area (BirdLife International, Retrieved February 22, 2025), and the first Canadian site to achieve 'Hemispheric Significance' in the Western Hemisphere Shorebird Reserve Network (WHSRN, Retrieved June 29, 2022). This layered protection underscores the site's irreplaceable role in the hemisphere's ecological network, comparable only to other critical shorebird habitats, including the Copper River Delta in Alaska or Delaware Bay in the United States (Clark et al., 1993).

3.4.1. Fundy Biosphere Region

Designated under the UNESCO Man and the Biosphere Programme, the Fundy Biosphere Region (Figure 3.3) is recognized for its exceptional biodiversity, dramatic landscapes, and cultural heritage (Fundy Biosphere, retrieved March 6, 2025). Shaped by the world's highest tides, the biosphere encompasses sea cliffs, beaches, forests, and mudflats that support diverse ecosystems and are culturally significant to the Mi'kmaq,

Wolastoqiyik, and Passamaquoddy peoples. Mary's Point is a core protected area within this conservation landscape.

Figure 3.3: Map of the Fundy Biosphere Region, New Brunswick, Canada (Canadian Geographic, 2013).

3.4.2. National Wildlife Area

Established in 1980 under the Canada Wildlife Act, the 990 ha Shepody National Wildlife Area (SNWA; Figure 3.4) protects outstanding wetland and coastal habitats, including salt marshes, intertidal mudflats, and the forested peninsula or Mary's Point, for migratory birds and waterfowl (Environment and Climate Change Canada, 2023; Government of Canada, 2016).

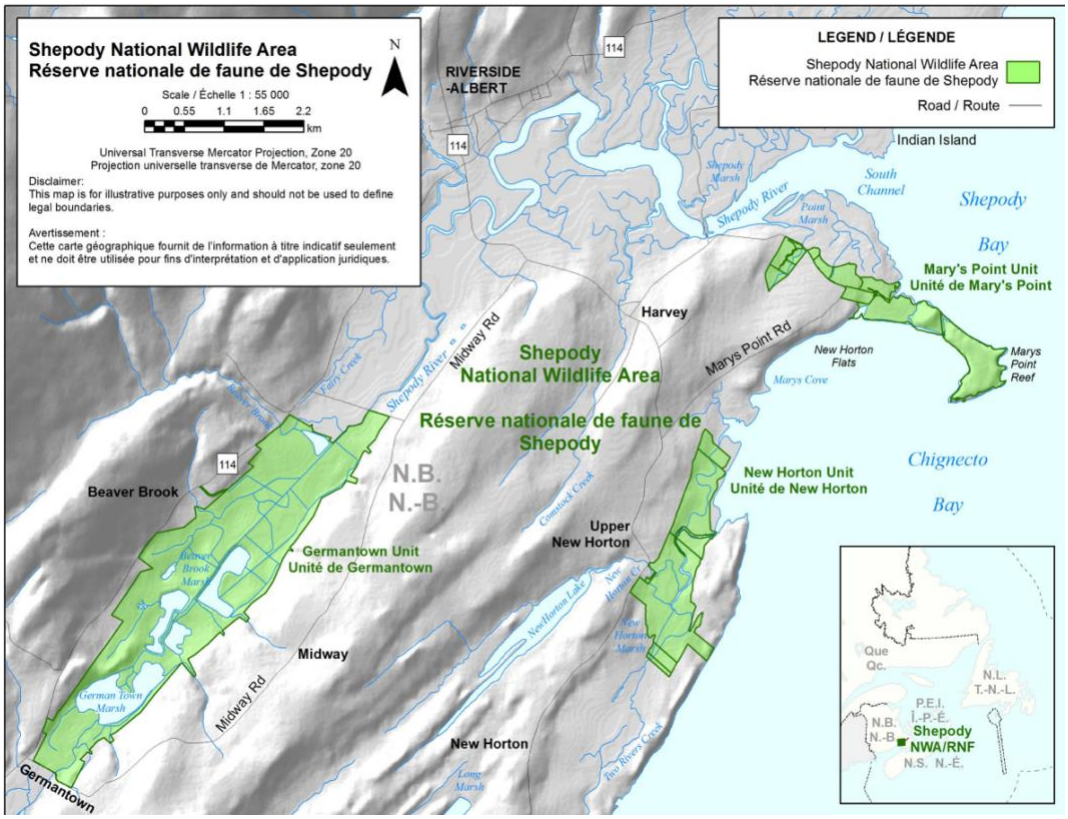

Figure 3.4. Protected regions under the designation of the Shepody National Wildlife Area (green) by the Government of Canada (Environment and Climate Change Canada, 2023).

3.4.3. Western Hemisphere Shorebird Reserve Network

To complete their near 3,000 km migration to Central and South America, nearly the entire population of eastern Semipalmated Sandpipers – about 1.8 million birds – relies on a critical late-summer stopover in the Bay of Fundy (Figure 3.5). As a site of Hemispheric Significance, Mary's Point specifically hosts flocks of more than 200,000 birds (Figure 3.6), drawn by the 80,000 ha of mudflats exposed by twice-daily tides (WHSRN, n.d., Retrieved June 29, 2022). These flats contain North America's densest populations of mud shrimp (*Corophium volutator*), offering the essential energy reserves required for the birds to sustain their long-distance flight.

Figure 3.5. Map of the Americas showing the migratory route of eastern Semipalmated Sandpipers, illustrating their journey between Arctic breeding grounds and South American wintering sites (Species at Risk, 2006).

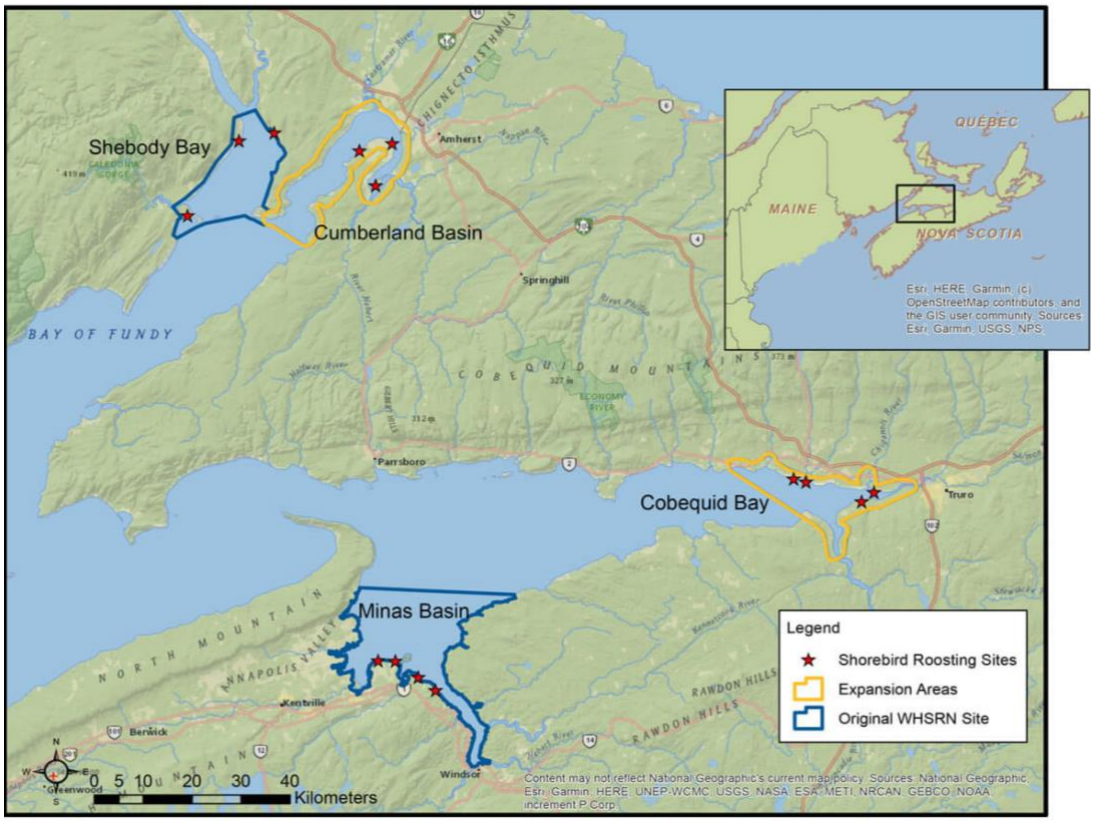

Figure 3.6. Mary's Point and other nearby WHSRN sites (WHSRN, n.d., Retrieved June 29, 2022).

3.4.4. Ramsar Wetland of International Importance

The 12,000-hectare Shepody Bay was designated a Ramsar site in 1987 (Figure 3.7) for its exceptional ecological integrity and its role in supporting vulnerable species, functioning as one of the most productive marine ecosystems in eastern North America (Ramsar, Retrieved April 8, 2025).

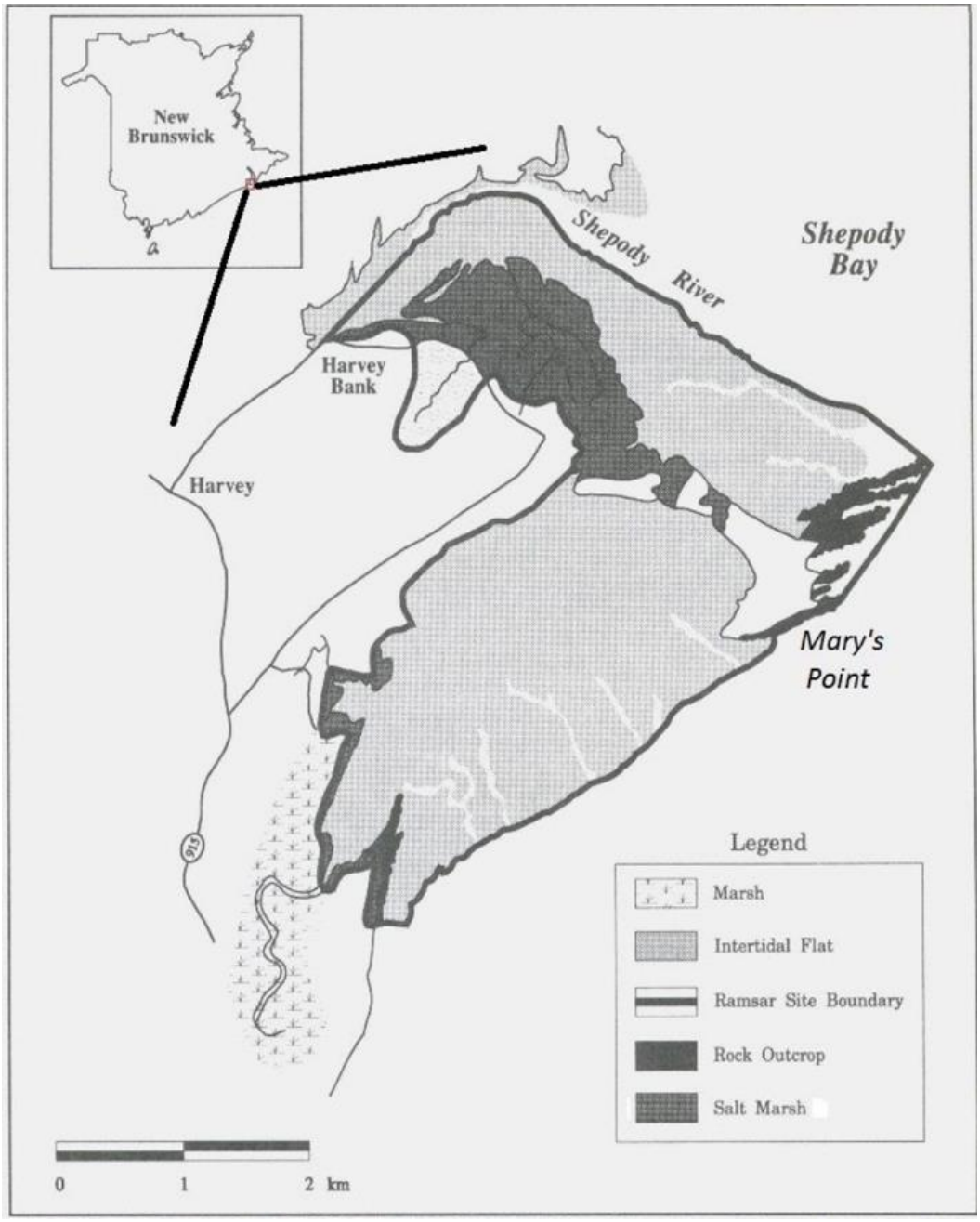

Figure 3.7. Map of Mary's Point unit of the Shepody NWA, and its additional RAMSAR Wetland of International Importance designation (Ramsar, Retrieved April 8, 2025).

3.5. Ecological threat of microplastics

Given the importance of Mary's Point as a critical migratory stopover for shorebirds, it is crucial to assess potential environmental threats to this protected coastal

habitat. While its designation under multiple conservation initiatives suggests a relatively undisturbed environment, no ecosystem is immune to global environmental pressures. Among these, microplastic pollution has become a pervasive issue in marine and coastal ecosystems.

The Semipalmated Sandpiper, which relies on the upper Bay of Fundy to rebuild fat stores during its 3,000+ km migration (Figure 3.7) (MacDonald et al., 2012), has traditionally been viewed as an intertidal forager, feeding primarily on *Corophim volutator*. However, recent studies (MacDonald et al., 2012; Gerwing et al., 2016; Quinn et al., 2017) indicated that these birds are more opportunistic foragers across both intertidal mudflats and upper beach areas (Gerwing et al., 2016; Quinn et al., 2017). Their diet includes a diverse array of marine, freshwater, and terrestrial prey, such as arachnids, crabs, bivalves, ctenophores, cnidarians, and fish (MacDonald et al., 2012; Gerwing et al., 2016). This dietary flexibility allows them to adapt to changing food source availability, but also likely increases their likelihood of ingesting pollutants present in their foraging habitats.

Microplastics, which have been widely documented in coastal sediments, pose a potential risk to shorebirds through inadvertent direct ingestion of particles with prey or trophic transfer via contaminated prey. While many shorebirds routinely ingest small amounts of natural sediment during foraging, microplastics present a greater concern due to their propensity to sorb and concentrate environmental toxins and their potential to chemically degrade into more bioavailable and harmful byproducts (Xu et al., 2020). Studies have identified microplastics in the digestive systems of multiple shorebird species (Hoang & Mitten, 2022; Mylius et al., 2023), raising concerns about their

potential physiological and ecological effects. Mylius et al. (2023) conducted a comprehensive global review of microplastic ingestion by shorebirds, encompassing 26 species across 10 countries. They found that approximately 53% of the world's shorebird population is exposed to microplastics through direct sediment ingestion and consumption of contaminated prey. Furthermore, migratory shorebirds, such as sandpipers, may serve as vectors for transporting plastic across ecosystems, further emphasizing the importance of assessing pollution levels at key stopover sites. However, to my knowledge, no published research has been conducted on microplastics in the Semipalmated Sandpipers.

To fully evaluate the potential risks of microplastic exposure to Semipalmated Sandpipers and other wildlife at Mary's Point, it is necessary to quantify the concentration and distribution of microplastics within the sediment. This study aims to address the knowledge gap by investigating the presence of microplastic pollution within this internationally recognized habitat for shorebirds.

4. Methodology

The present chapter outlines the procedures used to collect, prepare, extract, and analyze microplastic samples from beach sediments at the Mary's Point Beach of the Shepody National Wildlife Area, specifically the south-facing beach in Mary's Cove, landward of the New Horton (mud-) Flats and west of the headland of Mary's Point (Figure 3.4). Field methods, laboratory processing, extraction protocols, and quality control measures are described, including a novel multi-stage extraction technique.

4.1. Field Methods

The present study aimed to examine plastic pollution at depth (> 5 cm), thus requiring a coring method to extract sedimentary material. A hand-held, 4 cm internal diameter, 50 cm long, stainless-steel corer was used, rather than an auger, to preserve any sedimentary structures within the sediment column. The corer contained a removable internal plastic sleeve in which the sediment was collected. The south-facing sandy stretch of beach in Mary's Cove, west of Mary's Point, was targeted for coring, as a hand corer is not suitable for penetrating sediment containing pebbles, such as the north-facing beach, nor the near-surface relict gravel (and covered marsh) on the mudflats, which may block, break, or blunt the equipment. Fieldwork was conducted under the restrictions of sampling permits obtained from Environment and Climate Change Canada (e.g., to avoid times when migratory shorebirds were present). Effort was made to ensure samples were taken around low tide during the same tidal stage each year (following the 13th spring tide), which occurred on July 5th, 2022, and July 8th, 2024.

Cores were obtained from 3 m seaward of the spring-high-tide (strand) line, identified by the highest continuous trace of wrack (residual seaweed and macro-debris) on the beach. Extracting the core just seaward of the spring high tide was intended to limit the occurrence of wrack debris blocking coring, in addition to collecting material from a section of the beach affected by deposition, erosion, and sediment reworking. To ensure an unbiased characterization of the beach, a randomized sampling design was employed for both the 2022 and 2024 surveys. For each survey year, seven sampling locations were randomly generated within the defined beach boundaries, from the eastern extent (64°38'59.34"W) to the western extent (64°40'6.00"W) (Figure 4.1). This approach was chosen to provide a statistically representative snapshot of the sediment distribution across the active beach face and to allow for the objective identification of depositional patterns without researcher bias. At each coordinate, a 1 x 1 m square sampling grid was deployed, and through a random number generator, one of the 25 sub-squares was selected, within which coring occurred. In the case of surface or shallow subsurface pebbles or debris being present and inhibiting the coring in the selected sub-square, a new random sub-square would be generated.

A total of 14 sediment cores were collected, with seven obtained during fieldwork in 2022 and seven in 2024. Cores were numbered sequentially by year from west to east (Core 22-1 to 22-7 and Core 24-1 to 24-7), reflecting their relative positions along the sampling transect. While the physical length of the corer was 50 cm, actual recovery depth was governed by sedimentological core refusal. Coring was terminated upon reaching a highly compacted, relict gravel and pebble lag deposit beneath the active beach sand.

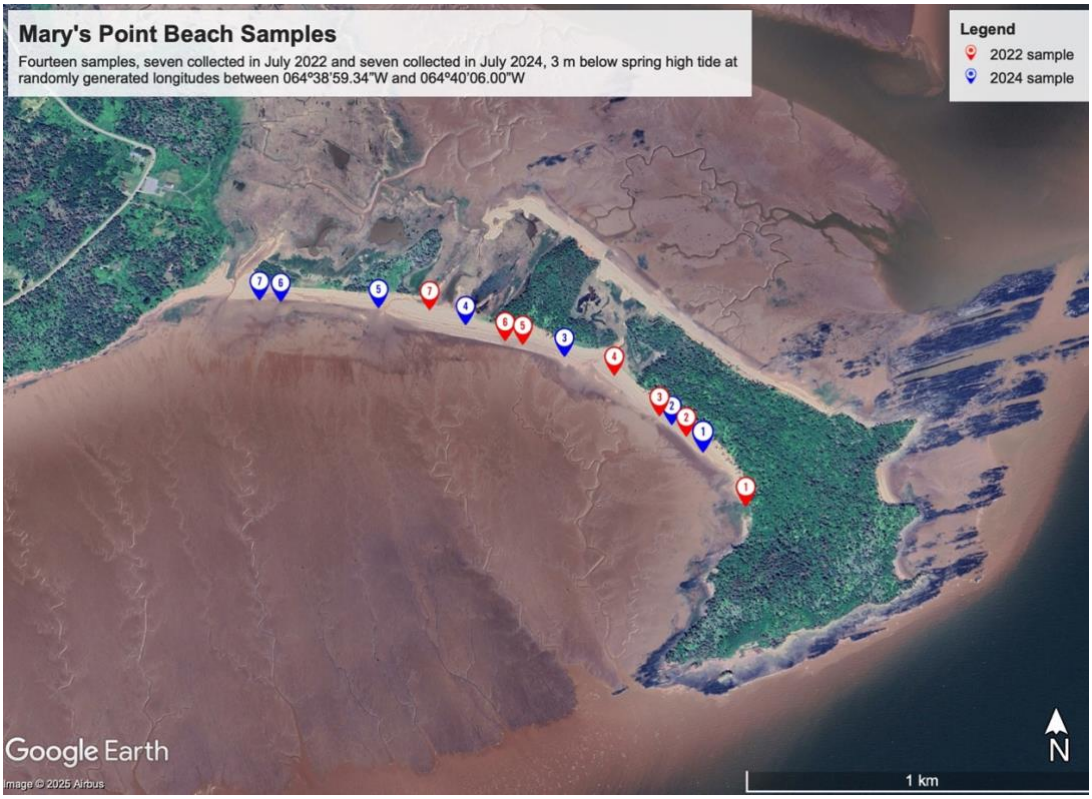

Figure 4.1. Fourteen core samples were taken from Mary's Point, New Brunswick, Canada, 3 m below the spring high tide line in 2022 and 2024. Samples were taken at randomly generated longitudes between the western (064º38'48.00" W) and eastern (064º39'45.00" W) ends of the beach.

After collection, the recovered cores were returned to the laboratory for drying, disaggregation, and preparation for extraction. Each core was sectioned into 4 cm increments from the surface downward, producing up to five depth intervals per core: (i) 0–4 cm, (ii) 4–8 cm, (iii) 8–12 cm, (iv) 12–16 cm, and (v) 16–20 cm (Table 4.1, 4.2). Because some cores did not penetrate as deeply due to the shallow refusal depth, fewer intervals were generated for these locations, resulting in a total of 30 processed interval samples for 2022 and 28 processed interval samples for 2024.

Table 4.2. Samples collected during 2022 field work on July 5th at Mary's Point Beach. Seven cores were extracted along the beach from east to west at randomly generated coordinates, along the spring high tide line. The spring high tide line was identified based on the continuous wrack present. Core 1 indicated the eastern-most location.

2022	Core 1	Core 2	Core 3	Core 4	Core 5	Core 6	Core 7
0–4 cm	22-1i	22-2i	22-3i	22-4i	22-5i	22-6i	22-7i
4–8 cm	22-1ii	22-2ii	22-3ii	22-4ii	22-5ii	22-6ii	22-7ii
8–12 cm	22-1iii	22-2iii	22-3iii	22-4iii	22-5iii	22-6iii	22-7iii
12–16 cm	22-1iv	22-2iv	22-3iv	22-4iv	22-5iv	22-6iv	22-7iv
16–20 cm	22-1v						22-7v

Table 4.1. Samples collected during 2024 field work on July 8th at Mary's Point Beach. Seven cores were extracted along the beach from east to west at randomly generated coordinates, along the spring high tide line. The spring high tide line was identified based on the continuous wrack present. Core 1 indicated the eastern-most location.

2024	Core 1	Core 2	Core 3	Core 4	Core 5	Core 6	Core 7
0–4 cm	24-1i	24-2i	24-3i	24-4i	24-5i	24-6i	24-7i
4–8 cm	24-1ii	24-2ii	24-3ii	24-4ii	24-5ii	24-6ii	24-7ii
8–12 cm	24-1iii	24-2iii	24-3iii	24-4iii	24-5iii	24-6iii	24-7iii
12–16 cm		24-2iv			24-5iv	24-6iv	24-7iv
16–20 cm					24-5v	24-6v	24-7v

4.2. Sediment preparation and analyses

Retrieved cores were kept in their coring sleeves until they were moved to the lab, where they were transferred into a halved cylindrical black PVC pipe (2022 samples) or aluminum trays (2024 samples) and covered with aluminum foil to prevent contamination. Since the coring sleeves and halved cylindrical pipes were of plastic, extra care was taken throughout the collection process to ensure no plastic was broken off these containers (of available options, black plastic was considered most easily identified if contaminating). Disaggregation or fracturing occurred in some, but not all, cores before processing.

Sediment cores were sliced lengthwise along their diameter with a stainless steel knife, to provide an additional view of any structures present, to retain half of the sediment for logging, and to allow for potential later re-analysis. The working half was divided top-down into individual samples corresponding approximately to 4 cm increments. The entirety of each 4 cm working-half increment was processed: samples were placed into labeled aluminum foil trays and oven-dried at 60 °C in a Fisher Isotemp Oven (100 series, model 126G) for 24 hours – a temperature and duration unlikely to cause degradation of microplastics (Zhang et al., 2021). Following drying, each sample was gently disaggregated, then dried for an additional 24 hours at 60 °C. Although the target was 4 cm per sample, actual thickness varied slightly (3.5 cm to 4.5 cm); therefore, each increment was weighed to record an accurate dry mass (see Appendix A for the full table of sample IDs). After microplastic extraction described below, the sediment was again dried at 40 °C using the same procedure as the pre-extraction drying, except at the lower temperature to minimize additional thermal stress on any residual microplastic particles.

Subsequently, the sediment was then shaken for 6 minutes through a stack of metal sieves with meshes at one-phi intervals (from +1 to +4 ϕ), and the fraction collected in each sieve was weighed to determine the grain size distribution (Mathalon & Hill, 2014; Hamdy et al., 2024). The mass of each fraction was determined using a cumulative weighing procedure: a collection tray was first tared, and the contents of the coarsest sieve were added and weighed; the contents of each subsequent sieve were then added successively, with the new total weight recorded after each addition (Frias et al., 2018). From these data, cumulative weight percentages were calculated, and the phi

values corresponding to the 16th, 50th, and 84th percentiles were determined by linear interpolation. These percentile values were then used to calculate the mean grain size (M_z) directly using the Folk and Ward (1957) formula: $M_z = \frac{\phi_{16}+\phi_{50}+\phi_{84}}{3}$. This granulometric analysis was performed after MP extraction, as shaking may fragment already degraded microplastics (Chubarenko et al., 2020) and lead to artificially high recorded abundances (Zhang et al., 2018). The prior extraction of MPs has a minimal influence on sediment weight measurements due to the low mass of plastic particles relative to the sediment grains (Hanvey et al., 2017; Tiwari et al., 2023).

4.3. Microplastic Extraction

Microplastic extraction from sediments remains highly variable across studies, with no universally adopted standard protocol. As reviewed in Section 2.3.2, most prior research relies on single-step density separations using a saturated solution of NaCl, owing to its affordability, non-toxicity, and ease of preparation (Hidalgo-Ruz et al., 2012; Simon-Sánchez et al., 2022). Other studies have employed high-density, but environmentally more problematic, solutions such as $ZnCl_2$ or NaI to recover denser polymers, such as PET or PVC, or oleophilic separations using oils to isolate hydrophobic plastics (e.g., Crichton et al., 2017). In most of the density and oleophilic extractions, only one solution was used, and extractions were often repeated simply to confirm particle removal (e.g., Hidalgo-Ruz et al., 2012). The methodology developed in this thesis builds upon and extends the work of Expósito et al. (2021), who used three distinct density phases, and Dodson et al. (2020), who followed a high-density extraction with an oleophilic step, resulting in a multi-step extraction protocol (Figure 4.2).

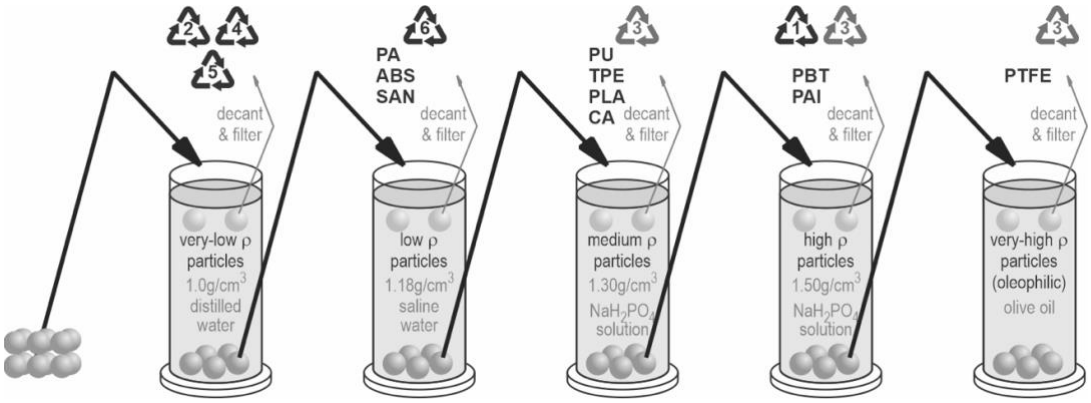

Figure 4.2. Illustration of methodology showing samples sequentially passed through increasing-density solutions, with decanting and filtration steps between each phase, concluding with an oleophilic extraction to remove particles with densities greater than 1.5 g/cm^3.

Herein, dried and disaggregated sediment samples were first weighed using a Mettler P1000 microbalance (±0.1 g). Samples were processed stepwise through a five-stage extraction protocol (Figure 4.2). The first four stages utilized solutions of increasing density: freshwater (1.0 g/cm^3), saturated NaCl (1.18 g/cm^3), and sodium dihydrogen phosphate (NaH_2PO_4). The NaH_2PO_4 solutions were prepared by saturating solute at 30 °C and 50 °C to achieve initial target densities of 1.3 g/cm^3 and 1.5 g/cm^3, respectively. Upon cooling, these solutions maintained a stable, supersaturated liquid phase at room temperature throughout the extraction process without crystallization. The extraction process concluded with a fifth phase involving a biphasic mixture of olive oil (0.92 g/cm^3) and water (1.0 g/cm^3). Each solution was added at a ratio of approximately 4 mL/g of dry sediment. The NaCl and NaH_2PO_4 solutions were prepared following Zhang et al. (2020).

At each stage, the mixture was stirred for 2 minutes (Hidalgo-Ruz et al., 2012; Lots et al., 2017) and allowed to settle undisturbed at room temperature for 24 hours.

The supernatant was carefully decanted, and vacuum filtered using a Whatman ME 25/21 ST 0.45-micron cellulose filter with a yellow plastic Nalgene reusable filtration unit until no solution remained. Remaining sediment sample was carried forward to the next denser solution and the process repeated to extract denser plastic particles, without rinsing (these stages were performed without rinsing of the prior solution that with hindsight could have been a useful additional step). In the final oleophilic step, following Crichton et al. (2017), a few millilitres of olive oil were added, along with tap water, to the sediment, mixed for 2 minutes, and allowed to settle. Microplastics preferentially floated into the oil layer, while sediment and the bulk of organic matter sank. The oil-rich supernatant was then filtered and rinsed with 20 mL of hexane (Scopetani et al., 2020) to reduce viscosity and facilitate passage through the membrane. See Appendix A for a complete list of sediment sample IDs and corresponding microplastic extraction IDs.

4.4. Particle Identification and Quality Control

4.4.1. Visual sorting and classification

Filtered particles from each extraction stage were examined under a binocular microscope at a magnification of up to 3x to distinguish likely plastics from false positives such as cotton, cellulose, or chitin: organic fibres and debris have been shown to comprise over half of recovered particles in some studies (Liu et al., 2022). Putative microplastics were counted, and additionally classified by shape (equant, fibre, film, fragment, and intertwined fibres) and colour (red, yellow, purple, brown, white/clear, black, other). Results were recorded for every extraction density step and sediment sample ID (Appendix B, Table B2).

4.4.2. Organic matter digestion

As a further validation step to assess the extent to which visually identified particles may have included non-plastic organic debris, a subset of 18 samples was selected for further treatment. The subset was chosen to capture both representative and worst-case conditions: one sample was selected from each core in both 2022 and 2024 (n=14) to ensure spatial and temporal coverage, and four additional samples (two per year) were selected based on visual complexity, such as a high abundance of particles, variety of shapes or colours, for a total of 18 samples analyzed. Following the recommendations of Pfeiffer & Fischer (2020), two millilitres of 10% sodium hypochlorite (NaClO) were added to 10 mL borosilicate glass test tubes (Aldrich Essentials, Sigma-Aldrich) to digest any organic matter potentially misidentified as microplastics. The test tubes were placed in a sand bath inside the Fisher Isotemp Oven (100 series, model 126G) for 24 hours. The first 8 hours of the sand bath heated the samples to 40–50 °C, while for the following 16 hours the samples were kept at room temperature (20 °C). After digestion, the contents of each tube were filtered through a Whatman ME 25/21 ST 0.45-micron filter. Each tube was then rinsed twice with water to recover any remaining particles.

Filters were examined under a binocular microscope, and particle counts were compared to pre-digestion values. Minimal particle loss (defined as ≤10%) was observed in all treated samples across both years (ranging from 6–9%), consistent with procedural tolerances outlined by Pfeiffer & Fischer (2020) and recovery benchmarks reported in comparative methodology reviews (e.g., Hartmann et al., 2019; Tirkey & Upadhyay,

2021). As a result, no further digestion trials of the remaining samples were deemed necessary.

4.4.3. Quality control

To ensure data accuracy and minimize sample contamination, a multi-faceted quality control protocol was implemented. First, environmental contamination was controlled by undertaking all measurements in rooms with limited airflow to reduce the settling of airborne dust and fibres. Cotton clothing was worn, as cotton sheds natural fibers more easily distinguishable from synthetic microplastics. All glassware and metal equipment were washed thoroughly and air-dried under aluminum foil tents before use to prevent contamination from airborne particles during preparation.

Second, a procedural blank was created to quantify background contamination and assess the recovery efficiency of the extraction protocol. The sediment for this blank was sourced from a siliciclastic Quaternary deposit exposed near Fredericton, NB (46°07’21.00” N, 66°36’49.00” W). The sample was collected at a location away from plant roots, where undisturbed primary sedimentary ripples, interpreted as glaciofluvial deltaic, were preserved. To prevent modern contamination, the immediate surface was first excavated with a shovel to remove any potential recent air-derived plastic that might have infiltrated the sediment pore network before the sample was cored. Twenty-one particles of known household plastic types were cut and mixed into 0.1 kg of the dried, pre-screened glacial sediment presumed to be free of modern plastic contamination. The doped sample was then processed through the entire five-stage extraction protocol. All 21 doped microplastics were successfully recovered, demonstrating high recovery efficiency. In addition, six contaminant particles were

recovered across all steps, equating to a background contamination level of approximately 60 MPs/kg, or less than 5% of the average particle count in the 2022 environmental samples. As this was a minor level of contamination, results were not blank corrected (Dodson et al., 2020).

4.4.4. Omission of additional identification steps

The methodology presented here relies on clearly documented visual classification of microplastics (Section 1.1.3), which remains the most consistently described and accessible method in the literature for particles larger than 300–500 μm (Hidalgo-Ruz et al., 2012; Simon-Sánchez et al., 2022). Whereas instrumental confirmation of polymer identity using either FTIR (not available in our research facility) or Raman spectroscopy is often cited as a confirmatory procedure in microplastic studies, during the literature review process, it became apparent that many of these studies fail to include sufficient methodological detail for their spectroscopic analyses to be replicable. For example, Crichton et al. (2017), Expósito et al. (2021), and (Simon-Sánchez et al., 2022) all report the use of FTIR or Raman spectroscopy; however, none provide essential methodological details such as particle selection criteria, spectral resolution, match thresholds, or preprocessing steps. This lack of transparency represents a significant barrier to reproducibility and hampers progress toward the standardization of microplastic analysis protocols. Compounding this challenge, comprehensive and up-to-date Raman reference spectra were not readily available within the study's timeframe, increasing the risk that genuine plastic particles could be incorrectly classified. Given these limitations, alongside the unavailability of a

micro-FTIR instrument, neither Raman nor FTIR spectroscopy was employed in this investigation.

4.5. Statistical Tests

All statistical analyses were conducted in R (version 4.5.0) using the `stats` and `tidyverse` packages, with a significance threshold set at $\alpha = 0.05$. Given frequent small sample sizes, categorical groupings, outliers, and the presence of non-normal distributions, non-parametric statistical tests were used throughout.

To account for non-independence of vertically stratified depth increments within sample tubes, sediment parameters were aggregated into core summaries ($n = 7$ replicate cores per sampling year) prior to temporal analysis. Differences in median grain size (ϕ) and total microplastic abundance (MP/kg) between 2022 and 2024 were evaluated using non-parametric, unpaired Mann-Whitney U tests (wilcox.test).

5. Results

5.1. Sampling Overview

The tidal-transgressive beach was accessed on clear, sunny days in both years and was found to be relatively clear of macro-waste. Observed surface debris was rare, consisting primarily of structural wood likely from disintegrated lobster traps, scattered polystyrene (PS) foam possibly from floats, and various coloured elastic bands matching those traditionally used to secure lobster claws. This macro-waste material is interpreted to have been transported to the beach face by regional tidal currents, likely originating from the village of Alma or active commercial fishing grounds within Chignecto Bay.

Across both sampling years, the processed depth-interval samples represented a cumulative total sediment weight of 2,648.5 g. Subsequent laboratory application of the microplastic extraction methodology outlined in Chapter 4 yielded 150 microplastic-containing fractions from the 2022 dataset and 140 fractions from the 2024 dataset. Full high-resolution individual core records are compiled in Appendix C.

5.1.1. Sediment characteristics

Visual logging of the cores reveals no distinct sedimentary structures, such as laminae, crossbedding, or evidence of bioturbation. The only indication of any structure is graded bedding, mostly fining upward, rarely coarsening upward (See Appendix C for sedimentary core logs). Grain size analysis confirms that all samples are dominated by the sand fraction (Appendix C). The spatiotemporal patterns of grain size are demonstrated in Figure 5.1 and detailed in the following sections.

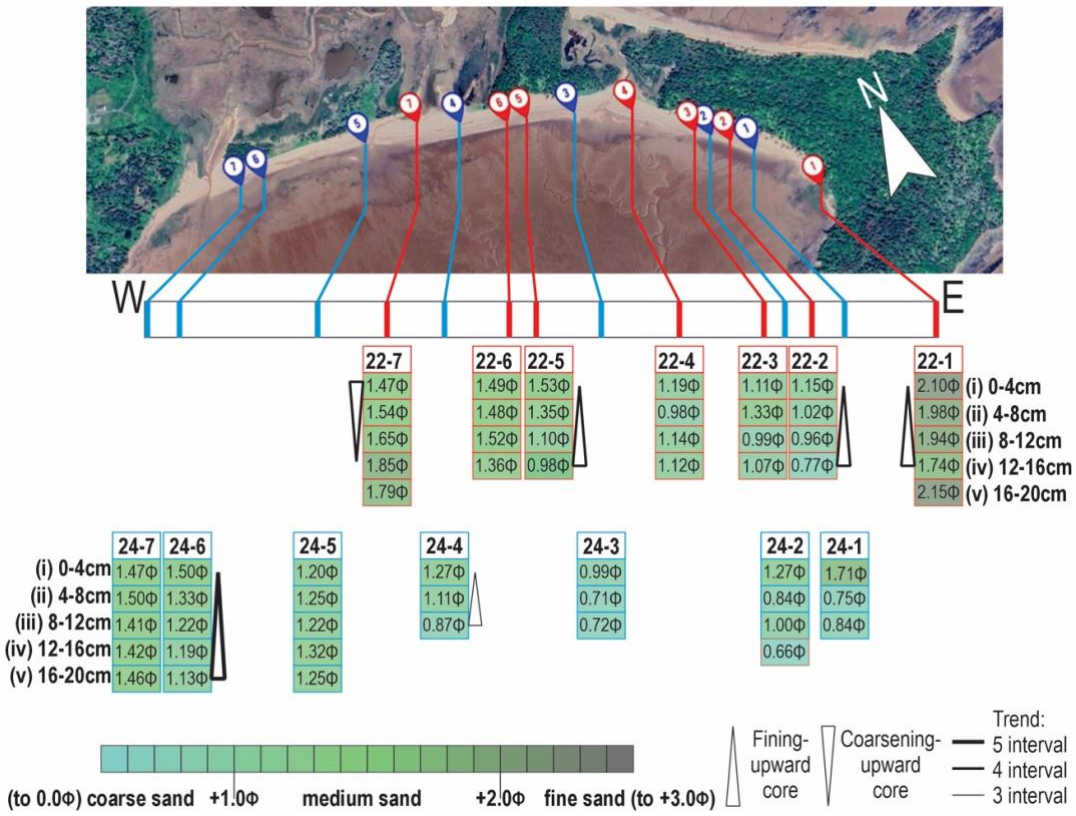

Figure 5.1. Core sample locations along the beach transect, with extrapolated heatmaps displaying mean grain size as a function of depth. Lighter colours represent coarser sediment (lower ϕ), and darker shades rrepresent finer material (higher ϕ). For descriptive display only; depth parameters were statistically aggregated by core to preserve strict data independence during temporal hypothesis testing (n = 14)

5.1.2. Temporal grain-size variation

The 2022 data show values ranging from 0.77 ϕ (22-2iv) to 2.15 ϕ (22-1v) with the mean grain size for all samples being 1.44 ϕ, a medium-grained sand. The 2024 sediment samples range from 0.66 ϕ (24-2iv) to 1.71 ϕ (24-1i) and have a mean grain size of 1.16 ϕ (Appendix C), a medium-grained sand. To account for the non-independence of vertically stratified depth increments sampled within individual cores, sediment parameters were aggregated into core summaries prior to inferential testing (n = 7 replicate cores per sampling year) by summing the weighted phi intervals and

calculating a mean grain size for each core. A Mann-Whitney U test performed on these independent core-level averages confirmed that overall mean grain size (ϕ) did not change significantly between 2022 and 2024 study periods (W = 33.5, p = 0.2769).

5.1.3. Spatial variation in grain size

Vertical grain size trends within the cores were generally subtle, with most down-hole variations spanning a range of less than 0.5 ϕ (Figure 5.1). While subsurface vertical variations are tracked stratigraphically via core logs (Appendix C), multi-dimensional spatial modeling of localized down-hole parameters remains beyond the exploratory scope of this baseline assessment. However, fining upward sequences were quantitatively observed across a few core fractions, most notably Core 22-2vi to i (1.31 to 1.72 ϕ), Core 22-5vi to i (1.58 to 2.09 ϕ), and Core 24-6v to i (1.64 to 1.99 ϕ).

Both sampling years display an overall westward-fining tendency along the western half of the shoreline. However, in 2022, the easternmost core (22-1, 064°38’59.70” W) is a very notable fine-grained outlier, with a mean grain size of 1.99 ϕ for the five samples – exceeding the upper outlier fence of 1.80 ϕ (1.5 x IQR Q_3). The next finest sediment for that year is the westernmost core. In 2024, the westernmost core (24-7, 064°39’05” W) contains the finest overall mean grain size (1.04 ϕ, outlier fence of 1.60 ϕ). The surface interval of the easternmost core in 2024 is also relatively fine, although deeper intervals at that location are coarser.

5.2. Microplastic abundance

A total of 1,806 microplastic particles were extracted from the 290 individual density fractions across the 58 samples between 2022 and 2024. Microplastic counts in

these samples were highly variable. The minimum abundance observed was 8 microplastics, recovered from 0.0745 kg of sediment in sample 24-4ii (107 MP/kg, or 0.107 MP/g), while the maximum observed was 88 microplastics, recovered from 0.0448 kg of sediment in sample 22-2i (1,964 MP/kg = 1.964 MP/g). The spatiotemporal distribution of this pollution is visualized in Figure 5.2 and detailed in the subsequent sections.

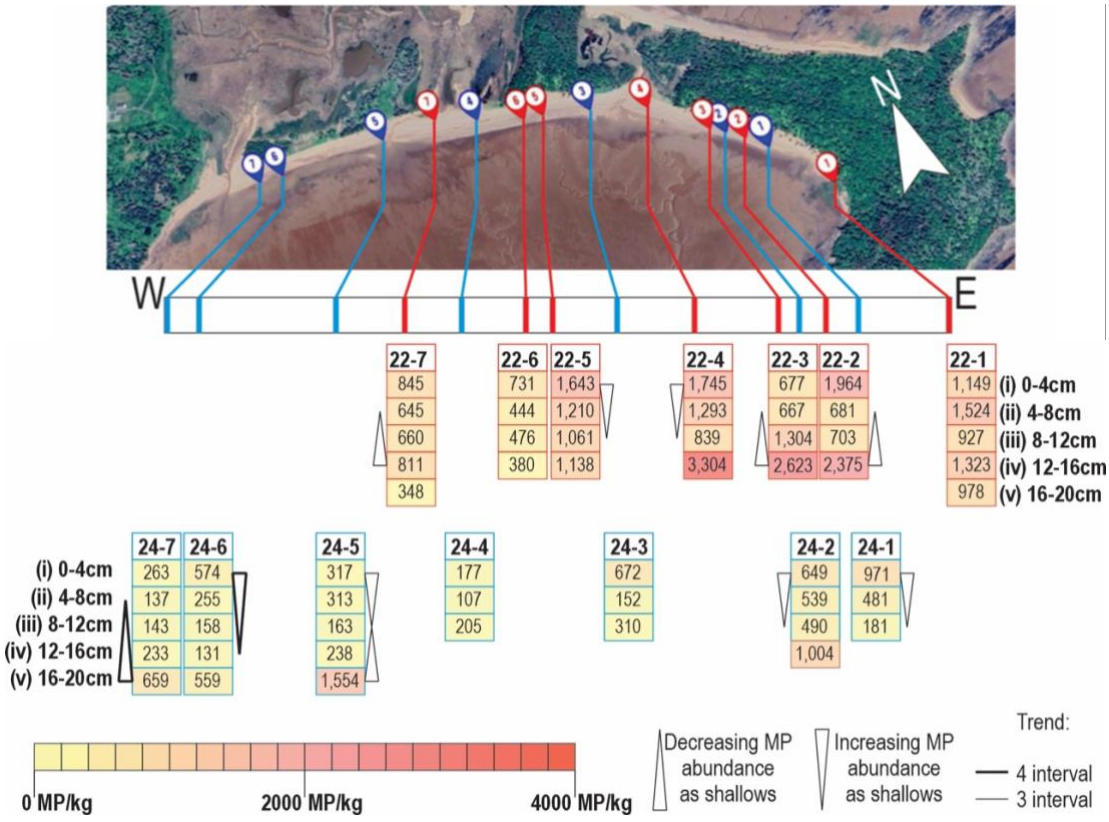

Figure 5.2. Spatiotemporal distribution of microplastic abundance (MP/Kg) by core and depth for (a) 2022 and (b) 2024. Cores are arranged along a relative west-to-east transect for each sampling year. Each cell represents the number of microplastic particles per gram recovered from a 4 cm sediment interval. Note that core numbers represent relative position only and are not co-located between years. The colour scale is standardized across both panels to allow for direct comparison of the overall abundance patterns, highlighting the higher concentrations found in 2022. This figure is for descriptive display only; depth parameters were statistically aggregated by core to preserve strict data independence during temporal hypothesis testing (n = 14)

Samples from 2022 contain a total of 1,254 microplastic particles, compared to 552 in 2024. This corresponds to a mean concentration of 990.8 ± 60 MP/kg in 2022 versus 343.5 ± 60 MP/kg in 2024. To evaluate annual baseline variations while maintaining data independence, total particle counts per core were divided by total core weights to generate a single independent concentration value per core (n = 7 per year). An unpaired Mann-Whitney U test executed on these independent core concentrations confirmed a highly significant temporal decline in overall microplastic abundance from 2022 to 2024 ($W = 47.0$, $p = 0.0023$).

5.2.1. Temporal Variation

This temporal shift was not uniform across all density fractions. The decrease in microplastics between the two years was most pronounced in the higher-density fractions. For example, the combined count of the higher density fractions (MDP, HDP, and VHDP) decreased from 812 particles in 2022 to 326 in 2024, a 60% reduction. In contrast, the lower-density fractions (VLDP and LDP) saw a smaller relative decrease from 442 to 226 particles, a 49% reduction. In 2022, the highest recovery came from the VHDP fraction (n = 435, 35%), whereas in 2024, the VLDP fraction yielded the most particles (n = 141, 26%). Descriptive separations show an asymmetric reduction heavily favoring high-density polymer tiers (MDP, HDP, and VHDP; 60% reduction), while true multi-group non-parametric multivariate modeling remains an avenue for future work.

5.2.2. Variation of microplastic characteristics

Fibres were the dominant microplastic shape in both 2022 (92.3%) and 2024 (92.0%), followed by films (4.9% and 3.8%) and fragments (2.9% and 2.9%). A small

number of fibre balls were identified in 2024 (1.3%) (Figure 5.3). Particle shape showed clear associations with particle density based on visual observations. Films were recovered almost exclusively from lower-density fractions (VLDP and LDP), while fragments were found predominantly in higher-density fractions (HDP and VHDP). Fibres occurred across all fractions but were most numerous in the VLDP and VHDP groups. Depth patterns were also evident in 2024: films were more common in shallow layers (4–8 cm), whereas fibre balls tended to appear in deeper layers (12–16 cm).

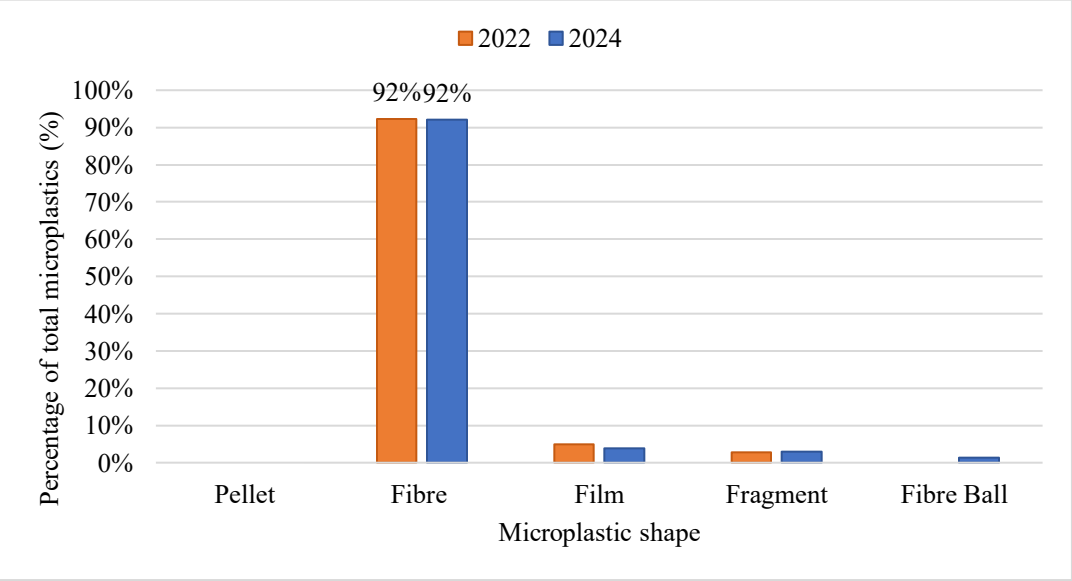

Figure 5.3. Relative abundance (%) of microplastic shapes (pellets, fibres, films, fragments, and fibre balls) recovered from sediment samples in 2022 and 2024, highlighting the consistent dominance of fibres across both sampling years.

The colour profile of recovered particles was consistent across the sampling period (Figure 5.4). The most prevalent colours were white/clear (49.0% in 2022, 44.2% in 2024), black (22.0% in 2022, 27.2% in 2024), and blue (14.4% in 2022, and 17.6% in 2024). Particle colour was strongly associated with density. In both years, black particles were disproportionately recovered from the densest (VHDP) fraction, while white/clear and blue particles were most numerous in the lower-density VLDP and LDP fractions. In contrast to shape, no significant associations were found between colour and either sediment depth of lateral position along the beach transect. See Appendix B, Table B3 for detailed cross-tabulations.

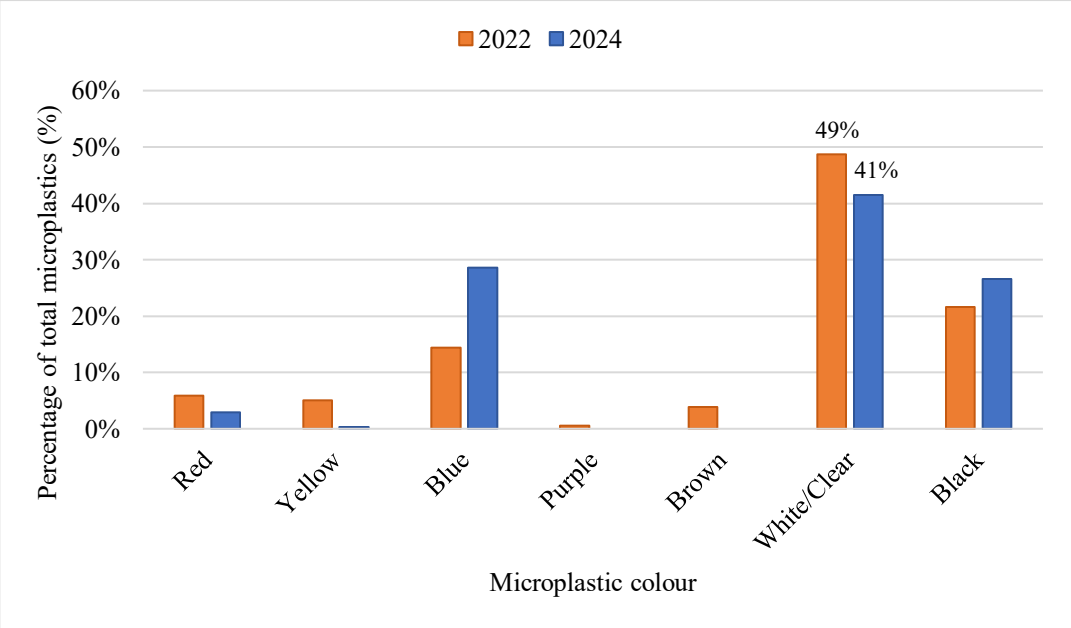

Figure 5.4. Relative abundance (%) of microplastic colours identified in 2022 and 2024, showing a stable colour profile between years with white/clear, black, and blue particles being the most prevalent.

6. Discussion

This discussion interprets the spatial and temporal baseline trends of clastic sediments and microplastic contaminants captured at Mary's Point. To provide a holistic geomorphic context, this chapter first models the hydrodynamic mechanisms and episodic cyclonic shocks driving baseline sorting across sampling years. Second, a quantitative synthesis of global high-density extraction literature is deployed to benchmark the scale of Mary's Point contamination within a global context. Finally, the distributions of recovered polymers are cross-examined to trace basin-wide provenance pathways and assess bioavailability constraints within the wider coastal food web.

6.1. Sediment Characteristics

When clastic datasets are properly aggregated into independent core summaries ($n = 14$) to account for vertical stratification within sample tubes, the overall beach face exhibits no statistically significant temporal variation in mean grain size ($p = 0.28$). High-energy storm events frequently induce significant net coarsening on exposed beaches through wave-driven winnowing of fine fractions (e.g., Lo et al., 2020; Misic et al., 2019). In the case of Mary's Point, the close proximity of the passing post-tropical cyclones Fiona (September 2022) and, particularly, Hurricane Lee (September 2023), might be expected to be primary agents of change (Fig. 6.1). However, although an increase in mean grain size (from +1.44 ϕ to +1.16 ϕ) occurs between the two sampling years, the increase is not statistically significant and the sand matrix at Mary's Point maintained its baseline medium-sand classification.

The lack of any significant change in grain size between 2022 and 2024 could relate to one or more of several factors. While bed shear stresses were sufficient to mobilize surface layers and truncate overlying sediment thickness, hydrodynamic energy may not have exceeded the threshold required to fundamentally alter the bulk grain-size distribution of the clastic matrix (e.g., Lo et al., 2020; Misic et al., 2019). The 2022 beach survey does not represent a pristine, pre-storm baseline; the system had also been impacted by preceding events such as hurricanes Dorian (late August 2019), Teddy (mid-September 2020), Elsa (early July 2021), and Ida (late August 2021) that passed through Maritimes Canada slightly further away from Mary's Point in the preceding years (Culligan et al., 2022; Georgiou et al., 2023) (Figure 6.1).

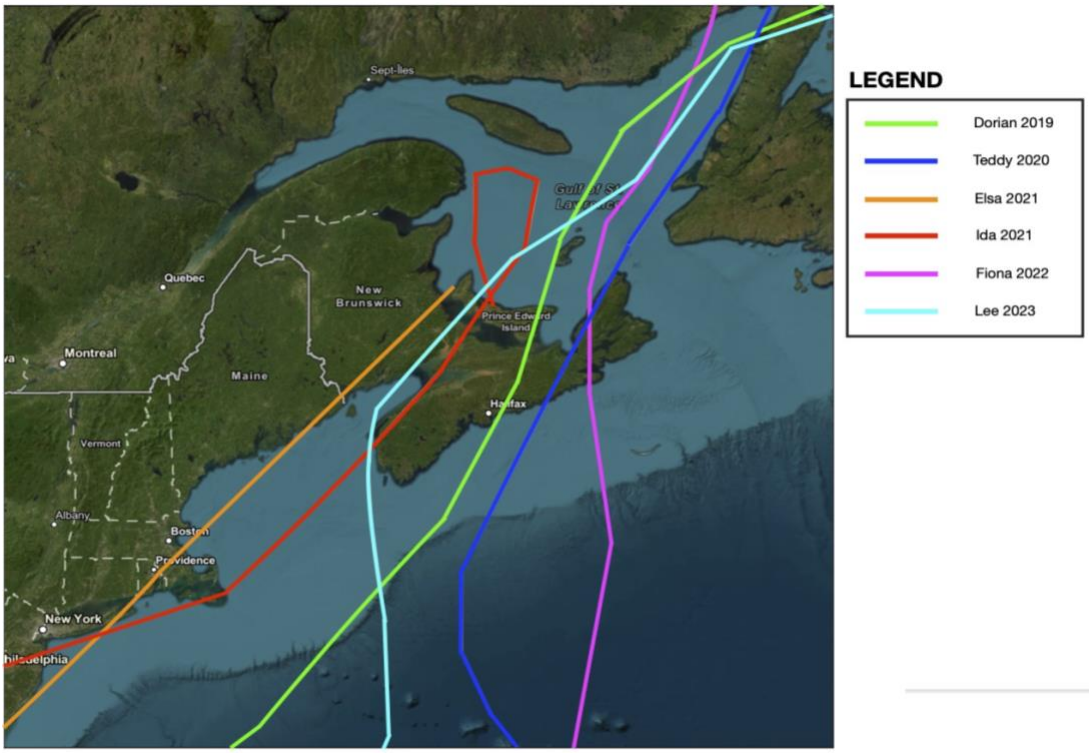

Figure 6.1. NOAA Historic Hurricane tracks showing hurricanes passing through a 180 Nautical Mile radius of Mary's Point, NB, Canada from 2019 to 2023.

Factors affecting only part of the beach may also play a role. The storms also may have introduced new sediment into the system. Associated storm surges can erode and undercut adjacent unconsolidated cliffs and dunes in the backshore, triggering mass movement events that deliver a fresh supply of sediment to parts of the beach. Depending on the granulometry of the eroded source material, cliff input can either promote localized coarsening or supply finer fractions that buffer and preserve overall grain-size equilibrium across the intertidal zone. Although the backshore cliffs west of Mary's Point were not sampled prior to permit expiration, this interplay between wave winnowing, cliff erosion, and subsequent tidal reworking illustrates the geomorphic resilience of the Mary's Point sand matrix.

Laterally, in both years, the beach exhibits a broad westward-fining trend in grain size, together with a localized, anomalous hotspot of fine-grained sediment at its easternmost end. The dominant westward-fining trend is consistent with a classic longshore drift system driven by the prevailing high-energy waves entering the embayment of Mary's Cove and the New Horton Flats from the southeast, south, and southwest (Figure 6.2b). As these waves strike the beach at an oblique angle, they generate a westward-flowing longshore drift that sorts sediment along the shoreline. The higher energy in the eastern and central section's transports both coarse and fine material, but as the drift progresses westward and its energy dissipates, its carrying capacity diminishes. This causes coarser particles to be deposited first, while finer particles remain in transport longer and are deposited further west, creating the observed fining-to-the-west pattern.

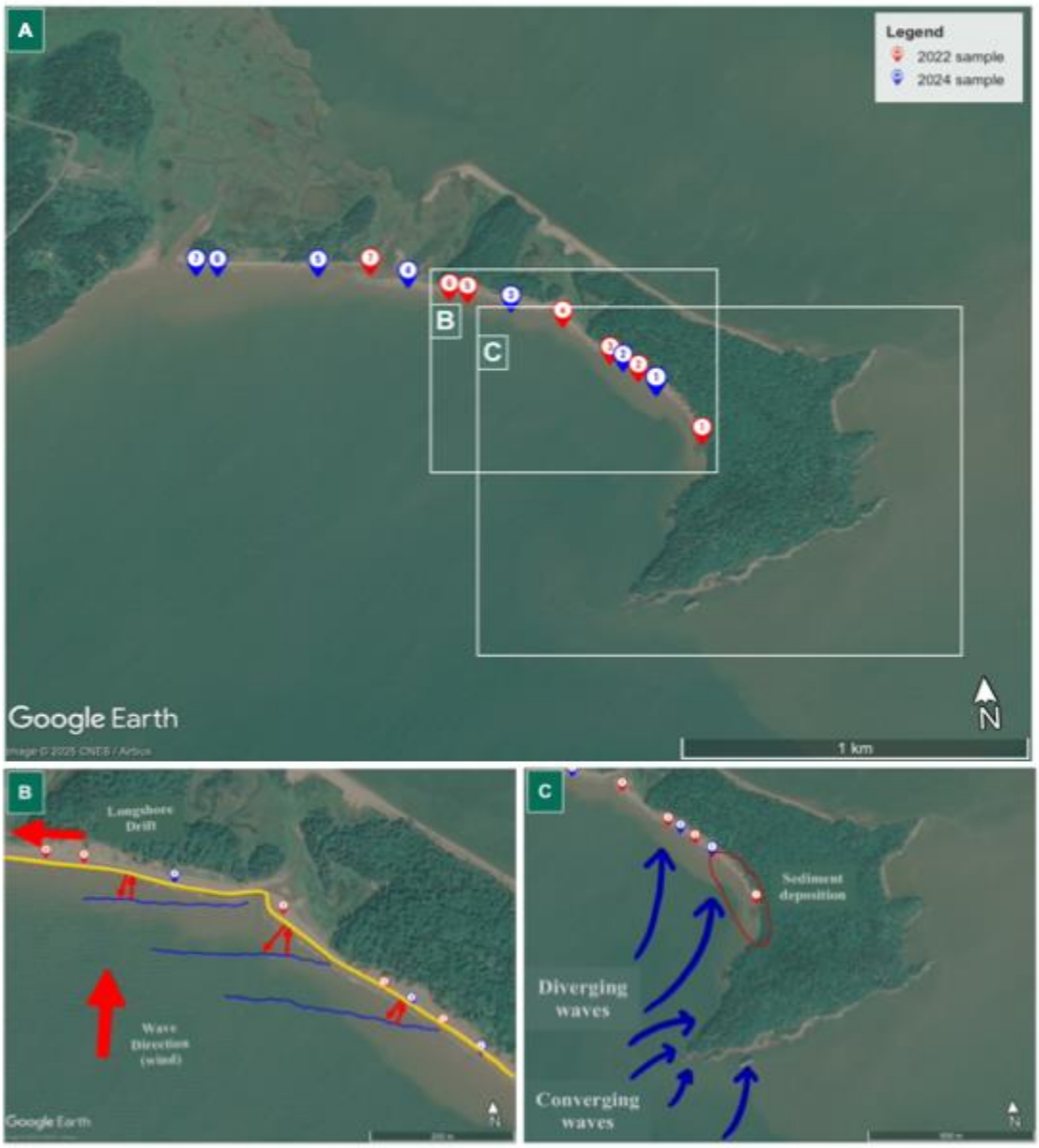

Figure 6.2. (a) Hydrodynamic processes at the study site, shown on satellite imagery from Google Earth. (b) The dominant southwest wave approach (blue line) relative to the shoreline (yellow line), indicating the potential for westward longshore drift (red arrows); (c) Wave diffraction around the eastern headland, which creates a sheltered, low-energy zone at the eastern end of the beach.

The formation of the fine-grained hotspot at the eastern end of the beach is explained by a combination of primary and secondary hydrodynamic processes. The primary mechanism is hydraulic sheltering, where the headland of Mary's Point

physically blocks and refracts the dominant southeasterly to southwesterly waves (Figure 6.2c). This creates a “wave shadow” zone at the immediate western edge of the headland, a region of hydrodynamic quiescence that drastically reduces wave energy and creates a sheltered environment suitable for deposition (Debrot et al., 1999).

While the dominant energy comes from the southwest, wind and waves approaching from the west or northwest would only have a very short fetch while travelling across Mary’s Cove, generating only a very weak, eastward-directed longshore drift. This current would only be capable of transporting the finest sediments (silt and clay), which would then be trapped against the natural barrier of the eastern headland, further contributing to the hotspot. Therefore, the eastern hotspot is likely a product of both hydraulic sheltering from the dominant wave climate and the accumulation of fine sediments transported by secondary, opposing longshore drift.

Tidal processes may also play a role, although the sampled section of the beach is only influenced by wave activity during high water, when tidal currents are minimal and flow velocities are reduced. Under these conditions, any residual tidal currents passing the headland tend to separate from the coastline, forming a slow, recirculating eddy in their lee (Guo et al., 2020). This low-velocity zone acts as a highly efficient sediment trap, creating a proximal sink for suspended particles that would otherwise remain in transport (Georgiou et al., 2023; Guo et al., 2020). Fine particles suspended in the water column, either brought in by tides or stirred up by wave action further offshore, can easily settle out in this calm, sheltered pocket (Debrot et al., 1999; Guo et al., 2020). This process, driven by tidal asymmetries that promote net sediment transport

into low-energy areas, explains why the very start of the longshore transport cell is paradoxically a depositional sink for fine material (Cheng et al., 2020).

Vertically, most cores show no systematic variation in sediment structure, (Figure 5.1). Fining-upward successions observed in some intervals may indicate gradual energy reduction during storm waning or slack high tide, whereas rare coarsening upward trends could signal sudden increases in energy, such as storm onset. Depending on the grain size of the unconsolidated cliffs and dunes in the backshore, mass movement, particularly grain flows or grain fall common in dry, unconsolidated sand may have contributed to either the fining- or coarsening-up. Overall, the discontinuous grading is consistent with high-energy coastal systems where episodic storm events dominate sediment reworking and disrupt any subtle sediment stratigraphic signals that might form during calmer periods (Misic et al., 2019; Flores-Cortés et al., 2022).

In several locations, particularly near the centre of the transect, coring was halted by a compact, resistant pebble layer that may be the relict glacial till, or post-glacial tidal gravel noted by Amos & Zaitlin (1991). This layer was encountered at a shallower depth in 2024 than in 2022, suggesting that the overlying sediment column was truncated by erosion during recent high-energy events. This truncation is consistent with the combined influence of storm waves and longshore drift: storms amplify wave energy, which scours upper sediment layers while accelerating the westward sediment transport along the shoreline. In this context, the observed erosion reflects both vertical removal of sediment and lateral redistribution driven by longshore currents during storm conditions.

Finally, the role of biogenic reworking (bioturbation) must be considered as a potential mechanism for modifying sediment structure. While visual logging of the cores revealed no distinct sedimentary structures or trace fossils such as burrows, the absence does not necessarily indicate that bioturbation was absent. Instead, it may reflect the complete obliteration of such features by biological activity. In intertidal systems, bioturbation can rapidly destroy sedimentary fabric and eliminate evidence of graded bedding or other structures within hours, mixing sediment and reducing the distinction of depositional layers (Keighley & Pickerill, 1995; Misic et al., 2019).

6.2. Microplastic Abundance and Distribution

6.2.1. Temporal and Spatial Variability

The major temporal finding of this study is the statistically significant decrease ($W = 47.0$, $p = 0.0023$) in microplastic abundance between 2022 and 2024. Variation in methodology can be excluded as an explanation. The only procedural change was that black PVC pipes were used for storing the 2022 samples, in contrast to aluminum trays in 2024, but microscopic analysis of the 2022 samples did not reveal an anomalous abundance of black, angular fragments that would be expected from PVC abrasion in the 2022 samples. Likewise, no documented change in fishing practices, clean up campaigns, leakage management, etc. has been reported to my knowledge and, given that global plastic production and input into marine environments is increasing, the major finding is unlikely to reflect a true reduction in regional pollution (Culligan et al., 2022).

Numerous studies have documented that high-energy events, such as storms and typhoons, can flush microplastics from coastal systems by resuspending surface sediments and redistributing particles (Balthazar-Silva et al., 2020; Lo et al., 2020; Lefebvre et al., 2021; Vermeiren et al., 2021; Pervez & Wang, 2022). For example, Lo et al. (2020) showed that storm-deposited sediment layers became significantly coarser following Typhoon Mangkhut as a result of onshore over wash and intense offshore wave activity. At Mary's Point, storms comparable to Hurricanes Fiona and Lee mobilized surface sand layers. Rather than rearranging the bulk mineral grain distribution, these high-energy hydrodynamics winnowed out the light, high-drag synthetic clast fraction (specifically the flexible secondary microfibres) and flushed them offshore. This process purged the active intertidal sediment budget of its lightweight plastics while leaving the mean bulk grain size profile statistically stable ($p = 0.28$), a relationship consistent with findings on the role of energetic events in flushing microplastics from coastal systems (Vermeiren et al., 2021; Pervez and Wang, 2022).

Inconsistent microplastic abundance along beach transects is a finding common in beach studies because local factors create high variability, likely in time as well as space (Lots et al., 2017; Lefebvre et al., 2021; Dimante-Deimantovica et al., 2023). This suggests that microplastic inputs at Mary's Point are relatively diffuse, or that dynamic surface processes including wave swash and longshore drift, or bioturbation, continually homogenize their horizontal distribution (Seemungal et al., 2022). Higher concentrations in microplastic abundance at deeper depth intervals (12–16 cm, 16–20 cm), suggest that surface layers act as the primary zone of deposition susceptible to erosion and redistribution. Deeper layers may retain older, buried particles that were incorporated

and retained from past depositional events but also accumulate microplastic originally entrained in swash that subsequently seeps into the sediment or is washed down by percolating rainwater or snow melt.

At least three additional conflating factors can be considered. First, wind (aeolian transport) plays a crucial role in sorting surficial microplastics, preferentially reworking smaller or less dense particles, such as fibres and films, from the intertidal zone to the backshore and creating distinct accumulation patterns (Moreira et al., 2016; Turner et al., 2020; Şener & Yabanli, 2023). Second, storms may have locally removed the uppermost layers where microplastics initially accumulate. In both years, cores from the central part of the beach penetrate to the same point in the subsurface, just above the coarse lag deposit, but the thickness of overlying sediment differs (Figure 6.3).

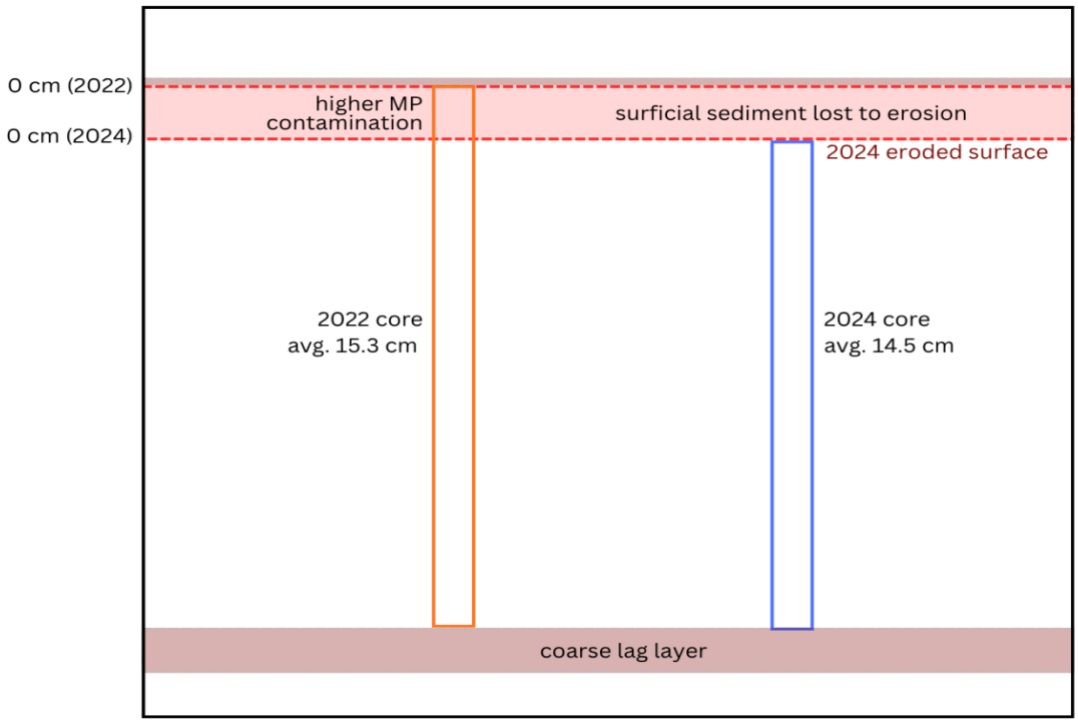

Figure 6.3. Conceptual sketch illustrating the effect of surface erosion on apparent core depth between 2022 and 2024.

In 2022, cores penetrated to a mean depth of 15.3 cm, whereas in 2024 they penetrated to a mean depth of only 14.6 cm, likely due to erosion washing away upper sediment layers. Although the 2024 cores contained less sediment overall, their lower mean MP/kg value may reflect the removal of the typically more highly contaminated surface layer, which was likely stripped away by erosion before sampling. Third, large volumes of microplastic-free Quaternary sediment can be delivered to the beach by storms and wave action that erodes backshore cliffs, such as near cores 1–3 and 5–6 in 2022 and cores 1-2 in 2024. This influx dilutes microplastic concentrations on a per-gram basis, even when mixed into the existing beach by wave reworking and bioturbation, demonstrating how local geology can override large-scale transport patterns in determining final depositional signatures (Figure 6.4) (Culligan et al., 2022)

6.2.2. . Microplastic Characteristics: Density, Shape and Colour

As discussed in Section 5.3.1, the temporal shift was not uniform across all density fractions. Descriptive separations show an asymmetric reduction heavily favoring high-density polymer tiers (MDP, HDP, and VHDP; 60% reduction), while multi-group multivariate modeling remains an avenue for future work. These patterns are consistent with expected hydrodynamic behavior: lower-density particles, particularly VLDP, are more mobile and more easily transported in the water column, whereas higher-density particles (HDP and VHDP) behave as bedload and may remain locally or become buried.

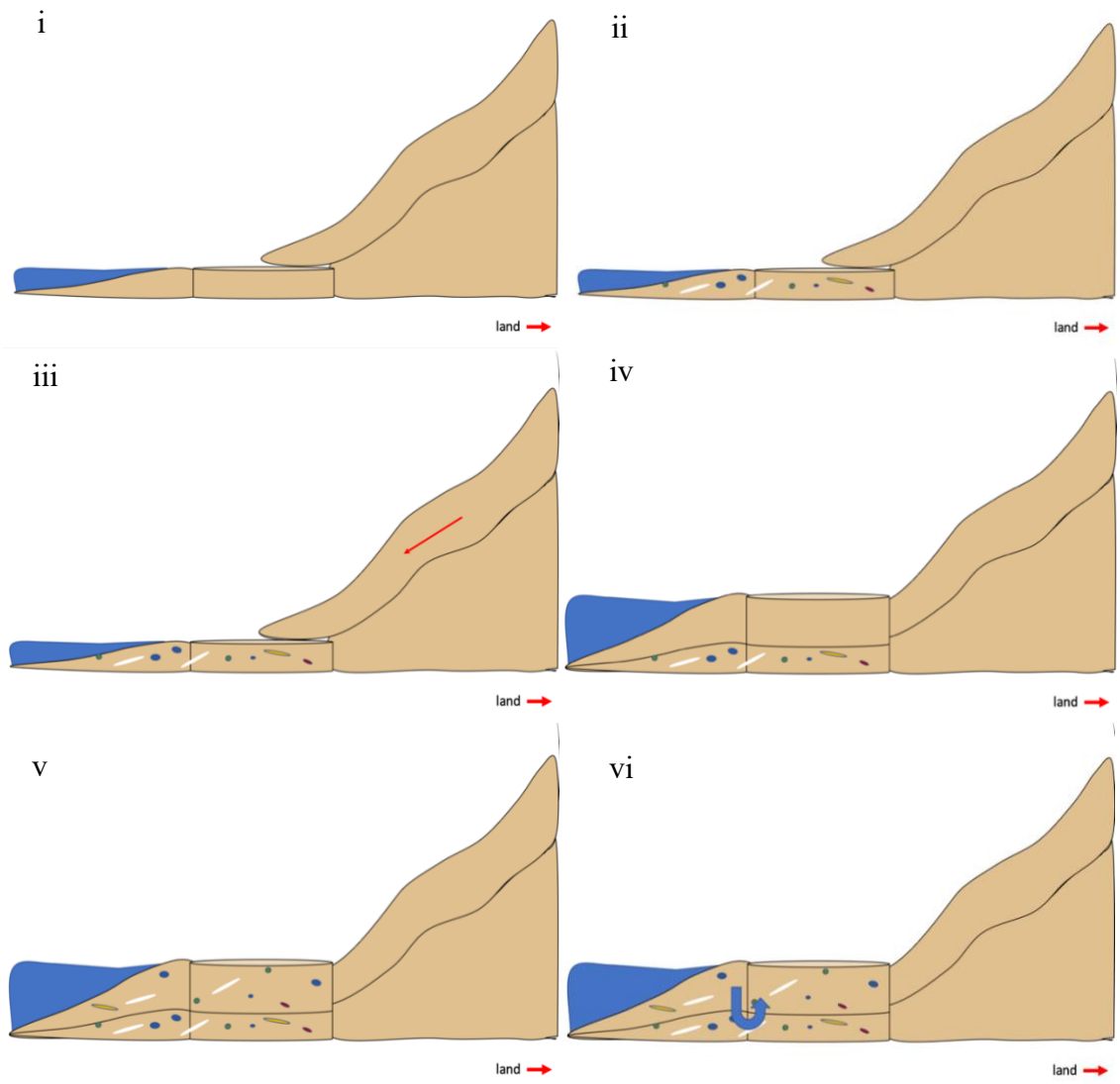

Figure 6.4. Schematic showing the dilution of microplastic contamination in the upper sedimentary layers. (i) initial environment, (ii) constant rate of microplastic accumulation from various sources, (iii) slope stability breached on backshore, (iv) increased sediment load deposition, (v) constant rate of microplastic accumulation from various sources, (vi) bioturbation and sediment reworking.

Fibres dominate the microplastic assemblage at Mary's Point, accounting for over 90% of total particles in both years. This finding aligns with many global beach sediment studies, where fibres frequently emerge as the most common shape due to their widespread use in textiles and fishing gear; their ability to bypass wastewater filtration;

and their physical properties that enable long-range transport (Hengstmann et al., 2017; Godoy et al., 2020). A review of 38 recent studies (Figure 6.5) illustrates that fibres were the most abundant shape in 19 cases, followed by fragments/foam (17 studies), and pellets/granules (2 studies).

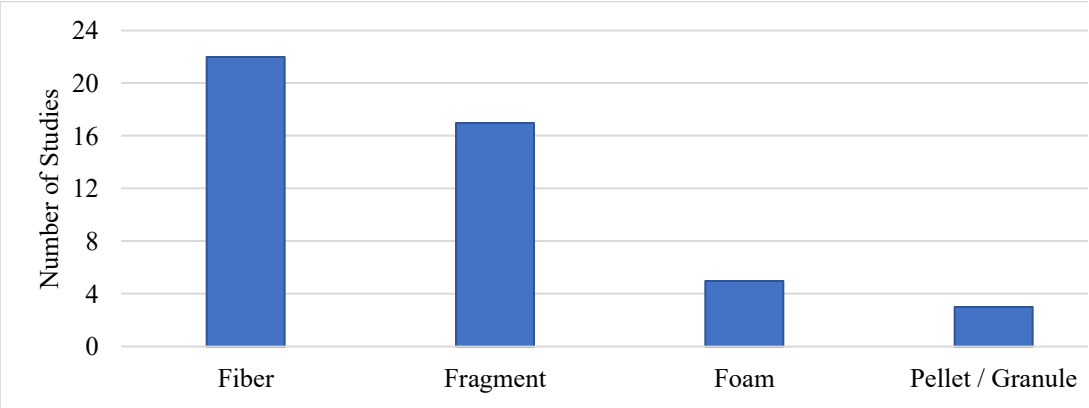

Figure 6.5. Frequency of dominant microplastic shapes reported in global beach and coastal sediment literature from recent studies (n=38). The chart illustrates the number of studies in which fibres, fragments, foam, or pellets were identified as the most prevalent shape Note: In cases where two shapes were reported as equally dominant (e.g., fibre and fragment in Godoy et al., 2020), the study was included in the count for both categories. (Ballent et al., 2016; Retama et al., 2016; Lots et al., 2017; Hengstmann et al., 2018; Koongolla et al., 2018; Li et al., 2018; Lo et al., 2018; Zhang et al., 2018; Zhao et al., 2018; Ghaffari et al., 2019; Sathish et al., 2019; Tziourrou et al., 2019; De-la-Torre et al., 2020; Godoy et al., 2020; Nguyen et al., 2020; Prarat et al., 2020; Rahman et al., 2020; Carvalho et al., 2021; Hossain et al., 2021; Jualaong et al., 2021; Manbohi et al., 2021; Schröder et al., 2021; Veerasingam et al., 2021; Wu et al., 2021; Abidli et al., 2022; Asensio-Montesinos et al., 2022; Gao et al., 2022; Jones et al., 2022; Kaviarasan et al., 2022; Nhon et al., 2022; Pervez & Wang, 2022; Terzi et al., 2022; Zhang et al., 2021; Khaleel et al., 2023; Le et al., 2023; Şener & Yabanli, 2023; Tasnim et al., 2023; Arjun et al., 2024; Bobchev et al., 2024; Borah et al., 2024; Gül, 2024; Hamdy et al., 2024; Piyumali et al., 2024).

Fibres dominate the microplastic assemblage at Mary's Point, accounting for over 90% of total particles in both years. This finding aligns with many global beach sediment studies, where fibres frequently emerge as the most common shape due to their widespread use in textiles and fishing gear; their ability to bypass wastewater filtration; and their physical properties that enable long-range transport (Hengstmann et al., 2017; Godoy et al., 2020). A review of 38 recent studies (Figure 6.5) illustrates that fibres were the most abundant shape in 19 cases, followed by fragments/foam (17 studies), and pellets/granules (2 studies).

However, fibres are also among the hardest to identify reliably. They are highly susceptible to airborne contamination and visually ambiguous under microscopy, creating the potential for overestimation in studies that rely exclusively on visual identification (Löder & Gerdts, 2015; Lusher et al., 2015; Schröder et al., 2021; Simon-Sánchez et al., 2022). In contrast, fragments and films were present in much lower proportions, a trend often linked to differential transport dynamics and rapid degradation into particles below the detection threshold (Misic et al., 2019; Nabizadeh et al., 2019). The near absence of primary microplastics such as pellets further suggests that contamination at Mary's Point originates mainly from secondary breakdown of larger items rather than direct industrial discharge (Laglbauer et al., 2014).

Clear associations between particle density and shape (films in VLDP & LDP, fragments in HDP & VHDP) suggest that particle shape and density influence how microplastics are distributed vertically within the sediment column. This pattern supports the interpretation that lighter, more flexible shapes remain concentrated near the surface where they are easily reworked by the waves and wind, while denser, more

compact shapes behave similarly to mineral grains and are more readily incorporated into deeper, older layers.

Colour profiles were dominated by white/clear, black, and blue particles, hues commonly associated with synthetic textiles and fishing gear (Andrady, 2011; Lots et al., 2017). The prevalence of darker, weathered colours indicates aged plastics transported over long distances rather than recent local litter (De-la-Torre et al., 2020; Hernández-Sánchez et al., 2021). Combined with the scarcity of fragments typical of recreational waste, this points to diffuse marine sources rather than immediate beach-based activity (Browne et al., 2011; Napper & Thompson, 2016).

Laundry-derived greywater is a major source of microplastic pollution in the Greater Moncton region, as synthetic textiles such as polyester and nylon shed millions of microfibres during routine wash cycles (Ocean Wise, 2021; TransAqua, 2024). Although the TransAqua wastewater treatment facility removes most suspended solids through secondary biological treatment, municipal systems are not designed to capture microplastics (Bodzek et al., 2024). Consequently, even with high removal efficiencies, the facility's capacity (up to 143 million litres per day) allows millions of microfibres to bypass filtration and enter the Petitcodiac River and, ultimately, the Bay of Fundy (Vandermeer, 2023). Fibres that are successfully removed often accumulate within sewage sludge; when these biosolids are applied to agricultural land, rainwater runoff can reintroduce microplastics into the watershed, eventually transporting them to marine environments (Ocean Diagnostics, 2024; Sustainability Directory, 2025).

Overall, the assemblage reflects a pollution signal shaped by regional household and fishing activity, along with global transport processes. Fibres and other buoyant

polymers likely also arrive via ocean currents and atmospheric fallout, while biofouling and storm-driven mixing promote burial of denser particles at depth (Ballent et al., 2016; Yang et al., 2021). This dynamic interplay underscores the role of Mary's Point as a sink for long-range plastic pollution rather than a hotspot of local input.

A broader ecological consideration links these sedimentary findings back to the biosphere: microplastics recovered from Mary's Point beach are not confined to the substrate but actively enter coastal food webs. Shorebirds, including the Semipalmated Sandpiper, routinely ingest sediment incidentally while foraging, and because microplastics are present in both the water column and benthic sediment, they can be consumed directly or indirectly through prey items such as amphipods, molluscs, and small crustaceans. Global syntheses confirm that many marine taxa ingest microplastics, with clear differences among groups in the types of particles taken up; for example, Marma et al. (2023) report that some taxa disproportionately ingest fibers while other ingest more films, reflecting variation in feeding mode, habitat, and particle availability. These patterns underscore that the overwhelmingly fibre-dominated assemblage at Mary's Point beach is not only a sedimentary signal, but also the type of particle most likely to be transferred through tropic pathways. Thus, the persistence and redistribution of microplastics on the beach have direct implications for wildlife in this internationally significant migratory stopover, reinforcing the need to evaluate contamination not only as a physical sedimentary phenomenon, but as a biologically relevant stressor within the coastal ecosystem.

6.3. Mary's Point Microplastic Pollution in a Global Context

The microplastic abundances at Mary's Point are best understood when placed in the context of global beach sediment studies. Two histograms illustrate how reported microplastic abundances vary across global beach-sediment studies (Figure 6.6). The first histogram shows studies that relied on low-density NaCl extraction; the second, those that employed higher-density solutions capable of recovering a wider range of polymers. The NaCl-based extractions tend to cluster at lower reported concentrations, reflecting systematic under-recovery of denser polymers such as PET and PVC. This highlights a critical point: if a less comprehensive method, such as simple NaCl flotation, had been employed, the reported abundance at Mary's Point would have been considerably lower. Less than 45% (33.1% in 2022, and 44.2% in 2024; equivalent to 415 and 244 MPs, respectively) of total microplastics were recovered in the initial low-density steps (Lots et al., 2017; Stolte et al., 2015; Zhang et al., 2020; Zobkov & Esiukova, 2018).

(a)

(b)

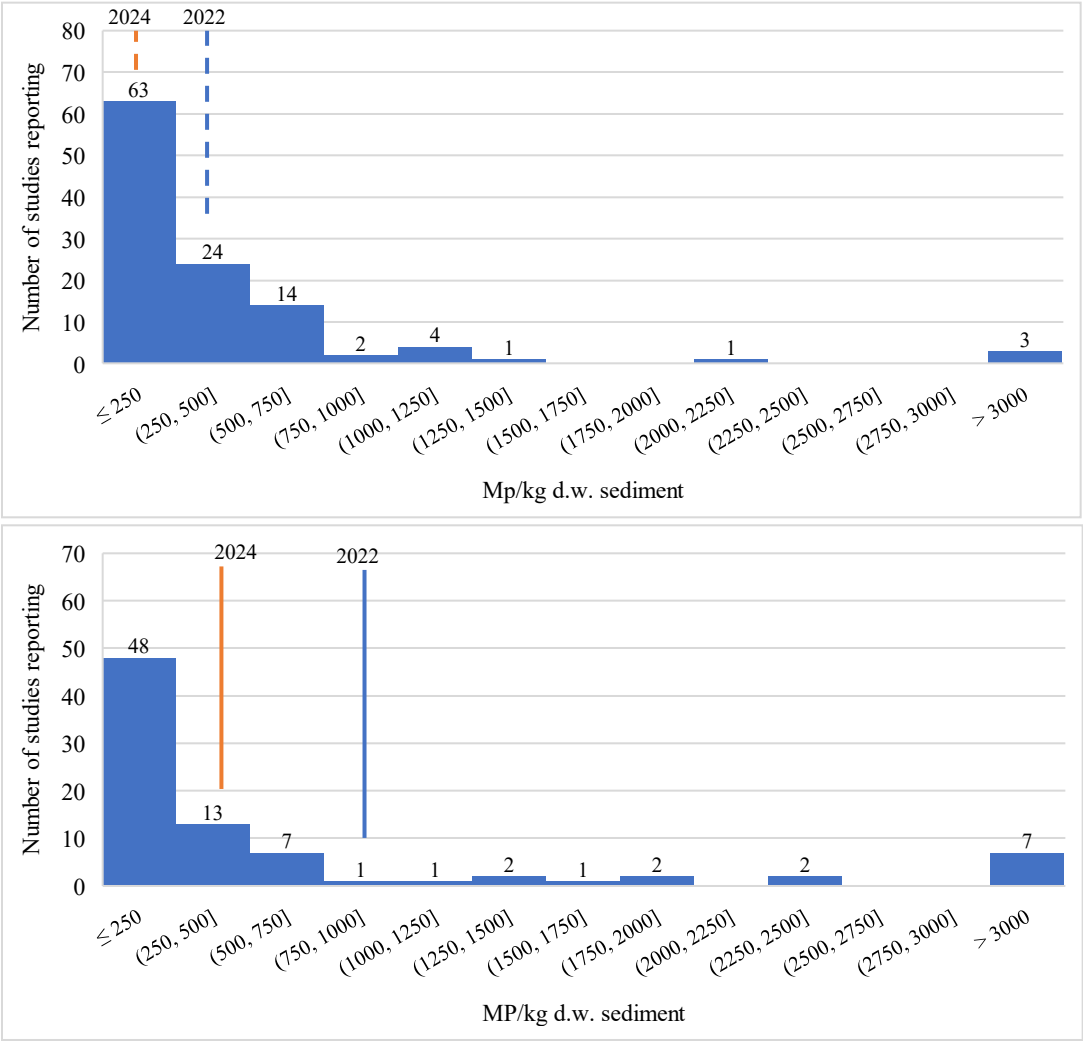

Figure 6.6. Global distribution of microplastic abundances (MP/kg) reported in beach-sediment studies between 2011 and 2024 (see Appendix D, Table D1). Studies are grouped into 13 bins of 250 MP/kg, with the final bin representing values > 3000 MP/kg. Panel (a) includes studies using low-density NaCl extraction (n = 112; ~1.18 g/cm^3), while panel (b) includes studies using higher-density extraction solutions (n = 84; e.g., $CaCl_2$, $ZnCl_2$, NaI, NaH_2PO_4). Vertical lines indicate mean microplastic abundance at Mary's Point: solid lines in panel (b) represent values derived from the full multi-step extraction protocol used in this study, whereas dashed lines in panel (a) show where the same samples would plot if only NaCl extraction had been employed.

Studies using higher-density extraction methods (Figure. 6.6b and this thesis) exhibit a broader and often higher distribution of MP/kg values reflecting greater extraction efficiency and, in some regions, also likely genuinely elevated contamination.

When compared against a box-and-whisker distribution of 201 beach studies that used high-density based extraction from 2011–2024 (Figure 6.7), the independent core concentration boundaries provide clear baseline benchmarks. In July 2022, the baseline rank median sits noticeably above the global upper quartile (Q_3 = 562 MP/kg) compiled from high-density extraction literature, identifying the beach as an elevated depositional zone during quiet climatic intervals. Conversely, following the scouring shocks of late 2023, the 2024 median contracts firmly down into the global interquartile range (Q_1–Q_3), matching moderate baseline signatures documented worldwide. These comparisons provide a useful visual benchmark, but their interpretive power is still limited by methodological inconsistencies across studies. Published density extraction studies vary widely in maximum density of the solution used, pre-treatment steps, solution toxicity, and whether organic matter was digested or denser polymers targeted (Zheng et al., 2021).

Building on this methodological context, the abundance of microplastics at Mary's Point beach, particularly in 2022, is comparable to or even exceeds that of several moderately impacted coastal areas when assessed using similarly rigorous, high-density extraction protocols. The findings also confirm that a site's protected status offers no immunity from pervasive plastic pollution, positioning it alongside other protected and remote coastlines that serve as sinks for debris transported over vast distances. Comparable assessments from other conservation areas reinforce this pattern, as seen in Table 6.1.

However, this study reveals that Mary's Point is not a static repository but a highly dynamic system. The significant environmental changes observed between 2022

and 2024 were driven by episodic, high-energy storm events resembling post-tropical cyclone Fiona and Hurricane Lee, which acted as powerful geomorphic agents, fundamentally purging the active clastic column and executing a statistically significant flushing of microplastic contaminants ($p = 0.0023$) from the beach reservoir.

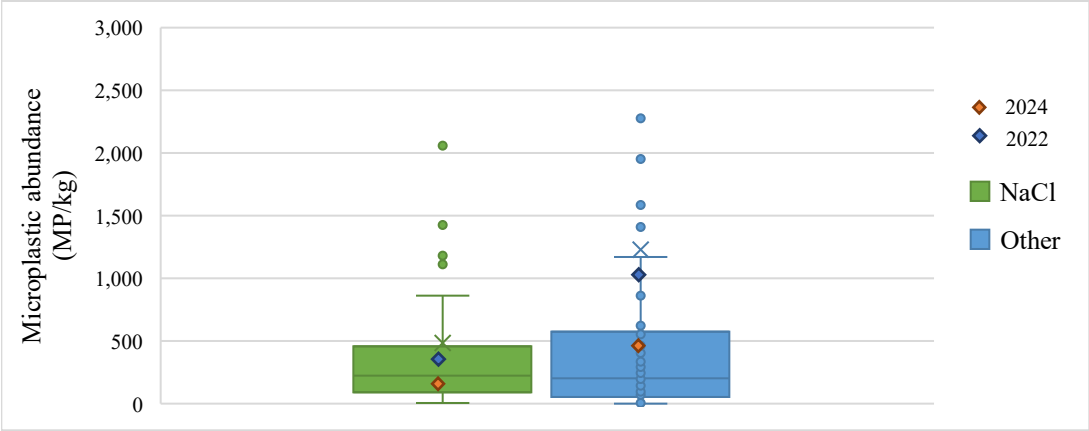

Figure 6.7. Global distribution of microplastic (MP) abundances in beach sediments reported in density-base extraction studies. Results are grouped by low-density NaCl extraction (~1.18 g/cm^3) and higher-density extraction solutions (e.g., $CaCl_2$, $ZnCl_2$, NaI, NaH_2PO_4, and Na_2WO_4), capable of recovering denser polymers. Boxes show the interquartile ranges (IQR), medians, means (x), and 1.5xIQR whiskers; outliers represent highly contaminated sites. For NaCl-only studies, Q1 = 89, Q3 = 433, IQR = 345, mean = 481, median = 221. For higher-density extraction studies, Q1 = 56, Q3 = 564, IQR = 508, mean = 1226, median = 204. Diamonds indicate mean MP abundance at Mary's Point for 2022 and 2024 derived from the multistep extraction (blue) and estimated NaCl-only recovery (green).

Table 6.1. Summary of reported microplastic abundances in protected coastal environments worldwide, highlighting that even ecologically significant or conservation-designated sites exhibit measurable levels of contamination across a range of geographic and environmental contexts.

Location / Site	**Protection Status / Context**	**Study**	**Reported Microplastic Abundance**	**Notes**
Bay of Biscay (Natura 2000 Special Protection Area for Birds)	Protected coastal habitat	Masiá et al. (2019)	145 MP/kg and 382 MP/kg (dry sand)	Two sampled beaches showing measurable contamination despite protected status
Telaščica Bay, Croatia (Marine Protected Area)	Marine Protected Area	Blašković et al. (2017)	32.3–377.8 MP/kg dry weight of sediment	Demonstrates microplastics as a abundant relative to meso and macroplastics
Spain – Seasonal Comparison	Coastal site (not specified as protected)	Novillo-Sanjuan et al. (2022)	Surface sediment: 5.66 ± 3.66 MPs/kg (July); 6.45 ± 4.42 MPs/kg (November)	Shows strong seasonal variability
The Ballestas Islands (TBI) & Paracas National Reserve (PNR), Peru	Protected coastal areas	De-La-Torre et al. (2023)	7.5–8.5 MP/kg	Contamination dominated by blue fibres
Bundala National Park (BNP) and Hikkaduwa Marine National Park (HNP), Sri Lanka	Marine protected area (MPA)	Sevwandi et al. (2021)	111±29 MPs/m^2 102±16 MPs/m^2	Fragments and polyethylene most abundant
Cispata, Columbia	Marine Protected Area (MPA)	Ordóñez 2022	(72 to 1 668 items/m^2 or from 42 to 1 825 items/kg of sediment) 8 to 36 items/m^2	More abundant in mangroves than beach sediment

Ultimately, the evidence from Mary's Point paints a clear picture of a complex environmental interplay. Even a remote, internationally recognized conservation area functions as a dynamic sink for diffuse, long-range pollution. Its capacity to retain contaminants is not constant but is fundamentally controlled by the powerful, episodic

reworking of its physical structure. This highlights that understanding the fate of microplastics in coastal environments requires an integrated approach that considers not just pollution sources, but the dynamic sedimentological context in which they are stored and remobilized.

7. Summary and Future Work

7.1. Summary of key findings

This study underscores the persistent challenges in global plastic waste management and microplastic research, and highlights the vulnerability of even protected coastal environments to contamination. Global recycling rates remain extremely low (6–9%), with the vast majority of plastic waste (79–80%) being mismanaged, ultimately entering landfills or the natural environment (Geyer et al., 2017; Thompson & De Falco, 2020; Kumar et al., 2021; Reddy et al., 2022; Fonseca et al., 2024). The ecological persistence and widespread transport of microplastics across air, water, and biotic vectors amplify the urgency for comprehensive mitigation strategies, potentially including extended producer responsibility, bans on single-use items, and investments in advanced recycling technologies (Zalasiewicz et al., 2016; Rahman et al., 2023).

A central conclusion of this research is that a significant barrier to understanding and combating global microplastic pollution is the dual challenge of inconsistent terminology (as outlined in Chapter 1) and divergent methodologies (Chapter 2). These persistent inconsistencies compromise data reliability and hamper the coherent global monitoring and meta-analysis essential for effective action (Hidalgo-Ruz et al., 2012; Jambeck et al., 2015; Shi et al., 2021). Methodological choices, particularly in extraction, profoundly shape reported microplastic loads.

Addressing this challenge, the detailed case study at Mary's Point, a site of international ecological importance with five overlapping conservation designations, demonstrates that even protected coastal environments accumulate significant

microplastic burdens. By employing a novel, multi-step extraction protocol that combines sequential density and oleophilic separations, this study successfully recovered a broad spectrum of polymers, including denser types, than is possible with the most commonly used saline-solution methods (Zhang et al., 2021; Soursou et al., 2023). This comprehensive approach revealed that less than 45% of total microplastics were captured in the initial low-density-solution steps, confirming that conventional methods systematically overlook the majority of plastic particles present.

The results from Mary's Point reveal a highly dynamic sorting system governed by episodic weather shocks. When stratographic increments are properly aggregated into independent core summary values ($n = 14$), the clastic data demonstrate that the bulk mineral sand matrix was geomorphically resilient, exhibiting no statistically significant temporal shift in mean grain size ($p = 0.28$) between sampling years. However, high-energy wave conditions from Hurricanes Fiona and Lee crossed a highly selective geomorphic shear threshold. Rather than structurally modifying bulk clastic profiles, the storm energy winnowed out the lightweight, high-drag synthetic contaminant payloads, executing a statistically significant flushing ($p = 0.0023$) of trapped microplastics from the intertidal column. This finding demonstrates that the beach's capacity to store pollutants is not static, nor ever-increasing, but is fundamentally controlled by high-energy hydrodynamic events.

The microplastic assemblage was dominated by weathered, secondary fibres, with a notable scarcity of primary industrial pellets, and fragments from local litter. This pollution signature, characterized by aged particles and a mix of polymer densities, points overwhelmingly to diffuse, long-range estuarine, oceanic, and atmospheric

transport as the primary contamination pathway, rather than direct, local sources. This confirms that Mary's Point functions as a dynamic sink for regional and possibly more global plastic pollution, with its complex distribution patterns shaped by the interplay of long-range transport and intense local reworking.

7.2. Limitations and future work

A primary challenge facing microplastic science is that the highly varied approaches and limited standardization across studies mean that results are not often directly comparable. This study, while methodologically robust, is also situated within this context. Furthermore, several specific limitations of this project highlight clear directions for future research. The use of a hand corer restricts sampling to the sand-dominated portion of the beach, excluding zones with gravel or pebble layers. While the approach would preserve sedimentary structures (none were found beyond simple graded bedding), it limits the spatial scope of the analysis. Polymer-specific identification using FTIR or Raman spectroscopy was not performed due to equipment constraints, meaning that polymer composition was inferred from density-based classifications rather than confirmed analytically.

Given the non-normal distributions and localized outlier patchiness characteristic of coastal contaminant datasets, non-parametric Mann-Whitney U tests were deployed on aggregated core units to evaluate temporal variations on the basis of rank medians rather than pooled sample means. This aggregation step was statistically required to respect data independence assumptions and eliminate vertical pseudoreplication vulnerabilities within core tubes. While temporal shifts were safely captured, collapsing

vertical segments functions as a study limitation since it cannot continuously model interactive 3D spatial grids or cross-shore profiles along the beach face.

Mean phi values were reported following established grain-size conventions, which enables direct comparison with regional and international sedimentological studies (e.g., Misic et al., 2019; Flores-Cortés et al., 2022; Papuga et al., 2022). This approach also maintains consistency with widely used granulometric frameworks. The multi-step extraction protocol used in this study was specifically designed to maximize recovery across the full range of polymer densities. This contrasts with the widespread reliance on single-step NaCl extractions in the global literature, which preferentially recover only low-density polymers and systematically underrepresent denser plastics such as PET, PVC, and rubber (e.g., Mexico: Flores-Cortés et al., 2022; Spain: Godoy et al., 2023; Bangladesh: Tasnim et al., 2023). As a result, while the protocol used here yields a more complete recovery relative to many published methods, comparisons with NaCl-only datasets must be interpreted with caution, as observed differences in total abundance may reflect variations in extraction efficiency rather than true environmental differences.

Future work should address the above limitations through several avenues. First, provided a suitable alternative to the hand-corer is available, sampling could be expanded beyond the high-tide line to include backshore zones, low-tide areas, and adjacent mudflats, providing a more complete picture of cross-shore contamination patterns and burial processes. To expand upon the spatial constraints of core-averaging, future long-term baseline tracking grids should implement a split-unit (split-plot / repeated-measures) mixed linear model. By nesting core identifiers as a random factor

within individual sampling years, vertical stratigraphy trends and depth-by-year interaction parameters can be mathematically tracked over time without sacrificing sample independence. Additionally, continued annual baseline monitoring at the high-tide line would also provide a valuable long-term dataset to further assess the impacts of storms and seasonal variability on the beach's function as a dynamic microplastic sink.

Second, this study did not include a granulometric analysis of the backshore cliffs west of Mary's Point because this work was not requested in the sampling permit for this protected beach and could not be completed within the thesis timeframe. Future research should prioritize this analysis to quantify the contribution of cliff erosion to beach sediment dynamics and determine whether storm-driven retreat introduces coarser or finer material. Understanding these inputs is critical for assessing how episodic erosion events influence sediment structure and microplastic retention, and for integrating these findings into predictive models of beach morphology under increasing storm frequency. Integrating this analysis with hydrodynamic modeling and long-term monitoring would help predict how storm frequency and intensity affect sediment structure and contaminant storage. Third, polymer-specific identification using FTIR, Raman spectroscopy, or Pyrolysis-GC/MS would confirm the composition of recovered particles. Additionally, refining organic matter digestion protocols and incorporating standardized QA/QC measures, such as procedural blanks and reagent filtration, will enhance analytical reliability. Finally, contributing to global efforts to harmonize microplastic extraction and reporting protocols will improve comparability across studies and support the development of robust, internationally recognized baselines for coastal contamination.

7.3. Broader implications and concluding remarks

Advancing microplastic research depends on more complete microplastic data collection, harmonized classification systems and robust QA/QC procedures to ensure data comparability across laboratories and regions (Tiwari et al., 2023; Thompson et al., 2024;). This study contributes to that goal by demonstrating a multi-step extraction protocol that recovers a broader spectrum of polymer densities than conventional single-solution methods. By establishing a transparent, reproducible approach that can be done using environmentally friendly procedures and at low cost to facilitate practical execution in low-resource regions, these findings provide a critical baseline for the Bay of Fundy and offer a model that can be adapted for other dynamic coastal environments. Collectively, this work underscores the urgent need for standardized methodologies to support global monitoring, inform policy, and guide targeted mitigation strategies in both protected and high-risk ecosystems. Ultimately, implementing these measures will not only improve scientific comparability but also strengthen conservation efforts by ensuring that management decisions are grounded in accurate, globally relevant data.

Bibliography

Abayomi, O. A., Range, P., Al-Ghouti, M. A., Obbard, J. P., Almeer, S. H., & Ben-Hamadou, R. (2017). Microplastics in coastal environments of the Arabian Gulf. Marine Pollution Bulletin, 124, 181–188. doi.org/10.1016/j.marpolbul.2017.07.011

Abdel Ghani, S. A., El-Sayed, A. A. M., Ibrahim, M. I. A., Ghobashy, M. M., Shreadah, M. A., & Shabaka, S. (2022). Characterization and distribution of plastic particles along Alexandria beaches, Mediterranean Coast of Egypt, using microscopy and thermal analysis techniques. Science of the Total Environment, 834, 1–10. doi.org/10.1016/j.scitotenv.2022.155363

Abdel Ghani, S. A., Shobier, A. H., El-Sayed, A. A. M., Shreadah, M. A., & Shabaka, S. (2023). Quantifying microplastics pollution in the Red Sea and Gulfs of Suez and Aqaba: Insights from chemical analysis and pollution load assessment. Science of the Total Environment, 901, 1–12. doi.org/10.1016/j.scitotenv.2023.166031

Abelouah, M. R., Ben-Haddad, M., Rangel-Buitrago, N., Hajji, S., El Alem, N., & Ait Alla, A. (2022). Microplastics pollution along the central Atlantic coastline of Morocco. Marine Pollution Bulletin, 174, 1–12. doi.org/10.1016/j.marpolbul.2021.113190

Abidli, S., Antunes, J., Ferreira, J., Lahbib, Y., Sobral, P., & El Menif, N. T. (2018). Microplastics in sediments from the littoral zone of the north Tunisian coast (Mediterranean Sea). Estuarine, Coastal and Shelf Science, 205, 1–9. doi.org/10.1016/j.ecss.2018.03.006

Adjornor, B. Y., Han, B., Zahran, E. M., Pichtel, J., & Wood, R. (2024). Transport and deposition of microplastics at the water–sediment interface: A case study of the White River near Muncie, Indiana. Hydrology, 11(9), 1–17. doi.org/10.3390/hydrology11090141

Ahmed Dar, A., Chen, Z., Sardar, M. F., & An, C. (2024). Navigating the nexus: climate dynamics and microplastics pollution in coastal ecosystems. Environmental Research, 252, 1–16. doi.org/10.1016/j.envres.2024.118971

Akkajit, P., Tipmanee, D., Cherdsukjai, P., Suteerasak, T., & Thongnonghin, S. (2021). Occurrence and distribution of microplastics in beach sediments along Phuket coastline. Marine Pollution Bulletin, 169, 1–11. doi.org/10.1016/j.marpolbul.2021.112496

Al Nahian, S., Rakib, M. R. J., Haider, S. M. B., Kumar, R., Mohsen, M., Sharma, P., & Khandaker, M. U. (2022). Occurrence, spatial distribution, and risk assessment of microplastics in surface water and sediments of Saint Martin Island in the Bay of Bengal. Marine Pollution Bulletin, 179, 1–13. doi.org/10.1016/j.marpolbul.2022.113720

Alava, J. J., Kazmiruk, T. N., Douglas, T., Schuerholz, G., Heath, B., Flemming, S. A., Bendell, L., & Drever, M. C. (2021). Occurrence and size distribution of microplastics in mudflat sediments of the Cowichan-Koksilah Estuary, Canada: A

baseline for plastic particles contamination in an anthropogenic-influenced estuary. Marine Pollution Bulletin, 173, 1–10. doi.org/10.1016/j.marpolbul.2021.113033

American Association of State Highway and Transportation Officials (AASHTO). (1997). The classification of soils and soil-aggregate mixtures for highway construction purposes. AASHTO designation M145–91. In Standard specifications for transportation materials and methods of sampling and testing, Part 1: Specifications (18th ed.) (18th ed.). American Association of State Highway and Transportation Officials.

Amorim, A. L. A. D., Ramos, J. A. A., & Nogueira Júnior, M. (2020). Ingestion of microplastic by ontogenetic phases of Stellifer brasiliensis (Perciformes, Sciaenidae) from the surf zone of tropical beaches. Marine Pollution Bulletin, 158, 1–5. doi.org/10.1016/j.marpolbul.2020.111214

Amos, C. (1987). Fine-grained sediment transport in Chignecto Bay, Bay of Fundy, Canada. Continental Shelf Research, 7(10), 278–343.

Amos, C., & Asprey, K. (1979). Geophysical and sedimentary studies in the Chignecto Bay System, Bay of Fundy – A progress report. Current Research, Part B, Geological Survey of Canada, 79(1B), 245–252.

Amos, C., & Zaitlin, B. (1991). The post-glacial evolution of Chignecto Bay, Bay of Fundy, and its modern environment of deposition. In D. G. Smith, G. E. Reinson, B. A. Zaitlan, & R. A. Rahmani (Eds.), Clastic Tidal Sedimentology (Vol. 16, pp. 59–90). Canadian Society of Petroleum Geologists. https://www.researchgate.net/publication/259621002

anak Alexander Tampang, A. M., & Mohan Viswanathan, P. (2022). Occurrence, distribution and sources of microplastics in beach sediments of Miri coast, NW Borneo. Chemosphere, 305, 1–10. doi.org/10.1016/j.chemosphere.2022.135368

Anderson, R. J., & Turner, A. (2024). Microplastic transport and deposition in a beach-dune system (Saunton Sands-Braunton Burrows, southwest England). Science of the Total Environment, 909, 1–10. doi.org/10.1016/j.scitotenv.2023.168535

Andrady, A. (2011). Microplastics in the marine environment. Marine Pollution Bulletin, 62(8), 1596–1605. doi.org/10.1016/j.marpolbul.2011.05.030

Araújo, M. C. B., Costa, M. F., Silva-Cavalcanti, J. S., Duarte, A. C., Reis, V., Rocha-Santos, T. A., da Costa, J. P., & Girão, V. (2022). Different faces of cigarette butts, the most abundant beach litter worldwide. Environmental Science and Pollution Research, 29(32), 48926–48936. doi.org/10.1007/s11356-022-19134-w

Arjun, H. S., Aiswriya, P., Muthuchamy, M., Krishnakumar, S., Singh, S. H., & Muthukumar, A. (2024). Distribution and characterization of microplastics along the coastal shoreline of Thiruvananthapuram District, Kerala, India. Water, Air, and Soil Pollution, 235(4), 1–15. doi.org/10.1007/s11270-024-07061-0

Asensio-Montesinos, F., Blaya-Valencia, G., Corbí, H., Beltrán-Sanahuja, A., & Sanz-Lázaro, C. (2022). Microplastic accumulation dynamics in two Mediterranean

beaches with contrasting inputs. Journal of Sea Research, 188, 1–9. doi.org/10.1016/j.seares.2022.102269

Asensio-Montesinos, F., Oliva Ramírez, M., González-Leal, J. M., Carrizo, D., & Anfuso, G. (2020). Characterization of plastic beach litter by Raman spectroscopy in South-western Spain. Science of the Total Environment, 744, 1–9. doi.org/10.1016/j.scitotenv.2020.140890

Aslam, H., Ali, T., Maruf Mortula, M., Attaelmanan, A.G. (2020). Evaluation of microplastics in beach sediments along the coast of Dubai, UAE. Marine Pollution Bulletin, 150, 1–12. doi.org/10.1016/j.marpolbul.2019.110739.

Atwood, E., Falcieri, F., Piehl, S., Bochow, M., Matthies, M., Franke, J., Carniel, S., Sclavo, M., Laforsch, C., Siegert, F. (2019). Coastal accumulation of microplastic particles emitted from the Po River, Northern Italy: Comparing remote sensing and hydrodynamic modelling with in situ sample collections. Marine Pollution Bulletin, 138, 561–574. doi.org/10.1016/j.marpolbul.2018.11.045

Azaaouaj, S., Nachite, D., Anfuso, G., & Er-Ramy, N. (2024). Abundance and distribution of microplastics on sandy beaches of the eastern Moroccan Mediterranean coast. Marine Pollution Bulletin, 200, 1–10. doi.org/10.1016/j.marpolbul.2024.116144

Balestra, V., Trunfio, F., Akyıldız, S. H., Marini, P., & Bellopede, R. (2024). Microparticles of anthropogenic origin (microplastics and microfibers) in sandy sediments: A case study from Calabria, Italy. Environmental Monitoring and Assessment, 196, 1–14. doi.org/10.1007/s10661-024-13159-z

Ballent, A., Corcoran, P. L., Madden, O., Helm, P. A., & Longstaffe, F. J. (2016). Sources and sinks of microplastics in Canadian Lake Ontario nearshore, tributary and beach sediments. Marine Pollution Bulletin, 110(1), 383–395. doi.org/10.1016/j.marpolbul.2016.06.037

Balthazar-Silva, D., Turra, A., Moreira, F. T., Camargo, R. M., Oliveira, A. L., Barbosa, L., & Gorman, D. (2020). Rainfall and tidal cycle regulate seasonal inputs of microplastic pellets to sandy beaches. Frontiers in Environmental Science, 8(123), 1–8. doi.org/10.3389/fenvs.2020.00123

Banik, P., Hossain, M. B., Nur, A. U., Choudhury, T. R., Liba, S. I., Yu, J., Noman, M. A., & Sun, J. (2022). Microplastics in sediment of Kuakata beach, Bangladesh: Occurrence, spatial distribution, and risk assessment. Frontiers in Marine Science, 9, 1–13. doi.org/10.3389/fmars.2022.860989

Bayo, J., Rojo, D., & Olmos, S. (2019). Abundance, morphology and chemical composition of microplastics in sand and sediments from a protected coastal area: The Mar Menor lagoon (SE Spain). Environmental Pollution, 252, 1357–1366. doi.org/10.1016/j.envpol.2019.06.024

Bellasi, A., Binda, G., Pozzi, A., Boldrocchi, G., & Bettinetti, R. (2021). The extraction of microplastics from sediments: An overview of existing methods and the proposal of a new and green alternative. Chemosphere, 278, 1–5. doi.org/10.1016/j.chemosphere.2021.130357

Béraud, E., Bednarz, V., Otto, I., Golbuu, Y., & Ferrier-Pagès, C. (2022). Plastics are a new threat to Palau's coral reefs. PLoS ONE, 17, 1–16. doi.org/10.1371/journal.pone.0270237

Besley, A., Vijver, M. G., Behrens, P., & Bosker, T. (2017). A standardized method for sampling and extraction methods for quantifying microplastics in beach sand. Marine Pollution Bulletin, 114, 77–83. doi.org/10.1016/j.marpolbul.2016.08.055

BirdLife International. (n.d.). Protecting the most important habitats for birds. BirdLife International. Retrieved February 22, 2025, from https://www.birdlife.org/

Bissen, R., & Chawchai, S. (2020). Microplastics on beaches along the eastern Gulf of Thailand – A preliminary study. Marine Pollution Bulletin, 157, 1–14. doi.org/10.1016/j.marpolbul.2020.111345

Blair, T. C., & McPherson, J. G. (1999). Grain-size and textural classification of coarse sedimentary particles. Journal of Sedimentary Research, 69(1), 6–19. archive.org/details/sim_journal-of-sedimentary-research_1999-01_69_1

Blašković, A., Fastelli, P., Čižmek, H., Guerranti, C., & Renzi, M. (2017). Plastic litter in sediments from the Croatian marine protected area of the natural park of TelašČica bay (Adriatic Sea). Marine Pollution Bulletin, 114(1), 583–586. doi.org/10.1016/j.marpolbul.2016.09.018

Blašković, A., Guerranti, C., Fastelli, P., Anselmi, S., & Renzi, M. (2018). Plastic levels in sediments close to Cecina river estuary (Tuscany, Italy). Marine Pollution Bulletin, 135, 1–5. doi.org/10.1016/j.marpolbul.2018.07.021

Bobchev, N., Berov, D., Klayn, S., & Karamfilov, V. (2024). High microplastic pollution in marine sediments associated with urbanised areas along the SW Bulgarian Black Sea coast. Marine Pollution Bulletin, 209, 1–10. doi.org/10.1016/j.marpolbul.2024.117150

Bodzek, M., Pohl, A., & Rosik-Dulewska, C. (2024). Microplastics in wastewater treatment plants: characteristics, occurrence and removal technologies. Water (Switzerland) (Vol. 16, Number 24). Multidisciplinary Digital Publishing Institute (MDPI). doi.org/10.3390/w16243574

Borah, A., Hande, O. M., Jayakumar, S., & Devipriya, S. P. (2024). Microplastic pollution in beach sediments in the Dapoli coast, Maharashtra, the western peninsular region of India. Regional Studies in Marine Science, 77, 1–7. doi.org/10.1016/j.rsma.2024.103640

Borrelle, S. B., Ringma, J., Law, K. L., Monnahan, C. C., Lebreton, L., Mcgivern, A., Murphy, E., Jambeck, J., Leonard, G. H., Hilleary, M. A., Eriksen, M., Possingham, H. P., De Frond, H., Gerber, L. R., Polidoro, B., Tahir, A., Bernard, M., Mallos, N., Barnes, M., & Rochman, C. M. (2020). Predicted growth in plastic waste exceeds efforts to mitigate plastic pollution. Science, 396, 1515–1518. doi.org/10.1126/science.aba3656

Bosker, T., Guaita, L., & Behrens, P. (2018). Microplastic pollution on Caribbean beaches in the Lesser Antilles. Marine Pollution Bulletin, 133, 442–447. doi.org/10.1016/j.marpolbul.2018.05.060

Browne, M. A., Crump, P., Niven, S. J., Teuten, E., Tonkin, A., Galloway, T., & Thompson, R. (2011). Accumulation of microplastic on shorelines worldwide: Sources and sinks. Environmental Science and Technology, 45(21), 9175–9179. doi.org/10.1021/es201811s

Canadian Geographic. (2013). Fundy Biosphere Region Map. In Canadian Geographic. canadiangeographic.ca/articles/fundys-amazing-places/

Cannas, S., Fastelli, P., Guerranti, C., & Renzi, M. (2017). Plastic litter in sediments from the coasts of south Tuscany (Tyrrhenian Sea). Marine Pollution Bulletin, 119(1), 372–375. doi.org/10.1016/j.marpolbul.2017.04.008

Carpenter, E. J., & Smith, K. L. (1972). Plastics on the Sargasso Sea Surface. Science, 175, 1240–1241. https://www.jstor.org/stable/1733709

Carretero, O., Gago, J., & Viñas, L. (2021). From the coast to the shelf: Microplastics in Rías Baixas and Miño River shelf sediments (NW Spain). Marine Pollution Bulletin, 162(111814), 1–7. doi.org/10.1016/j.marpolbul.2020.111814

Carvalho, J. P. S., Silva, T. S., & Costa, M. F. (2021). Distribution, characteristics and short-term variability of microplastics in beach sediment of Fernando de Noronha Archipelago, Brazil. Marine Pollution Bulletin, 166, 1–10. doi.org/10.1016/j.marpolbul.2021.112212

Castro, R. O., Silva, M. L. D., Marques, M. R. C., & Araújo, F. V. D. (2020). Spatio-temporal evaluation of macro, meso and microplastics in surface waters, bottom and beach sediments of two embayments in Niterói, RJ, Brazil. Marine Pollution Bulletin, 160, 1–21. doi.org/10.1016/j.marpolbul.2020.111537

Chen, M. C., & Chen, T. H. (2020). Spatial and seasonal distribution of microplastics on sandy beaches along the coast of the Hengchun Peninsula, Taiwan. Marine Pollution Bulletin, 151, 1–7. doi.org/10.1016/j.marpolbul.2019.110861

Cheng, G., Wang, Y. P., Voulgaris, G., Du, J., Sheng, J., Xiong, J., & Xing, F. (2020). Sediment exchange between channel and sand ridges in the southern Yellow Sea: The importance of tidal asymmetries. Continental Shelf Research, 205, 1–14. doi.org/10.1016/j.csr.2020.104169

Cheung, C. K. H., & Not, C. (2023). Impacts of extreme weather events on microplastic distribution in coastal environments. Science of the Total Environment, 904, 1–9. doi.org/10.1016/j.scitotenv.2023.166723

Chouchene, K., Prata, J. C., da Costa, J., Duarte, A. C., Rocha-Santos, T., & Ksibi, M. (2021). Microplastics on Barra beach sediments in Aveiro, Portugal. Marine Pollution Bulletin, 167, 1–5. doi.org/10.1016/j.marpolbul.2021.112264

Chubarenko, I. P., Esiukova, E. E., Bagaev, A. V., Bagaeva, M. A., & Grave, A. N. (2018). Three-dimensional distribution of anthropogenic microparticles in the body

of sandy beaches. Science of the Total Environment, 628, 1340–1351. doi.org/10.1016/j.scitotenv.2018.02.167

Chubarenko, I., Esiukova, E., Khatmullina, L., Lobchuk, O., Grave, A., Kileso, A., & Haseler, M. (2020). From macro to micro, from patchy to uniform: Analyzing plastic contamination along and across a sandy tide-less coast. Marine Pollution Bulletin, 156, 1–10. doi.org/10.1016/j.marpolbul.2020.111198

Chubarenko, I., Esiukova, E., Zobkov, M., & Isachenko, I. (2022). Microplastics distribution in bottom sediments of the Baltic Sea Proper. Marine Pollution Bulletin, 179, 1–11. doi.org/10.1016/j.marpolbul.2022.113743

Claessens, M., Meester, S. De, Landuyt, L. Van, Clerck, K. D, & Janssen, C. R. (2011). Occurrence and distribution of microplastics in marine sediments along the Belgian coast. Marine Pollution Bulletin, 62(10), 2199–2204. doi.org/10.1016/j.marpolbul.2011.06.030

Clark, K. E., Niles, L. J., & Burger, J. (1993). Abundance and distribution of migrant shorebirds in Delaware Bay. The Condor, 95, 694–705.

Cole, M., Lindeque, P., Halsband, C., & Galloway, T. S. (2011). Microplastics as contaminants in the marine environment: A review. Marine Pollution Bulletin, 62(12), 2588–2597. doi.org/10.1016/j.marpolbul.2011.09.025

Colton, J. B., Knapp, F. D., & Burns, B. R. (1974). Plastic Particles in Surface Waters of the Northwestern Atlantic. Science, 185, 491–497. https://www.jstor.org/stable/1738284

Constant, M., Kerhervé, P., Mino-Vercellio-Verollet, M., Dumontier, M., Sànchez Vidal, A., Canals, M., & Heussner, S. (2019). Beached microplastics in the Northwestern Mediterranean Sea. Marine Pollution Bulletin, 142, 263–273. doi.org/10.1016/j.marpolbul.2019.03.032

Corcoran, P. L., Norris, T., Ceccanese, T., Walzak, M. J., Helm, P. A., & Marvin, C. H. (2015). Hidden plastics of Lake Ontario, Canada and their potential preservation in the sediment record. Environmental Pollution, 204, 17–25. doi.org/10.1016/j.envpol.2015.04.009

Cordova, M. R., Ulumuddin, Y. I., Purbonegoro, T., Puspitasari, R., Rositasari, R., Yogaswara, D., Kaisupy, M. T., Wibowo, S. P. A., Subandi, R., Sani, S. Y., Sulistiowati, S., Nugraheni, I. K., Rahman, L., Rahmawati, Al Rahmadhani, S., Khoirunnisa, T. A., Nurhasanah, Muhtadi, A., Lestari, S. P., & Cragg, S. M. (2024). Abundance and characterization of microplastic pollution in the wildlife reserve, Ramsar site, recreational areas, and national park in northern Jakarta and Kepulauan Seribu, Indonesia. Chemosphere, 348, 1–12. doi.org/10.1016/j.chemosphere.2023.140761

Courtene-Jones, W., Martínez Rodríguez, A., & Handy, R. D. (2022). From microbes to ecosystems: a review of the ecological effects of biodegradable plastics. Emerging Topics in Life Sciences, 6, 423–433. doi.org/10.1042/ETLS20220015

Craggs, S., Keighley, D., Waldron, J. W. F., & Park, A. (2017). Salt tectonics in an intracontinental transform setting: Cumberland and Sackville basins, southern New Brunswick, Canada. Basin Research, 29(3), 266–283. doi.org/10.1111/bre.12152

Crichton, E. M., Noël, M., Gies, E. A., & Ross, P. S. (2017). A novel, density-independent and FTIR-compatible approach for the rapid extraction of microplastics from aquatic sediments. Analytical Methods, 9(9), 1419–1428. doi.org/10.1039/c6ay02733d

Culligan, N., Liu, K. biu, Ribble, K., Ryu, J., & Dietz, M. (2022). Sedimentary records of microplastic pollution from coastal Louisiana and their environmental implications. Journal of Coastal Conservation, 26(1), 1–14. doi.org/10.1007/s11852-021-00847-y

Cundell, A. M. (1974). Plastics in the marine environment. Environmental Conservation, 1(1), 63–68. https://www.jstor.org/stable/44519666

Da Silva, H., Murphy, F., Amigo, J. M., Stedmon, C., & Strand, J. (2020). Classification and quantification of microplastics (<100 μm) using a focal plane array-fourier transform infrared imaging system and machine learning. Analytical Chemistry, 92(20), 13724–13733. doi.org/10.1021/acs.analchem.0c01324

Dahms, H. T. J., & Greenfield, R. (2024). A review of the environments, biota, and methods used in microplastics research in South Africa. South African Journal of Science, 120(5–6), 1–9. doi.org/10.17159/sajs.2024/16669

Daniel, D. B., Ashraf, P. M., & Thomas, S. N. (2022). Impact of 2018 Kerala flood on the abundance and distribution of microplastics in marine environment off Cochin, Southeastern Arabian Sea, India. Regional Studies in Marine Science, 53, 1–12. doi.org/10.1016/j.rsma.2022.102367

Dashtgard, S. E., & Gingras, M. K. (2007). Tidal controls on the morphology and sedimentology of gravel-dominated deltas and beaches: Examples from the Megatidal Bay of Fundy, Canada. Journal of Sedimentary Research, 77(12), 1063–1077. doi.org/10.2110/jsr.2007.093

Dashtgard, S. E., Gingras, M. K., & Butler, K. E. (2006). Sedimentology and stratigraphy of a transgressive, muddy gravel beach: Waterside Beach, Bay of Fundy, Canada. Sedimentology, 53(2), 279–296. doi.org/10.1111/j.1365-3091.2006.00773.x

Davidson, B., Batista, K., Samrah, S., Rios Mendoza, L. M., & Pujara, N. (2022). Microplastic contamination of sediments across and within three beaches in western Lake Superior. Journal of Great Lakes Research, 48, 1563–1572. doi.org/10.1016/j.jglr.2022.09.011

de Falco, F., Di Pace, E., Cocca, M., & Avella, M. (2019). The contribution of washing processes of synthetic clothes to microplastic pollution. Scientific Reports, 9(1), 1–11. doi.org/10.1038/s41598-019-43023-x

de Miranda, C. O., Schaefer, C. E. G. R., de Souza, J. J. L. L., Guimarães, L. M., Maia, P. S., & Ivar Do Sul, J. A. (2023). Low numbers of large microplastics on environmentally-protected Antarctic beaches reveals no widespread contamination:

insights into beach sedimentary dynamics. Anais Da Academia Brasileira de Ciencias, 95, 1–21. doi.org/10.1590/0001-3765202320230283

de Ruijter, V. N., Milou, A., & Costa, V. (2019). Assessment of microplastics distribution and stratification in the shallow marine sediments of Samos island, Eastern Mediterranean sea, Greece. Mediterranean Marine Science, 20, 736–744. doi.org/10.12681/mms.19131

De-la-Torre, G. E., Dioses-Salinas, D. C., Castro, J. M., Antay, R., Fernández, N. Y., Espinoza-Morriberón, D., & Saldaña-Serrano, M. (2020). Abundance and distribution of microplastics on sandy beaches of Lima, Peru. Marine Pollution Bulletin, 151, 1–7. doi.org/10.1016/j.marpolbul.2019.110877

De-la-Torre, G. E., Dioses-Salinas, D. C., Pizarro-Ortega, C. I., Forero López, A. D., Fernández Severini, M. D., Rimondino, G. N., Malanca, F. E., Dobaradaran, S., Aragaw, T. A., Mghili, B., & Ayala, F. (2023). Plastic and paint debris in marine protected areas of Peru. Science of the Total Environment, 901, 1–16. doi.org/10.1016/j.scitotenv.2023.165788

De-la-Torre, G. E., Pizarro-Ortega, C. I., Dioses-Salinas, D. C., Ribeiro, V. V., Urizar Garfias Reyes, D. F., Ben-Haddad, M., Rakib, M. R. J., & Dobaradaran, S. (2023). Micro- and mesoplastic pollution along the coast of Peru. Environmental Science and Pollution Research, 30, 71396–71408. doi.org/10.1007/s11356-023-27707-6

Dean, B. Y., Corcoran, P. C., & Helm, P. A. (2018). Factors influencing microplastic abundances in nearshore, tributary and beach sediments along the Ontario shoreline of Lake Erie. Journal of Great Lakes Research, 44, 1002–1009. doi.org/10.1016/j.jglr.2018.07.014

Debrot, A. O., Tiel, A. B., & Bradshaw, J. E. (1999). Beach Debris in Curaçao. Marine Pollution Bulletin, 38(9), 795–801. 10.1016/S0025-326X(99)00043-0

Deswati, D., Tetra, O. N., Febriani, U., Suparno, S., Pardi, H., & Putra, A. (2023). Detection of microplastic in sediments at beach tourism area of Muaro Lasak, Padang City, West Sumatra, Indonesia. AACL Bioflux, 16, 2765–2780. bioflux.com.ro/docs/2023.2765-2780.pdf

Dimante-Deimantovica, I., Bebrite, A., Skudra, M., Retike, I., Viška, M., Bikše, J., Barone, M., Prokopovica, A., Svipsta, S., & Aigars, J. (2023). The baseline for micro- and mesoplastic pollution in open Baltic Sea and Gulf of Riga beach. Frontiers in Marine Science, 10, 1–17. doi.org/10.3389/fmars.2023.1251068

Dodson, G. Z., Shotorban, A. K., Hatcher, P. G., Waggoner, D. C., Ghosal, S., & Noffke, N. (2020). Microplastic fragment and fiber contamination of beach sediments from selected sites in Virginia and North Carolina, USA. Marine Pollution Bulletin, 151, 1–11. doi.org/10.1016/j.marpolbul.2019.110869

Dou, P. C., Mai, L., Bao, L. J., & Zeng, E. Y. (2021). Microplastics on beaches and mangrove sediments along the coast of South China. Marine Pollution Bulletin, 172, 1–8. doi.org/10.1016/j.marpolbul.2021.112806

Doucet, C. V., Labaj, A. L., & Kurek, J. (2021). Microfiber content in freshwater mussels from rural tributaries of the Saint John River, Canada. Water, Air, and Soil Pollution, 232(1), 1–12. doi.org/10.1007/s11270-020-04958-4

Dowarah, K., & Devipriya, S. P. (2019). Microplastic prevalence in the beaches of Puducherry, India and its correlation with fishing and tourism/recreational activities. Marine Pollution Bulletin, 148, 123–133. doi.org/10.1016/j.marpolbul.2019.07.066

Doyen, P., Hermabessiere, L., Dehaut, A., Himber, C., Decodts, M., Degraeve, T., Delord, L., Gaboriaud, M., Moné, P., Sacco, J., Tavernier, E., Grard, T., & Duflos, G. (2019). Occurrence and identification of microplastics in beach sediments from the Hauts-de-France region. Environmental Science and Pollution Research, 26, 28010–28021. doi.org/10.1007/s11356-019-06027-8

Duncan, E. M., Arrowsmith, J., Bain, C., Broderick, A. C., Lee, J., Metcalfe, K., Pikesley, S. K., Snape, R. T. E., van Sebille, E., & Godley, B. J. (2018). The true depth of the Mediterranean plastic problem: Extreme microplastic pollution on marine turtle nesting beaches in Cyprus. Marine Pollution Bulletin, 136, 334–340. doi.org/10.1016/j.marpolbul.2018.09.019

Dutta, S., Sethulekshmi, S., & Shriwastav, A. (2022). Abundance, morphology, and spatio-temporal variation of microplastics at the beaches of Mumbai, India. Regional Studies in Marine Science, 56, 1–9. doi.org/10.1016/j.rsma.2022.102722

Egessa, R., Nankabirwa, A., Basooma, R., & Nabwire, R. (2020). Occurrence, distribution and size relationships of plastic debris along shores and sediment of northern Lake Victoria. Environmental Pollution, 257, 1–9. doi.org/10.1016/j.envpol.2019.113442

Environment and Climate Change Canada (ECCC). (2016, April 25). Shepody National Wildlife Area pamphlet. Government of Canada. https://www.canada.ca/en/environment-climate-change/services/national-wildlife-areas/locations/shepody/pamphlet.html

Environment and Climate Change Canada (ECCC). (2022). Grindstone Island - 00160. Government of Canada. https://www.tides.gc.ca/en/stations/160

Environment and Climate Change Canada. (2023, March 27). Shepody National Wildlife Area. Government of Canada. https://www.canada.ca/en/environment-climate-change/services/national-wildlife-areas/locations/shepody.html

Esiukova, E., Lobchuk, O., Haseler, M., & Chubarenko, I. (2021). Microplastic contamination of sandy beaches of national parks, protected and recreational areas in southern parts of the Baltic Sea. Marine Pollution Bulletin, 173, 1–11. doi.org/10.1016/j.marpolbul.2021.113002

Expósito, N., Rovira, J., Sierra, J., Folch, J., & Schuhmacher, M. (2021). Microplastics levels, size, morphology and composition in marine water, sediments and sand beaches. Case study of Tarragona coast (western Mediterranean). Science of the Total Environment, 786, 1–18. doi.org/10.1016/j.scitotenv.2021.147453

Fader, G. (2005). Glacial, post glacial, present and projected sea levels, Bay of Fundy. Atlantic Marine Geological Consulting Ltd., 1–20.

Fader, G. B. ., King, L. H. ., & MacLean, B. (1977). Surficial geology of the Eastern Gulf of Maine and Bay of Fundy. Geological Survey of Canada, 19, 1–23.

Felsing, S., Kochleus, C., Buchinger, S., Brennholt, N., Stock, F., & Reifferscheid, G. (2018). A new approach in separating microplastics from environmental samples based on their electrostatic behavior. Environmental Pollution, 234, 20–28. doi.org/10.1016/j.envpol.2017.11.013

Fischer, E. K., Paglialonga, L., Czech, E., & Tamminga, M. (2016). Microplastic pollution in lakes and lake shoreline sediments - A case study on Lake Bolsena and Lake Chiusi (central Italy). Environmental Pollution, 213, 648–657. doi.org/10.1016/j.envpol.2016.03.012

Fisner, M., Majer, A. P., Balthazar-Silva, D., Gorman, D., & Turra, A. (2017). Quantifying microplastic pollution on sandy beaches: the conundrum of large sample variability and spatial heterogeneity. Environmental Science and Pollution Research, 24(15), 13732–13740. doi.org/10.1007/s11356-017-8883-y

Flores-Cortés, M., Armstrong-Altrin, & John S. (2022). Textural characteristics and abundance of microplastics in Tecolutla beach sediments, Gulf of Mexico. Environmental Monitoring and Assessment, 194(10), 1–14. doi.org/10.1007/s10661-022-10447-4

Flores-Ocampo, I. Z., & Armstrong-Altrin, J. S. (2023). Abundance and composition of microplastics in Tampico beach sediments, Tamaulipas State, southern Gulf of Mexico. Marine Pollution Bulletin, 191, 1–11. doi.org/10.1016/j.marpolbul.2023.114891

Folk, R.L. & Ward, W.C. (1957) a study in the significance of grain-size parameters. Journal of Sedimentary Petrology, 27, 3–26. doi.org/10.1306/74D70646-2B21-11D7-8648000102C1865D

Fong, Y. K., Kek, H. Y., Tan, H., Othman, M. H. D., Leng, P. C., Wong, S. L., & Wong, K. Y. (2024). State-of-the-art microplastic sampling sources, identification approaches and possible transformation to wealth. Chemical Engineering Transactions , 113, 331–336. doi.org/10.3303/CET24113056

Fonseca, J., Antunes, V., & Freire, A. C. (2024). Contributions to incorporation of non-recyclable plastics in bituminous mixtures. Sustainability (Switzerland), 16(22), 1–18. doi.org/10.3390/su16229945

Forsythe, C. (2016). The quantification of microplastics in intertidal sediments in the Bay of Fundy, Canada by [MSc]. University of British Columbia.

Frias, J. P. G. L., & Nash, R. (2019). Microplastics: Finding a consensus on the definition. Marine Pollution Bulletin, 138, 145–147. doi.org/10.1016/j.marpolbul.2018.11.022

Frias, J., Pagter, E., Nash, R., O'Connor, I., Carretero, O., Filgueiras, A., Viñas, L., Gago, J., Antunes, J., Bessa, F., Sobral, P., Goruppi, A., Tirelli, V., Pedrotti, M. L.,

Suaria, G., Aliani, S., Lopes, C., Raimundo, J., Caetano, M., & Gerdts, G. (2020). Standardised protocol for monitoring microplastics in sediments (Deliverable 4.2)..doi.org/10.25607/OBP-723

Fulfer, V. M., & Walsh, J. P. (2023). Extensive estuarine sedimentary storage of plastics from city to sea: Narragansett Bay, Rhode Island, USA. Scientific Reports, 13, 1–11. doi.org/10.1038/s41598-023-36228-8

Fuller, S., & Gautam, A. (2016). A procedure for measuring microplastics using pressurized fluid extraction. Environmental Science and Technology, 50(11), 5774–5780. doi.org/10.1021/acs.est.6b00816

Fundy Biosphere (n.d.). Fundy Biosphere Region. Fundy Biosphere Region. Retrieved March 6, 2025, from https://www.fundy-biosphere.ca/

Furlan, I., Fornari, M., Sawakuchi, A. O., Giannini, P. C. F., Dipold, J., de Freitas, A. Z., Wetter, N. U., & Semensatto, D. (2024). Morphodynamics drive the transport and accumulation of anthropogenic microparticles in tropical coastal depositional systems in southeastern Brazil. Science of the Total Environment, 957, 1–14. doi.org/10.1016/j.scitotenv.2024.177479

Gao, F., Li, J., Hu, J., Sui, B., Wang, C., Sun, C., Li, X., & Ju, P. (2021). The seasonal distribution characteristics of microplastics on bathing beaches along the coast of Qingdao, China. Science of the Total Environment, 783, 1–11. doi.org/10.1016/j.scitotenv.2021.146969

Gao, S. N., Wang, S., Liu, H., Han, S., Wei, J., & Liu, H. (2023). Distribution and characteristics of microplastics in the tidal flats of Sanya Bay, China. Journal of Marine Environmental Engineering, 11(1), 79–89. doi.org/10.32908/JMEE.v11.2023041301

Gao, Z., Wontor, K., Cizdziel, J. V., & Lu, H. (2022). Distribution and characteristics of microplastics in beach sand near the outlet of a major reservoir in north Mississippi, USA. Microplastics and Nanoplastics, 2(1), 1–13. doi.org/10.1186/s43591-022-00029-z

Garcês, A., & Pires, I. (2024). The detrimental impacts of plastic pollution on wildlife. Research in Ecology, 6, 42–46. doi.org/10.30564/re.v6i2.6294

Georgiou, I. Y., Messina, F., Sakib, M. M., Zou, S., Foster-Martinez, M., Bregman, M., Hein, C. J., Fenster, M. S., Shawler, J. L., McPherran, K., & Trembanis, A. C. (2023). Hydrodynamics and sediment-transport pathways along a mixed-energy spit-inlet system: A modeling study at chincoteague Inlet (Virginia, USA). Journal of Marine Science and Engineering, 11(5), 1–22. doi.org/10.3390/jmse11051075

Gerwing, T., Hamilton, D., Barbeau, M., Haralampides, K., & Yamazaki, G. (2017). Short-term response of a downstream marine system to the partial opening of a tidal-river causeway. Estuaries and Coasts, 40(3), 717–725. doi.org/10.1007/s12237-016-0173-2

Gerwing, T., Kim, J. H., Hamilton, D., Barbeau, M., & Addison, J. (2016). Diet reconstruction using next-generation sequencing increases the known ecosystem usage by a shorebird. Auk, 133(2), 168–177. doi.org/10.1642/AUK-15-176.1

GESAMP. (2019). Guidelines for the monitoring and assessment of plastic litter and microplastics in the ocean. In P. Kershaw, A. Turra, & F. Galgani (Eds.), Rep. and Stud. GESAMP (Vol. 99). United Nations Environment Programme (UNEP). https://www.gesamp.org

Geyer, R., Jambeck, J. R., & Law, K. L. (2017). Production, use, and fate of all plastics ever made. Science Advances, 3, 1–5. doi.org/10.1126/sciadv.1700782

Ghaffari, S., Bakhtiari, A. R., Ghasempouri, S. M., & Nasrolahi, A. (2019). The influence of human activity and morphological characteristics of beaches on plastic debris distribution along the Caspian Sea as a closed water body. Environmental Science and Pollution Research, 26(25), 25712–25724. doi.org/10.1007/s11356-019-05790-y

Ghanadi, M., Joshi, I., Dharmasiri, N., Jaeger, J. E., Burke, M., Bebelman, C., Symons, B., & Padhye, L. P. (2024). Quantification and characterization of microplastics in coastal environments: Insights from laser direct infrared imaging. Science of the Total Environment, 912, 1–14. doi.org/10.1016/j.scitotenv.2023.168835

Ghayebzadeh, M., Aslani, H., Taghipour, H., & Mousavi, S. (2020). Contamination of the Caspian Sea southern coast sediments with microplastics: A marine environmental problem. Marine Pollution Bulletin, 160, 1–19. doi.org/10.1016/j.marpolbul.2020.111620

Go, M., Ybañez, A., Illano, A., Cababat, F., & De La Calzada, L. (2024). Microplastics in beach sediments, seawater, and common fish in tourist destinations. Global Journal of Environmental Science and Management, 10, 1993–2008. doi.org/10.22034/gjesm.2024.04.30

Godoy, V., Prata, J. C., Blázquez, G., Almendros, A. I., Duarte, A. C., Rocha-Santos, T., Calero, M., & Martín-Lara, M. Á. (2020). Effects of distance to the sea and geomorphological characteristics on the quantity and distribution of microplastics in beach sediments of Granada (Spain). Science of the Total Environment, 746, 1–11. doi.org/10.1016/j.scitotenv.2020.142023

Godoy, V., Prata, J. C., Pérez, A., da Costa, J. P., Rocha-Santos, T., & Duarte, A. C. (2023). Microplastics in sediments from a sandy beach in Costa Nova (Aveiro, Portugal). Sustainability, 15, 1–10. doi.org/10.3390/su15076186

Graca, B., Szewc, K., Zakrzewska, D., Dołęga, A., & Szczerbowska-Boruchowska, M. (2017). Sources and fate of microplastics in marine and beach sediments of the Southern Baltic Sea—a preliminary study. Environmental Science and Pollution Research, 24, 7650–7661. doi.org/10.1007/s11356-017-8419-5

Grbic, J., Nguyen, B., Guo, E., You, J. B., Sinton, D., & Rochman, C. M. (2019). Magnetic extraction of microplastics from environmental samples. Environmental Science and Technology Letters, 6(2), 68–72. doi.org/10.1021/acs.estlett.8b00671

Guerranti, C., Cannas, S., Scopetani, C., Fastelli, P., Cincinelli, A., & Renzi, M. (2017). Plastic litter in aquatic environments of Maremma Regional Park (Tyrrhenian Sea, Italy): Contribution by the Ombrone river and levels in marine sediments. Marine Pollution Bulletin, 117(1–2), 366–370. doi.org/10.1016/j.marpolbul.2017.02.021

Gül, M. R. (2023). Short-term tourism alters abundance, size, and composition of microplastics on sandy beaches. Environmental Pollution, 316, 1–9. doi.org/10.1016/j.envpol.2022.120561

Gül, M. R. (2024). Factors influencing the three-dimensional distribution of microplastics on sandy beaches: A case study from the Turkish Coast of the Black Sea. Turkish Journal of Fisheries and Aquatic Sciences, 24(12), 1–12. doi.org/10.4194/TRJFAS26559

Guo, B., Ahmadian, R., Evans, P., & Falconer, R. A. (2020). Studying the wake of an island in a macro-tidal estuary. Water (Switzerland), 12(5), 1–18. doi.org/10.3390/W12051225

Habumugisha, T., Zhang, Z., Uwizewe, C., Yan, C., Ndayishimiye, J. C., Rehman, A., & Zhang, X. (2024). Toxicological review of micro- and nano-plastics in aquatic environments: Risks to ecosystems, food web dynamics and human health. Ecotoxicology and Environmental Safety, 278, 1–15. doi.org/10.1016/j.ecoenv.2024.116426

Hahladakis, J., Velis, C., Weber, R., Iacovidou, E., Purnell, P. (2018). An overview of chemical additives present in plastics: Migration, release, fate and environmental impact during their use, disposal and recycling. Journal of Hazardous Materials, 344, 179–199, doi.org/10.1016/j.jhazmat.2017.10.014

Hamdy, N., Osman, A. M., Awad, H., & Shaaban, N. A. (2024). Monitoring of microplastics in the marine environment and their ecological risks, the coastline of Alexandria, Egypt as a case study. Egyptian Journal of Aquatic Biology and Fisheries, 28, 221–242. doi.org/10.21608/ejabf.2024.367795

Hanvey, J. S., Lewis, P. J., Lavers, J. L., Crosbie, N. D., Pozo, K., & Clarke, B. O. (2017). A review of analytical techniques for quantifying microplastics in sediments. Analytical Methods, 9(9), 1369–1383, doi.org/10.1039/c6ay02707e

Hartmann, N. B., Hüffer, T., Thompson, R. C., Hassellöv, M., Verschoor, A., Daugaard, A. E., Rist, S., Karlsson, T., Brennholt, N., Cole, M., Herrling, M. P., Hess, M. C., Ivleva, N. P., Lusher, A. L., & Wagner, M. (2019). Are we speaking the same language? Recommendations for a definition and categorization framework for plastic debris. Environmental Science and Technology, 53(3), 1039–1047. doi.org/10.1021/acs.est.8b05297

Hengstmann, E., Gräwe, D., Tamminga, M., & Fischer, E. K. (2017). Marine litter abundance and distribution on beaches on the Isle of Rügen considering the influence of exposition, morphology and recreational activities. Marine Pollution Bulletin, 115(1–2), 297–306. doi.org/10.1016/j.marpolbul.2016.12.026

Hengstmann, E., Tamminga, M., vom Bruch, C., & Fischer, E. K. (2018). Microplastic in beach sediments of the Isle of Rügen (Baltic Sea) - Implementing a novel glass

elutriation column. Marine Pollution Bulletin, 126, 263–274. doi.org/10.1016/j.marpolbul.2017.11.010

Hernández-Sánchez, C., González-Sálamo, J., Díaz-Peña, F. J., Fraile-Nuez, E., & Hernández-Borges, J. (2021). Arenas Blancas (El Hierro island), a new hotspot of plastic debris in the Canary Islands (Spain). Marine Pollution Bulletin, 169, 1–12. doi.org/10.1016/j.marpolbul.2021.112548

Hidalgo-Ruz, V., Gutow, L., Thompson, R. C., & Thiel, M. (2012). Microplastics in the marine environment: A review of the methods used for identification and quantification. Environmental Science and Technology, 46(6), 3060–3075. doi.org/10.1021/es2031505

Hien, T. T., Nhon, N. T. T., Thu, V. T. M., Quyen, D. T. T., & Nguyen, N. T. (2020). The distribution of microplastics in beach sand in Tien Giang Province and Vung Tau City, Vietnam. Journal of Engineering and Technological Sciences, 52, 208–221. doi.org/10.5614/j.eng.technol.sci.2020.52.2.6

Ho, N. H. E., & Not, C. (2019). Selective accumulation of plastic debris at the breaking wave area of coastal waters. Environmental Pollution, 245, 702–710. doi.org/10.1016/j.envpol.2018.11.041

Hoang, T., & Mitten, S. (2022). Microplastic accumulation in the gastrointestinal tracts of nestling and adult migratory birds. Science of the Total Environment, 838, 1–10. doi.org/10.1016/j.scitotenv.2022.155827

Hopewell, J., Dvorak, R., & Kosior, E. (2009). Plastics recycling: challenges and opportunities. Philosophical transactions of the royal society. Biological Sciences, 364, 2115–2126, doi.org/10.1098/rstb.2008.0311

Hossain, M. B., Banik, P., Nur, A. U., & Rahman, T. (2021). Abundance and characteristics of microplastics in sediments from the world's longest natural beach, Cox's Bazar, Bangladesh. Marine Pollution Bulletin, 163, 1–7. doi.org/10.1016/j.marpolbul.2020.111956

Hurley, R. R., Lusher, A. L., Olsen, M., & Nizzetto, L. (2018). Validation of a method for extracting microplastics from complex, organic-rich, environmental matrices. Environmental Science and Technology, 52(13), 7409–7417. doi.org/10.1021/acs.est.8b01517

International Organization for Standardization, Technical Committee ISO/TC 61, Plastics Subcommittee SC 14, Environmental aspects, & European Committee for Standardization Technical Committee 249 “Plastics”. (2023). Principles for the analysis of microplastics present in the environment = Principles d’analyse des microplastiques présents dans l’environnement. International Organization for Standardization. (First edition 2023-09).

Jambeck, J. R., Geyer, R., Wilcox, C., Siegler, T. R., Perryman, M., Andrady, A., Narayan, R., & Law, K. L. (2015). Plastic waste inputs from land into the ocean. Science, 347, 768–771. doi.org/10.1126/science.l260879

Jaouani, R., Mouneyrac, C., Châtel, A., Amiard, F., Dellali, M., Beyrem, H., Michelet, A., & Lagarde, F. (2022). Seasonal and spatial distribution of microplastics in sediments by FTIR imaging throughout a continuum lake - lagoon- beach from the Tunisian coast. Science of the Total Environment, 838, 1–12. doi.org/10.1016/j.scitotenv.2022.156519

Jarosz, K., Borek-Dorosz, A., Drozdek, M., Rokicińska, A., Kiełbasa, A., Janus, R., Setlak, K., Kuśtrowski, P., Zapotoczny, S., & Michalik, M. (2024). Abiotic weathering of plastic: Experimental contributions towards understanding the formation of microplastics and other plastic related particulate pollutants. Science of the Total Environment, 917, 1–17. doi.org/10.1016/j.scitotenv.2024.170533

Jaubet, M. L., Hines, E., Elías, R., & Garaffo, G. V. (2021). Factors driving the abundance and distribution of microplastics on sandy beaches in a Southwest Atlantic seaside resort. Marine Environmental Research, 171, 1–9. doi.org/10.1016/j.marenvres.2021.105472

Jeevanandam, M., Talelign, W., Biru, A., Sakthi, J. S., Silva, J. D., Saravanan, P., & Jonathan, M. P. (2022). Evidences of microplastics in Hawassa Lake, Ethiopia: A first-hand report. Chemosphere, 296, 1–7. doi.org/10.1016/j.chemosphere.2022.133979

Jiang, J., He, L., Zheng, S., Liu, J., & Gong, L. (2024). A review of microplastic transport in coastal zones. Marine Environmental Research, 196, 1–14. doi.org/10.1016/j.marenvres.2024.106397

Jocelyn, T. F., Areanely, C. S. A., Carolina, M. S., Sara, O. B., Alethia, V. M., & Carlos, Á. Z. J. (2023). Presence of microplastics deposited in Sargassum sp. on sandy beaches. Regional Studies in Marine Science, 66, 1–9. doi.org/10.1016/j.rsma.2023.103152

Johannessen, C., & Shetranjiwalla, S. (2021). Role of structural morphology of commodity polymers in microplastics and nanoplastics formation: fragmentation, effects and associated toxicity in the aquatic environment. In Reviews of Environmental Contamination and Toxicology (Vol. 259, pp. 123–169). Springer Nature Switzerland. doi.org/10.1007/398_2021_80

Jones, J. S., Guézou, A., Medor, S., Nickson, C., Savage, G., Alarcón-Ruales, D., Galloway, T. S., Muñoz-Pérez, J. P., Nelms, S. E., Porter, A., Thiel, M., & Lewis, C. (2022). Microplastic distribution and composition on two Galápagos island beaches, Ecuador: Verifying the use of citizen science derived data in long-term monitoring. Environmental Pollution, 311, 1–8. doi.org/10.1016/j.envpol.2022.120011

Jones, J. S., Porter, A., Muñoz-Pérez, J. P., Alarcón-Ruales, D., Galloway, T. S., Godley, B. J., Santillo, D., Vagg, J., & Lewis, C. (2021). Plastic contamination of a Galapagos Island (Ecuador) and the relative risks to native marine species. Science of the Total Environment, 789, 1–13. doi.org/10.1016/j.scitotenv.2021.147704

Jong, M. C., Tong, X., Li, J., Xu, Z., Chng, S. H. Q., He, Y., & Gin, K. Y. H. (2022). Microplastics in equatorial coasts: Pollution hotspots and spatiotemporal variations

associated with tropical monsoons. Journal of Hazardous Materials, 424, 1–12. doi.org/10.1016/j.jhazmat.2021.127626

Jualaong, S., Pransilpa, M., Pradit, S., & Towatana, P. (2021). Type and distribution of microplastics in beach sediment along the coast of the eastern gulf of Thailand. Journal of Marine Science and Engineering, 9(12), 1–12. doi.org/10.3390/jmse9121405

Jualaong, S., Towatana, P., Pradit, S., & Puttapreecha, R. (2023). Type and distribution of microplastic contamination in beach sediment along the coast of the lower Gulf of Thailand. Applied Ecology and Environmental Research, 21, 2671–2682. doi.org/10.15666/aeer/2103_26712682

Kanak, K., Ahmed, M. K., Islam, M. S., Hasan, M., Chowdhury, K. M. A., & Hossain, K. B. (2024). Microplastic pollution along the coastal island shorelines of Bangladesh: Distribution, patterns, and abundance. Heliyon, 10, 1–16. doi.org/10.1016/j.heliyon.2024.e40723

Karami, A., Golieskardi, A., Choo, C. K., Romano, N., Ho, Y. Bin, & Salamatinia, B. (2017). A high-performance protocol for extraction of microplastics in fish. Science of the Total Environment, 578, 485–494. doi.org/10.1016/j.scitotenv.2016.10.213

Kaviarasan, T., Dhineka, K., Sambandam, M., Sivadas, S. K., Sivyer, D., Hoehn, D., Pradhan, U., Mishra, P., & Ramana Murthy, M. (2022). Impact of multiple beach activities on litter and microplastic composition, distribution, and characterization along the southeast coast of India. Ocean and Coastal Management, 223, 1–12. doi.org/10.1016/j.ocecoaman.2022.106177

Keene, J., & Turner, A. (2023). Microplastics in coastal urban sediments: Discrepancies in concentration and character revealed by different approaches to sample processing. Science of the Total Environment, 865, 1–7. doi.org/10.1016/j.scitotenv.2022.161140

Keerthika, K., Padmavathy, P., Rani, V., Jeyashakila, R., Aanand, S., & Kutty, R. (2022). Spatial, seasonal and ecological risk assessment of microplastics in sediment and surface water along the Thoothukudi, south Tamil Nadu, south-east India. Environmental Monitoring and Assessment, 194, 1–18. doi.org/10.1007/s10661-022-10468-z

Keighley, D. G., & Pickerill, R. K. (1995). The ichnotaxa Palaeophycus and Planolites: Historical perspectives and recommendations. Ichnos, 3(4), 301–309. doi.org/10.1080/10420949509386400

Kelly, A., Rodemann, T., Meiners, K., Auman, H., Bowman, J., & Lannuzel, D. (2025). Microplastic isolation in biomass-laden sea-ice samples: A low-cost method for particle isolation and automated polymer analysis. Polar Biology, 48, 1–12. doi.org/10.1007/s00300-025-03399-1

Kelly, N. E., Trela, O., Gavel, H., & Kuylen, A. V. (2024). Plastic and anthropogenic microfiber pollution on exposed sandy beaches in Nova Scotia, Canada. Water Emerging Contaminants and Nanoplastics, 3, 1–13. doi.org/10.20517/wecn.2023.66

Kenyon, K. W., & Kridler, E. (1969). Laysan Albatrosses Swallow Indigestible Matter. The Auk, 86(2), 339–343. digitalcommons.usf.edu/auk/vol86/iss2/15

Khaleel, R., Valsan, G., Rangel-Buitrago, N., & Warrier, A. K. (2023). Microplastics in the marine environment of St. Mary's Island: implications for human health and conservation. Environmental Monitoring and Assessment, 195(9). doi.org/10.1007/s10661-023-11651-6

Khaleel, R., Valsan, G., Rangel-Buitrago, N., & Warrier, A. K. (2022). Hidden problems in geological heritage sites: The microplastic issue on Saint Mary's Island, India, Southeast Arabian Sea. Marine Pollution Bulletin, 182, 1–14. doi.org/10.1016/j.marpolbul.2022.114043

Khuyen, V. T. K., Le, D. V., Fischer, A. R., & Dornack, C. (2021). Comparison of microplastic pollution in beach sediment and seawater at UNESCO Can Gio Mangrove Biosphere Reserve. Global Challenges, 5, 1–10. doi.org/10.1002/gch2.202100044

Kneel, S., Stephens, C. G., Rolston, A., Mendes, A. M., Morrison, L., & Linnane, S. (2024). Microplastic contamination of intertidal sediment and cockles (Cerastoderma edule). Marine Pollution Bulletin, 205, 1–16. doi.org/10.1016/j.marpolbul.2024.116568

Kodavanti, S., & Loganathan, B. G. (2016). Brominated flame retardants: spatial and temporal trends in the environment and biota from the Pacific Basin countries. In S. Masunaga, B. G. Logananthan, J. S. Khim, & P. R. S. Kodavanti (Eds.), AGS Symposium Series (Vol. 1244, pp. 21–48). American Chemical Society. pubs.acs.org/sharingguidelines

Koh, J., Bairoliya, S., Salta, M., Cho, Z. T., Fong, J., Neo, M. L., Cragg, S., & Cao, B. (2023). Sediment-driven plastisphere community assembly on plastic debris in tropical coastal and marine environments. Environment International, 179, 1–12. doi.org/10.1016/j.envint.2023.108153

Koongolla, J., Andrady, A. L., Terney Pradeep Kumara, P. B., & Gangabadage, C. S. (2018). Evidence of microplastics pollution in coastal beaches and waters in southern Sri Lanka. Marine Pollution Bulletin, 137, 277–284. doi.org/10.1016/j.marpolbul.2018.10.031

Korez, Š., Gutow, L., & Saborowski, R. (2019). Microplastics at the strandlines of Slovenian beaches. Marine Pollution Bulletin, 145, 334–342. doi.org/10.1016/j.marpolbul.2019.05.054

Kumar, A. S., & Varghese, G. K. (2021). Microplastic pollution of Calicut beach - Contributing factors and possible impacts. Marine Pollution Bulletin, 169, 1–11. doi.org/10.1016/j.marpolbul.2021.112492

Kumar, R., Verma, A., Shome, A., Sinha, R., Sinha, S., Jha, P. K., Kumar, R., Kumar, P., Shubham, Das, S., Sharma, P., & Prasad, P. V. (2021). Impacts of plastic pollution on ecosystem services, sustainable development goals, and need to focus on circular economy and policy interventions. Sustainability, 13(17), 1–40. doi.org/10.3390/su13179963

Kumkar, P., Verma, C. R., Hysek, Pise, M., Żółtowska, S., Gosavi, S. M., Mercl, F., Božik, M., Praus, L., Hanková, K., Rinn, R., Klouček, P., Petrtýl, M., & Kalous, L. (2023). Contaminants and their ecological risk assessment in beach sediments and water along the Maharashtra coast of India: A comprehensive approach using microplastics, heavy metal(loid)s, pharmaceuticals, personal care products and plasticisers. Science of the Total Environment, 892, 1–19. doi.org/10.1016/j.scitotenv.2023.164712

Laglbauer, B. J. L., Franco-Santos, R. M., Andreu-Cazenave, M., Brunelli, L., Papadatou, M., Palatinus, A., Grego, M., & Deprez, T. (2014). Macrodebris and microplastics from beaches in Slovenia. Marine Pollution Bulletin, 89(1–2), 356–366. doi.org/10.1016/j.marpolbul.2014.09.036

Laun, J., & Wang, Y. H. (2024). Abundance, morphology, spatial-temporal distribution and sources of microplastics in Shilaoren Beach, Qingdao, China. Regional Studies in Marine Science, 74, 1–10. doi.org/10.1016/j.rsma.2024.103422

Le, X. T. T., Nguyen, D. T., Pham, M. T., Trinh, M. V., Le, P. C., & Do, M. (2023). Risk assessment of microplastic exposure: A case study near a refinery factory at the central coast of Vietnam. Marine Pollution Bulletin, 196, 1–11. doi.org/10.1016/j.marpolbul.2023.115636

Lefebvre, C., Rojas, I. J., Lasserre, J., Villette, S., Lecomte, S., Cachot, J., & Morin, B. (2021). Stranded in the high tide line: Spatial and temporal variability of beached microplastics in a semi-enclosed embayment (Arcachon, France). Science of the Total Environment, 797, 1–12. doi.org/10.1016/j.scitotenv.2021.149144

Lekshmi, N. M., Kumar, S. S., Ashraf, P. M., Nehala, S. P., Edwin, L., & Turner, A. (2023). Occurrence and characteristics of fibreglass-reinforced plastics and microplastics on a beach impacted by abandoned fishing boats: A case study from Chellanam, India. Marine Pollution Bulletin, 192, 1–8. doi.org/10.1016/j.marpolbul.2023.114980

Lenz, M., Brennecke, D., Haeckel, M., Knickmeier, K., & Kossel, E. (2023). Spatio-temporal variability in the abundance and composition of beach litter and microplastics along the Baltic Sea coast of Schleswig-Holstein, Germany. Marine Pollution Bulletin, 190, 1–13. doi.org/10.1016/j.marpolbul.2023.114830

Leslie, H. A., Brandsma, S. H., van Velzen, M. J. M., & Vethaak, A. D. (2017). Microplastics en route: Field measurements in the Dutch river delta and Amsterdam canals, wastewater treatment plants, North Sea sediments and biota. Environment International, 101, 133–142. doi.org/10.1016/j.envint.2017.01.018

Leusch, F. D., Lu, H. C., Perera, K., Neale, P. A., & Ziajahromi, S. (2023). Analysis of the literature shows a remarkably consistent relationship between size and abundance of microplastics across different environmental matrices. Environmental Pollution, 319, 1–9. doi.org/10.1016/j.envpol.2022.120984

Li, J., Liu, H., & Paul Chen, J. (2018). Microplastics in freshwater systems: A review on occurrence, environmental effects, and methods for microplastics detection. Water Research, 137, 362–374. doi.org/10.1016/j.watres.2017.12.056

Li, J., Mao, X., Xing, R., Wang, Z., Sun, Q., Liu, H., Wu, Y., & Li, Y. (2023). Microplastics pollution and their potential impact in marine systems: A case study in Shandong Peninsula, China. ACS ES&T Water, 3, 2373–2383. doi.org/10.1021/acsestwater.3c00087

Li, J., Shan, E., Zhao, J., Teng, J., & Wang, Q. (2023). The factors influencing the vertical transport of microplastics in marine environment: A review. Science of the Total Environment, 870, 1–11. doi.org/10.1016/j.scitotenv.2023.161893

Li, J., Zhang, H., Zhang, K., Yang, R., Li, R., & Li, Y. (2018). Characterization, source, and retention of microplastic in sandy beaches and mangrove wetlands of the Qinzhou Bay, China. Marine Pollution Bulletin, 136, 401–406. doi.org/10.1016/j.marpolbul.2018.09.025

Li, Q., Su, L., Ma, C., Feng, Z., & Shi, H. (2022). Plastic debris in coastal macroalgae. Environmental Research, 205, 1–9. doi.org/10.1016/j.envres.2021.112464

Li, X., Wu, F., Zhang, C., & Wang, T. (2024). The effects of rainfall events on the composition and diversity of microplastics on beaches in Xiamen city on a short-term scale. Toxics, 12, 1–15. doi.org/10.3390/toxics12050375

Li, Y., Liu, C., Yang, H., He, W., Li, B., Zhu, X., Liu, S., Jia, S., Li, R., & Tang, K. H. D. (2024). Leaching of chemicals from microplastics: A review of chemical types, leaching mechanisms and influencing factors. Science of the Total Environment, 906, 1–15. doi.org/10.1016/j.scitotenv.2023.167666

Li, Y., Xiao, P., Donnici, S., Cheng, J., Tang, C. (2023). Spatial and seasonal distribution of microplastics in various environmental compartments around Sishili Bay of North Yellow Sea, China. Marine Pollution Bulletin, 186, 1–10, doi.org/10.1016/j.marpolbul.2022.114372

Li, Y., Zhang, H., & Tang, C. (2020). A review of possible pathways of marine microplastics transport in the ocean. Anthropocene Coasts, 3(1), 6–13. doi.org/10.1139/anc-2018-0030

Liebezeit, G., & Dubaish, F. (2012). Microplastics in beaches of the East Frisian Islands Spiekeroog and Kachelotplate. Bulletin of Environmental Contamination and Toxicology, 89(1), 213–217. doi.org/10.1007/s00128-012-0642-7

Liu, Y., Jiang, W. Y., Liao, Y., Sun, R., Hu, J., Lu, Z., Chang, M., Yang, J., Dai, Z., Zhou, C., Hong, P., Qian, Z. J., Sun, S., Ren, L., Liang, Y. Q., Zhang, Y., & Li, C. (2022). Separation of false-positive microplastics and analysis of microplastics via a two-phase system combined with confocal Raman spectroscopy. Journal of Hazardous Materials, 440, 1–11. doi.org/10.1016/j.jhazmat.2022.129803

Lloyd-Jones, T., Dick, J., Lane, T., Cunningham, E., & Kiriakoulakis, K. (2023). Occurrence and sources of microplastics on Arctic beaches: Svalbard. Marine Pollution Bulletin, 196, 1–11. doi.org/10.1016/j.marpolbul.2023.115586.

Lo, H. S., Lee, Y. K., Po, B. H. K., Wong, L. C., Xu, X., Wong, C. F., Wong, C. Y., Tam, N. F. Y., & Cheung, S. G. (2020). Impacts of Typhoon Mangkhut in 2018 on the

deposition of marine debris and microplastics on beaches in Hong Kong. Science of the Total Environment, 716, 1–9. doi.org/10.1016/j.scitotenv.2020.137172

Lo, H. S., Xu, X., Wong, C. Y., & Cheung, S. G. (2018). Comparisons of microplastic pollution between mudflats and sandy beaches in Hong Kong. Environmental Pollution, 236, 208–217. doi.org/10.1016/j.envpol.2018.01.031

Löder, M. G. J., & Gerdts, G. (2015). Methodology used for the detection and identification of microplastics—a critical appraisal. In Marine Anthropogenic Litter (Chapter 8, pp. 201–227). Springer International Publishing. doi.org/10.1007/978-3-319-16510-3_8

López-Velázquez, K., Duque-Olivera, K. G., Santiago-Gordillo, D. A., Hoil-Canul, E. R., Guzmán-Mar, J. L., Villanueva-Rodríguez, M., Ronderos-Lara, J. G., Castillo-Quevedo, C., & Cabellos-Quiroz, J. L. (2024). Microplastics on sandy beaches of Chiapas, Mexico. Regional Studies in Marine Science, 70, 1–10. doi.org/10.1016/j.rsma.2024.103381

Lots, F. A. E., Behrens, P., Vijver, M. G., Horton, A. A., & Bosker, T. (2017). A large-scale investigation of microplastic contamination: Abundance and characteristics of microplastics in European beach sediment. Marine Pollution Bulletin, 123(1–2), 219–226. doi.org/10.1016/j.marpolbul.2017.08.057

Lucas, Z. (1992). Monitoring Persistent Litter in the Marine Environment on Sable Island, Nova Scotia. Marine Pollution Bulletin, 7(4), 192–199. doi.org/10.1016/0025-326X(92)90529-F

Luo, Y., Sun, C., Li, C., Liu, Y., Zhao, S., Li, Y., Kong, F., Zheng, H., Luo, X., Chen, L., & Li, F. (2022). Spatial patterns of microplastics in surface seawater, sediment, and sand along Qingdao coastal environment. Frontiers in Marine Science, 9, 1–17. doi.org/10.3389/fmars.2022.916859

Lusher, A. L., Bråte, I. L. N., Munno, K., Hurley, R. R., & Welden, N. A. (2020). Is it or isn't it: the importance of visual classification in microplastic characterization. Applied Spectroscopy, 74(9), 1139–1153. doi.org/10.1177/0003702820930733

Lusher, A. L., Tirelli, V., O'Connor, I., & Officer, R. (2015). Microplastics in Arctic polar waters: The first reported values of particles in surface and sub-surface samples. Scientific Reports, 5, 1–9. doi.org/10.1038/srep14947

Lv, S., Cui, K., Zhao, S., Li, Y., Liu, R., Hu, R., Zhi, B., Gu, L., Wang, L., Wang, Q., & Shao, Z. (2024). Continuous generation and release of microplastics and nanoplastics from polystyrene by plastic-degrading marine bacteria. Journal of Hazardous Materials, 465, 1–12. doi.org/10.1016/j.jhazmat.2023.133339

MacDonald, E. C., Ginn, M. G., & Hamilton, D. J. (2012). Variability in foraging behavior and implications for diet breadth among Semipalmated Sandpipers staging in the upper Bay of Fundy. Condor, 114(1), 135–144. doi.org/10.1525/cond.2012.100246

Machendiranathan, M., Hu, Y., Chen, W. C., Tan, A., Xie, L., Chen, F., Jin, G., Ranith, R. P., & Senthilnathan, L. (2022). Consequences of anthropogenic activities and

beach dynamics on vertical distribution of microplastics in the mid-intertidal sediments of Donghai Island, China. Water Science and Technology, 86(6), 1342–1357. doi.org/10.2166/wst.2022.276

Machendiranathan, M., Jin, G., Huang, H., Liang, T., Lin, Z., Lin, H., Xie, L., & Chen, F. (2025). Vertical distribution of microplastics in coastal sediments of Xuwen Coral Reef National Nature Reserve, China. Journal of Oceanology and Limnology, 43, 422–432. doi.org/10.1007/s00343-024-3292-9

Malla-Pradhan, R., Suwunwong, T., Phoungthong, K., Joshi, T. P., & Pradhan, B. L. (2022). Microplastic pollution in urban Lake Phewa, Nepal: The first report on abundance and composition in surface water of lake in different seasons. Environmental Science and Pollution Research, 29, 39928–39936. doi.org/10.1007/s11356-021-18301-9

Manbohi, A., Mehdinia, A., Rahnama, R., Dehbandi, R., & Hamzehpour, A. (2021). Spatial distribution of microplastics in sandy beach and inshore-offshore sediments of the southern Caspian Sea. Marine Pollution Bulletin, 169, 1–12. doi.org/10.1016/j.marpolbul.2021.112578

Mandal, A., Singh, N., Mondal, A., Talib, M., Basu, R., Biswas, M. K., & Darbha, G. K. (2023). The extent of microplastic pollution along the eastern coast of India: Focussing on marine waters, beach sand, and fish. Marine Pollution Bulletin, 194, 1–12. doi.org/10.1016/j.marpolbul.2023.115265

Mao, X., Xu, Y., Cheng, Z., Yang, Y., Guan, Z., Jiang, L., & Tang, K. (2022). The impact of microplastic pollution on ecological environment: a review. Frontiers in Bioscience - Landmark Ed, 27(2), 1–7. doi.org/10.31083/j.fbl2702046

Marmara, D., Katsanevakis, S., Brundo, M. V., Tiralongo, F., Ignoto, S. & Krasakopoulou, E. (2023). Microplastics ingestion by marine fauna with a particular focus on commercial species: a systematic review. Frontiers in Marine Science, 1–16. doi.org/10.3389/fmars.2023.1240969

Masiá, P., Ardura, A., & Garcia-Vazquez, E. (2019). Microplastics in special protected areas for migratory birds in the Bay of Biscay. Marine Pollution Bulletin, 146, 993–1001. doi.org/10.1016/j.marpolbul.2019.07.065

Masiá, P., Ardura, A., Gaitán, M., Gerber, S., Rayon-Viña, F., & Garcia-Vazquez, E. (2021). Maritime ports and beach management as sources of coastal macro-, meso-, and microplastic pollution. Environmental Science and Pollution Research, 28, 30722–30731. doi.org/10.1007/s11356-021-12821-0

Masud, A., Gül, M., Küçükuysal, C., Buluş, E., & Şahin, Y. M. (2023). Effect of lithological properties of beach sediments on plastic pollution in Bodrum Peninsula (SW Türkiye). Marine Pollution Bulletin, 190, 1–14. doi.org/10.1016/j.marpolbul.2023.114895

Masura, J., & Marine Debris Program (U.S.). (2015). Laboratory methods for the analysis of microplastics in the marine environment : recommendations for quantifying synthetic particles in waters and sediments. NOAA Marine Debris Program,

National Oceanic and Atmospheric Administration, U.S. Department of Commerce. https://purl.fdlp.gov/GPO/gpo188064

Mataji, A., Taleshi, M. S., & Balimoghaddas, E. (2020). Distribution and characterization of microplastics in surface waters and the Southern Caspian Sea coasts sediments. Archives of Environmental Contamination and Toxicology, 78(1), 86–93. doi.org/10.1007/s00244-019-00700-2

Mathalon, A., & Hill, P. (2014). Microplastic fibers in the intertidal ecosystem surrounding Halifax Harbor, Nova Scotia. Marine Pollution Bulletin, 81(1), 69–79. doi.org/10.1016/j.marpolbul.2014.02.018

Matsumoto, M., Ito, H., Tateishi, A., Kobayashi, Y., Satoh, K., Numata, K., & Miyakawa, H. (2023). Effects of polycaprolactone degradation products on the water flea, Daphnia magna: Carbodiimide additives have acute and chronic toxicity. Journal of Applied Toxicology, 43(12), 1840–1848. doi.org/10.1002/jat.4516

Mayoma, B. S., Sørensen, C., Shashoua, Y., & Khan, F. R. (2020). Microplastics in beach sediments and cockles (*Anadara antiquata*) along the Tanzanian coastline. Bulletin of Environmental Contamination and Toxicology, 105, 513–521. doi.org/10.1007/s00128-020-02991-x

Mazurkiewicz, M., Martinez, P. S., Konwent, W., Deja, K., Kotwicki, L., & Węsławski, J. M. (2022). Plastic contamination of sandy beaches along the southern Baltic – a one season field survey results. Oceanologia, 64, 769–780. doi.org/10.1016/j.oceano.2022.07.004

Minor, E. C., Lin, R., Burrows, A., Cooney, E. M., Grosshuesch, S., & Lafrancois, B. (2020). An analysis of microlitter and microplastics from Lake Superior beach sand and surface-water. Science of the Total Environment, 744, 1–13. doi.org/10.1016/j.scitotenv.2020.140824

Misic, C., Covazzi Harriague, A., & Ferrari, M. (2019). Hydrodynamic forcing and sand permeability influence the distribution of anthropogenic microparticles in beach sediment. Estuarine, Coastal and Shelf Science, 230, 1–11. doi.org/10.1016/j.ecss.2019.106429

Misra, A., Zambrzycki, C., Kloker, G., Kotyrba, A., Anjass, M. H., Franco Castillo, I., Mitchell, S. G., Güttel, R., & Streb, C. (2020). Water purification and microplastics removal using magnetic polyoxometalate-supported ionic liquid phases (magPOM-SILPs). Angewandte Chemie, 132(4), 1618–1622. doi.org/10.1002/ange.201912111

Missawi, O., Bousserrhine, N., Zitouni, N., Maisano, M., Boughattas, I., De Marco, G., Cappello, T., Belbekhouche, S., Guerrouache, M., Alphonse, V., & Banni, M. (2021). Uptake, accumulation and associated cellular alterations of environmental samples of microplastics in the seaworm Hediste diversicolor. Journal of Hazardous Materials, 406, 1–11. doi.org/10.1016/j.jhazmat.2020.124287

Mohan, P. M., Tiwari, S., Karuvelan, M., Malairajan, S., Mageswaran, T., & Sachithanandam, V. (2022). A baseline study of meso and microplastic

predominance in pristine beach sediment of the Indian tropical island ecosystem. Marine Pollution Bulletin, 181, 1–12. doi.org/10.1016/j.marpolbul.2022.113825

Mondal, C., Mondal, N., Moon, U. M., Biswas, S. J., & Hossain, A. (2023). Contamination of microplastics in the marine food web with special reference to seafood: Present status and future concern. In Spatial Modeling of Environmental Pollution and Ecological Risk (pp. 175–207). Elsevier. doi.org/10.1016/B978-0-323-95282-8.00035-3

Monteiro, S. S., Rocha-Santos, T., Prata, J. C., Duarte, A. C., Girão, A. V., Lopes, P., Cristovão, T., & da Costa, J. P. (2022). A straightforward method for microplastic extraction from organic-rich freshwater samples. Science of the Total Environment, 815, 1–11. doi.org/10.1016/j.scitotenv.2022.152941

Moreira, F. T., Balthazar-Silva, D., Barbosa, L., & Turra, A. (2016). Revealing accumulation zones of plastic pellets in sandy beaches. Environmental Pollution, 218, 313–321. doi.org/10.1016/j.envpol.2016.07.006

Morét-Ferguson, S., Law, K. L., Proskurowski, G., Murphy, E. K., Peacock, E. E., & Reddy, C. M. (2010). The size, mass, and composition of plastic debris in the western North Atlantic Ocean. Marine pollution bulletin, 60(10), 1873–1878. doi.org/10.1016/j.marpolbul.2010.07.020

Morra, J. (2021). Characterizing microplastic pollution in aquatic sediments from Southwestern British Columbia, Canada [Dissertation, Simon Fraser University]. https://www.central.bac-lac.gc.ca/.redirect?app=damspub&id=0011e3d8-4525-453c-85cc-6e7ee73cfb4e

Munari, C., Infantini, V., Scoponi, M., Rastelli, E., Corinaldesi, C., & Mistri, M. (2017). Microplastics in the sediments of Terra Nova Bay (Ross Sea, Antarctica). Marine Pollution Bulletin, 122(1–2), 161–165. doi.org/10.1016/j.marpolbul.2017.06.039

Mylius, K. A., Lavers, J. L., Woehler, E. J., Rodemann, T., Keys, B. C., & Rivers-Auty, J. (2023). Foraging strategy influences the quantity of ingested micro- and nanoplastics in shorebirds. Environmental Pollution, 319, 1–9. doi.org/10.1016/j.envpol.2022.120844

Nabizadeh, R., Sajadi, M., Rastkari, N., & Yaghmaeian, K. (2019). Microplastic pollution on the persian gulf shoreline: a case study of Bandar Abbas city, Hormozgan Province, Iran. Marine Pollution Bulletin, 145, 536–546. doi.org/10.1016/j.marpolbul.2019.06.048

Nadon, G. C., & Middleton, G. (1985). The stratigraphy and sedimentology of the Fundy Group (Triassic) of the St. Martins area, New Brunswick. Canadian Journal of Earth Science, 22, 1183–1203. doi.org/10.1139/e85-121

Naidoo, T., Glassom, D., & Smit, A. J. (2015). Plastic pollution in five urban estuaries of KwaZulu-Natal, South Africa. Marine Pollution Bulletin, 101(1), 473–480. doi.org/10.1016/j.marpolbul.2015.09.044

Naji, A., Esmaili, Z., & Khan, F. R. (2017). Plastic debris and microplastics along the beaches of the Strait of Hormuz, Persian Gulf. Marine Pollution Bulletin, 114, 1057–1062. doi.org/10.1016/j.marpolbul.2016.11.032

Napper, I. E., & Thompson, R. C. (2016). Release of synthetic microplastic plastic fibres from domestic washing machines: Effects of fabric type and washing conditions. Marine Pollution Bulletin, 112(1–2), 39–45. doi.org/10.1016/j.marpolbul.2016.09.025

National Oceanic and Atmospheric Administration. What are microplastics? National Oceanic and Atmospheric Administration. Retrieved March 2, 2025, from oceanservice.noaa.gov/facts/microplastics.html

National Oceanic and Atmospheric Administration. "NOAA National Ocean Service Education: Coastal Pollution Tutorial." NOAA's National Ocean Service, October 22, 2019. oceanservice.noaa.gov/education/tutorial-coastal/marine-debris/md04-sub-01.html

Nchimbi, A. A., Shilla, D. A., Kosore, C. M., Shilla, D. J., Shashoua, Y., & Khan, F. R. (2022). Microplastics in marine beach and seabed sediments along the coasts of Dar es Salaam and Zanzibar in Tanzania. Marine Pollution Bulletin, 185, 1–6. doi.org/10.1016/j.marpolbul.2022.114305

Nel, H. A., Sambrook Smith, G. H., Harmer, R., Sykes, R., Schneidewind, U., Lynch, I., & Krause, S. (2020). Citizen science reveals microplastic hotspots within tidal estuaries and the remote Scilly Islands, United Kingdom. Marine Pollution Bulletin, 161, 1–12. doi.org/10.1016/j.marpolbul.2020.111776

Nematollahi, M. J., Keshavarzi, B., Mohit, F., Moore, F., & Busquets, R. (2022). Microplastic occurrence in urban and industrial soils of Ahvaz metropolis: A city with a sustained record of air pollution. Science of the Total Environment, 819, 1–12. doi.org/10.1016/j.scitotenv.2021.152051

Nguyen, Q. A. T., Nguyen, H. N. Y., Strady, E., Nguyen, Q. T., Trinh-Dang, M., & Vo, M. (2020). Characteristics of microplastics in shoreline sediments from a tropical and urbanized beach (Da Nang, Vietnam). Marine Pollution Bulletin, 161, 1–10. doi.org/10.1016/j.marpolbul.2020.111768

Nhon, N. T. T., Nguyen, N. T., Hai, H. T. N., & Hien, T. T. (2022). Distribution of microplastics in beach sand on the Can Gio coast, Ho Chi Minh City, Vietnam. Water, 14(18), 1–18. doi.org/10.3390/w14182779

Nichols, E. C., Lavers, J. L., Archer-Rand, S., & Bond, A. L. (2021). Assessing plastic size distribution and quantity on a remote island in the South Pacific. Marine Pollution Bulletin, 167, 1–9. doi.org/10.1016/j.marpolbul.2021.112366

Noël, M., Wong, C., Ross, P. S., Patankar, S., Etemadifar, A., Morales-Caselles, C., Lyons, S., & Delisle, K. (2022). Microplastics distribution in sediment and mussels along the British Columbia Coast, Canada. Marine Pollution Bulletin, 185, 1–10. doi.org/10.1016/j.marpolbul.2022.114273

Novillo-Sanjuan, O., Raga, J. A., & Tomás, J. (2022). Microdebris in three Spanish Mediterranean beaches located at a sporadic loggerhead turtles' (Caretta caretta) nesting area. Regional Studies in Marine Science, 49, 1–11. doi.org/10.1016/j.rsma.2021.102116

Obuzor, G. U., & Onyedikachi, U. B. (2023). Chemical leaching into food and the environment poses health hazards. In Sustainable Development Goals Series: Part F2785 (pp. 129–148). Springer. doi.org/10.1007/978-3-031-34963-8_14

Ocean Diagnostics. (2024, November 26). Press release: New report tackles microfibre pollution crisis, outlines solutions. Ocean Diagnostics. oceandiagnostics.com/ocean-diagnostics-blog/press-release-microfibre-report

Ocean Wise. (2021, July 20). Microfibers from our clothes are polluting the ocean, but new study offers hopeful solutions. Ocean Wise. ocean.org/media/microfibers-from-our-clothes-are-polluting-the-ocean-but-new-study-offers-hopeful-solutions/

OECD. (2024a). Extended Producer Responsibility: Basic facts and key principles.

OECD. (2024b). Policy Scenarios for Eliminating Plastic Pollution by 2040. OECD. doi.org/10.1787/76400890-en

Ordóñez, O. G. (2022). Microplastic pollution in mangroves and beaches of the Cispata marine protected area, Colombian Caribbean Coast. Revista Ciencias Marinas y Costeras, 14(2), 9–25. doi.org/10.15359/revmar.14-2.1

Pagter, E., Frias, J., & Nash, R. (2018). Microplastics in Galway Bay: A comparison of sampling and separation methods. Marine Pollution Bulletin, 135, 932–940. doi.org/10.1016/j.marpolbul.2018.08.013

Pal, D., Prabhakar, R., Barua, B., Zekker, I., Burlakovs, J., Krauklis, A., Hogland, W., & Vincevica-Gaile, Z. (2024). Microplastics in aquatic systems: A comprehensive review of its distribution, environmental interactions, and health risks. Environmental Science and Pollution Research, 32, 56–88. doi.org/10.1007/s11356-024-35741-1

Paler, M. K. O., Malenab, M. C. T., Maralit, J. R., & Nacorda, H. M. (2019). Plastic waste occurrence on a beach off southwestern Luzon, Philippines. Marine Pollution Bulletin, 141, 416–419. doi.org/10.1016/j.marpolbul.2019.02.006

Pan, I., & Umapathy, S. (2024). Probiotics an emerging therapeutic approach towards gut-brain-axis oriented chronic health issues induced by microplastics: A comprehensive review. Heliyon, 10(11), 1–28. doi.org/10.1016/j.heliyon.2024.e32004

Papuga, K., Kaszubkiewicz, J., Kawałko, D., & Kreimeyer, M. (2022). Effect of organic matter removal by hydrogen peroxide on the determination of soil particle size distribution using the dynamometer method. Agriculture (Switzerland), 12(2), 1–14. doi.org/10.3390/agriculture12020226

Paradinas, L. M., James, N. A., Quinn, B., Dale, A., & Narayanaswamy, B. E. (2021). A new collection tool-kit to sample microplastics from the marine environment

(sediment, seawater, and biota) using citizen science. Frontiers in Marine Science, 8, 1–15. doi.org/10.3389/fmars.2021.657709

Pasquier, G., Doyen, P., Chaïb, I., & Amara, R. (2024). Do tidal fluctuations affect microplastics distribution and composition in coastal waters? Marine Pollution Bulletin, 200, 1–10. doi.org/10.1016/j.marpolbul.2024.116166

Patchaiyappan, A., Ahmed, S. Z., Dowarah, K., Jayakumar, S., & Devipriya, S. P. (2020). Occurrence, distribution and composition of microplastics in the sediments of South Andaman beaches. Marine Pollution Bulletin, 156, 1–10. doi.org/10.1016/j.marpolbul.2020.111227

Patchaiyappan, A., ZakiAhmed, S., Dowarah, K., Khadanga, S. S., Singh, T., Jayakumar, S., Thirunavukkarasu, C., & Devipriya, S. P. (2021). Prevalence of microplastics in the sediments of Odisha beaches, southeastern coast of India. Marine Pollution Bulletin, 167, 1–10. doi.org/10.1016/j.marpolbul.2021.112265

Patidar, K., Ambade, B., & Alshehri, M. (2024). Microplastics and associated polycyclic aromatic hydrocarbons in surface water and sediment of the Bay of Bengal coastal area, India: Sources, pathway and ecological risk. Environmental Geochemistry and Health, 46, 1–19. doi.org/10.1007/s10653-024-01926-3

Patti, T. B., Fobert, E. K., Reeves, S. E., & Burke da Silva, K. (2020). Spatial distribution of microplastics around an inhabited coral island in the Maldives, Indian Ocean. Science of the Total Environment, 748, 1–10. doi.org/10.1016/j.scitotenv.2020.141263

Pelegrini, K., Pereira, T. C. B., Wertheimer, C. C. S., De Souza Teodoro, L., De Souza Basso, N. R., Ligabue, R. A., & Bogo, M. R. (2024). Microplastics beach pollution: Composition, quantification and distribution on the southern coast of Brazil. Water, Air, and Soil Pollution, 235, 1–21. doi.org/10.1007/s11270-024-07541-3

Pervez, R., & Wang, Y. H. (2022). Microplastic distribution within core sediments of beach and its responses to anthropogenic activities. Marine Pollution Bulletin, 174(113256), 1–9. doi.org/10.1016/j.marpolbul.2021.113256

Pervez, R., Lai, Y., Song, Y., Li, X., & Lai, Z. (2023). Impact of microplastic pollution on coastal ecosystems using comprehensive beach quality indices. Marine Pollution Bulletin, 194, 1–10. doi.org/10.1016/j.marpolbul.2023.115300

Pervez, R., Wang, Y., Mahmood, Q., & Jattak, Z. (2020). Stereomicroscopic and Fourier transform infrared (FTIR) spectroscopic characterization of the abundance, distribution and composition of microplastics in the beaches of Qingdao, China. Analytical Letters, 53, 2960–2977. doi.org/10.1080/00032719.2020.1763379

Petrovic, A., Westphal, H., Hodhodi, B., Slootmaker, T., Koberg, A., & Naji, A. (2022). Influence of windward versus leeward settings on microplastic distribution in beach sediments of Kish Island, Gulf region. Regional Studies in Marine Science, 55, 1–14. doi.org/10.1016/j.rsma.2022.102585

Pfeiffer, F., & Fischer, E. K. (2020). Various digestion protocols within microplastic sample processing—evaluating the resistance of different synthetic polymers and

the efficiency of biogenic organic matter destruction. Frontiers in Environmental Science, 8, 1–9. doi.org/10.3389/fenvs.2020.572424

Pieper, C., Martins, A., Zettler, E., Loureiro, C. M., Onink, V., Heikkilä, A., Epinoux, A., Edson, E., Donnarumma, V., de Vogel, F., Law, K. L., & Amaral-Zettler, L. (2020). Into the med: searching for microplastics from space to deep-sea. In M. Cocca, E. Di Pace, M. Errico, G. Gentile, A. Montarsolo, R. Mossotti, & M. Avella (Eds.), Proceedings of the 2nd International Conference on Microplastic Pollution in the Mediterranean Sea. ICMPMS 2019 (pp. 129–138). Springer, Cham. doi.org/10.1007/978-3-030-45909-3_21

Piñon-Colin, T. D. J., Rodriguez-Jimenez, R., Pastrana-Corral, M. A., Rogel-Hernandez, E., & Wakida, F. T. (2018). Microplastics on sandy beaches of the Baja California Peninsula, Mexico. Marine Pollution Bulletin, 131, 63–71. doi.org/10.1016/j.marpolbul.2018.03.055

Piperagkas, O., & Papageorgiou, N. (2021). Changes in (micro and macro) plastic pollution in the sediment of three sandy beaches in the Eastern Mediterranean Sea, in relation to seasonality, beach use and granulometry. Marine Pollution Bulletin, 173, 1–8. doi.org/10.1016/j.marpolbul.2021.113014

Piperagkas, O., Papageorgiou, N., & Karakassis, I. (2019). Qualitative and quantitative assessment of microplastics in three sandy Mediterranean beaches, including different methodological approaches. Estuarine, Coastal and Shelf Science, 219, 169–175. doi.org/10.1016/j.ecss.2019.02.016

Piyumali, H., Sewwandi, M., Atugoda, T., Wijesekara, H., Mahatantila, K., & Vithanage, M. (2024). Microplastic abundance, characteristics, and heavy metal contamination in coastal environments of Western Sri Lanka. Physics and Chemistry of the Earth, 136, 1–11. doi.org/10.1016/j.pce.2024.103770

Plastics Europe. (2021). Plastics - the Facts 2021. Plastics Europe. plasticseurope.org/wp-content/uploads/2021/12/Plastics-the-Facts-2021-web-final.pdf

Pohl, A., & Bodzek, M. (2023). Alkylphenols and bisphenol A in the aquatic environment and their leaching from plastic products – a review. Desalination and Water Treatment, 315, 446–457. doi.org/10.5004/dwt.2023.30176

Prarat, P., & Hongsawat, P. (2022). Microplastic pollution in surface seawater and beach sand from the shore of Rayong province, Thailand: Distribution, characterization, and ecological risk assessment. Marine Pollution Bulletin, 174, 1–13. doi.org/10.1016/j.marpolbul.2021.113200

Prarat, P., Thanayotmethi, T., Sriboonyapirat, T., Donsomchit, P., Hongsawat, P., & Chouychai, B. (2020). Preliminary study of abundance and characteristics of microplastics on beach sediment along the Coast of Rayong Province, Thailand. IOP Conference Series: Earth and Environmental Science, 581(1), 1–7. doi.org/10.1088/1755-1315/581/1/012033

Prata, J. C., da Costa, J. P., Girão, A. V., Lopes, I., Duarte, A. C., & Rocha-Santos, T. (2019). Identifying a quick and efficient method of removing organic matter

without damaging microplastic samples. Science of the Total Environment, 686, 131–139. doi.org/10.1016/j.scitotenv.2019.05.456

Purushothaman, A., Vishnudattan, N. K., Nehala, S. P., Meghamol, M. D., Neethu, K. V., Joseph, J., Nandan, S. B., Padmakumar, K. B., & Thomas, L. C. (2023). Patterns and variability in the microplastic contamination along the southwest coast of India with emphasis on submarine groundwater discharge sites. Marine Pollution Bulletin, 194, 1–14. doi.org/10.1016/j.marpolbul.2023.115432

Quinn, J. T., Hamilton, D. J., & Hebert, C. E. (2017). Fatty acid composition and concentration of alternative food of semipalmated sandpipers (Calidris pusilla) in the upper Bay of Fundy, Canada. Canadian Journal of Zoology, 95(8), 565–573. doi.org/10.1139/cjz-2016-0246

Rahimi, A. R., & Garciá, J. M. (2017). Chemical recycling of waste plastics for new materials production. Nature Reviews Chemistry, 1, 1–11. doi.org/10.1038/s41570-017-0046

Rahman, M. A., Mojumdar, S., Rahman, S. A., Ahmed, T., & Marimuthu, K. (2023). Plastic pollutions in the ocean: their sources, causes, effects and control measures. Journal of Biological Studies, 6(1), 38–52.

Rahman, S. M. A., Robin, G. S., Momotaj, M., Uddin, J., & Siddique, M. A. M. (2020). Occurrence and spatial distribution of microplastics in beach sediments of Cox's Bazar, Bangladesh. Marine Pollution Bulletin, 160, 1–10. doi.org/10.1016/j.marpolbul.2020.111587

Raimundo, G. I., Sousa, M. C., & Dias, J. M. (2020). Numerical modelling of plastic debris transport and accumulation throughout Portuguese Coast. Journal of Coastal Research, 95, 1252–1257. doi.org/10.2112/SI95-242.1

Ramos-Vázquez, M. A., Verma, S. K., Armstrong-Altrin, J. S., James, R. A., & Madhavaraju, J. (2024). Characterization of microplastics in marine sediments from the Gulf of Tehuantepec, Mexican Pacific. Carpathian Journal of Earth and Environmental Sciences, 19(2), 255–264. doi.org/10.26471/cjees/2024/019/296

Ramsar. (n.d.). Canada 21: Shepody Bay, New Brunswick. In Ramsar. Retrieved April 8, 2025, from rsis.ramsar.org/

Rangel-Buitrago, N., Arroyo-Olarte, H., Trilleras, J., Arana, V. A., Mantilla-Barbosa, E., Gracia, C. A., Mendoza, A. V., Neal, W. J., Williams, A. T., & Micallef, A. (2021). Microplastics pollution on Colombian Central Caribbean beaches. Marine Pollution Bulletin, 170, 1–13. doi.org/10.1016/j.marpolbul.2021.112685

Ranjani, M., Veerasingam, S., Venkatachalapathy, R., Jinoj, T. P. S., Guganathan, L., Mugilarasan, M., & Vethamony, P. (2022). Seasonal variation, polymer hazard risk and controlling factors of microplastics in beach sediments along the southeast coast of India. Environmental Pollution, 305, 1–11. doi.org/10.1016/j.envpol.2022.119315

Rayhan, A. B. M. S., Wang, J., Islam, M. M., Hossain, K. B., Chen, B., Ke, H., & Cai, M. (2024). Tidal variability and microplastics distribution: Source analysis in

Dongshan Bay beach sediments, South China. Journal of Oceanology and Limnology, 43, 459–473. doi.org/10.1007/s00343-024-4089-6

Razeghi, N., Hamidian, A. H., Wu, C., Zhang, Y., & Yang, M. (2021). Microplastic sampling techniques in freshwaters and sediments: a review. In Environmental Chemistry Letters (Vol. 19, Number 6, pp. 4225–4252). Springer Science and Business Media Deutschland GmbH. doi.org/10.1007/s10311-021-01227-6

Reddy, N. G., Vidya, A., & Sri Mullapudi, R. (2022). Review of the utilization of plastic wastes as a resource material in civil engineering infrastructure applications. Journal of Hazardous, Toxic, and Radioactive Waste, 26(4), 1–13. doi.org/10.1061/(asce)hz.2153-5515.0000717

Reid, J. (2013). Finding Kluskap: A journey into Mi'kmaw myth (W. Deal, G. Gundaker, T. Kassam, W. Kort, L. Patton, & R. Sugirtharajah, Eds.). The Pennsylvania State University Press.

Retama, I., Jonathan, M. P., Shruti, C., Velumani, S., Sarkar, S. K., Roy, P. D., & Rodríguez-Espinosa, P. F. (2016). Microplastics in tourist beaches of Huatulco Bay, Pacific coast of southern Mexico. Marine Pollution Bulletin, 113(1–2), 530–535. doi.org/10.1016/j.marpolbul.2016.08.053

Rey, S. F., Franklin, J., & Rey, S. J. (2021). Microplastic pollution on island beaches, Oahu, Hawai'i. PLoS ONE, 16, 1–13. doi.org/10.1371/journal.pone.0247224

Rezaie, A., & Forghani, S. (2022). A Novel Method for Removal of Hazardous Microplastics from Water Using Magnets. Journal of Environmental Health and Sustainable Development, 7(4), 1775–1776. doi.org/10.18502/JEHSD.V7I4.11428

Rochman, C., Browne, M. A., Underwood, A. J., Van Franeker, J., Thompson, R., & Amaral-Zettler, L. (2016). The ecological impacts of marine debris: Unraveling the demonstrated evidence from what is perceived. Ecology, 97(2), 302–312. doi.org/10.1890/14-2070.1

Rodrigues, C., Rodríguez, Y., Frias, J., Carriço, R., Sobral, P., Antunes, J., Duncan, E. M., & Pham, C. K. (2024). Microplastics in beach sediments of the Azores archipelago, NE Atlantic. Marine Pollution Bulletin, 201, 1–8. doi.org/10.1016/j.marpolbul.2024.116243

Rogowska, W., Skorbiłowicz, E., Skorbiłowicz, M., & Trybułowski, Ł. (2021). Microplastics in coastal sediments of Ełckie lake (Poland). Studia Quaternaria, 38, 109–116. doi.org/10.24425/sq.2021.136827

Ronda, A. C., Menéndez, M. C., Tombesi, N., Álvarez, M., Tomba, J. P., Silva, L. I., & Arias, A. H. (2023). Microplastic levels on sandy beaches: Are the effects of tourism and coastal recreation really important? Chemosphere, 316, 1–14. doi.org/10.1016/j.chemosphere.2023.137842

Rothstein, S. I. (1973). Plastic particle pollution of the surface of the Atlantic Ocean: evidence from a seabird. The Condor, 75, 344–345.

Ryan, A. C., Allen, D., Allen, S., Maselli, V., LeBlanc, A., Kelleher, L., Krause, S., Walker, T. R., & Cohen, M. (2023). Transport and deposition of ocean-sourced

microplastic particles by a North Atlantic hurricane. Communications Earth and Environment, 4(1), 1–10. doi.org/10.1038/s43247-023-01115-7

Sabaliauskaitė, V., Kataržytė, M., Rubavičiūtė, R., Tiškus, E., & Balčiūnas, A. (2024). Beach wrack as a potential microplastic hot spot in the South-Eastern Baltic Sea environment. Marine Pollution Bulletin, 209, 1–10. doi.org/10.1016/j.marpolbul.2024.117139

Sagawa, N., Kawaai, K., & Hinata, H. (2018). Abundance and size of microplastics in a coastal sea: Comparison among bottom sediment, beach sediment, and surface water. Marine Pollution Bulletin, 133, 532–542. doi.org/10.1016/j.marpolbul.2018.05.036

Sajorne, R. E., Cayabo, G. D. B., Gajardo, L. J. A., Mabuhay-Omar, J. A., Creencia, L. A., & Bacosa, H. P. (2022). Disentangling microplastic pollution on beach sand of Puerto Princesa, Palawan Island, Philippines: Abundance and characteristics. Sustainability, 14, 1–11. doi.org/10.3390/su142215303

Samrat Hossain, M., Saifullah, A. S. M., Uddin, M. J., & Hasibur Rahaman, M. (2024). Assessment of microplastics in coastal ecosystem of Bangladesh. Ecotoxicology and Environmental Safety, 281, 1–14. doi.org/10.1016/j.ecoenv.2024.116622

Sánchez-García, N., & Sanz-Lázaro, C. (2023). Darwin's paradise contaminated by marine debris: Understanding their sources and accumulation dynamics. Environmental Pollution, 324, 1–8. doi.org/10.1016/j.envpol.2023.121310

Sathish, N., Jeyasanta, K. I., & Patterson, J. (2019). Abundance, characteristics and surface degradation features of microplastics in beach sediments of five coastal areas in Tamil Nadu, India. Marine Pollution Bulletin, 142, 112–118. doi.org/10.1016/j.marpolbul.2019.03.037

Scaria, S. S., Balasubramanian, B., Dandin, S., Meyyazhagan, A., Pappuswamy, M., Sattanathan, G., Liu, W. C., Kadanthottu Sebastian, J., & Park, S. (2023). Review on impacts of micro- and nano-plastic on aquatic ecosystems and mitigation strategies. Aquatic Toxicology, 265, 1–14. doi.org/10.1016/j.aquatox.2023.106759

Schröder, K., Kossel, E., & Lenz, M. (2021). Microplastic abundance in beach sediments of the Kiel Fjord, Western Baltic Sea. Environmental Science and Pollution Research, 28, 26515–26528. doi.org/10.1007/s11356-020-12220-x/Published

Scopetani, C., Chelazzi, D., Martellini, T., Pellinen, J., Ugolini, A., Sarti, C., & Cincinelli, A. (2021). Occurrence and characterization of microplastic and mesoplastic pollution in the Migliarino San Rossore, Massaciuccoli Nature Park (Italy). Marine Pollution Bulletin, 171, 1–8. doi.org/10.1016/j.marpolbul.2021.112712

Scopetani, C., Chelazzi, D., Mikola, J., Leiniö, V., Heikkinen, R., Cincinelli, A., & Pellinen, J. (2020). Olive oil-based method for the extraction, quantification and identification of microplastics in soil and compost samples. Science of the Total Environment, 733(139338), 1–7. doi.org/10.1016/j.scitotenv.2020.139338

Seemungal, R., Darsan, J., & Wilson, M. (2022). The influence of coastal geomorphology and human activity on plastic debris distribution on a micro-tidal recreational beach on the north coast of Trinidad. Journal of Coastal Conservation, 26(3), 1–16. doi.org/10.1007/s11852-021-00846-z

Şener, İ., & Yabanlı, M. (2023). Macro- and microplastic abundance from recreational beaches along the South Aegean Sea (Türkiye). Marine Pollution Bulletin, 194, 1–11. doi.org/10.1016/j.marpolbul.2023.115329

Sevwandi, W. L. S., Andrady, A. L., Kumara, P. B. T. P., Maes, T., & Gangabadage, C. S. (2021). Microplastics pollution in Marine Protected Areas of Southern Sri Lanka. Marine Pollution Bulletin, 168, 1–10. doi.org/10.1016/j.marpolbul.2021.112462

Shaji, S., Vannarath, A., Rao, Y. R. S., & Sundaram, B. (2024). Distribution, characteristics and ecological risk of microplastics in beach sediments along the northern coast of Andhra Pradesh, India. Regional Studies in Marine Science, 77, 1–16. doi.org/10.1016/j.rsma.2024.103716

Sharma, N., & Vuppu, S. (2023). In silico study of enzymatic degradation of bioplastic by microalgae: an outlook on microplastic environmental impact assessment, challenges, and opportunities. Molecular Biotechnology, 23, 1–31. doi.org/10.1007/s12033-023-00886-w

Sheikhi, H., & Mirzaei, R. (2023). Occurrence and abundance of macro, meso and microplastics along the coasts of the Persian Gulf (case study: Bushehr Province coast). Marine Pollution Bulletin, 194, 1–10. doi.org/10.1016/j.marpolbul.2023.115261

Shen, L., & Worrell, E. (2024). Plastic recycling. In C. Meskers, E. Worrell, & M. A. Reuter (Eds.), Handbook of Recycling (Second, pp. 497–510). Elsevier. doi.org/10.1016/B978-0-323-85514-3.00014-2

Shi, W., Cui, T., Wu, H., LeBlanc, G. A., Wang, F., & Lihui, A. N. (2021). A proposed nomenclature for microplastic contaminants. Marine Pollution Bulletin, 172, 1–4. doi.org/10.1016/j.marpolbul.2021.112960

Shinde, R., Rabari, V., Duggal, R., Patel, A., Alharbi, S. A., Ansari, M. J., & Trivedi, J. (2024). An assessment of microplastic contamination in beach sediment of Maharashtra State, India, with special reference to anthropogenic activities. Water Environment Research, 96, 1–14. doi.org/10.1002/wer.11033

Simon-Sánchez, L., Grelaud, M., Franci, M., & Ziveri, P. (2022). Are research methods shaping our understanding of microplastic pollution? A literature review on the seawater and sediment bodies of the Mediterranean Sea. Environmental Pollution, 292, 1–14. doi.org/10.1016/j.envpol.2021.118275

Simon-Sánchez, L., Grelaud, M., Garcia-Orellana, J., & Ziveri, P. (2019). River deltas as hotspots of microplastic accumulation: The case study of the Ebro River (NW Mediterranean). Science of the Total Environment, 687, 1186–1196. doi.org/10.1016/j.scitotenv.2019.06.168

Sivaraman, M., Fan, L., & Yan, W. (2024). Quantitative analysis of microplastics in beach sand via low-temperature solvent extraction and thermal degradation: Effects of particle size and sample depth. Science of the Total Environment, 953, 1–10. doi.org/10.1016/j.scitotenv.2024.176009

Soil Survey Staff. (1951). Soil survey manual. U.S. Department of Agriculture Handbook 18. Soil Conservation Service.

Soursou, V., Campo, J., & Picó, Y. (2023). A critical review of the novel analytical methods for the determination of microplastics in sand and sediment samples. Trends in Analytical Chemistry, 166(117190), 1–15. doi.org/10.1016/j.trac.2023.117190

Soursou, V., Campo, J., & Picó, Y. (2024). Spatio-temporal variation and ecological risk assessment of microplastics along the touristic beaches of a Mediterranean coast transect (Valencia province, East Spain). Journal of Environmental Management, 354, 1–13. doi.org/10.1016/j.jenvman.2024.120315

SpecialChem SA. (n.d.). Density of Plastics: Technical Properties. Omnexus: The Material Selection Platform. Retrieved March 1, 2023, from omnexus.specialchem.com/polymer-properties/properties/density

Species At Risk. (2006, January 6). Fall Shorebird Migration. Species at Risk. https://www.speciesatrisk.ca/fundyshorebirds/shorebirds/migration.html

Srihari, S., Subramani, T., Prapanchan, V. N., & Li, P. (2023). Human health risk perspective study on characterization, quantification and spatial distribution of microplastics in surface water, groundwater and coastal sediments of thickly populated Chennai coast of South India. Human and Ecological Risk Assessment, 29, 222–244. doi.org/10.1080/10807039.2022.2154635

Stea, R. R., Seaman, A. A., Pronk, T., Parkhill, M. A., Allard, S., & Utting, D. (2011). The Appalachian Glacier Complex in Maritime Canada. In Developments in Quaternary Science (Vol. 15, pp. 631–659). doi.org/10.1016/B978-0-444-53447-7.00048-9

Stolte, A., Forster, S., Gerdts, G., & Schubert, H. (2015). Microplastic concentrations in beach sediments along the German Baltic coast. Marine Pollution Bulletin, 99(1–2), 216–229. doi.org/10.1016/j.marpolbul.2015.07.022

Strady, E., Dang, T. H., Dao, T. D., Dinh, H. N., Do, T. T. D., Duong, T. N., Duong, T. T., Hoang, D. A., Kieu-Le, T. C., Le, T. P. Q., Mai, H., Trinh, D. M., Nguyen, Q. H., Tran-Nguyen, Q. A., Tran, Q. V., Truong, T. N. S., Chu, H., & Vo, C. (2021). Baseline assessment of microplastic concentrations in marine and freshwater environments of a developing Southeast Asian country, Vietnam. Marine Pollution Bulletin, 162, 1–10. doi.org/10.1016/j.marpolbul.2020.111870

Sujathan, S., Kniggendorf, A. K., Kumar, A., Roth, B., Rosenwinkel, K. H., & Nogueira, R. (2017). Heat and bleach: a cost-efficient method for extracting microplastics from return activated sludge. Archives of Environmental Contamination and Toxicology, 73(4), 641–648. doi.org/10.1007/s00244-017-0415-8

Summers, E., Du, J., Park, K., Wharton, M., & Kaiser, K. (2024). Importance of the water-sediment bed interactions in simulating microplastic particles in an estuarine system. Frontiers in Marine Science, 11, 1–17. doi.org/10.3389/fmars.2024.1414459

Sundar, S., Chokkalingam, L., Roy, P. D., & Usha, T. (2021). Estimation of microplastics in sediments at the southernmost coast of India (Kanyakumari). Environmental Science and Pollution Research, 28, 18495–18500. doi.org/10.1007/s11356-020-10333-x

Sunil, M., N, M., Charles, M., Chidangil, S., Kumar, S., & Lukose, J. (2024). Visualization and characterisation of microplastics in aquatic environment using a home-built micro-Raman spectroscopic set up. Journal of Environmental Management, 354, 1–15. doi.org/10.1016/j.jenvman.2024.120351

Sunitha, T. G., Monisha, V., Sivanesan, S., Vasanthy, M., Prabhakaran, M., Omine, K., Sivasankar, V., & Darchen, A. (2021). Micro-plastic pollution along the Bay of Bengal coastal stretch of Tamil Nadu, South India. Science of the Total Environment, 756, 1–12. doi.org/10.1016/j.scitotenv.2020.144073

Sustainability Directory. (2025, December 19). How do wastewater treatment plants handle microplastics and microfibers? Sustainability Directory. pollution.sustainability-directory.com/learn/how-do-wastewater-treatment-plants-handle-microplastics-and-microfibers/

Taher, N. Z., Shabaka, S., Soliman, Y. A., & Younis, A. M. (2023). Assessment of microplastic pollution in the Gulf of Suez: Abundance and polymeric composition in beach sediments. Egyptian Journal of Aquatic Biology and Fisheries, 27(4), 671–682. doi.org/10.21608/ejabf.2023.312078

Tasnim, J., Ahmed, M. K., Hossain, K. B., & Islam, M. S. (2023). Spatiotemporal distribution of microplastic debris in the surface beach sediment of the southeastern coast of Bangladesh. Heliyon, 9(11), 1–13. doi.org/10.1016/j.heliyon.2023.e21864

Tata, T., Belabed, B. E., Bououdina, M., & Bellucci, S. (2020). Occurrence and characterization of surface sediment microplastics and litter from North African coasts of Mediterranean Sea: Preliminary research and first evidence. Science of the Total Environment, 713, 1–10. doi.org/10.1016/j.scitotenv.2020.136664

Terzi, Y., Gedik, K., Eryaşar, A. R., Öztürk, R. Ç., Şahin, A., & Yılmaz, F. (2022). Microplastic contamination and characteristics spatially vary in the southern Black Sea beach sediment and sea surface water. Marine Pollution Bulletin, 174, 1–10. doi.org/10.1016/j.marpolbul.2021.113228

Thepwilai, S., Wangritthikraikul, K., Chawchai, S., & Bissen, R. (2021). Testing the factors controlling the numbers of microplastics on beaches along the western Gulf of Thailand. Marine Pollution Bulletin, 168, 1–12. doi.org/10.1016/j.marpolbul.2021.112467

Thompson, R. C., & De Falco, F. (2020). Marine litter: are there solutions to this environmental challenge? Nature, 39–44). doi.org/10.1007/978-3-030-45909-3_8

Thompson, R. C., Courtene-Jones, W., Boucher, J., Pahl, S., Raubenheimer, K., & Koelmans, A. A. (2024). Twenty years of microplastic pollution research-what have we learned? Science (New York, N.Y.), 386, 1–12. doi.org/10.1126/science.adl2746

Thompson, R. C., Olsen, Y., Mitchell, R. P., Davis, A., Rowland, S. J., John, A. W. G., Mcgonigle, D., & Russell, A. E. (2004). Lost at sea: where is all the plastic? 304, 838.

Thushari, G. G. N., & Senevirathna, J. D. M. (2020). Plastic pollution in the marine environment. Heliyon, 6(8), 1–16. doi.org/10.1016/j.heliyon.2020.e04709

Tirkey, A., & Upadhyay, L. S. B. (2021). Microplastics: An overview on separation, identification and characterization of microplastics. Marine Pollution Bulletin, 170, 1–12. doi.org/10.1016/j.marpolbul.2021.112604

Tiwari, M., Rathod, T. D., Ajmal, P. Y., Bhangare, R. C., & Sahu, S. K. (2019). Distribution and characterization of microplastics in beach sand from three different Indian coastal environments. Marine Pollution Bulletin, 140, 262–273. doi.org/10.1016/j.marpolbul.2019.01.055

Tiwari, M., Sahu, S. K., Rathod, T., Bhangare, R. C., Ajmal, P. Y., Pulhani, V., & Vinod Kumar, A. (2023). Comprehensive review on sampling, characterization and distribution of microplastics in beach sand and sediments. Trends in Environmental Analytical Chemistry, 40, 1–13. doi.org/10.1016/j.teac.2023.e00221

Tong, N. X., Khuyen, V. T. K., & Thao, N. T. T. (2023). Combining fluorescence microscope and FTIR to investigate microplastics in sand at Vung Tau beaches. EnvironmentAsia, 16, 137–148. doi.org/10.14456/ea.2023.28

TransAqua. (2024). GMWC Infrastructure Report Card. https://www.transaqua.ca

Trenhaile, A. S., Pepper, D. A., Trenhaile, R. W., & Dalimonte, M. (1998). Stack and notch development, Hopewell Rocks, New Brunswick. Canadian Geographer, 42(1), 94–99. doi.org/10.1111/j.1541-0064.1998.tb01556.x

Truchet, D. M., López, A. D. F., Ardusso, M. G., Rimondino, G. N., Buzzi, N. S., Malanca, F. E., Spetter, C. V., & Severini, M. D. F. (2021). Microplastics in bivalves, water and sediments from a touristic sandy beach of Argentina. Marine Pollution Bulletin, 173, 1–11. doi.org/10.1016/j.marpolbul.2021.113023

Tuong Vy, N. T., Nha Khanh, D. N., Hai Khoa, L., Tan Phat, N., Kim Phuong, L., Mon, D., Tuan Nhi, P., Mong Lan, N. T., Ngoc Thanh, D., The Anh, N., Lan Anh, T. N., Minh Dan, L., Nhat Tri, H., & Kim Phuong, N. T. (2024). Assessment of microplastics pollution level on clam farming and bathing beaches: A case study of Thanh Phu in Ben Tre, Vietnam. International Journal of Environmental Health Research, 35, 959–971. doi.org/10.1080/09603123.2024.2377306

Turner, A., Amos, S. L., & Williams, T. (2021). Coastal dunes as a sink and secondary source of marine plastics: A study at Perran Beach, southwest England. Marine Pollution Bulletin, 173, 1–8. doi.org/10.1016/j.marpolbul.2021.113133

Turner, A., Arnold, R., & Williams, T. (2020). Weathering and persistence of plastic in the marine environment: Lessons from LEGO. Environmental Pollution, 262, 1–7. doi.org/10.1016/j.envpol.2020.114299

Turra, A., Manzano, A. B., Dias, R. J. S., Mahiques, M. M., Barbosa, L., Balthazar-Silva, D., & Moreira, F. T. (2014). Three-dimensional distribution of plastic pellets in sandy beaches: Shifting paradigms. Scientific Reports, 4, 1–7. doi.org/10.1038/srep04435

Tuuri, E. M., & Leterme, S. C. (2023). How plastic debris and associated chemicals impact the marine food web: A review. Environmental Pollution, 321, 1–12. doi.org/10.1016/j.envpol.2023.121156

Tyler, C. R., Parsons, A., Rogers, N. J., Lange, A., Brown, A. R., Hester, R. E., & Harrison, R. M. (2019). Plasticisers and their impact on wildlife. In R. E. Hester & R. M. Harrison (Eds.), Issues in Environmental Science and Technology (Vol. 47, pp. 106–130). The Royal Society of Chemistry. https://www.rsc.org

Tziourrou, P., Megalovasilis, P., Tsounia, M., & Karapanagioti, H. K. (2019). Characteristics of microplastics on two beaches affected by different land uses in Salamina Island in Saronikos Gulf, east Mediterranean. Marine Pollution Bulletin, 149, 1–6. doi.org/10.1016/j.marpolbul.2019.110531

Udden, J. A. (1914). Mechanical Composition of Clastic Sediments. Bulletin of the Geological Society of America, 25, 655–744.

Uddin, S., Fowler, S. W., & Saeed, T. (2020). Microplastic particles in the Persian/Arabian Gulf – A review on sampling and identification. Marine Pollution Bulletin, 154, 1–12. doi.org/10.1016/j.marpolbul.2020.111100

Ulfah, M., Ziliwu, I. N., Agustina, S., Octavina, C., Khairunnisa, & Yucharoen, M. (2024). Microplastic accumulation in coral reef ecosystems at Peukan Bada district, Aceh Besar. Ecological Engineering and Environmental Technology, 25, 291–300. doi.org/10.12912/27197050/187209

Urban-Malinga, B., Zalewski, M., Jakubowska, A., Wodzinowski, T., Malinga, M., Pałys, B., & Dąbrowska, A. (2020). Microplastics on sandy beaches of the southern Baltic Sea. Marine Pollution Bulletin, 155, 1–9. doi.org/10.1016/j.marpolbul.2020.111170

Van Cauwenberghe, L., Claessens, M., Vandegehuchte, M. B., Mees, J., & Janssen, C. R. (2013). Assessment of marine debris on the Belgian Continental Shelf. Marine Pollution Bulletin, 73, 161–169. doi.org/10.1016/j.marpolbul.2013.05.026

Vandermeer, E. (2023, February 9). New Canadian minimum standards for marine protected areas are an important step in reversing wildlife loss. World Wildlife Fund. wwf.ca/media-releases/new-canadian-minimum-standards-for-marine-protected-areas-are-an-important-step-in-reversing-wildlife-loss/

Veerasingam, S., Vethamony, P., Valliyil, Aboobacker, M., Giraldes, A. E., Dib, S., & Al-Khayat, J. A. (2021). Factors influencing the vertical distribution of microplastics in the beach sediments around the Ras Rakan Island, Qatar.

Environmental Science and Pollution Research, 1–10. doi.org/10.1007/s11356-020-12100-4/Published

Vermeiren, P., Lercari, D., Muñoz, C. C., Ikejima, K., Celentano, E., Jorge-Romero, G., & Defeo, O. (2021). Sediment grain size determines microplastic exposure landscapes for sandy beach macroinfauna. Environmental Pollution, 286, 1–9. doi.org/10.1016/j.envpol.2021.117308

Vetrimurugan, E., Jonathan, M. P., Sarkar, S. K., Rodríguez-González, F., Roy, P. D., Velumani, S., & Sakthi, J. S. (2020). Occurrence, distribution and provenance of micro plastics: A large scale quantitative analysis of beach sediments from southeastern coast of South Africa. Science of the Total Environment, 746, 1–11. doi.org/10.1016/j.scitotenv.2020.141103

Vidyasakar, A., Krishnakumar, S., Kasilingam, K., Neelavannan, K., Bharathi, V. A., Godson, P. S., Prabha, K., & Magesh, N. S. (2020). Characterization and distribution of microplastics and plastic debris along Silver Beach, Southern India. Marine Pollution Bulletin, 158, 1–9. doi.org/10.1016/j.marpolbul.2020.111421

Volgare, M., Castaldo, R., Errico, M. E., Gentile, G., Avolio, R., Ambrogi, V., & Cocca, M. (2021). The effect of the detergent on microfibre release during the washing process of polyester textiles. 2021 IEEE International Workshop on Metrology for the Sea: Learning to Measure Sea Health Parameters, MetroSea 2021 - Proceedings, 444–448. doi.org/10.1109/MetroSea52177.2021.9611615

Walther, B. A., & Bergmann, M. (2022). Plastic pollution of four understudied marine ecosystems: a review of mangroves, seagrass meadows, the Arctic Ocean and the deep seafloor. Emerging Topics in Life Sciences, 6(4), 371–387. doi.org/10.1042/ETLS20220017

Wang, L. C., Lin, J. C. T., Dong, C. D., Chen, C. W., & Liu, T. K. (2021). The sorption of persistent organic pollutants in microplastics from the coastal environment. Journal of Hazardous Materials, 420, 1–12. doi.org/10.1016/j.jhazmat.2021.126658

Wentworth, C. K. (1922). A Scale of Grade and Class Terms for Clastic Sediments. The Journal of Geology, 30(5), 377–392. https://www.jstor.org/stable/30063207

WHSRN. (n.d.). Bay of Fundy. Western Hemispheric Shorebird Reserve Network. Retrieved June 29, 2022, from whsrn.org/whsrn_sites/bay-of-fundy/

Wu, F., Li, X., Zhang, C., & Wang, T. (2024). Spatiotemporal distribution and diversity of microplastics in the sediment of beaches in Xiamen city, China. Journal of Oceanology and Limnology, 43, 396–405. doi.org/10.1007/s00343-024-3277-8

Wu, X., Zhong, C., Wang, T., & Zou, X. (2023). Assessment on the pollution level and risk of microplastics on bathing beaches: A case study of Liandao, China. Environmental Monitoring and Assessment, 195, 1–20. doi.org/10.1007/s10661-023-10994-4

Wu, X., Zhong, C., Wang, T., Zou, X., Zang, Z., Li, Q., & Chen, H. (2021). Occurrence and distribution of microplastics on recreational beaches of Haichow Bay, China.

Environmental Science and Pollution Research, 28, 6132–6145. doi.org/10.1007/s11356-020-10987-7/Published

Xu, N., Zhu, Z., Li, S., Ouyang, X., Zhu, Q., Gao, W., Cai, Y., & Yang, Z. (2023). The role of bio-geomorphic feedbacks in shaping microplastic burial in blue carbon habitats. Science of the Total Environment, 861, 1–8. doi.org/10.1016/j.scitotenv.2022.160220

Xu, X., Wong, C. Y., Tam, N. F. Y., Lo, H. S., & Cheung, S. G. (2020). Microplastics in invertebrates on soft shores in Hong Kong: Influence of habitat, taxa and feeding mode. Science of the Total Environment, 715, 1–10. doi.org/10.1016/j.scitotenv.2020.136999

Yabanlı, M., Yozukmaz, A., Şener, İ., & Ölmez, Ö. T. (2019). Microplastic pollution at the intersection of the Aegean and Mediterranean Seas: A study of the Datça Peninsula (Turkey). Marine Pollution Bulletin, 145, 47–55. doi.org/10.1016/j.marpolbul.2019.05.003

Yang, L., Zhang, Y., Kang, S., Wang, Z., & Wu, C. (2021). Microplastics in freshwater sediment: A review on methods, occurrence, and sources. Science of the Total Environment, 754, 1–20. doi.org/10.1016/j.scitotenv.2020.141948

Yaranal, N. A., Subbiah, S., & Mohanty, K. (2021). Distribution and characterization of microplastics in beach sediments from Karnataka (India) coastal environments. Marine Pollution Bulletin, 169, 1–8. doi.org/10.1016/j.marpolbul.2021.112550

Yona, D., Setyawan, F. O., Putri, S. E. N., Iranawati, F., Kautsar, M. A., & Isobe, A. (2023). Microplastic distribution in beach sediments: Comparison between the north and south waters of East Java Island, Indonesia. Jurnal Ilmiah Perikanan dan Kelautan, 15, 303–315. doi.org/10.20473/jipk.v15i2.41065

Yu, R. S., & Singh, S. (2023). Microplastic pollution: threats and impacts on global marine ecosystems. Sustainability (Switzerland), 15(17), 1–21. doi.org/10.3390/su151713252

Yu, X., Ladewig, S., Bao, S., Toline, C. A., Whitmire, S., & Chow, A. T. (2018). Occurrence and distribution of microplastics at selected coastal sites along the southeastern United States. Science of the Total Environment, 613-614, 298–305. doi.org/10.1016/j.scitotenv.2017.09.100

Yu, X., Peng, J., Wang, J., Wang, K., & Bao, S. (2016). Occurrence of microplastics in the beach sand of the Chinese inner sea: The Bohai Sea. Environmental Pollution, 214, 722–730. doi.org/10.1016/j.envpol.2016.04.080

Zahari, N. Z., Vincent, S. D., Cleophas, F. N., Budin, K., & Sabullah, M. K. (2023). Abundance, distribution, and characterization of microplastics on two recreational beaches in Kota Kinabalu, Sabah, Malaysia. Water, 15(15), 1–13. doi.org/10.3390/w15152681

Zalasiewicz, J., Waters, C. N., Ivar do Sul, J. A., Corcoran, P. L., Barnosky, A. D., Cearreta, A., Edgeworth, M., Gałuszka, A., Jeandel, C., Leinfelder, R., McNeill, J. R., Steffen, W., Summerhayes, C., Wagreich, M., Williams, M., Wolfe, A. P., &

Yonan, Y. (2016). The geological cycle of plastics and their use as a stratigraphic indicator of the Anthropocene. Anthropocene, 13, 4–17. doi.org/10.1016/j.ancene.2016.01.002

Zhang, H. (2017). Transport of microplastics in coastal seas. Estuarine, Coastal and Shelf Science, 199, 74–86. doi.org/10.1016/j.ecss.2017.09.032

Zhang, J., Fu, D., & Wang, L. (2025). The relation and consistency of nanoplastics analysis to microplastics. In Analysis of Microplastics and Nanoplastics (pp. 275–279). Elsevier. doi.org/10.1016/B978-0-443-15779-0.00009-2

Zhang, K., Hamidian, A. H., Tubić, A., Zhang, Y., Fang, J. K. H., Wu, C., & Lam, P. K. S. (2021). Understanding plastic degradation and microplastic formation in the environment: A review. Environmental Pollution, 274, 1–14. doi.org/10.1016/j.envpol.2021.116554

Zhang, K., Shi, H., Peng, J., Wang, Y., Xiong, X., Wu, C., & Lam, P. K. S. (2018). Microplastic pollution in China's inland water systems: A review of findings, methods, characteristics, effects, and management. Science of the Total Environment, 630, 1641–1653. doi.org/10.1016/j.scitotenv.2018.02.300

Zhang, T., Li, D., Liu, Y., Li, Y., Yu, Y., An, X., Jiang, Y., Wang, J., Shi, H., & Lin, L. (2024). Microplastic distribution characteristics and sources on beaches that serve as the largest nesting ground for green turtles in China. Toxics, 12, 1–10. doi.org/10.3390/toxics12020109

Zhang, X., Yu, K., Zhang, H., Liu, Y., He, J., Liu, X., & Jiang, J. (2020). A novel heating-assisted density separation method for extracting microplastics from sediments. Chemosphere, 256, 1–6. doi.org/10.1016/j.chemosphere.2020.127039

Zhao, J., Ran, W., Teng, J., Liu, Y., Liu, H., Yin, X., Cao, R., & Wang, Q. (2018). Microplastic pollution in sediments from the Bohai Sea and the Yellow Sea, China. Science of the Total Environment, 640–641, 637–645. doi.org/10.1016/j.scitotenv.2018.05.346

Zheng, Y., Li, J., Sun, C., Cao, W., Wang, M., Jiang, F., & Ju, P. (2021). Comparative study of three sampling methods for microplastics analysis in seawater. Science of the Total Environment, 765, 1–8. doi.org/10.1016/j.scitotenv.2020.144495

Zingg, T. (1935). Beitrag zur schotteranalys [Ph.D.]. University of Zurich.

Zobkov, M. B., & Esiukova, E. E. (2018). Microplastics in a Marine Environment: Review of Methods for Sampling, Processing, and Analyzing Microplastics in Water, Bottom Sediments, and Coastal Deposits. Oceanology, 58(1), 137–143. doi.org/10.1134/S0001437017060169

Appendix A – Sample ID's

Table A1. Core ID's and microplastic extraction ID's for 2022.

Sediment Samples				Microplastic Sample Extraction				
Core #	Depth Interval	Depth Id	Sample Id	1.0 g/cm^3 Freshwater (A)	1.2 g/cm^3 NaCl (B)	1.3 g/cm^3 NaH_2PO_4 (30^{o}C) (C)	1.5 g/cm^3 NaH_2PO_4 (50^{o}C) (D)	Olive Oil (E)
1	0 - 4 cm	i	2022-1i	2022-1i (A)	2022-1i (B)	2022-1i (C)	2022-1i (D)	2022-1i (E)
1	4 - 8 cm	ii	2022-1ii	2022-1ii (A)	2022-1ii (B)	2022-1ii (C)	2022-1ii (D)	2022-1ii (E)
1	8 - 12 cm	iii	2022-1iii	2022-1iii (A)	2022-1iii (B)	2022-1iii (C)	2022-1iii (D)	2022-1iii (E)
1	12 - 16 cm	iv	2022-1iv	2022-1iv (A)	2022-1iv (B)	2022-1iv (C)	2022-1iv (D)	2022-1iv (E)
1	16 - 20 cm	v	2022-1v	2022-1v (A)	2022-1v (B)	2022-1v (C)	2022-1v (D)	2022-1v (E)
2	0 - 4 cm	i	2022-2i	2022-2i (A)	2022-2i (B)	2022-2i (C)	2022-2i (D)	2022-2i (E)
2	4 - 8 cm	ii	2022-2ii	2022-2ii (A)	2022-2ii (B)	2022-2ii (C)	2022-2ii (D)	2022-2ii (E)
2	8 - 12 cm	iii	2022-2iii	2022-2iii (A)	2022-2iii (B)	2022-2iii (C)	2022-2iii (D)	2022-2iii (E)
2	12 - 16 cm	iv	2022-2iv	2022-2iv (A)	2022-2iv (B)	2022-2iv (C)	2022-2iv (D)	2022-2iv (E)
3	0 - 4 cm	i	2022-3i	2022-3i (A)	2022-3i (B)	2022-3i (C)	2022-3i (D)	2022-3i (E)
3	4 - 8 cm	ii	2022-3ii	2022-3ii (A)	2022-3ii (B)	2022-3ii (C)	2022-3ii (D)	2022-3ii (E)
3	8 - 12 cm	iii	2022-3iii	2022-3iii (A)	2022-3iii (B)	2022-3iii (C)	2022-3iii (D)	2022-3iii (E)
3	12 - 16 cm	iv	2022-3iv	2022-3iv (A)	2022-3iv (B)	2022-3iv (C)	2022-3iv (D)	2022-3iv (E)
4	0 - 4 cm	i	2022-4i	2022-4i (A)	2022-4i (B)	2022-4i (C)	2022-4i (D)	2022-4i (E)
4	4 - 8 cm	ii	2022-4ii	2022-4ii (A)	2022-4ii (B)	2022-4ii (C)	2022-4ii (D)	2022-4ii (E)
4	8 - 12 cm	iii	2022-4iii	2022-4iii (A)	2022-4iii (B)	2022-4iii (C)	2022-4iii (D)	2022-4iii (E)
4	12 - 16 cm	iv	2022-4iv	2022-4iv (A)	2022-4iv (B)	2022-4iv (C)	2022-4iv (D)	2022-4iv (E)
5	0 - 4 cm	i	2022-5i	2022-5i (A)	2022-5i (B)	2022-5i (C)	2022-5i (D)	2022-5i (E)
5	4 - 8 cm	ii	2022-5ii	2022-5ii (A)	2022-5ii (B)	2022-5ii (C)	2022-5ii (D)	2022-5ii (E)
5	8 - 12 cm	iii	2022-5iii	2022-5iii (A)	2022-5iii (B)	2022-5iii (C)	2022-5iii (D)	2022-5iii (E)
5	12 - 16 cm	iv	2022-5iv	2022-5iv (A)	2022-5iv (B)	2022-5iv (C)	2022-5iv (D)	2022-5iv (E)
6	0 - 4 cm	i	2022-6i	2022-6i (A)	2022-6i (B)	2022-6i (C)	2022-6i (D)	2022-6i (E)
6	4 - 8 cm	ii	2022-6ii	2022-6ii (A)	2022-6ii (B)	2022-6ii (C)	2022-6ii (D)	2022-6ii (E)
6	8 - 12 cm	iii	2022-6iii	2022-6iii (A)	2022-6iii (B)	2022-6iii (C)	2022-6iii (D)	2022-6iii (E)
6	12 - 16 cm	iv	2022-6iv	2022-6iv (A)	2022-6iv (B)	2022-6iv (C)	2022-6iv (D)	2022-6iv (E)
7	0 - 4 cm	i	2022-7i	2022-7i (A)	2022-7i (B)	2022-7i (C)	2022-7i (D)	2022-7i (E)
7	4 - 8 cm	ii	2022-7ii	2022-7ii (A)	2022-7ii (B)	2022-7ii (C)	2022-7ii (D)	2022-7ii (E)
7	8 - 12 cm	iii	2022-7iii	2022-7iii (A)	2022-7iii (B)	2022-7iii (C)	2022-7iii (D)	2022-7iii (E)
7	12 - 16 cm	iv	2022-7iv	2022-7iv (A)	2022-7iv (B)	2022-7iv (C)	2022-7iv (D)	2022-7iv (E)
7	16 - 20 cm	v	2022-7v	2022-7v (A)	2022-7v (B)	2022-7v (C)	2022-7v (D)	2022-7v (E)

Table A2. Core ID's and microplastic extraction ID's for 2024.

Sediment Samples				Microplastic Sample Extraction				
Core #	Depth Interval	Depth Id	Sample Id	1.0 g/cm^3 Freshwater (A)	1.2 g/cm^3 NaCl (B)	1.3 g/cm^3 NaH_2PO_4 (30°C) (C)	1.5 g/cm^3 NaH_2PO_4 (50°C) (D)	Olive Oil (E)
1	0 - 4 cm	i	2024-1i	2024-1i (A)	2024-1i (B)	2024-1i (C)	2024-1i (D)	2024-1i (E)
1	4 - 8 cm	ii	2024-1ii	2024-1ii (A)	2024-1ii (B)	2024-1ii (C)	2024-1ii (D)	2024-1ii (E)
1	8 - 12 cm	iii	2024-1iii	2024-1iii (A)	2024-1iii (B)	2024-1iii (C)	2024-1iii (D)	2024-1iii (E)
2	0 - 4 cm	i	2024-2i	2024-2i (A)	2024-2i (B)	2024-2i (C)	2024-2i (D)	2024-2i (E)
2	4 - 8 cm	ii	2024-2ii	2024-2ii (A)	2024-2ii (B)	2024-2ii (C)	2024-2ii (D)	2024-2ii (E)
2	8 - 12 cm	iii	2024-2iii	2024-2iii (A)	2024-2iii (B)	2024-2iii (C)	2024-2iii (D)	2024-2iii (E)
2	12 - 16 cm	iv	2024-2iv	2024-2iv (A)	2024-2iv (B)	2024-2iv (C)	2024-2iv (D)	2024-2iv (E)
3	0 - 4 cm	i	2024-3i	2024-3i (A)	2024-3i (B)	2024-3i (C)	2024-3i (D)	2024-3i (E)
3	4 - 8 cm	ii	2024-3ii	2024-3ii (A)	2024-3ii (B)	2024-3ii (C)	2024-3ii (D)	2024-3ii (E)
3	8 - 12 cm	iii	2024-3iii	2024-3iii (A)	2024-3iii (B)	2024-3iii (C)	2024-3iii (D)	2024-3iii (E)
4	0 - 4 cm	i	2024-4i	2024-4i (A)	2024-4i (B)	2024-4i (C)	2024-4i (D)	2024-4i (E)
4	4 - 8 cm	ii	2024-4ii	2024-4ii (A)	2024-4ii (B)	2024-4ii (C)	2024-4ii (D)	2024-4ii (E)
4	8 - 12 cm	iii	2024-4iii	2024-4iii (A)	2024-4iii (B)	2024-4iii (C)	2024-4iii (D)	2024-4iii (E)
5	0 - 4 cm	i	2024-5i	2024-5i (A)	2024-5i (B)	2024-5i (C)	2024-5i (D)	2024-5i (E)
5	4 - 8 cm	ii	2024-5ii	2024-5ii (A)	2024-5ii (B)	2024-5ii (C)	2024-5ii (D)	2024-5ii (E)
5	8 - 12 cm	iii	2024-5iii	2024-5iii (A)	2024-5iii (B)	2024-5iii (C)	2024-5iii (D)	2024-5iii (E)
5	12 - 16 cm	iv	2024-5iv	2024-5iv (A)	2024-5iv (B)	2024-5iv (C)	2024-5iv (D)	2024-5iv (E)
5	16 - 20 cm	v	2024-5v	2024-5v (A)	2024-5v (B)	2024-5v (C)	2024-5v (D)	2024-5v (E)
6	0 - 4 cm	i	2024-6i	2024-6i (A)	2024-6i (B)	2024-6i (C)	2024-6i (D)	2024-6i (E)
6	4 - 8 cm	ii	2024-6ii	2024-6ii (A)	2024-6ii (B)	2024-6ii (C)	2024-6ii (D)	2024-6ii (E)
6	8 - 12 cm	iii	2024-6iii	2024-6iii (A)	2024-6iii (B)	2024-6iii (C)	2024-6iii (D)	2024-6iii (E)
6	12 - 16 cm	iv	2024-6iv	2024-6iv (A)	2024-6iv (B)	2024-6iv (C)	2024-6iv (D)	2024-6iv (E)
6	16 - 20 cm	v	2024-6v	2024-6v (A)	2024-6v (B)	2024-6v (C)	2024-6v (D)	2024-6v (E)
7	0 - 4 cm	i	2024-7i	2024-7i (A)	2024-7i (B)	2024-7i (C)	2024-7i (D)	2024-7i (E)
7	4 - 8 cm	ii	2024-7ii	2024-7ii (A)	2024-7ii (B)	2024-7ii (C)	2024-7ii (D)	2024-7ii (E)
7	8 - 12 cm	iii	2024-7iii	2024-7iii (A)	2024-7iii (B)	2024-7iii (C)	2024-7iii (D)	2024-7iii (E)
7	12 - 16 cm	iv	2024-7iv	2024-7iv (A)	2024-7iv (B)	2024-7iv (C)	2024-7iv (D)	2024-7iv (E)
7	16 - 20 cm	v	2024-7v	2024-7v (A)	2024-7v (B)	2024-7v (C)	2024-7v (D)	2024-7v (E)

Appendix B – Microplastic Abundance Results

Table B1. Microplastic abundance results per sample (by depth and core) in 2022

2022	Core 1	Core 2	Core 3	Core 4	Core 5	Core 6	Core 7
0–4 cm	50	88	26	52	57	45	31
4–8 cm	64	39	30	56	42	30	33
8–12 cm	43	32	51	46	35	21	33
12–16 cm	68	38	48	38	38	17	40
16–20 cm	45						18

Table B2. Microplastic abundance results per sample (by depth and core) in 2024

2024	Core 1	Core 2	Core 3	Core 4	Core 5	Core 6	Core 7
0–4 cm	61	37	35	12	17	34	23
4–8 cm	30	32	13	8	15	17	10
8–12 cm	8	20	21	13	12	10	10
12–16 cm		26			18	8	13
16–20 cm					23	8	18

Table B3. 2022 microplastic abundance results per sample (by depth and core)

Year	Sample	mean_phi	MP_Total	MP_H_2O	MP_NaCl	MP_NaH_2PO_4 30C	MP_NaH_2PO_4 50C	MP_Oil	Shape_FibreBall	Shape_Equant	Shape_Fibre	Shape_Film	Shape_Fragment	Colour_Red	Colour_Blue	Colour_Black	Colour_White/Clear	Colour_Other
2022	1i	2.66	61	20	6	5	4	26	0	0	23	7	3	7	4	11	26	13
	1ii	2.52	70	4	11	11	28	16	0	0	14	31	2	2	10	8	38	12
	1iii	2.46	46	11	11	10	12	2	0	0	2	13	3	0	2	5	32	7
	1iv	2.21	77	6	22	7	11	31	0	0	28	14	1	4	8	10	40	15
	1v	2.71	49	9	9	6	5	20	0	0	18	5	1	0	2	19	25	3
	2i	1.72	152	54	31	25	15	27	0	0	24	18	1	11	15	16	98	12
	2ii	1.61	42	7	5	12	8	10	0	0	8	11	1	0	4	5	32	1
	2iii	1.56	36	5	2	5	16	8	0	0	7	15	2	1	1	12	22	0
	2iv	1.31	83	6	45	7	9	16	0	0	16	12	2	5	6	18	48	6
	2v	0.00	0	0	0	0	0	0	0	0	0	0	0	0	0	0	0	0
	3i	1.71	26	5	1	8	5	7	0	0	6	8	0	0	3	2	20	1
	3ii	1.91	30	6	5	5	8	6	0	0	4	12	1	1	1	6	21	1
	3iii	1.59	73	7	4	11	6	45	0	0	45	9	1	5	11	10	42	5
	3iv	1.56	62	7	9	3	3	40	0	0	40	4	3	7	9	8	37	1
	3v	0.00	0	0	0	0	0	0	0	0	0	0	0	0	0	0	0	0
	4i	1.76	60	9	8	5	9	29	0	0	27	8	3	5	7	8	32	8
	4ii	1.55	68	23	5	9	13	18	0	0	18	14	5	2	6	14	34	12
	4iii	1.72	61	8	17	5	13	18	0	0	17	15	2	1	3	5	46	6
	4iv	1.68	51	0	9	6	11	25	0	0	25	11	0	5	9	8	28	1
	4v	0.00	0	0	0	0	0	0	0	0	0	0	0	0	0	0	0	0
	5i	2.09	61	11	11	9	14	16	0	0	15	15	0	1	2	22	36	0
	5ii	1.92	42	7	4	8	7	16	0	0	16	5	2	4	7	8	18	5
	5iii	1.67	43	2	7	6	3	25	0	0	25	5	0	1	5	7	29	1
	5iv	1.56	38	9	8	5	5	11	0	0	11	7	0	1	4	8	25	0
	5v	0.00	0	0	0	0	0	0	0	0	0	0	0	0	0	0	0	0
	6i	2.01	51	14	3	4	6	24	0	0	22	7	1	3	5	13	25	5
	6ii	1.98	34	5	5	5	1	18	0	0	18	1	0	2	5	10	16	1
	6iii	2.07	22	2	2	6	0	12	0	0	11	0	1	1	3	2	15	1
	6iv	1.94	17	2	2	5	7	1	0	0	1	6	1	0	3	3	11	0
	6v	0.00	0	0	0	0	0	0	0	0	0	0	0	0	0	0	0	0
	7i	2.14	33	13	0	2	2	16	0	0	16	2	0	2	10	12	9	0
	7ii	2.11	33	8	3	2	7	13	0	0	13	7	0	1	9	8	13	2
	7iii	2.20	52	6	2	2	2	40	0	0	40	2	0	6	6	14	24	2
	7iv	2.39	46	3	1	12	4	26	0	0	26	4	0	1	22	9	13	1
	7v	2.30	45	6	0	1	1	37	0	0	36	2	0	0	6	5	31	3

Table B4. 2024 microplastic abundance results per sample (by depth and core)

Year	Sample	mean_phi	MP_Total	MP_H_2O	MP_NaCl	MP_NaH_2PO_4_30C	MP_NaH_2PO_4_50C	MP_Oil	Shape_FibreBall	Shape_Equant	Shape_Fibre	Shape_Film	Shape_Fragment	Colour_Red	Colour_Blue	Colour_Black	Colour_White/Clear	Colour_Other
2024	1i	2.20	61	13	11	5	10	22	0	0	22	10	0	2	9	11	39	0
	1ii	1.32	30	5	2	7	6	10	0	0	10	6	0	0	5	15	10	0
	1iii	1.38	8	3	0	0	4	1	0	0	1	4	0	0	2	3	3	0
	1iv	0.00	0	0	0	0	0	0	0	0	0	0	0	0	0	0	0	0
	1v	0.00	0	0	0	0	0	0	0	0	0	0	0	0	0	0	0	0
	2i	1.80	37	3	3	9	15	7	0	0	5	17	2	0	5	15	17	0
	2ii	1.37	32	5	3	6	16	2	0	0	1	16	2	0	5	4	23	0
	2iii	1.56	20	6	5	1	2	6	1	0	6	1	0	0	7	5	7	0
	2iv	1.24	26	7	4	5	1	9	3	0	9	1	0	0	12	6	5	0
	2v	0.00	0	0	0	0	0	0	0	0	0	0	0	0	0	0	0	0
	3i	1.52	35	14	11	4	5	1	0	0	0	5	1	1	2	18	14	0
	3ii	1.28	13	4	3	1	3	2	0	0	2	3	1	0	3	6	4	0
	3iii	1.27	21	13	3	0	1	4	0	0	4	1	0	0	2	5	14	0
	3iv	0.00	0	0	0	0	0	0	0	0	0	0	0	0	0	0	0	0
	3v	0.00	0	0	0	0	0	0	0	0	0	0	0	0	0	0	0	0
	4i	1.81	12	1	1	2	4	4	1	0	4	2	1	0	4	3	4	0
	4ii	1.64	8	0	2	4	0	2	1	0	2	0	0	0	4	0	3	0
	4iii	1.40	13	1	4	3	4	1	1	0	1	4	0	0	6	2	4	0
	4iv	0.00	0	0	0	0	0	0	0	0	0	0	0	0	0	0	0	0
	4v	0.00	0	0	0	0	0	0	0	0	0	0	0	0	0	0	0	0
	5i	1.75	17	3	6	2	2	4	0	0	4	2	0	1	4	10	2	0
	5ii	1.81	15	3	1	3	3	5	0	0	5	3	1	1	4	6	4	0
	5iii	1.78	12	1	5	0	0	6	0	0	6	1	1	0	7	1	4	0
	5iv	1.87	18	12	1	0	1	4	0	0	3	1	0	1	8	5	4	0
	5v	1.81	23	8	5	5	1	4	0	0	4	1	1	2	10	5	5	1
	6i	2.00	34	6	12	2	4	10	0	0	8	5	3	1	17	3	13	0
	6ii	1.88	17	9	1	1	4	2	0	0	1	6	0	1	5	6	5	0
	6iii	1.78	10	4	0	1	2	3	0	0	3	2	0	1	5	0	4	0
	6iv	1.74	8	1	2	2	0	3	0	0	3	0	0	0	3	2	2	1
	6v	1.68	8	0	2	2	1	3	0	0	3	1	0	1	2	2	3	0
	7i	1.96	23	7	5	3	2	6	0	0	5	3	0	2	8	8	5	0
	7ii	2.01	10	3	1	1	3	2	0	0	2	4	1	0	4	1	5	0
	7iii	1.90	10	2	2	3	1	2	0	0	2	1	0	1	6	2	1	0
	7iv	1.90	13	3	3	4	3	0	0	0	0	5	0	1	3	1	8	0
	7v	1.95	18	4	5	3	1	5	0	0	3	6	2	0	6	2	10	0

Appendix C – Sediment Analysis

Legend:

Figure C1. Core 22-1. Stratigraphic log for Core 22-1, collected on July 5th, 2022. The core consists of brown medium-sandstone and reached a total recovery of 19.0 cm. The log illustrates consistent grain size throughout, while microplastic (MP) abundance shows vertical variability, notably featuring a localized lens of high contamination at 12–16 cm.

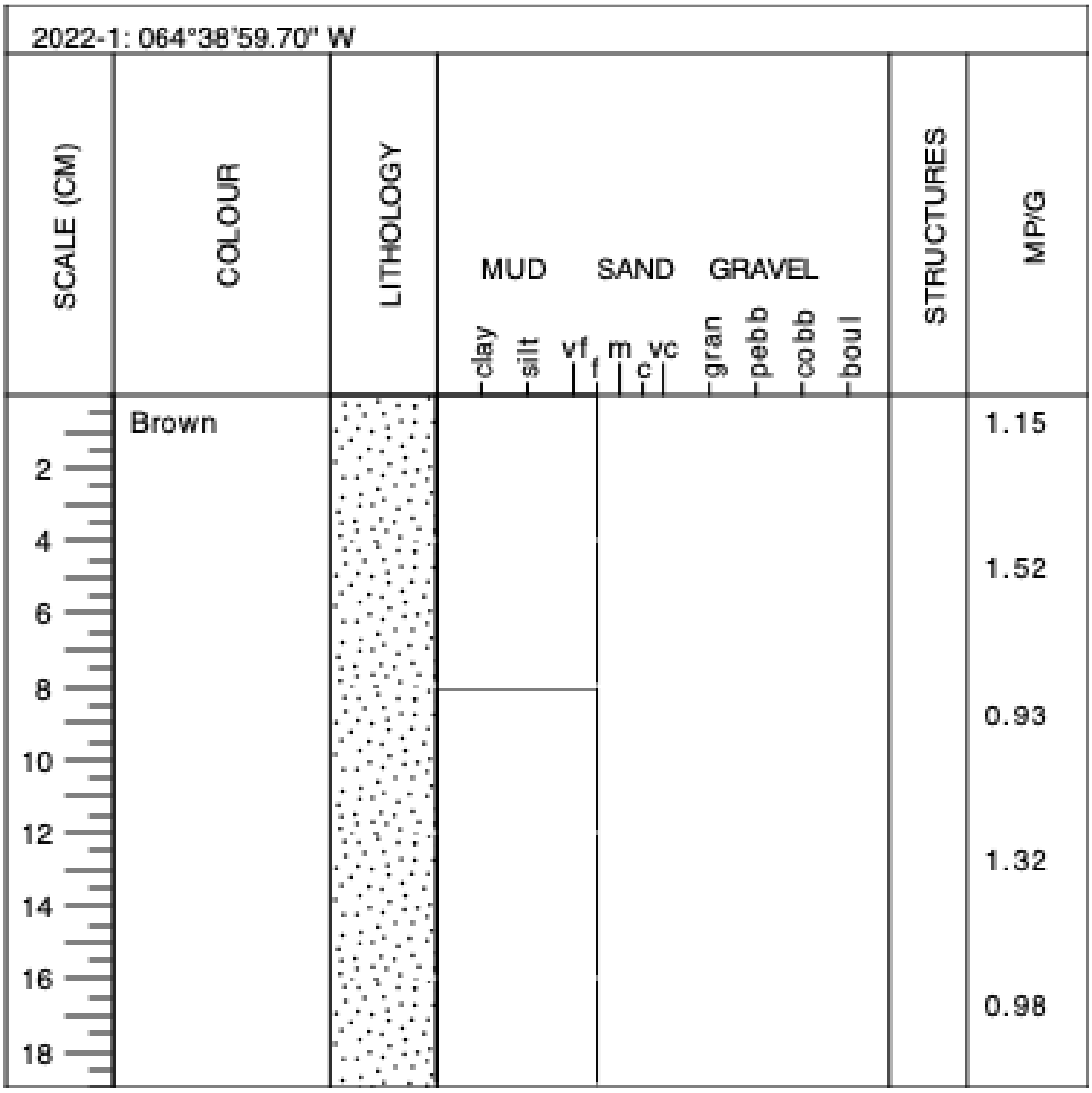

Figure C2. Core 22-2. Stratigraphic log for Core 22-2, collected on July 5th, 2022. Composed of brown medium-sandstone with a total recovery of 14.0 cm, the log illustrates consistent grain size and variable MP abundance. Notable peaks in contamination occur at the surface (0–4 cm) and at depth (12–14 cm).

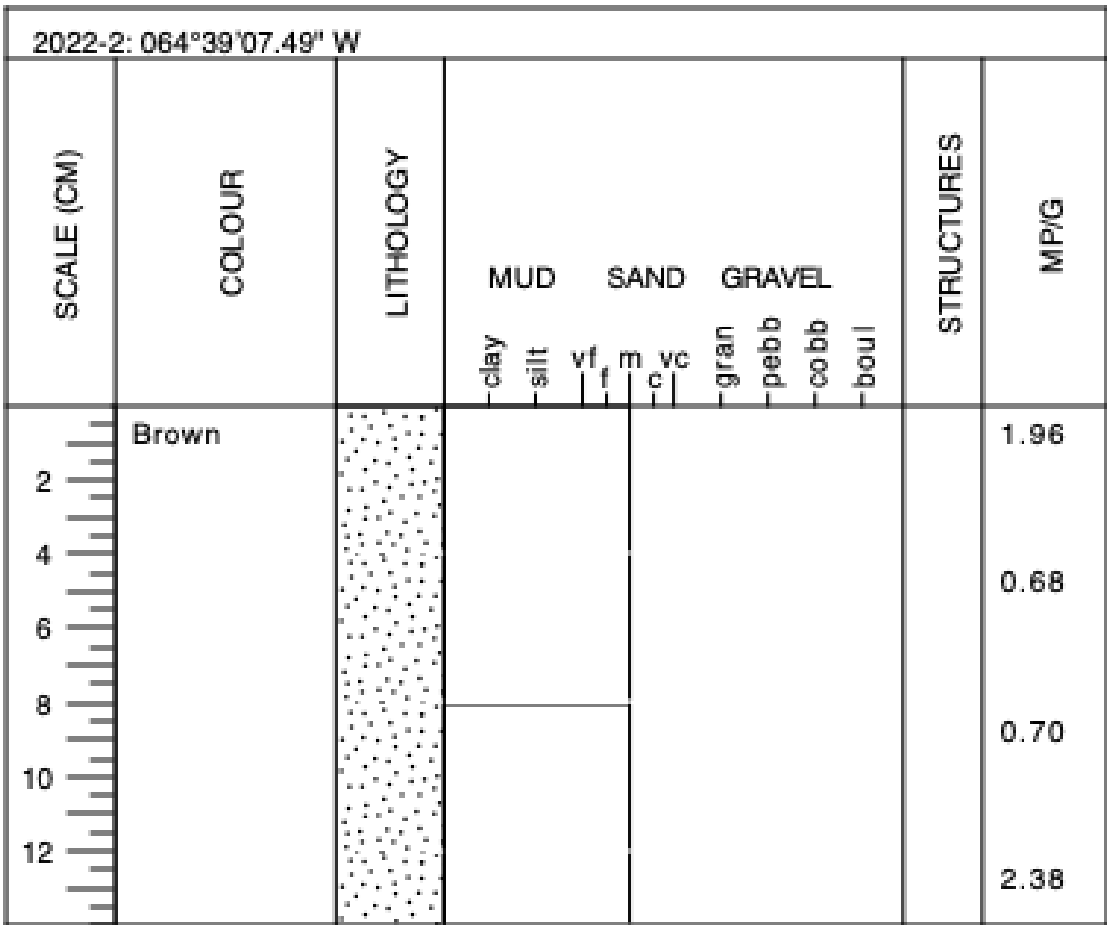

Figure C3. Core 22-3. Stratigraphic log for Core 22-3, collected on July 5th, 2022. The core reached a total recovery of 15.0 cm and is characterized as brown medium-sandstone. While grain size remains consistent, MP abundance varies vertically, with high contamination observed at depth (8–15 cm).

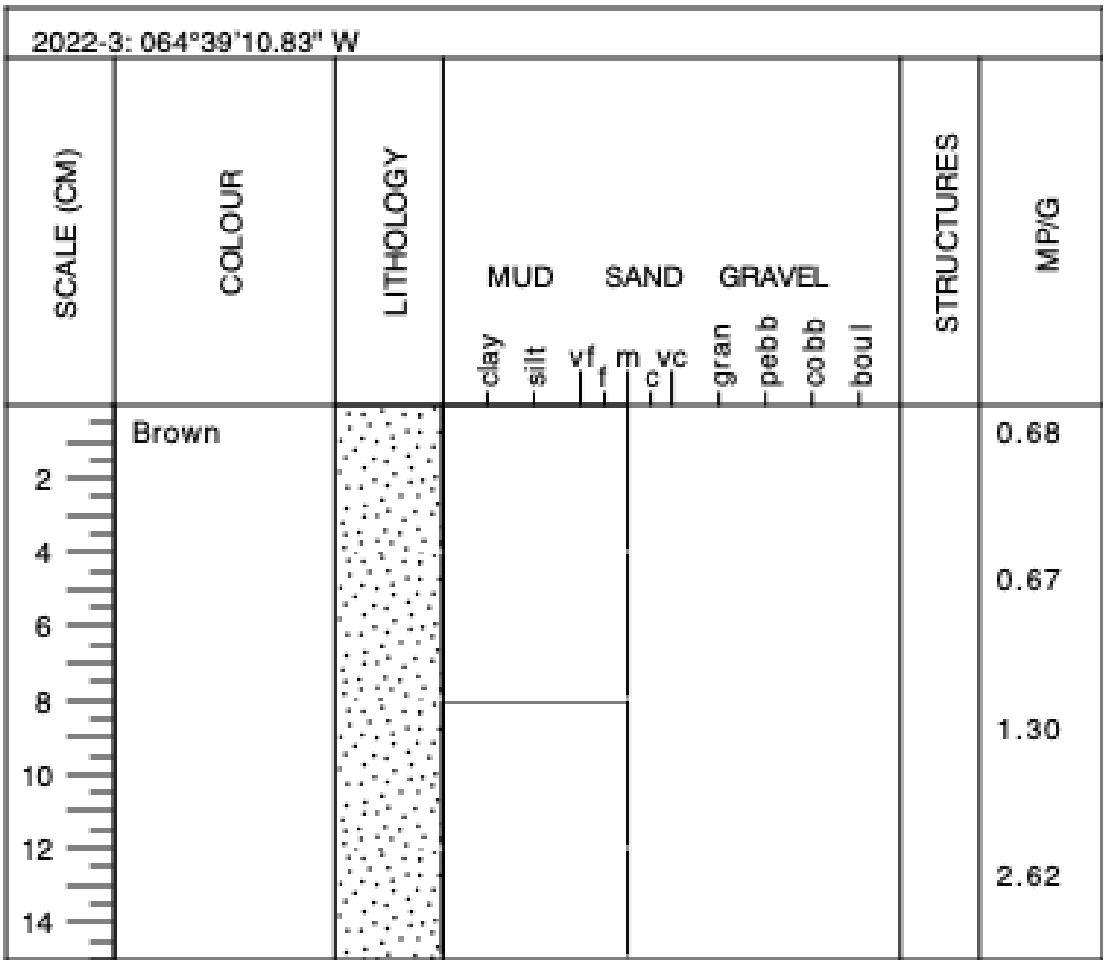

Figure C4. Core 22-4. Stratigraphic log for Core 22-4, collected on July 5th, 2022. Reaching a total recovery of 13.0 cm, this brown medium-sandstone core exhibits consistent grain size. The log reveals vertical variability in MP abundance, highlighted by a localized lens of low contamination at 8–12 cm.

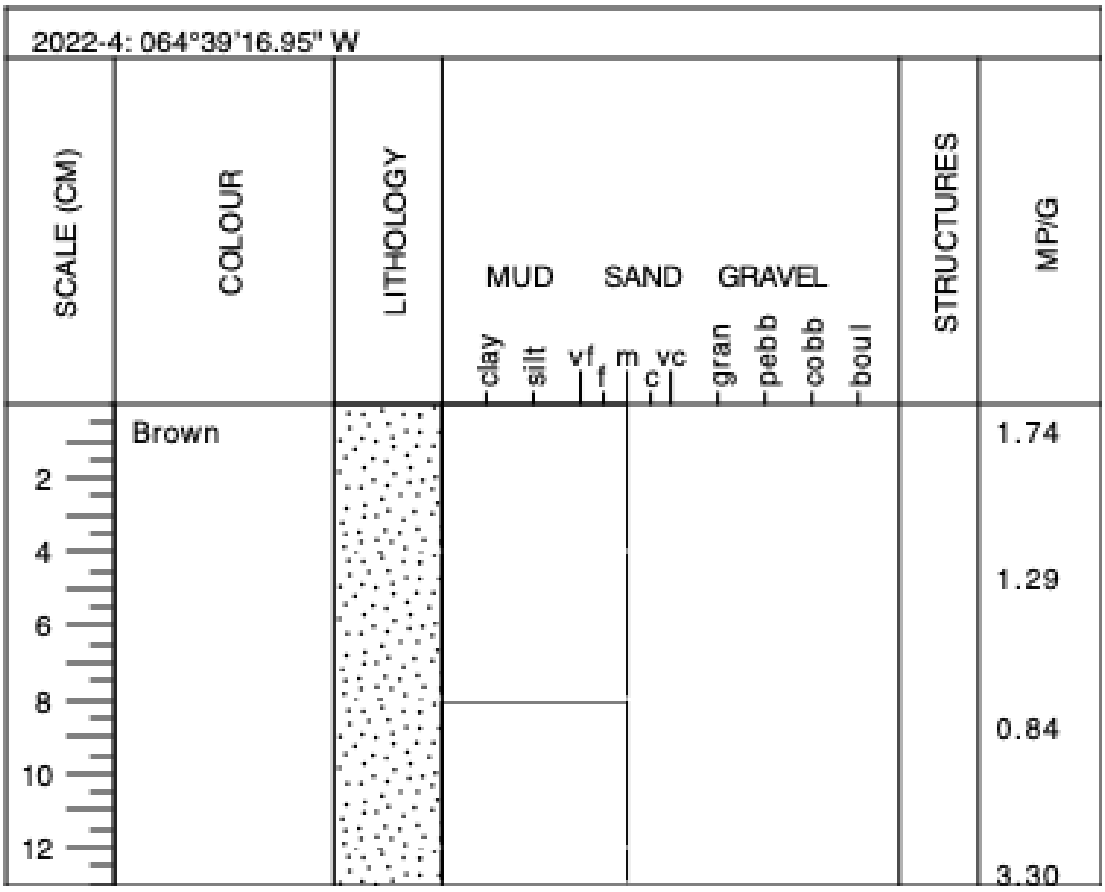

Figure C5. Core 22-5. Stratigraphic log for Core 22-5, collected on July 5th, 2022. Total core recovery reached 13.0 cm. The lithology transitions from brown fine-sandstone to medium-sandstone at a depth of 4 cm. The log illustrates slight variability in both grain size and MP abundance throughout the profile.

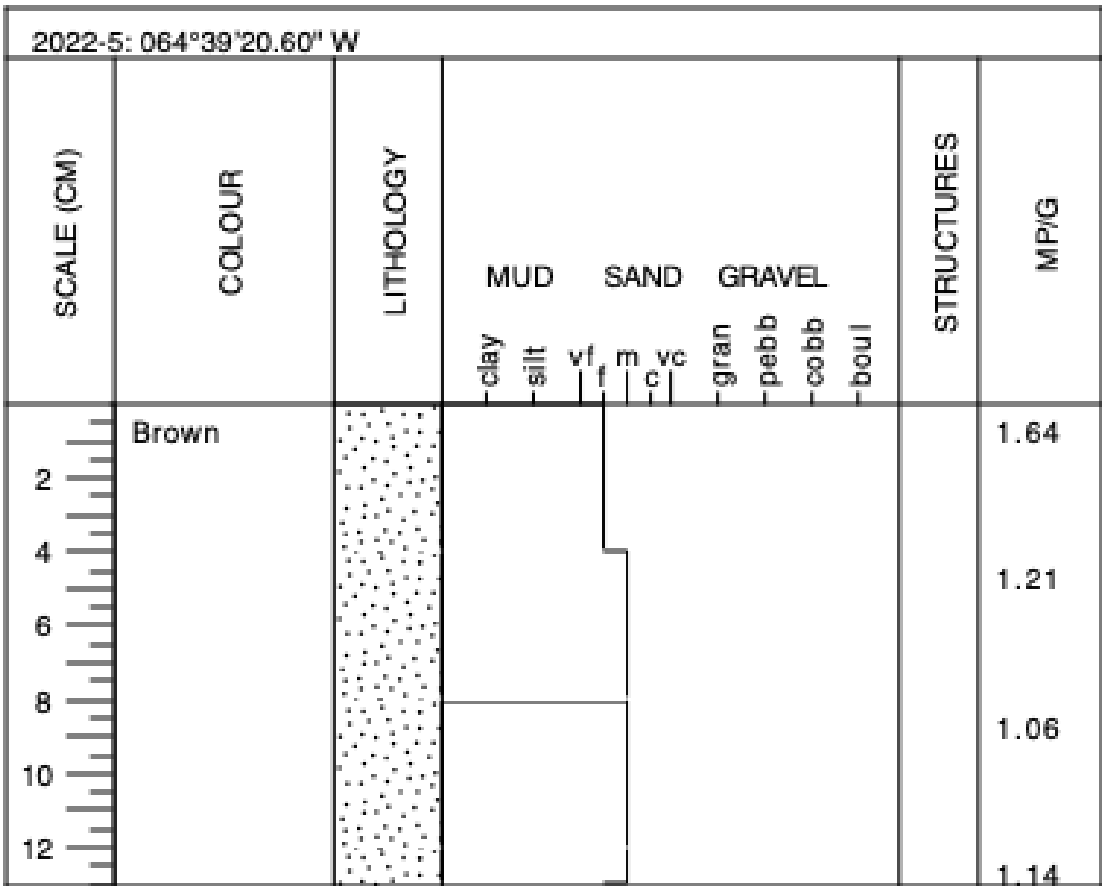

Figure C6. Core 22-6. Stratigraphic log for Core 22-6, collected on July 5th, 2022. The core reached 13.0 cm and consists primarily of brown medium-sandstone, featuring a medium-coarse lens from 8–12 cm. The log illustrates slight variability in grain size and a generally lower MP abundance.

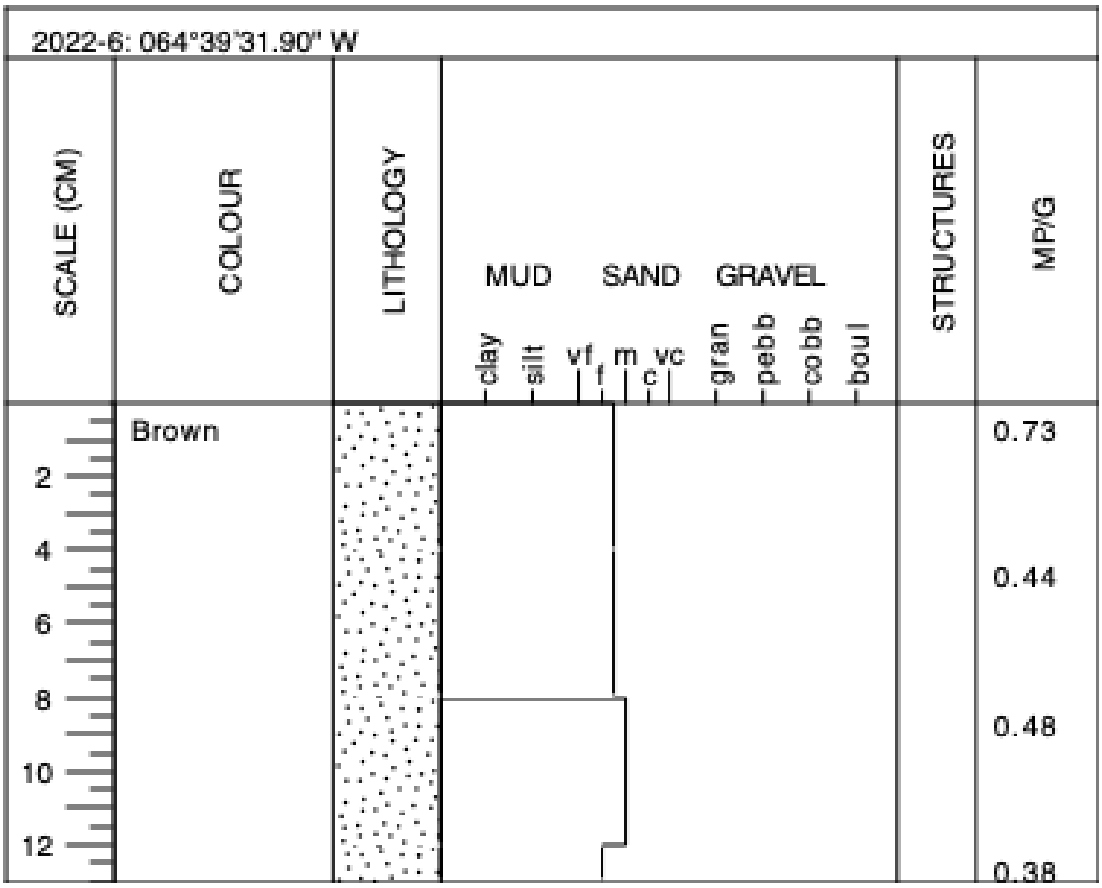

Figure C7. Core 22-7. Stratigraphic log for Core 22-7, collected on July 5th, 2022. Composed of brown medium-sandstone with a total recovery of 20.0 cm, the log illustrates consistent grain size and MP abundance. A localized low-contamination lens is noted at 16–20 cm.

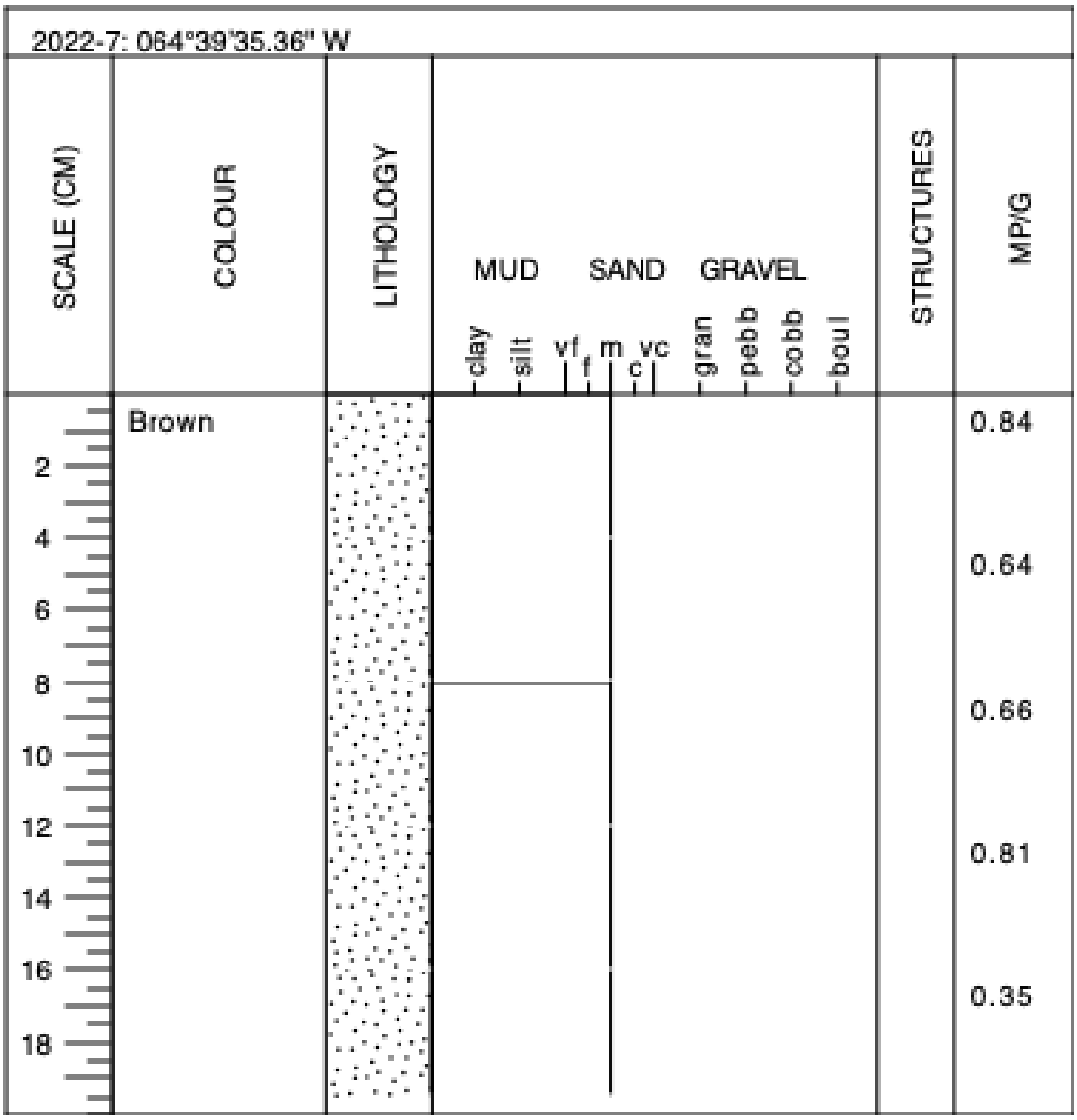

Figure C8. Core 24-1. Stratigraphic log for Core 24-1, collected on July 8th, 2024. Total recovery reached 12.0 cm, with the lithology transitioning from brown to red-brown medium-sandstone at 8.5 cm. The log illustrates an increase in grain size and a corresponding decrease in MP abundance with depth.

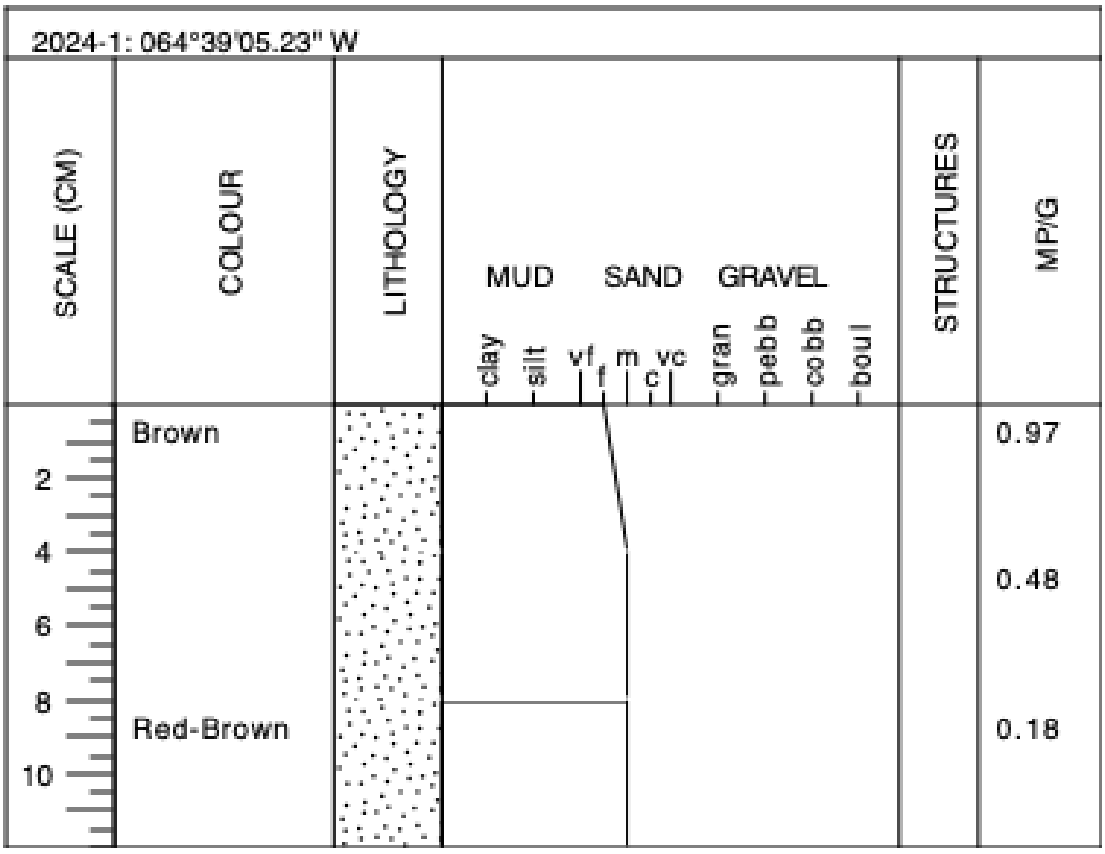

Figure C9. Core 24-2. Stratigraphic log for Core 24-2, collected on July 8th, 2024. The core reached a total recovery of 14.0 cm, shifting from brown medium-sandstone to red-brown at 10.5 cm. Pebble and conglomerate lenses are present at 8–10 cm and 12–14 cm. MP abundance is variable, with high contamination localized at 12–14 cm.

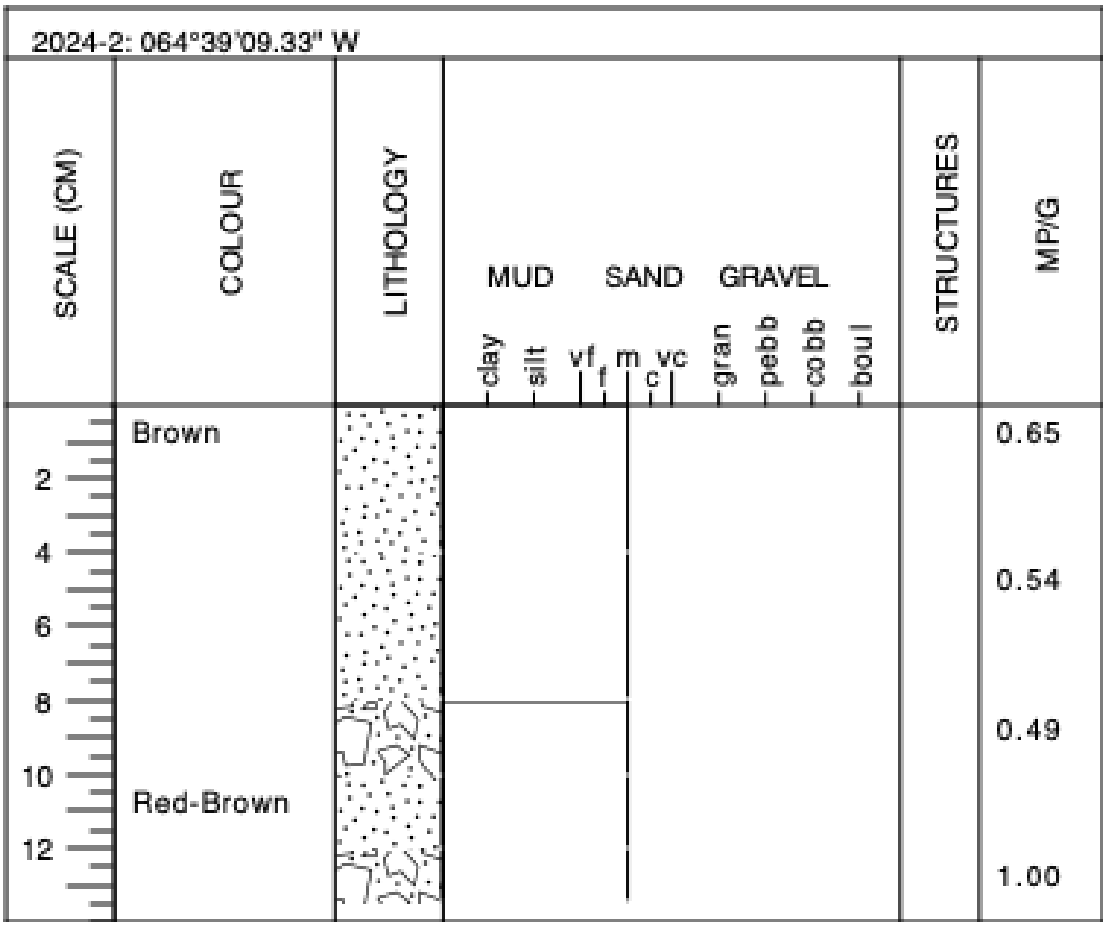

Figure C10. Core 24-3. Stratigraphic log for Core 24-6, collected on July 8th, 2024. Total recovery reached 17.0 cm, with a lithological transition from brown sandstone to red-brown conglomerate at 12 cm. The log illustrates variable MP abundance, featuring high contamination at the surface (0–4 cm) and at depth (16–17 cm).

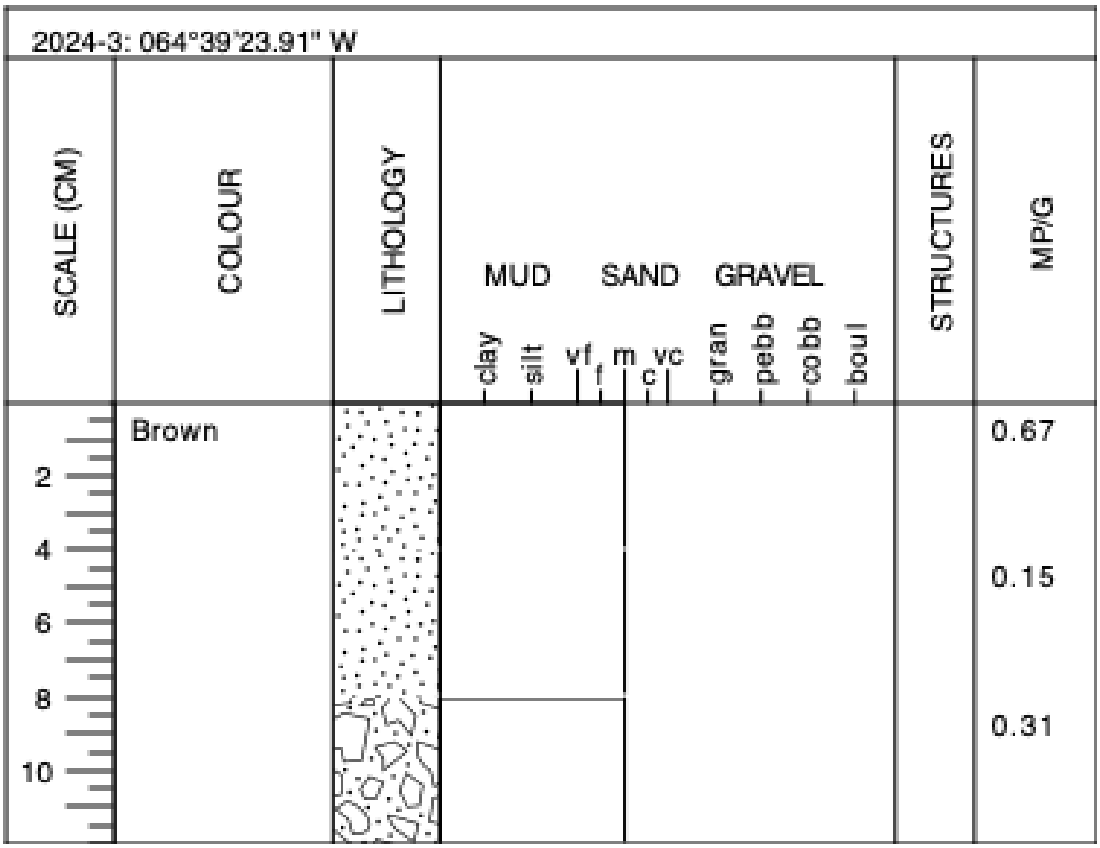

Figure C11. Core 24-4. Stratigraphic log for Core 24-4, collected on July 8th, 2024. Composed of brown medium-grained sandstone with a total recovery of 12.0 cm, the log illustrates consistent grain size and MP abundance throughout the profile.

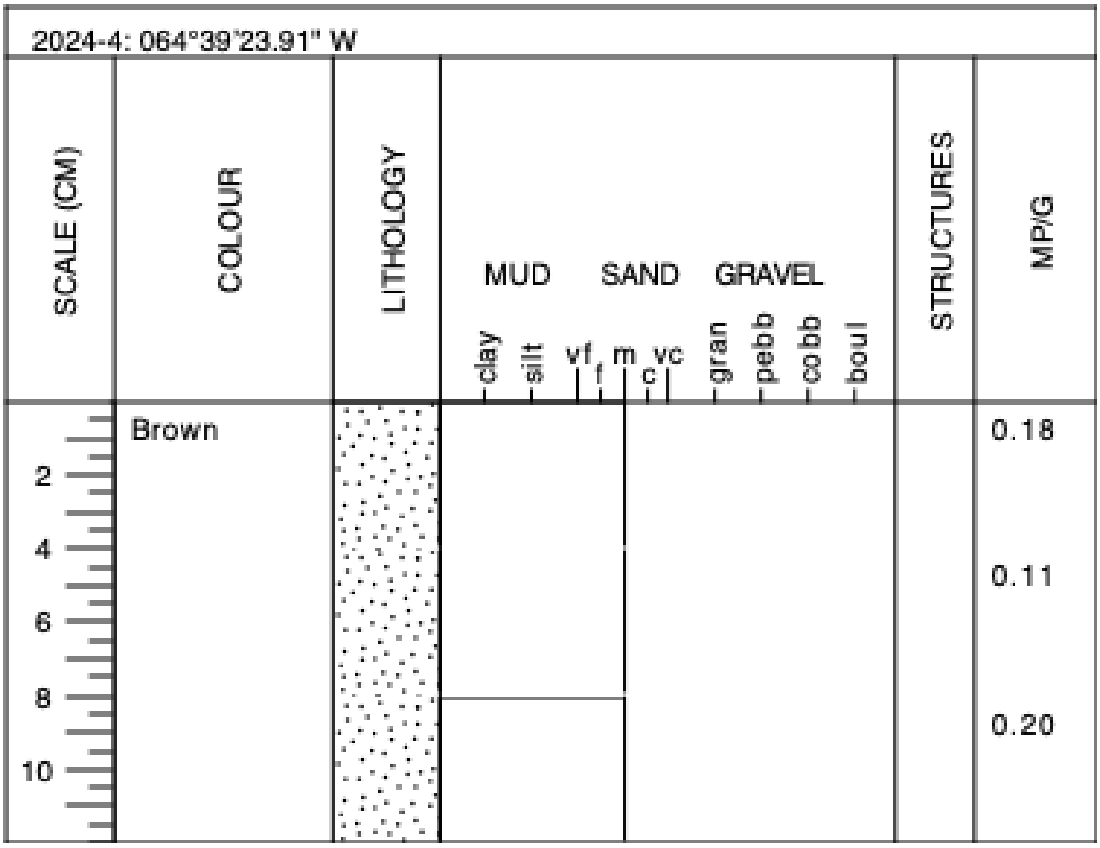

Figure C12. Core 24-5. Stratigraphic log for Core 24-5, collected on July 8th, 2024. The core consists of brown sandstone and reached 17.0 cm; a small pebble/conglomerate lens at 16 cm inhibited deeper coring. The log illustrates near-consistent grain size and variable MP abundance, with a localized high-contamination lens at 16–17 cm.

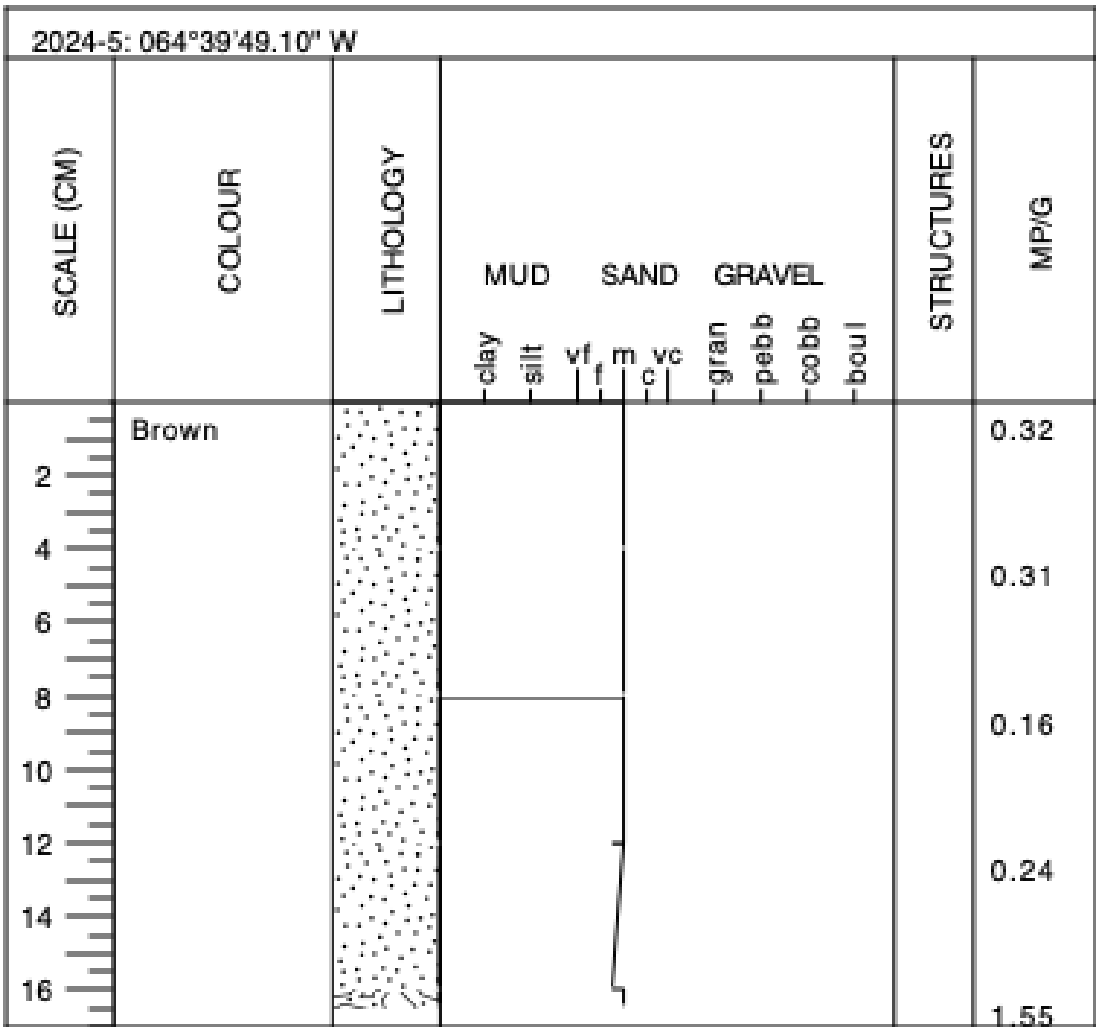

Figure C13. Core 24-6. Stratigraphic log for Core 24-6, collected on July 8th, 2024. Total recovery reached 17.0 cm, with a lithological transition from brown sandstone to red-brown conglomerate at 12 cm. The log illustrates variable MP abundance, featuring high contamination at the surface (0–4 cm) and at depth (16–17 cm).

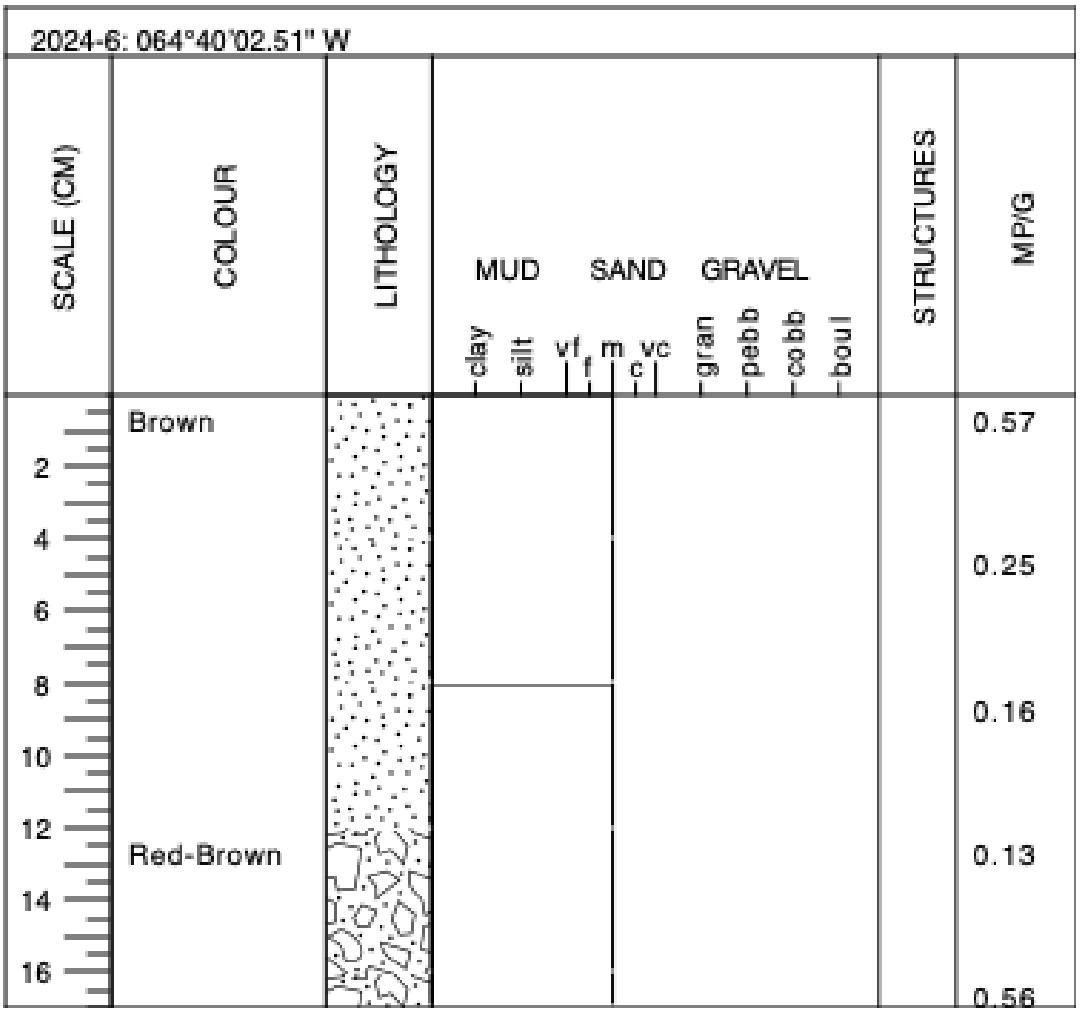

Figure C14. Core 24-7. Stratigraphic log for Core 24-7, collected on July 8th, 2024. The core reached 18.0 cm, transitioning from brown to red-brown sandstone at 9 cm. The log illustrates near-consistent grain size and variable MP abundance, notably a localized lens of higher contamination at 16–18 cm.

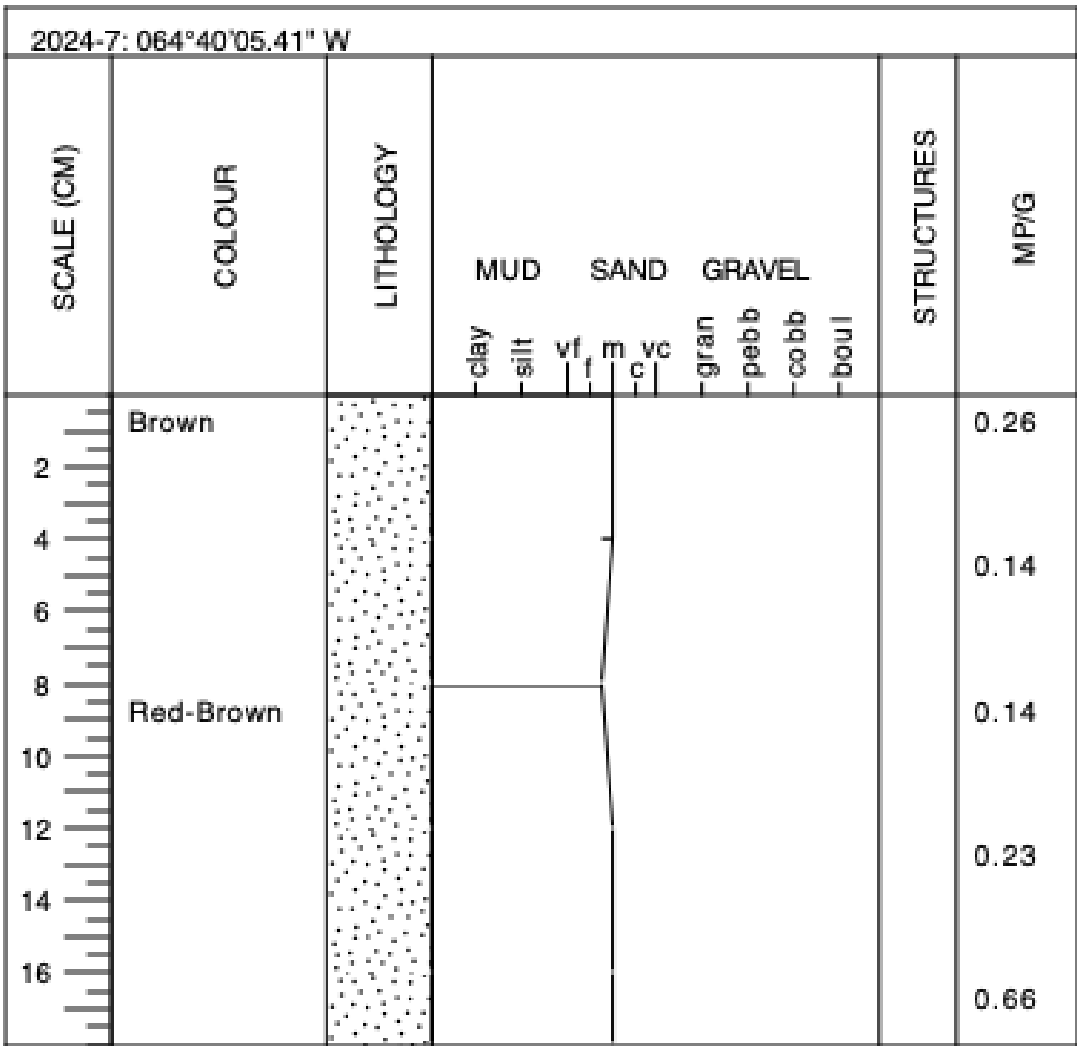

Table C1. Grain size analysis of samples collected in 2022.

				Weight (g)					Abundance (%)						
Year	**Core**	**Depth-mid**	**Depth-range**	**1ϕ**	**2 ϕ**	**3 ϕ**	**4 ϕ**	**Pan**	**1ϕ**	**2 ϕ**	**3 ϕ**	**4 ϕ**	**Pan**	**Mean-phi**	**St.Dev**
2022	1	2	0-4	0.8	31.1	28.8	5.9	1.9	1%	45%	42%	9%	3%	2.10	0.2
2022	1	6	4-8	0.3	23.7	16.6	1.9	0.8	1%	55%	38%	4%	2%	1.98	0.2
2022	1	10	8-12	4.0	22.9	16.1	3.2	1.1	8%	48%	34%	7%	2%	1.94	0.2
2022	1	14	12-16	5.0	26.0	11.8	0.7	0.3	11%	59%	27%	2%	1%	1.74	0.2
2022	1	18	16-20	2.0	17.8	20.4	4.9	1.7	4%	38%	44%	10%	4%	2.15	0.2
2022	2	2	0-4	17.6	23.0	2.4	0.6	0.6	40%	52%	5%	1%	1%	1.15	0.2
2022	2	6	4-8	29.5	23.3	2.5	0.8	1.0	52%	41%	4%	1%	2%	1.02	0.2
2022	2	10	8-12	27.3	13.5	2.0	1.0	1.2	61%	30%	4%	2%	3%	0.96	0.3
2022	2	14	12-16	12.2	3.3	0.5	0.1	0.1	75%	20%	3%	1%	1%	0.77	0.3
2022	2	18	16-20												
2022	3	2	0-4	17.7	18.5	2.1	0.6	0.9	44%	46%	5%	2%	2%	1.11	0.2
2022	3	6	4-8	11.6	28.2	4.7	1.0	0.3	25%	62%	10%	2%	1%	1.33	0.3
2022	3	10	8-12	22.5	14.2	1.7	0.6	1.0	56%	36%	4%	2%	3%	0.99	0.2
2022	3	14	12-16	7.9	10.2	0.0	0.0	0.0	44%	56%	0%	0%	0%	1.07	0.3
2022	3	18	16-20												
2022	4	2	0-4	10.8	17.0	1.9	0.4	0.3	36%	56%	6%	1%	1%	1.19	0.2
2022	4	6	4-8	25.0	15.8	2.0	0.6	0.7	57%	36%	5%	1%	2%	0.98	0.3
2022	4	10	8-12	23.3	26.8	3.5	0.9	0.8	42%	48%	6%	2%	1%	1.14	0.2
2022	4	14	12-16	5.0	6.2	0.6	0.1	0.1	42%	52%	5%	1%	1%	1.12	0.2
2022	4	18	16-20												
2022	5	2	0-4	3.3	26.2	4.2	0.5	0.4	10%	76%	12%	1%	1%	1.53	0.3
2022	5	6	4-8	9.4	26.3	3.9	0.3	0.6	23%	65%	10%	1%	1%	1.35	0.3
2022	5	10	8-12	15.0	15.6	1.8	0.4	0.5	45%	47%	5%	1%	2%	1.10	0.2
2022	5	14	12-16	15.7	9.9	1.3	0.4	0.5	56%	36%	5%	1%	2%	0.98	0.2
2022	5	18	16-20												
2022	6	2	0-4	7.1	47.4	5.0	0.6	0.5	12%	78%	8%	1%	1%	1.49	0.3
2022	6	6	4-8	7.5	44.1	4.8	0.3	0.4	13%	77%	8%	1%	1%	1.48	0.3
2022	6	10	8-12	4.5	33.8	5.0	0.5	0.5	10%	76%	11%	1%	1%	1.52	0.3
2022	6	14	12-16	10.0	29.9	4.3	0.5	0.7	22%	66%	9%	1%	2%	1.36	0.3
2022	6	18	16-20												
2022	7	2	0-4	6.4	26.0	0.8	3.3	1.5	17%	68%	2%	9%	4%	1.47	0.3
2022	7	6	4-8	3.8	39.7	6.1	0.5	0.7	7%	78%	12%	1%	1%	1.54	0.3
2022	7	10	8-12	2.5	37.3	7.9	0.7	1.0	5%	76%	16%	1%	2%	1.65	0.3
2022	7	14	12-16	2.3	31.4	12.5	1.1	2.4	5%	63%	25%	2%	5%	1.85	0.3
2022	7	18	16-20	2.8	33.7	13.0	1.0	1.0	5%	65%	25%	2%	2%	1.79	0.3

Table C2. Grain size analysis of samples collected in 2024.

				Weight (g)					Abundance (%)						
Year	**Core**	**Depth-mid**	**Depth-range**	**1ϕ**	**2 ϕ**	**3 ϕ**	**4 ϕ**	**Pan**	**1ϕ**	**2 ϕ**	**3 ϕ**	**4 ϕ**	**Pan**	**Mean-phi**	**St.Dev**
2024	1	2	0-4	2.8	44.8	14.6	0.2	0.1	4%	72%	23%	0%	0%	2.2	0.3
2024	1	6	4-8	29.4	6.0	1.6	0.5	0.4	78%	16%	4%	1%	1%	1.3	0.3
2024	1	10	8-12	29.1	9.8	1.9	0.1	0.5	70%	24%	5%	0%	1%	1.4	0.3
2024	1	14	12-16												
2024	1	18	16-20												
2024	2	2	0-4	12.9	35.6	1.6	0.1	0.3	26%	70%	3%	0%	1%	1.8	0.3
2024	2	6	4-8	38.8	15.3	1.8	0.5	0.2	69%	27%	3%	1%	0%	1.4	0.3
2024	2	10	8-12	31.7	21.7	4.3	0.2	0.4	54%	37%	7%	0%	1%	1.6	0.2
2024	2	14	12-16	20.1	3.5	0.7	0.2	0.1	82%	14%	3%	1%	0%	1.2	0.3
2024	2	18	16-20												
2024	3	2	0-4	23.1	19.7	1.1	0.1	0.2	52%	45%	2%	0%	0%	1.5	0.3
2024	3	6	4-8	58.7	12.4	1.6	0.6	0.8	79%	17%	2%	1%	1%	1.3	0.3
2024	3	10	8-12	46.0	10.5	1.3	0.5	0.3	78%	18%	2%	1%	1%	1.3	0.3
2024	3	14	12-16												
2024	3	18	16-20												
2024	4	2	0-4	14.2	36.7	3.0	0.1	0.3	26%	68%	6%	0%	1%	1.8	0.3
2024	4	6	4-8	26.0	31.3	2.9	0.4	0.2	43%	51%	5%	1%	0%	1.6	0.3
2024	4	10	8-12	34.7	15.5	1.8	0.3	0.3	66%	29%	3%	1%	1%	1.4	0.3
2024	4	14	12-16												
2024	4	18	16-20												
2024	5	2	0-4	15.6	26.8	3.3	0.2	0.2	34%	58%	7%	0%	0%	1.8	0.3
2024	5	6	4-8	12.6	23.1	4.0	0.3	0.1	31%	58%	10%	1%	0%	1.8	0.2
2024	5	10	8-12	20.6	34.6	5.9	0.4	0.1	33%	56%	10%	1%	0%	1.8	0.2
2024	5	14	12-16	15.2	39.8	5.8	0.3	0.3	25%	65%	9%	0%	0%	1.9	0.3
2024	5	18	16-20	4.0	8.0	1.0	0.1	0.1	30%	61%	8%	1%	1%	1.8	0.3
2024	6	2	0-4	4.4	40.0	3.8	0.1	0.1	9%	83%	8%	0%	0%	2.0	0.4
2024	6	6	4-8	13.4	32.7	6.6	0.1	0.1	25%	62%	12%	0%	0%	1.9	0.3
2024	6	10	8-12	19.2	26.9	6.3	0.3	0.2	36%	51%	12%	1%	0%	1.8	0.2
2024	6	14	12-16	18.3	25.8	4.7	0.2	0.2	37%	52%	10%	0%	0%	1.7	0.2
2024	6	18	16-20	5.3	6.3	0.8	0.1	0.1	42%	50%	6%	1%	1%	1.7	0.2
2024	7	2	0-4	8.0	55.8	5.0	0.1	0.1	12%	81%	7%	0%	0%	2.0	0.3
2024	7	6	4-8	5.5	48.0	5.4	0.1	0.1	9%	81%	9%	0%	0%	2.0	0.3
2024	7	10	8-12	9.9	43.0	3.6	0.1	0.1	17%	76%	6%	0%	0%	1.9	0.3
2024	7	14	12-16	7.6	35.1	2.7	0.1	0.1	17%	77%	6%	0%	0%	1.9	0.3
2024	7	18	16-20	2.9	18.1	1.5	0.1	0.0	13%	80%	7%	0%	0%	1.9	0.3

Table C3. Mean grain size by core in 2022 and 2024.

Year	Core #	1 ϕ	2 ϕ	3 ϕ	4 ϕ	pan	mean ϕ
2022	1	5%	49%	38%	7%	2%	1.99
2022	2	53%	39%	5%	2%	2%	0.60
2022	3	42%	49%	6%	2%	2%	1.01
2022	4	45%	46%	6%	1%	1%	0.98
2022	5	32%	57%	8%	1%	1%	1.08
2022	6	14%	75%	9%	1%	1%	1.48
2022	7	7%	70%	17%	3%	3%	1.70
2024	1	43%	43%	13%	1%	1%	1.04
2024	2	54%	40%	4%	1%	1%	0.58
2024	3	72%	24%	2%	1%	1%	0.50
2024	4	45%	50%	5%	0%	0%	0.97
2024	5	31%	59%	9%	1%	0%	1.07
2024	6	28%	61%	10%	0%	0%	1.09
2024	7	13%	79%	7%	0%	0%	1.46

Appendix D – Meta-Analysis of Data

A comprehensive literature search was conducted using the Scopus search engine with the keywords “microplastic*” and “beach” applied to the Article Title, Abstract, and Keywords fields. The following specific query was utilized:

(TITLE-ABS-KEY (microplastic*) AND TITLE-ABS-KEY (beach)) AND PUBYEAR < 2025 AND (LIMIT-TO (DOCTYPE, "ar") AND (LIMIT-TO (LANGUAGE, "English"))

This search targeted peer-reviewed research articles published in English before 2025. To maintain data comparability, articles were excluded if they reported measurements by volume or area, focused on non-beach locations (e.g., subtidal zones, mangroves), utilized non-density/oleophilic extraction methods, or presented unclear methodologies. For each study, the extraction solution, study region and sample zone [High Tide (HT), Low Tide (LT), Back Shore (BS), Intertidal (IT), Strand Line (StL), Dune (D), Fore Shore (FS), Beach, and Mud Flat] were recorded. The mean value, or the highest mean value from a reported range across different sub-environments, adjacent beaches, or timeframes, was recorded. While this search was extensive, it may not be exhaustive.

Full bibliographic details for all publications listed in Table D1 are provided in the preceding Bibliography section of this thesis (pages 110–147).

Table D1. Summary of peer-reviewed beach sediment microplastic studies (2011–2024)

Unique Publications	Salt	Study region	Sample zone	MP Mean (MP/kg)	Range (MP/kg)
Abayomi et al., 2017	NaCl & KI	Middle East	HT	22	6 – 38

Abdel Gahni et al., 2022	NaCl	Africa	beach	398	
Abdel Ghandi et al., 2023	NaCl & NaI	Africa	beach	476.5	23 – 930
Abelouah et al., 2022	NaCl	Africa	IT-StL	20940	7680 – 34200
Abidli et al., 2018	NaCl	Africa	beach	301	141 – 461
Akkajit et al., 2021	NaCl	Asia	IT	183	
Al Nahian et al., 2022	$ZnCl_2$	Asia	beach	317	
Amorim et al., 2024	NaCl	Europe	beach	470	200 – 740
anak Alexander Tampang & Mohan Viswanathan, 2022	$ZnCl_2$	Asia	IT	2275	920 – 3630
Anderson et al., 2024	$ZnCl_2$	Europe	LT-IT-HT	300	40 – 560
Arjun et al., 2024	NaCl	Asia	LT-HT	28.2	
Asensio-Montesinos et al., 2022	NaCl	Europe	HT	47	23 – 71
Aslam et al., 2020	KI	Middle East	HT	71	8 – 134
Atwood et al., 2019	$ZnCl_2$	Europe	HT	40	1 – 79
Azaaouaj et al., 2024	NaCl	Africa	StL	44	40 – 48
Balestra et al., 2024	NaCl	Europe	FS-BS	861	606 – 1116
Ballent et al., 2016	Na_2WO_4	North America	beach	670	
Banik et al., 2022	$ZnCl_2$	Asia	HT	234	157 – 311
Bayo et al., 2019	NaCl	Europe	IT	87	8 – 166
Ben-Haddad et al., 2022	NaCl	Africa	IT	1181.5	915 – 1448
Beraud et al., 2022	NaCl	Oceania	HT	255	170 – 340
Besley et al. ., 2017	NaCl	Europe	IT-HT-BS	504	426 – 582
Bissen & Chawchai., 2020	NaCl	Asia	HT	11880	1360 – 22400
Blašković et al., 2018	NaCl	Europe	LT-BS	131.5	72 – 191
Bobchev et al., 2024	NaCl	Europe	HT	324	184 – 464
Borah et al., 2024	$ZnCl_2$	Asia	LT	122	91 – 153
Bosker et al., 2018	NaCl	Caribbean	IT-HT-BS	344	68 – 620
Cannas et al., 2017	NaCl	Europe	LT-BS	376	286 – 466
Castro et al., 2020	NaCl	South America	beach	245	69 – 421
Chen and Chen., 2020	NaCl	Asia	HT	280	80 – 480
Cheung and Not., 2023	NaCl	Asia	HT	235	
Chouchene et al., 2021	NaCl	Europe	IT	167.5	15 – 320
Chubarenko et al., 2018	$ZnCl_2$	Europe	beach	35	7 – 63
Chubarenko et al., 2020	$ZnCl_2$	Europe	HT-BS	115	
Chubarenko et al., 2024	$ZnCl_2$	Europe	LT-HT	95	
Claessens et al., 2011	NaCl	Europe	LT-BS	108.5	92 – 125
Constant et al., 2019	NaCl	Europe	HT-StL-BS	99.5	12 – 187
Cordova et al., 2024	$ZnCl_2$	Asia	IT-StL	81	51 – 111
Daniel et al., 2022	$ZnCl_2$	Asia	HT	58	
Davidson et al., 2022	$ZnCl_2$	North America	beach	65	
De la Torre., 2023	NaCl	South America	SL	8	7.5 – 8.5
de Ruijter et al ., 2019	NaCl	Europe	IT-StL-BS	19	1 – 37
Dean et al., 2018	Na_2WO_4	North America	LT-HT-BS	102.5	59 – 146
Deswati et al., 2023	NaCl	Asia	beach	2058	6 – 4110
Dimante-Deimantovica et al., 2023	NaCl	Europe	HT	3	2 – 4
Dodson et al., 2020	CsCl & Oil	North America	LT-ST-D	1410	
Dou et al., 2021	NaCl	Asia	LT-IT-HT	3200	
Dowarah & Devipraya., 2019	NaCl	Asia	HT	720	
Doyen et al., 2019	NaCl	Europe	LT-IT-HT	40.5	33 – 48
Dutta et al., 2022	$ZnCl_2$	Asia	HT	290	50 – 530

Egessa et al ., 2020	NaCl	Africa	StL	120.5	1 – 240
Esiukova et al., 2021	$ZnCl_2$	Europe	IT-HT	228.5	20 – 437
Exposito et al., 2021	H_2O & NaCl & $ZnCl_2$	Europe	IT	21.5	1 – 42
Fischer et al., 2016	NaCl	Europe	IT-HT-BS	187.5	109 – 266
Flores-Cortez et al., 2022	NaCl	North America	beach	241	
Flores-Ocampo & Armstrong-Altrin., 2023	NaCl & $ZnCl_2$	North America	beach	13475	12800 – 14150
Fulfer& Walsh., 2023	NaI	North America	LT-IT-HT-BS	1170	396 – 1944
Furlan et al., 2024	$ZnCl_2$	South America	FS-BS	16950	16500 – 17400
Gao et al., 2021	$ZnCl_2$	Asia	beach	17.5	13 – 22
Ghanadi et al., 2024	$CaCl_2$	Oceania	LT-IT-HT	2300	2067 – 2533
Ghayebzadeh et al., 2020	$ZnCl_2$	Asia	beach	183.5	140 – 227
Go et al., 2024	NaCl	Asia	HT	130	
Go et al., 2025	NaCl	Asia	HT	80	
Godoy et al., 2020	NaCl	Europe	IT-StL	33.5	22 – 45
Godoy et al., 2023	NaCl	Europe	LT-IT-HT	200	
Graca et al., 2017	NaCl	Europe	beach	39	25 – 53
Guerranti et al., 2017	NaCl	Europe	beach	241	200 – 282
Gül, M., 2023	NaCl	Middle East	LT-IT-HT	25	20 – 30
Hamdy et al., 2024	NaCl	Africa	IT	507	147 – 867
Hien et al., 2020	$ZnCl_2$	Asia	LT-IT-HT	23.5	2 – 45
Hossein et al., 2021	$ZnCl_2$	Asia	LT	289.5	200 – 379
Jaouani et al., 2022	NaCl	Africa	beach	131	
Jaubet et al., 2021	$CaCl_2$	South America	HT	622.5	184 – 1061
Jebashalomi et al., 2024	NaCl	Asia	LT-IT-HT-BS	821	335 – 344
Jones et al., 2021	$ZnCl_2$	South America	HT	75	
Jong et al ., 2022	NaCl	Asia	LT-IT-HT	658	
Jualaong et al., 2021	NaCl	Asia	IT-HT	16.5	
Jualaong et al., 2023	NaCl	Asia	LT-HT	572	
Kanak et al., 2024	NaCl	Asia	LT-IT-HT	175	
Kaviarasan et al ., 2022	NaCl	Asia	IT-BS	500	244 – 756
Keene and Turner., 2023	$ZnCl_2$	Europe	beach & mud flat	240	
Keerthika et al ., 2022	$ZnCl_2$	Asia	beach	49	19 – 79
Kelly et al., 2024	NaCl & NaI	North America	LT-IT-HT	50	
Kelly et al., 2025	NaCl & NaI	North America	LT-IT-HT	55.8	
Khaleel et al., 2022	$ZnCl_2$	Asia	HT	113	8 – 218
Khuyen et al., 2021	NaCl	Asia	IT-HT-BS	59	32 – 86
Korez et al ., 2019	NaCl	Europe	StL	9	7 – 11
Kumkar et al., 2023	NaCl	Asia	LT-HT	108	
Laglbauer et al., 2014	NaCl	Europe	IT-BS	133	
Laun et al., 2024	NaCl	Asia	LT-IT-HT-BS	600	452 – 748
Le et el., 2023	NaCl & $ZnCl_2$	Asia	LT-IT-HT	1582	
Lekshmi et al., 2023	$ZnCl_2$	Asia	HT	93.5	32 – 155
Lenz et al., 2023	SPT	Europe	beach	4	
Li et al., 2023	$CaCl_2$ then $ZnCl_2$	Asia	HT	143	96 – 190
Li, J et al., 2018	$CaCl_2$	Asia	LT	3266	

Li, J et al., 2023	NaCl	Asia	beach	174	
Li, Y et al., 2022	$CaCl_2$	Asia	IT	406	
Li,Y et al., 2024	NaCl	Asia	HT	245	
Liebezeit & Dubaish., 2012	$ZnCl_2$	Europe	LT-D	671	
Llyod-Jones et al., 2023	SPT	Europe	StL	1450	700 – 2200
Lo, Lee et al., 2020	$ZnCl_2$	Asia	HT	261.5	188 – 335
Lo, Xu et al., 2018	$ZnCl_2$	Asia	LT-IT-StL	17	
Lopez-Velazquez et al., 2024	NaCl	North America	HT	36	19 – 53
Luo et al., 2020	$ZnCl_2$	Asia	LT-IT-HT	3602	
Machendiranathan et al., 2022	NaCl	Asia	IT	32	
Machendiranathan et al., 2024	NaCl	Asia	beach	119	
Malla-Pradhan et al., 2022	NaCl	Asia	beach	89	55 – 123
Manbohi et al., 2021	$ZnCl_2$	Asia	beach	197	
Mandal et al., 2023	$ZnCl_2$	Asia	beach	3.5	1 – 6
Masia et al., 2019	NaCl	Europe	IT	263.5	145 – 382
Masia et al., 2021	NaCl	Europe	IT	144	58 – 230
Masud et al., 2023	NaCl	Middle East	StL-BS	280	155 – 405
Mathalon & Hill, 2014	NaCl	North America	LT-IT-HT	5000	2000 – 8000
Mayoma et al., 2020	NaCl	Africa	IT	127.5	15 – 240
Mazurkiewicz et al., 2022	$ZnCl_2$	Europe	HT-BS	327	118 – 536
Minor et al., 2020	NaCl	North America	HT-StL	27.5	
Misic et al., 2019	NaCl & $ZnCl_2$	Europe	HT	416	
Missawi et al., 2020	$ZnCl_2$	Africa	beach	367.5	129 – 606
Mohan et al., 2022	NaCl & NaI	Asia	HT	274	73 – 475
Nahla et al., 2023	NaCl & NaI	Africa	beach	204	
Naji et al., 2017	NaCl & NaI	Asia	IT	630	2 – 1258
Nchimbi et al., 2022	NaCl	Africa	IT	592	320 – 864
Nel et al., 2020	$ZnCl_2$	Europe	LT-IT-HT	462	97 – 827
Nematollahi et al., 2020	$ZnCl_2$	Asia	LT	15	
Nhon et al., 2022	$ZnCl_2$	Asia	LT-IT-HT	4	1 – 7
Nichols et al., 2021	$ZnCl_2$	Oceania	HT	1960	
Novillo-Sanjuan et al.., 2022	NaCl	Europe	HT	52	37 – 67
Paler et al., 2019	NaCl	Asia	beach	260	
Paradinas et al., 2021	Oleo	Europe	IT	185	
Patchaiyappan et al., 2020	NaCl	Asia	HT	567.5	162 – 973
Patchaiyappan et al., 2021	NaCl	Asia	HT	279.5	181 – 378
Patidar et al., 2024	NaCl	Asia	beach	59	94 – 24
Patti et al., 2020	$ZnCl_2$	Asia	beach	242	
Pelegrini et al., 2024	NaCl	South America	LT-HT	650	
Pervez & Wang., 2020	NaCl	Asia	StL	466	268 – 664
Pervez et al ., 2020	NaCl	Asia	HT	253.5	208 – 299
Pervez et al., 2023	NaCl	Asia	HT	664	
Petrovic et al., 2022	$ZnCl_2$	Asia	HT	555	530 – 580
Pinon-Colin et al., 2018	NaCl	North America	HT	174.5	16 – 230
Piperagkas et al., 2019	NaCl & NaI	Europe	LT-IT-HT	45	5 – 85
Piperagkas et al., 2021	NaCl & NaI	Europe	LT-IT-HT	80.5	6 – 155
Piyumali et al., 2024	NaCl	Asia	beach	66.5	42 – 91
Prarat&Hongsawat., 2022	NaCl	Asia	HT	331	80 – 582
Purushothaman et al., 2023	NaCl	Asia	LT	1205	
Rahman et al., 2020	$ZnCl_2$	Asia	LT-HT	8	
Ramos-Vazquez et al., 2024	oil	North America	HT	0	

Rangel-Buitrago et al., 2021	NaCl	South America	IT	1109	
Ranjani et al., 2022	NaCl	Asia	LT-HT-BS	398	76 – 720
Rayhan et al., 2024	NaCl	Asia	LT-IT-HT	78	
Retama et al., 2016	$ZnCl_2$	North America	HT	1950	1600 – 2300
Rodrigues et al ., 2024	NaCl	Europe	IT-HT-BS	13	
Rogowska et al ., 2021	NaCl	Europe	beach	29.5	28 – 31
Ronda et al., 2023	NaCl	South America	LT-IT-HT	1133	
Sa et al., 2022	$ZnCl_2$	Europe	beach	581	102 – 1060
Sagawa et al., 2018	NaCl	Asia	HT	625	5 – 1245
Sajorne et al., 2022	NaCl	Asia	HT	14.5	6 – 23
Samrat et al., 2024	NaCl	Asia	LT	140	40 – 160
Sanchez-Garcia & Sanz-Lazaro., 2023	NaCl	South America	StL	727	
Sathish et al., 2019	$ZnCl_2$	Asia	LT-HT	236	33 – 439
Schroder et al ., 2021	$CaCl_2$	Europe	HT	16	2 – 30
Scopetani et al., 2021	NaCl	Europe	HT-BS	207	191 – 223
Sener & Yabanli., 2023	NaCl	Middle East	HT-StL	177	
Shaji et al., 2024	$ZnCl_2$	Asia	HT	564	
Sheikhi & Mirzaei., 2023	NaCl	Asia	beach	137	
Shinde et al., 2024	NaCl	Asia	HT	365	300 – 430
Simon-Sanchez et al., 2019	NaCl	Europe	HT	422	
Srihari et al., 2023	NaCl & $ZnCl_2$	Asia	FS	25.5	9 – 42
Sundar et al., 2021	$ZnCl_2$	Asia	LT	860	
Sunitha et al., 2021	NaI	Asia	beach	348.5	331 – 366
Tasnim et al., 2023	NaCl	Asia	HT	246.66	
Tata et al., 2020	NaCl	Africa	beach	416	183 – 649
Terzi et al., 2022	$ZnCl_2$	Middle East	HT	91	9 – 173
Thepwilai et al ., 2021	NaCl	Asia	IT	1423.5	20 – 2827
Tiwari et al., 2019	$CaCl_2$	Asia	beach	113	45 – 181
Tong et al., 2023	NaCl	Asia	HT	60	50 – 70
Truchet et al., 2021	NaCl	South America	IT	370	330 – 410
Tuong Vy et al., 2024	$ZnCl_2$	Asia	LT-IT-HT	45.5	40 – 51
Ulfah et al., 2024	$ZnCl_2$	Asia	0	50	32 – 68
Urban-Malinga et al., 2020	NaCl	Europe	HT	185.5	76 – 295
van Cauwenberghe et al., 2013	NaI	Europe	IT	6	
Veerasingam et al.., 2021	NaCl	Middle East	beach	62	
Vetrimurugan et al ., 2020	$ZnCl_2$	Africa	IT	10925	5150 – 16700
Vidyasakar et al., 2020	$ZnCl_2$	Asia	beach	204	
Wang et al., 2021	NaCl	Asia	IT	150	110 – 190
Wu et al ., 2023	NaCl	Asia	LT-IT-HT	133.5	113 – 154
Wu et al., 2021	NaCl & NaI	Asia	beach	107	
Wu et al., 2023	NaCl	Asia	LT-IT-HT	135	
Wu et al., 2024	NaCl	Asia	IT	271	
Yabanli et al.., 2019	NaCl	Middle East	HT	736.5	350 – 1123
Yaranal et al.., 2021	NaCl	Asia	HT	664	
Yona et al., 2023	NaCl	Asia	StL	78.5	54 – 103
Yu et al., 2016	NaCl	Asia	IT	132.5	102 – 163
Yu et al., 2018	NaCl	North America	IT	243	43 – 443
Zahari et al., 2023	NaCl	Asia	LT	408	
Zhang et al., 2020	NaH_2PO_4	Asia	HT	6665	6 – 38
Zhang et al., 2024	NaCl	Asia	LT-IT-HT	286	

Curriculum Vitae

Candidate's Full Name: Claire Gullison

Universities Attended:

St. Thomas University, Bachelor of Education, July 2026.

University of Western Ontario, Master of Science in Geology (Transferred), April 2024. Supervisor: Dr. Patricia Corcoran

University of New Brunswick, Bachelor of Science in Earth Science (Honours), May 2023. Supervisor: Dr. Dave Keighley

Conference Abstracts / Proceedings:

Feng, J., Taillon, M. E., Al-Samarraie, D., Doshi, S., Gullison, C., & Corcoran, P. (2024). Microplastic pollution in water, sediment, soils, and air of Southwestern Ontario, Great Lakes Basin. In Proceedings of the 67th Annual Conference of the International Association of Great Lakes Research (p. 69). Journal of Great Lakes Research. *(Co-author; presented by J. Feng)*

Gullison, C., & Keighley, D. (2023). Microplastic in beach sediment from Mary's Point, Shepody National Wildlife Area, Southeast New Brunswick, Canada. In Proceedings of the 49th Annual Colloquium and General Meeting of the Atlantic Geoscience Society (p. 46). Atlantic Geoscience, 59. https://doi.org/10.4138/atlgeo.2023.002 . *(Presented by C. Gullison)*

Gullison, C., & Keighley, D. (2022). Microplastic in beach sediment from Mary's Point, Shepody National Wildlife Area, Southeast New Brunswick, Canada. In Proceedings of the 72nd Atlantic Universities Geoscience Conference (p. 295). Atlantic Geoscience, 58. https://doi.org/10.4138/atlgeo.2022.013. *(Presented by C. Gullison)*

Teaching Experience:

Practicum Teacher (Field Placements), School of Education, St. Thomas University, 2025–2026.

Graduate Teaching Assistant, Department of Earth Sciences, University of New Brunswick, 2024–2025.

Graduate Teaching Assistant, Department of Earth Sciences, University of Western Ontario, 2023–2024.

Awards:

Accelerated Master's Funding, School of Graduate Studies, University of New Brunswick, 2024 ($8,000).

RNB Graduate Merit Award, 2024, 2025 ($10,000 total).

Jayang Lee Memorial Fellowship, Department of Earth Sciences, University of New Brunswick, 2024 ($1,000).

Larry Mayer Prize in Ocean Mapping & Marine Geoscience, University of New Brunswick, 2024 ($1,500).

Western Graduate Research Scholarships, University of Western Ontario, 2023 ($3,000)

Dean's List, University of New Brunswick, 2019–2023 (4 consecutive years).

Science Atlantic Best Paper Award, October 2022 ($600).

NSERC Undergraduate Student Researcher Award (USRA), May 2021 ($6,000).

Robert Quartermain Geology Scholarship, University of New Brunswick, 2020, 2021, 2022 ($18,000 total).

Eileen M. Iwanicki Scholarship, University of New Brunswick, 2021, 2022 ($10,000 total).

Rosemary A. Wilcox Memorial Scholarship in Earth Science, University of New Brunswick, 2022 ($6,000).

Mackenzie Watson Bursary in Geology, University of New Brunswick, 2022 ($4,000).

Major Drilling Scholarship, University of New Brunswick, 2021 ($2,000).

Roy Kempster Memorial Scholarship, CIM-NB, 2022 ($2,000).

Abraham Gesner Geoscience Scholarship, University of New Brunswick, 2020, 2022 ($1,000 total).

William and Lois Paine Founder's Scholarship, University of New Brunswick, 2019 ($500).